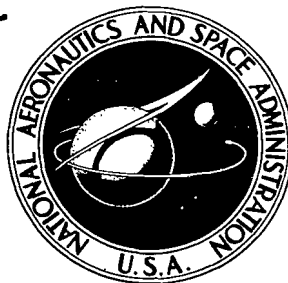


**NASA TECHNICAL
TRANSLATION**



NASA TT F-223

NASA TT F-223



ROCKET FLIGHT ENGINEERING

by Eugen Sänger

Verlag von R. Oldenbourg, Munich and Berlin, 1933.

NATIONAL AERONAUTICS AND SPACE ADMINISTRATION • WASHINGTON, D. C. • SEPTEMBER 1965

Document Processing Errors

Document: NASA-TT-F-223

Document Problems: TEXT CWT

PAGES VI, 194, 196, 290



ROCKET FLIGHT ENGINEERING

By Eugen Sanger

Translation of "Raketenflugtechnik."
Verlag von R. Oldenbourg, Munich and Berlin, 1933.

NATIONAL AERONAUTICS AND SPACE ADMINISTRATION

For sale by the Clearinghouse for Federal Scientific and Technical Information
Springfield, Virginia 22151 - Price \$7.00

TABLE OF CONTENTS

Introduction

0.	General	p. 3
1.	Propulsive Forces	p. 6
10.	Propulsive Forces. General	p. 11
11.	Theory of Rocket Motors. General	p. 13
111.	Processes in the Combustion Chamber	p. 18
112.	Processes in the Nozzle	p. 21
1121.	Nozzle Processes on the Assumption of Ideal Gases	p. 21
1122.	Effects of Friction on Nozzle Processes	p. 42
1123.	Deviations from the Gas Equation	p. 48
1124.	Shape of the Nozzle	p. 58
12.	Efficiency of a Rocket Motor. General	p. 59
121.	Internal Efficiency	p. 60
122.	External Efficiency. General	p. 64
1221.	External Efficiency for Flight in a Space Free from Gravity and Resistance	p. 67
1222.	External Efficiency for Flight against Gravity in a Space Free from Resistance	p. 72
1223.	External Efficiency in Flight in a Space Free from Gravity against a Resistance	p. 77
123.	Overall Efficiency	p. 80
13.	Propellants	p. 83
131.	Requirements as to Propellants	p. 83

132.	Independent Propellants.....	p.85
133.	Dependent Propellants (Combustants).....	p.86
134.	Liquid Oxygen Carriers	p.88
135.	Liquefied Gases	p.91
136.	Choice of the Most Suitable Propellant.....	p.93
137.	Propellant Tables.....	p.97
14.	Power of a Rocket Motor. General.....	p.106
141.	The Second-Thrust.....	p.107
142.	Internal Power	p.117
143.	External Power.....	p.118
2.	Air Forces	p.120
20.	Air Forces. General.....	p.123
21.	Lift in the Subsonic Region. General.....	p.125
211.	Two-Dimensional Theory of Lift on a Single Wing in Incompressible Flow.....	p.125
212.	Three-Dimensional Theory of Lift on a Single Wing in Incompressible Flow.....	p.129
213.	Two-Dimensional Theory of Lift for a Single Wing in a Compressible Flow.....	p.132
214.	Three-Dimensional Theory of Lift for a Single Wing in a Compressible Flow.....	p.135
215.	Results of Experiments on Wing Profiles at Low Speed.....	p.136
216.	Results of Experiments on Wing Profiles at High Speed.....	p.136
22.	Lift in the Supersonic Region. General	p.140
221.	Two-Dimensional Theory of Lift on the Single Wing in Purely Supersonic Flow.....	p.140

2211.	Flow around a Projecting Edge	p. 140
2212.	Flow around a Convex Surface.....	p. 156
2213.	Flow around a Leading Edge	p. 159
2214.	Flow around a Concave Surface	p. 169
2215.	Air Forces on Supersonic Profiles.....	p. 170
2216.	The Flat Plate	p. 176
2217.	The Curved Plate	p. 183
2218.	Separation Effects in the Supersonic Region.....	p. 186
2219.	Boundary and Sum Curves for Lift on the Suction and Pressure Sides from $v = 0$ to $v = 8000$ m/sec	p. 186
222.	The Three-Dimensional Theory of Airfoil Lift under Conditions of Purely Supersonic Flow	p. 193
223.	Principles of Airfoil Design in the Supersonic Region.....	p. 194
23.	Resistance in the Subsonic Region. General.....	p. 195
231.	Frictional Resistance	p. 196
232.	Form Resistance	p. 200
233.	Induced Drag.....	p. 205
234.	Overall Resistance	p. 207
24.	Resistance in the Supersonic Region. General.....	p. 211
241.	Frictional Resistance.....	p. 213
242.	Form Resistance	p. 217
243.	Wave Resistance.....	p. 226
244.	Overall Resistance	p. 241
2441.	Boundary and Sum Curves for the Total Drag	p. 243

2442.	Siacchi's Mean-Value Curve.....	p. 247
2443.	Krupp's Aerodynamic Drag Tables.....	p. 249
2444.	Graphical Correlation of the Various Test Results	p. 249
245.	Shapes with Favorable Supersonic Drag.....	p. 250
25.	Fuselage and Wing Design for a Rocket Aircraft.....	p. 258
251.	Design of Fuselage.....	p. 258
252.	Design of Wings	p. 265
2521.	Design of Wing Profile	p. 265
25211.	Study of Supersonic Profiles in the Subsonic Region	p. 267
25212.	Study of Supersonic Profiles in the Supersonic Region	p. 267
25213.	Study of Supersonic Profiles in the Hypersonic Region.....	p. 274
25214.	Characteristic Curves of the Supersonic Profile.....	p. 275
2522.	Design of Wing Contour.....	p. 277
253.	External Design of Rocket Aircraft	p. 278
3.	Flight Paths	p. 280
30.	Flight Paths. General.....	p. 282
31.	Structure of the Atmosphere. General	p. 284
311.	Composition and General Properties of the Atmosphere	p. 284
312.	Air Density as a Function of Flight Altitude	p. 289
313.	Speed of Sound as a Function of Flight Altitude.....	p. 293
314.	Acceleration due to Gravity as a Function of Flight Altitude....	p. 295
32.	The High-Altitude Flight Phase.....	p. 296
321.	Centrifugal Force	p. 297

322.	Aerodynamic Lift.....	p. 299
323.	Gross Flying Weight.....	p. 301
324.	Height and Flight Velocity of the High-Altitude Mid-Course Trajectory.....	p. 302
33.	Ascent Path.....	p. 306
330.	Ascent Path, General.....	p. 306
331.	Differential Equation of the Ascent Path.....	p. 307
332.	Approximate Ascent Path in the Subsonic Region.....	p. 313
333.	Approximate Ascent Path in the Supersonic Region	p. 321
334.	Efficiency of Ascent Path.....	p. 325
34.	Descent Path. General.....	p. 329
341.	Descent Path in the Supersonic Region	p. 330
342.	Descent Path in the Subsonic Region.....	p. 334
343.	Features of the Descent Path	p. 334
35.	Performance of a Rocket Aircraft. General.....	p. 337
351.	Range of a Rocket Aircraft	p. 338
352.	Cruising and Maximum Speeds of a Rocket Aircraft	p. 342
353.	Flight Altitudes of a Rocket Aircraft	p. 344

FOREWORD

The main object of this book is to direct discussion of rocket flight into serious channels and to free it from its former fantastic notions, which have, understandably but technically undesirably, prevented sober consideration by engineers busy with many other matters.

The principles of rocket flight considered together here in part reflect known facts, but ones which are widely scattered in the literature and whose relation to rocket flight is often scarcely apparent at first sight.

One of the major and essential purposes of this book is to collect as far as possible the material on hand for the designer. The sources that have been employed are conscientiously quoted. Where such references are not given, it is to be assumed that we have lines of thought which either are of general technical validity or have been developed by the author himself.

Rocket flight is above all a technical problem, and the book is directed primarily to the engineer and his ways of thinking. All studies are presented from the technical point of view rather than from the physical one. Important facts whose mathematical demonstration is to be found in the specialist literature, but which are evident to the engineer as such without fundamental proof, are merely mentioned as such where appropriate.

If the specialist finds that some special topic or other has been too superficially treated in one of the innumerable specialized sections, it is to be hoped that it will be excused on the ground that a complete treatment of every discipline involved in rocket technology would demand an altogether exceptionally many-sided technical knowledge, which could be acquired only as a result of many years' acquaintance with the material.

For this reason, and in accordance with the scope of the book, only the major relationships in rocket technology can be discussed, out of the vast amount of material. It might be possible in a later edition to deal with some especially important particular topics, such as the effects of gas dissociation on the behavior of rocket motors, temperature relations of motor walls, control and stability of rocket vehicles, various flight paths, heating consequent on air friction and compression, possible uses of high-pressure rocket motors, and so on; this might make possible description of the research leading to each result.

Structural details, of course, are not discussed for the present although there is no opposition to this.

The author wishes to record his thanks to various sources for interest in the writing and publication of this book.

First of all there is my respected head of division, Professor F. Rinagl of the Technical Research Institute at Vienna Technical University, for the greatest assistance in this work. The author also wishes to thank him as an active and tireless investigator of all problems, even those far from commonplace, for this most valuable advice and support.

In addition, the author wishes to express his thanks to his esteemed instructor in aeronautical sciences, Dr. R. Katzmayer of the Institute of Aerial Machines at this university, and also to Professor A. Lechner for much help in correcting and improving the draft, to Professor E. Wist for generous communication of his researches on nozzles subject to high thermal stress, to Dr. F. Müller for extensive advice (especially on special aspects of chemistry), and to W. Blauhut for reading the manuscript and proofs.

Finally, I owe many thanks to Dr. von Linde, general director of the German Linde Ice Machines Corp. (Deutsche Linde Eismaschinen AG), to the Association of Friends of the Vienna Technical University, which in spite of the difficulties of the times made possible the appearance of this book by providing a grant, and finally to the publishers, R. Oldenbourg of Munich, for the care taken in printing this book.

Vienna, Spring 1933
Technical Research Institute
of the Technical University

Dr. Eugen Sänger

O. GENERAL

By rocket flight is meant here the motion of such a vehicle within the general air space, the propulsive force being provided by a rocket motor. 1

Rocket flight in the narrow sense is taken to be motion in the upper levels of the stratosphere with a speed such that inertial forces arising from the curvature of the path have a marked effect on the lift.

This type of rocket flight is the next major development from tropospheric flight, which has been the product of the last thirty years; it is also the forerunner of space travel, the greatest technical problem of the present time.

This forerunner and the installation of a space station* are the noblest tasks of rocketry, but for the present they are still not realizable.

There are also several directly practical purposes to be served. Rocket flight should especially:

1. Provide rapid intercontinental travel around the globe with the highest possible terrestrial speeds.

2. Advance scientific research in certain fields, especially geophysics and astrophysics.

3. If necessary provide a war weapon of exceptional power.

These three purposes can now be reckoned as in part technically feasible. The present book is concerned with the technical basis of the realization of this first stage of rocket flight.

Any travel technique generally, and hence rocketry in particular, must be concerned with all three basic demands on a means of travel, namely performance, economy, and reliability.

*In cosmonauts' plans this is a vehicle that revolves around the Earth outside the sensible atmosphere with a speed such that the weight is balanced by the centripetal force. The space station would serve as starting point for flights to even greater heights.

Rocketry is in the very earliest stage of development. For the present, economy and reliability must take second place to performance in our demands on it. /2

For this reason I consider mainly the principles of performance in rocket flight, which are primary at present and in respect of the ultimate purpose, namely the emplacement in orbit of a space station.

Aspects of rocket flight that should become very much more important than in ordinary propeller aircraft are flight speed, ceiling height, and range.

The mechanical basis for flight performance is provided by the forces exerted on the vehicle.

The external forces occurring in rocket flight are as for ordinary propeller aircraft, namely drive, air, weight, and inertial forces.

The quantitative relationships between these are considerably altered, of course.

This is especially so for drive and air forces, so these are considered in particular detail in two of the three main sections of this book.

There is little new to be said about the gravitational attraction of the Earth, and the inertial forces are a consequence of the other forces; these will be dealt with in the treatment of flight performance in the third section.

This third section deals further with the calculation of response of the rocket vehicle to the forces and with the result in the form of the flight path.

These discussions of performance show, amongst other things, that:

Rocket vehicles for the first experiments can be built on the basis of the theoretical knowledge and available techniques, extension to ranges of up to about five thousand kilometers between stops being feasible. These long-range flights take the rocket vehicle to a path at a height of about fifty kilometers in the stratosphere. Further, the rocket vehicle would attain in these long-range flights a maximum flight speed of about 4000 m/sec and an average cruising speed of up to about 1000 m/sec.

These values represent upper limits and may be subject to modification, on account of the uncertainty of many assumptions made in the calculation.

Other and technically equally possible assumptions would allow perhaps of even higher ceilings at the expense of range.

Considerably longer ranges or higher flight speeds appear hardly conceivable except in the light of essentially new discoveries, especially as regards propellants, or as a result of expenditures scarcely to be considered as economic.

Especially it would seem that attainment of orbital velocities in the upper levels of the atmosphere (and hence the escape to altitudes for space stations) is not for certain possible with techniques presently known. /3

The discovery of appropriate techniques is a problem for future development.

Performance presently attainable leads us to expect that rocket vehicles excel ordinary propeller aircraft by about a factor twenty as regards maximum speed and cruising speed, and by about a factor five as regards ceiling height.

The ranges between landings meanwhile remain comparable.

Constructional details are most conveniently ignored in all discussions, although any calculation of flight performance must naturally be based on a certain design of the rocket vehicle.

For this purpose we assume the form of currently standard aircraft.

The following performance calculations are then concerned with a rocket aircraft having a spindle-shaped fuselage bearing rigid free wings and the usual land or water undercarriage and controls. The single rocket nozzle is assumed to be at the rear of the fuselage.

The process of flight by a rocket aircraft is externally exactly the same as that of an ordinary aircraft.

To sum up, we may say that the difficulties to be overcome in rocket flight are not fundamental but rather merely ones of construction.

Constructional difficulties are nothing uncommon to the modern engineer, though.

The main theoretical design principles are dealt with in the following publications.

1. PROPULSIVE FORCES

Literature for Propulsive Forces Section

A. Books

- Gaedicke, Der gefahrlose Menschenflug (Safe Manned Flight). /4
Hephästos-Verlag, Hamburg, 1911.
- Pelterie, Considérations sur les résultats de l'allégement indéfini des moteurs. (Considerations of the Results of the Undefined Tractive Effort of Motors), Journal de physique, 1913.
- Ziolkowsky [Tsiolkovskiy], Erforschung der Welträume mittels Reaktionsschiffen (Exploration of Space by Reaction Spaceships). Kaluga-Leningrad, 1914.
- Goddard, A Method of Reaching Extreme Altitudes. Smithsonian Institute, Washington, 1919.
- Ziolkowsky [Tsiolkovskiy], Eine Rakete in den kosmischen Raum. (A Rocket in Space). I. Kaluga, 1924.
- Hohmann, Die Erreichbarkeit der Himmelskörper (The Attainability of Celestial Bodies) R. Oldenbourg, München, 1925.
- Oberth, Die Rakete zu den Planetenräumen (Rocket Into Interplanetary Space). R. Oldenbourg, München, 1928.
- Pelterie, L'exploration par fusées de la très haute atmosphère et la possibilité des voyages interplanétaires (Rocket Exploration of the Upper Atmosphere and the Possibility of Interplanetary Travel). Paris, 1927.
- Ley, Die Möglichkeit der Weltraumfahrt (The Possibility of Space Travel). Hachmeister und Thal, Leipzig, 1928.
- Ziolkowsky, Erste praktische Vorversuche mit Reaktionsraumschiffen (First Practical Preliminary Experiment With Reaction Spaceships). VI. Kaluga, 1928.

- Scherschefsky, Die Rakete für Fahrt und Flug (The Rocket for Travel and Flight). Volckmann, Berlin, 1929.
- Noordung, Das Problem der Befahrung des Weltraumes (The Problem of Space Navigation). R. C. Schmidt, Berlin, 1929.
- Oberth, Wege zur Raumschiffahrt (Ways to Space Flight). R. Oldenbourg, München, 1929.
- Rakete, Zeitschrift des Vereins für Raumschiffahrt. (Journal of Society for Space Flight) Breslau, 1927/29.
- Rynin, Weltraumfahrten, Träume, Legenden und Phantasien (Spaceflight: Dreams, Legends and Fantasies). Leningrad, 1928.
- Rynin, Die Raumschiffahrt in der zeitgenössischen Belletristik (Spaceflight in Contemporary Literature). Soikin Press, Leningrad, 1928.
- Kondratjuk [Kondrat'yuk], Die Eroberung der Planetenräume (The Conquest of Interplanetary Space). Novosibirsk, 1929.
- Perelmann, Weltraumfahrten (Astronautics). VI. Aufl. Moskau, 1929.
- Rynin, Theorie der Bewegung durch direkten Rückstoss (Theory of Direct-Reaction Movement). T. H., Leningrad, 1929.
- Ziolkowsky, Fernflug- und Mehrfachraketen (Long-Distance and Multiple Rockets). Kaluga, 1929.
- Rynin, Raketen und Vortriebsmittel direkter Reaktion (Rockets and Direct-Reaction Propellants). Soikin Press, Leningrad, 1929.
- Ziolkowsky, Ziele der Raumschiffahrt (Goals of Space Travel). Kaluga, 1929.
- Ziolkowsky, Den Sternfahrern (Travelers to the Stars). Kaluga, 1930.
- Ziolkowsky, Das neue Flugzeug (The New Airplane). Kaluga, 1930.
- Biermann, Weltraumschiffahrt (Space Travel). Bremen, 1931.
- Rynin, Sternnavigation, Zwischenplanetenverkehr (Astronautics and Interplanetary Travel). Acad. Sci. USSR Press, Leningrad, 1932.

B. Articles

These occur in the periodical literature and in books; ones in which only particular points are relevant are given in footnotes at the appropriate point. /5

Some recent journal articles having a generally relevant content are as follows:

Manigold, Der Vorstoss in den Weltraum (The Advance Into Space). ZFM Vol. II, 1927.

Iademann, Zum Raketenproblem (On the Rocket Problem). ZFM Vol. 8, 1927.

Semper, Die Rakete (The Rocket). ZFM Vol. 14, 1928.

Lippisch, Raketenversuche mit Flugzeugen und Flugzeugmodellen (Rocket Experiments With Aircraft and Aircraft Models). ZFM Vol. 12, 1928.

Senftleben, Zur Mechanik der Weltraumraketen (Mechanics of Space Rockets). ZFM Vol. 14, 1928.

Senftleben, Zur Frage der Wirtschaftlichkeit des Raketenantriebes für irdische Fahrzeuge (On the Problem of the Economy of Rocket Drive for Terrestrial Vehicles). ZFM Vol. 16, 1928.

Lorenz, Die Möglichkeit der Weltraumfahrt (The Possibility of Space Travel). ZVDI, 1927.

Hamel, Über eine mit dem Problem der Rakete zusammenhängende Aufgabe der Variationsrechnung (On a Problem of Variational Calculus Relating to the Rocket Problem). A. F. angew. Math. u. Mech., 1927.

Lorenz, Der Raketenflug in der Stratosphäre (Rocket Flight in the Stratosphere). Jahrbuch der WGL 1928.

Schrenk-Schiller, Die Rakete als Kraftmaschine (The Rocket as a Power Engine). DVL-Bericht 24, 1928.

Lorenz, Die Ausführbarkeit der Weltraumfahrt (The Feasibility of Space Travel). Jahrbuch d. WGL 1928.

Everling-Iademann, Verkehrstechn (Transportation Engineering Weekly). Woche, 1929.

Dallwitz-Wegner, Über Raketenpropeller und die Unmöglichkeit der Weltraumschiffahrt mittels Raketenschiffen (The Rocket Propeller and the Impossibility of Space Travel by Means of Rocket Ships). Autotechnik, 1929.

Oestrich, Die Aussichten des Strahlantriebes für Flugzeuge unter besonderer Berücksichtigung des Abgas-Strahlantriebes (Prospects for Jet Propulsion of Aircraft, Especially for Exhaust Gas - Jet Propulsion). Jahrbuch d. DVL, 1931.

Crocco, Iperaviazione e Superaviazione (Hypersonic and Supersonic Flight). Rivista Aeronautica Bd. 7, 1931.

MEANINGS OF THE PRINCIPAL AND REGULARLY USED SYMBOLS [UNITS]
IN THE PROPULSIVE FORCES SECTION

$p_0, T_0, \gamma_0, \rho_0, a_0$	Pressure*, temperature, unit weight, density, and speed of sound for the stationary gases in the combustion chamber before burning [kg/m^2 , °, kg/m^3 , $\text{kg}\text{-sec}^2/\text{m}^4$, m/sec]
$p', T', \gamma', \rho', a'$	The same when the gas is flowing with the speed of sound (critical state)
p, T, γ, ρ, a	The above at any point in the nozzle
$p_m, T_m, \gamma_m, \rho_m, a_m$	The above at the mouth of the nozzle
$p_a, T_a, \gamma_a, \rho_a, a_a$	The above in the external space

*In accordance with the usual practice of aerodynamics and gas dynamics, the pressure reckoned per m^2 is denoted by a lower-case letter.

f'	Least cross section of the nozzle, in which the gas flows with the speed of sound a' [m^2]
f, f_m	Any cross section, mouth cross section of nozzle [m^2]
$V, V_0, V'V_m, V_a$	Specific volume of gas corresponding to the above [m^3/kg]
c, c_0, c', c_m, c_a	Flow speed corresponding to the above ($c_0 = c_a = 0, c' = a'$) [m/sec]
R	Gas constant in the equation of state $pV = RT$ for the gas [m/deg]
T	Absolute temperature [$^{\circ}$]
$g = 9.81 \text{ m/sec}^2$	Acceleration due to gravity [m/sec^2]
$n = c_p/c_v$	Exponent in $pV^n = \text{constant}$; ratio of the specific heats at constant pressure and constant volume [pure number]
μ	Outflow coefficient [pure number]
G	Amount of gas flowing through a cross section of the nozzle in a second [kg]
ν	Molecular weight of gas; in some places the kinematic viscosity [m^2/sec]
m	Exhaust mass $m = G/g$ [$kg^* = kg\text{-sec}^2/m$]
M	Mass of aircraft [kg^*]
kg^*	Mass kilogram ($1 \text{ kg}^* = 9.81 \text{ kg}$ near Earth)
$A = 1/427$	Mechanical equivalent of heat, value of one $m\text{-kg}$ in [$kcal$]

E

Usually the (thermochemical) energy content of unit weight of the unburnt rocket gas. In some places the heat value of the combustible material [kg-m/kg]

10. PROPULSIVE FORCES: GENERAL

Flight in the upper reaches of the stratosphere at very high speeds cannot employ the presently usual propulsion system with air-breathing engine and air-screw; even the solution of the supercharger and airscrew problems becomes impracticable for the air densities in question, while the weight of the power plant increases too greatly at the increasing flight speeds.

A flight speed of about 200 km/h near the ground corresponds at the following heights:

$$H = 0, 10, 20, 30, 40, \text{ and } 50 \text{ km}$$

to the following flight speeds respectively for unaltered lift pressure:

$$v = 200, 366, 750, 1780, 2650, \text{ and } 5280 \text{ km/h}$$

If we assume for convenience that ϵ (the aspect ratio) is constant at $1/10$, the drive power increases at least linearly with the speed, being for an all-up weight t as follows:

$$1/G = 74, 136, 278, 660, 985, \text{ and } 1970 \text{ PS/t.}$$

If now we make the most favorable assumption, namely that the motor power remains constant at all heights, and take 2PS as effective propeller power per kg of power plant, then the weight of the power plant as a fraction of the all-up weight is as follows:

3.7, 6.8, 13.9, 33, 49.2, and 98.4 %.

The residual part of the all-up weight is such that flight becomes absolutely impossible at a height of about 30 km (speed 1780 km/h) and uneconomic at about 20 km (750 km/h).

/7

In fact, the actual limits are lower, on account of the restricted possibilities of supercharging and propeller speed, as well as on account of the poor aerodynamic relationships at high speeds; it is scarcely to be envisaged that this can be altered by reduction in the plant weight per unit power.

For these and other reasons we have to consider rocket motors in order to attain the very high flight speeds desired, which in part demand new principles for efficient rocket power plants, whereby later heights in the outer atmosphere may be attained.

Much relevant theoretical work has been done as regards the mode of operation of rocket motors. Truly valuable information beyond the current position can come only from practical trials, so this section is concerned with a concise survey of the available theoretical knowledge, especially in respect of rocket flight within the atmosphere, which concerns us here; new features are introduced only on a few points.

Significant research is presently in progress on the topics dealt with in section 1 at the Technical Research Institute of the Technical University, Vienna. It is probable that various essentially new evidence on propulsive forces will be available when this is concluded.

As regards machine design, the problem of the design of a rocket motor has a certain resemblance to that of a gas turbine.

In accordance with the usual classification we can distinguish the principal modes of operation of liquid-fueled rockets:

a) Explosion rockets without precompression of the mixture (the mixture consisting of a liquid or vaporized combustant and gaseous oxygen or air).

b) Explosion rockets with precompression of the mixture.

c) Explosion rockets with liquid propellants only (combustant and oxygen used both in liquid form).

d) Constant-pressure rockets with precompression of the mixture.

e) Constant-pressure rockets with liquid propellants.

Types a) and b) will not be considered, in view of the low efficiency, which is already known from the corresponding gas turbines.

Type d) is also ruled out for the purposes of flight, on account of the high power demand of the compressor. /8

There remain to be considered only explosion and constant-pressure rockets with liquid propellants, of which the first provide lower combustion-chamber temperatures and the second higher efficiencies.

Rockets driven by powder will also not be discussed, for reasons that will appear later.

11. THEORY OF ROCKET MOTORS: GENERAL

All powered vehicles traveling in liquid or gaseous media (ships, aircraft, and so on) derive their propulsive forces from the principle of reaction, the propulsive force arising from the reaction of the mass of the water or air projected backwards by the propeller, airscrew, paddles, oars, etc.

The true rocket drive to be considered here is different from this old principle only in so far as that the thrust

$$P \cdot dt = d(mc)$$

is provided not by the projection backwards of large masses at low speed but by the projection of relatively small masses of gas that (in the simplest case) are carried by the vehicle and that are ejected with high speeds to give the same thrust:

$$P \cdot dt = d(m_1 c_1).$$

The rocket principle derives from the theory of momentum, which states that the time variation of the momentum $J = mc$ is equal to the resultant of the external forces:

$$d(mc) / dt = P,$$

and further from Newton's principle of action and reaction, which states that the ejected mass m exerts a force P equal to that exerted by the ejecting body.

If a mass (gas, air, liquid, and so on) is ejected by means of any device (airscrew, propeller, paddle, oar, rocket, and so on) so that the momentum in time dt undergoes a change $d(mc)$, then the ejected mass exerts on the device a reaction force of magnitude

/9

$$P = d(mc) / dt,$$

which is equivalent to an external propulsive force.

The production of the ejection velocity in the body arises in almost all cases from the combustion of propellants. The speed c_{th} theoretically producible in a mass m by 1 kg of propellant of calorific value E is

$$c_{th} = \sqrt{2 E/m}$$

(from $E = mc_{th}^2/2$); m is quite generally the mass of the accelerated

body, which naturally can include the mass of the burned propellant under some circumstances, but for pure rockets the mass of the propellant is the only available mass.

This theoretical speed is valid for practical discussions (subject to correction for the internal efficiency of the motor) as well as for theoretical studies, but this is not very obvious with regard to rocket performance.

We therefore choose as basis for comparison the theoretical thrust

$$J_{th} = m \cdot c_{th} = \sqrt{2 E m},$$

which in every obvious form indicates the force that can be exerted back on the vehicle for 1 sec when 1 kg of the propellant is burnt and a mass m becomes available for ejection.

Figure 1 shows this theoretical thrust for the presently most convenient combustant (gasoline) amongst others as a function of the ejected mass m , the upper limit being the product from the combustion and ejection of 1 kg of C_8H_{18} with 3.50 kg of O_2 . In addition, the

figure gives the m corresponding to the power plant of an ordinary fast racing aircraft, which corresponds to the second limit to the m/J curve. The masses are even larger for slower aircraft. This shows clearly that the propulsion of large masses m with small speeds c provides greater drive from a fixed amount of propellant. The highest possible over-all efficiency is naturally of decisive importance. As we shall see in more detail later on, it is a basic feature of any reaction drive that the external efficiency of the entire drive is greatest when the ejection velocity is of the same order as the flight speed. This explains the high efficiency of airscrew propulsion at the usual speeds (see the curve for c in Fig. 1); the figure also enables us to establish the mass relationships involved in the flight speeds needed in true rocket flight. Further, it shows clearly that pure rocket drive is the one of choice for very high extraterrestrial speeds and that rocket drive differs from airscrew drive not as regards principle but merely as regards parameters.

On the other hand, any reaction drive (and especially rocket drive) differs from the drive of an ordinary land vehicle (railroad, automobile, etc) fundamentally in that in the latter a constant motor power L provides a drive force P related to the speed v in accordance with the basic mechanical equation

/10

/11

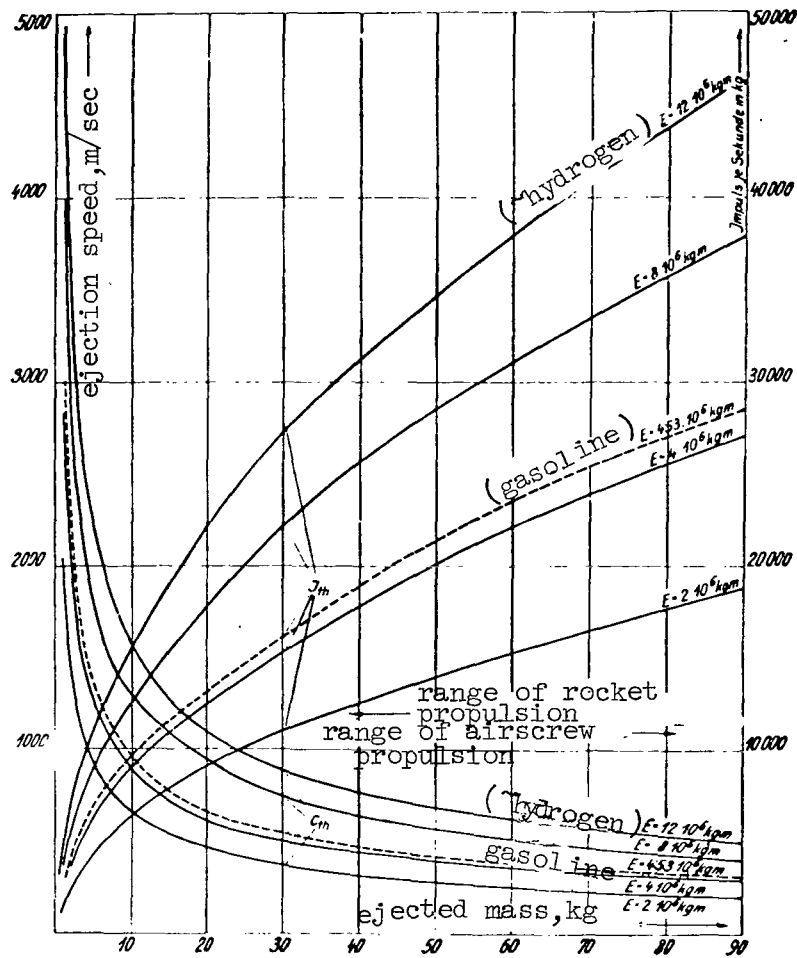
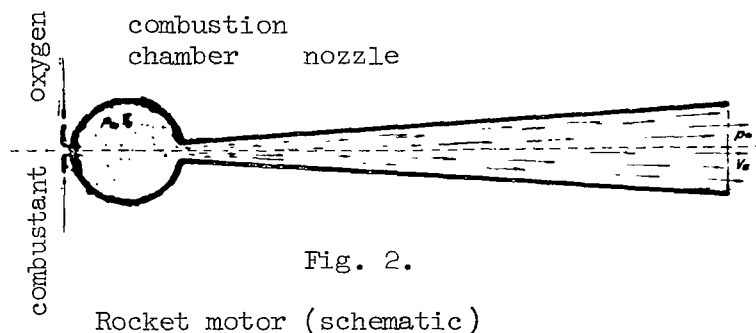


Fig. 1.

Relation of the theoretical ejection speed $c_{th} = (2E/m)^{1/2}$ and the theoretical thrust $J_{th} = (2Em)^{1/2}$ per kilogram of combustant (calorific value).

$$L = P \cdot v.$$

Reaction drive provides constant force as well as constant internal motor power, these being largely independent of the speed. The required derivation of the basic relation between these three quantities is to be found via a special relation between the motor power and the flight speed, the external efficiency being very greatly dependent on the flight speed. We shall have more to say on this later on, as it involves concepts entirely foreign to the normal drive of land vehicles.



In an aircraft the relations are: conversion of thermochemical energy of the combustant to a force from gas pressure in a cylinder on a piston, which is transferred via connecting rod, crank, and other connecting gearing to the airscrew, final conversion to an external propulsive force being by acceleration of the surrounding body of air.

Figure 2 shows in a simple fashion the design of a rocket motor, in which the pressure resulting from the thermochemical energy of propellant burnt in a cylinder accelerates the combustion products

directly, which flow out through an outlet in the cylinder.

The reaction force of the accelerated emerging gas provides the thrust directly.

A rocket motor consists essentially of a pressure (combustion) chamber (often called an oven in the rocket literature) and of an integral nozzle attached to this, which facilitates the outflow of the highly compressed gas in the combustion chamber.

The theory of rocket motors ('internal ballistics of rockets') is the next topic to be considered; this falls into two parts:

1. Combustion processes in the combustion chamber, in which the latent energy of the propellant is converted to pressure and heat energy of a gas mixture.

/12

2. Flow processes in the nozzle, in which the potential and heat energies made available in the combustion chamber are converted to kinetic energy as far as possible without loss and so are made usable.

In fact, the combustion and flow processes cannot be distinguished so sharply, for vigorous combustion continues in the narrow part of the nozzle, while part of the pressure energy is of course converted to motion in the combustion chamber itself before the nozzle is reached.

The processes whereby the combustant and the gas containing oxygen are introduced are of no interest here, although they are vital to the actual construction.

All the arguments present here, especially those concerning speed, energy, momentum, and so on, are conducted in a coordinate system linked to the rocket, which means that the state of motion of the rocket itself is immaterial.

111. Processes in the Combustion Chamber

The task of the combustion chamber is to convert the latent thermochemical energy of the propellant into pressure and heat energy of a gas mixture. The processes involved have much in common with the corresponding processes in an explosion motor, so it would be idle at the present stage of development of rocket motors to enter into skull-cracking detail over much that has not yet been finally elucidated for the explosion motor. This is more so over the basic questions of ignition, constant pressure as against variable pressure, and so on. The latter circumstance determines,

for example, whether the propellant and oxygen carrier must be introduced into the combustion chamber against the full steady combustion-chamber pressure (which is possible only for the liquid state) or whether the combustion-chamber pressure may be reduced periodically in a variable-pressure motor to facilitate the injection of propellant in the region of minimum pressure. In the latter case the propellant could perhaps be injected in gaseous form (fresh gas).

The pressure and temperature in the combustion chamber are kept as low as possible, to minimize heat losses and constructional difficulties. In particular, only the pressure required to produce the theoretical exit velocity of the gas is necessary. We equate the maximum exit velocity derived later on*, $c_{\max} = \sqrt{2gp_0 V_0^{\kappa/(\kappa-1)}}$,

/13

to the theoretical exit velocity $c_{th} = \sqrt{2gE}$ to get for the pressure required the simple expression

$$p_0 = \frac{\kappa - 1}{\kappa} \frac{E}{V_0},$$

which is also derivable on the basis of ideal gas expansion at constant volume. Here by p_0 is to be understood the final pressure

producible in the combustion chamber from the total energy content

E of a kg of gas. The initial energy (that corresponding to the pressure and temperature of the injected propellant or fresh gas) and also latent heats of evaporation are neglected. On the other hand, the energy needed for the injection must be taken from pumps themselves powered by the thermochemical energy of the propellant. The combustion causes the pressure increase p_0 , part of the energy being tapped off

* see p. /23.

to inject the propellant, which is at normal pressure in the tank.

The final pressure is dependent on the nature of the gas (n) and especially on the gas density in the combustion chamber; it increases with the latter for a given energy content E . The amount m of gas needed per second to provide a specified sustained thrust $J = mc$ for a given maximum attainable c is provided by a moderate combustion-chamber pressure p_0 . On the other hand, it may happen

that on technical grounds the maximum permissible pressure p_0 and the chamber capacity V_{cham} are already specified, in which case the weight of gas that can be introduced into the chamber is

$$G = \frac{p_0 V_{\text{cham}}^n}{(n - 1)E}.$$

The size of the chamber itself is of no theoretical importance and can be determined only on other grounds.

The rise in gas temperature behaves somewhat as does the rise in pressure and can be derived approximately from the following relation on the assumption of normal pressure and temperature relationships, provided that the low latent heats of evaporation are negligible:

$$T_0 = 0.03 p_0.$$

If these temperatures lie in the region of appreciable dissociation of the combustant, it is to be expected that n will become variable and that the full heat energy E will not in fact be available as gas pressure and gas temperature, especially since the last part of the combustion occurs in the nozzle.

112. Processes in the Nozzle

The purpose of the nozzle is to convert the energy made available in the form of gas pressure and elevated gas temperature in the oven into kinetic energy of the outflowing gas with the least possible loss and so to make it directly usable.

This purpose has been completely fulfilled if

$$c = c_{th} = \sqrt{2 E/m}$$

Any cooling or expansion of the gas in the state of exit is generally of only minor significance, so we need not consider more closely any possible further recovery of energy. In fact, the highest exit speeds reached are rather lower, on account of unavoidable losses.

1121. Nozzle Processes on the Assumption of Ideal Gases

Flow processes of gases in nozzles for the most part cannot be calculated in accordance with the laws of hydrodynamics.

Classical hydrodynamics assumes that the fluids are inviscid and incompressible.

The relationships derived on these assumptions for the behavior of fluids do not agree in many respects with actual relationships observed in nature.

Only by assuming viscosity in certain parts of a moved fluid can we obtain practical calculation results. Here incompressibility of the fluid for the moment still remains assured.

Liquids differ from gases in that the first alter in volume in response to external pressure only to a relatively very small extent, whereas Boyle's law ($pV = \text{constant}$) applies to gases.

This means that the compressibility may with every justification be neglected in relation to the motion of liquids. But for gases also the volume changes are frequently so small that it is permissible to neglect them (conventional aerodynamics). In this case the equations of motion are the same as those for liquids.

If the ratio of the pressure q of the flow becomes rather larger in relation to the elastic modulus E of the medium, the volume changes may come to have an important influence on the flow and so must be taken into account. This leads us to an extension of aerodynamics to the case in which the flowing medium is

compressible, namely gas dynamics, the science of the motion of gaseous bodies.

In place of the relations named one uses in practice the ratio of the flow speed v [m/sec] to the speed of sound a , v/a being known as the Mach number.

In practice, gases can be taken as incompressible up to speeds of about $v = 0.2a$; allowance for the compressibility must be made at greater flow speeds, and the flow must be examined by reference to the laws of gas dynamics rather than those of hydrodynamics.

The field of gas dynamics also includes steady motions of liquids such that the flow speed is comparable with the speed of sound, which practically never occurs (e.g., $a = 1400$ m/sec for water).

On the other hand, flow processes in gases in response to a force distribution such as to produce appreciable pressure differences belong to the field of meteorology, while nonstationary processes of motion involving large volume changes belong to the field of acoustics.

Gas dynamics has acquired technical importance particularly in the following fields in turn:

Ballistics, steam turbines, airscrew design, design of fast vehicles (especially racing aircraft and racing automobiles), and finally plans for rocket flight.

Gas dynamics in rocketry is of importance for the deduction of flow relations of the propellant gases in the nozzle of the rocket motor and for the establishment of external airflow relations for the vehicle.

For this reason we shall enter into more detail over the principles of gas dynamics, which serve extensively as principles for further discussion of rocket-flight technology, especially aerodynamic forces.

We disregard the viscosity of the gas at first in the subsequent treatment and deal with it, in so far as it is of importance in relation to boundary-layer processes, in the section on aerodynamic forces.

We also disregard the thermal conductivity in any form by virtue of the rapidity of changes in the gas-dynamic state, and so we assume that volume and pressure changes consequent on temperature equalization caused by conduction and radiation are negligible. Appreciable deviations from these assumptions should appear only in the spatially extremely narrow boundary-layer slow flows, especially at the outer wall of the vehicle.

Changes in the basic properties of the gases must strictly be considered in relation to propellant gas flow and to very high rocket velocities; these arise from absorption and release of energy in the flowing gas as a consequence of dissociation effects in the very hot gas. These special relationships are considered in a specialized section.

This leaves us with the compressibility of gases to be considered in detail first.

Any change in pressure produces a consequent change in volume of the gas, and any change of volume equally involves a related change of temperature. Thermodynamics* provides the following principles to describe these relationships:

The first law of thermodynamics (equivalence of heat and work); it states the law of conservation of energy for processes involving heat phenomena:

$$1 \text{ kcal} = 427 \text{ mkg}; \quad A = 1/427 \quad (1)$$

The total energy E in kg-m per unit weight of a body (liquid, vapor, gas) consists of:

The internal energy (heat content at constant volume) in kcal:

$$U = c_v T = Q - A \int p \, dV \text{ (heat equation)} \quad (2)$$

(in which Q is the heat produced in the change of state in kcal);

The external work (to overcome the external pressure) in kgm:

$$L = \int p \, dV, \quad (3)$$

*See, for example: H. Mache, Einführung in die Theorie der Wärme (Introduction to the Theory of Heat), Berlin, 1921; Schüle, Technische Thermodynamik (Technical Thermodynamics), Berlin, 1923, Hütte I, 26 ed. p. 508 and ff.

the pressure energy*

$$L_p = \int V \, d p \quad (4)$$

(external work and pressure energy together give the expansion energy

$$L + L_p = p V, \quad (5)$$

The kinetic energy $v^2/2g$ and
The potential energy h .

$$E = U/A + \int p \, d V + \int V \, d p + v^2/2g + h \quad (\text{thermodynamics energy equation}) \quad (6)$$

The total energy of a body at rest in a space free from gravity is called the enthalpy J (heat content at constant pressure, in kcal):

$$J = c_p T = U + A p V \quad (7)$$

The heat equation then allows us to put for the changes in

*Or "technical work" (Zerkowitz: *Thermodynamik der Turbomaschinen* (Thermodynamics of Turbines), 1912).

state of a gas at rest that

$$A \cdot \Delta E = \Delta J = Q + A \int V dp \quad (8)$$

By Δ is always meant the finite change of a quantity as a result of change in state.

The energy equation enables us to put for gas-dynamics purposes that

$$A (v_2^2 - v_1^2) / 2g + \Delta J = Q \text{ (gas-dynamics energy equation)} \quad (9)$$

The second law of thermodynamics, which implies that no periodically acting machine of any kind can persistently produce mechanical work while cooling a heat source, itself otherwise alters nothing.

In a reversible change of state (i.e., in steady or equilibrium processes) the available energy is

$$dQ = T dS, \quad (10)$$

in which the entropy $S = \int dQ/T$ is a formal parameter for the state

of the body; this can be calculated from the other parameters of the state, namely p , V , T , U , and J , via the heat equation. The sum of the entropies of all the bodies involved remains constant in a reversible process; the sum of the entropies increases in an irreversible process (e.g., throttling, inelastic collisions, friction, heat conduction, etc). The entropy of an isolated system can never decrease.

The equation of state completely defines the state of a body in

terms of two state parameters, and all other parameters are calculable from these two. The most important equation of state is that containing p , V , and T ; this cannot in general be expressed analytically and so is given as a diagram of state, such as J-S (Mollier) diagram or a T-S diagram.

The relation for the special case of an ideal gas, which is valid as a limit, is

$$p V = R T \text{ (gas equation)} \quad (11)$$

and this will be assumed in the arguments below; here R is the gas constant (29.27 under normal conditions for air, or 19.27 for carbon dioxide).

The specific heats are related by

$$c_p - c_v = A R \quad (12)$$

without relation to the temperature; c_p and c_v increase with temperature, but their ratio

$$\kappa = c_p / c_v \quad (13)$$

is constant for monatomic gases ($\kappa = 1.666$), is almost constant for diatomic ones ($\kappa = 1.40$), and is rather more dependent on temperature for polyatomic ones.

The enthalpy of a gas of state pV in a gravity-free space is

$$J = \frac{\kappa}{\kappa - 1} A p V$$

from (7), (12), and (11).

The gas equation and the two laws of thermodynamics enable one to calculate numerous special changes of state for an ideal gas, e.g. (with subscripts 1 and 2 denoting the respective quantities before and after the change):

Volume constant ($V = \text{const.}$, Δp , ΔT):

$$\begin{aligned} p_1/p_2 &= T_1/T_2 \text{ from (11);} & Q &= \Delta U = c_v \Delta T \text{ from (2) =} \\ & & &= AV\Delta p/(\kappa - 1) \text{ from (11) and (12)} \end{aligned}$$

$$L = 0 \text{ from (3);} \quad \Delta J = \kappa AV\Delta p/(\kappa - 1) \text{ from (8).}$$

Pressure constant ($p = \text{const.}$, ΔT , ΔV), as for burning in the combustion chamber:

$$\begin{aligned} V_1/V_2 &= T_1/T_2 \text{ from (11)} & Q &= \Delta J = c_p \Delta T \text{ from (8) =} \\ & & &= Ap\Delta V\kappa/(\kappa - 1) \text{ from (14)} \end{aligned}$$

$$\begin{aligned} L &= p\Delta V \text{ from (3)} & \Delta J &= Q = Ap\Delta V\kappa/(\kappa - 1) \\ & & &\text{from (8).} \end{aligned}$$

Temperature constant (isotherm, $T = \text{const.}$, ΔV , Δp), as in isothermal flow in a nozzle:

$$\begin{aligned} p_1/p_2 &= V_2/V_1 \text{ from (11)} & Q &= ATR \ln (V_2/V_1) \text{ from (2)} \\ & & &\text{and (11)} \end{aligned}$$

$$pV = \text{constant from (11)}$$

$$L = Q/A \text{ from (2) and (3)}$$

$$\Delta U = 0 \text{ from (2)}$$

$$\Delta J = 0 \text{ from (7).}$$

Entropy constant (adiabatic, $S = \text{const.}$, Δp , ΔV , ΔT), as in adiabatic flow in a nozzle:

$$p V^\kappa = \text{const}; \quad p_1/p_2 = (V_2/V_1)^\kappa \text{ (from 2, 6, 12, 11)}$$

$$TV^{\kappa-1} = \text{const}; \quad T_1/T_2 = (V_2/V_1)^{\kappa-1} \text{ (from 2, 6, 12, 11)}$$

$$\frac{T}{p}^{(1-\kappa)/\kappa} = \text{const}; \quad T_1/T_2 = (p_2/p_1)^{(1-\kappa)/\kappa} \text{ (from 2, 6, 12, 11)}$$

$$Q = 0 \text{ (from 10)}$$

$$L = \Delta U/A \text{ (from 2, 3)}$$

$$= p_1 V_1 / (\kappa - 1) \cdot (1 - T_2/T_1) =$$

$$= p_1 V_1 / (\kappa - 1) \cdot [1 - (p_2/p_1)^{(\kappa-1)/\kappa}] \text{ (from 2, 3, 12, 11)}$$

$$\Delta J = - \kappa A L \text{ (from 8).}$$

Table 1 gives the evaluation of this relation for adiabatic expansion.

Usually gas-dynamic flows are such that the gas neither gains nor loses heat during the motion, so $Q = 0$. This gives us then an adiabatic nozzle flow.

The gas-dynamic energy equation

TABLE 1

p_1/p_2	$\kappa = 1.4$		$\kappa = 1.3$	
	v_2/v_1	T_1/T_2	v_2/v_1	T_1/T_2
1.1	1.070	1.028	1.076	1.022
1.5	1.336	1.123	1.366	1.098
2.0	1.641	1.219	1.705	1.174
5	3.156	1.583	3.449	1.449
10	5.188	1.931	5.885	1.701
15	6.919	2.168	8.030	1.868
20	8.498	2.354	10.02	1.996
25	9.967	2.508	11.89	2.102
30	11.35	2.643	13.68	2.192
35	12.67	2.761	15.41	2.272
40	13.94	2.869	17.07	2.343
50	16.34	3.055	20.24	2.467
70	20.75	3.366	26.31	2.667
100	26.85	3.733	34.6	2.898
150	35.90	4.188	47.0	3.163
200	43.96	4.550	58.9	3.405
300	58.6	5.094	80.0	3.733
500	84.7	5.889	119	4.188
1000	139	7.178	203	4.921

$$A (v^2 - v_0^2)/2g + \Delta J = Q$$

and the relation for adiabatic changes of state

$$Q = 0,$$

$$\Delta J = - A p_1 V_1 \frac{n}{n-1} [1 - (p_2/p_1)^{(n-1)/n}]$$

give the flow speed c at any point in the nozzle as a function of the gas pressure p at that point and of the initial state p_0, V_0 ,

$v = 0$ in the combustion chamber:

$$\begin{aligned} c &= \sqrt{2 g \frac{n}{n-1} p_0 V_0 [1 - (p/p_0)^{(n-1)/n}]} = \\ &= \sqrt{\frac{2n}{n-1} p_0 / \rho_0 \cdot [1 - (p/p_0)^{(n-1)/n}]} . \end{aligned}$$

The condition of continuity for the constancy of the motion:

/20

$$G = f_1 v_1 / V_1 = f_2 v_2 / V_2$$

gives the cross section f at any point required to take the amount of gas G flowing out per second:

$$f = G / \sqrt{2g \frac{n}{n-1} p_0 / V_0} \cdot [(p/p_0)^{2/n} - (p/p_0)^{(n+1)/n}] .$$

The evaluation of this equation gives a minimum in the flow cross section at the 'critical' pressure p' :

$$p'/p_0 = \left(\frac{2}{n+1} \right)^{n/(n-1)}$$

(e.g., for a diatomic gas such as air, with $n = 1.4$ and $p' = 0.528 p_0$)
this being

$$f' = G / \left(\frac{2}{n+1} \right)^{1/(n-1)} \sqrt{2g \frac{n}{n+1} p_0 / V_0} .$$

A nozzle, of correct shape therefore narrows first to the throat cross section f' and then gradually widens to a cross section f_m at the exit (Laval nozzle, Fig. 3).

The proper basis of this shape of nozzle is the fact that in the equation of continuity

$$f/G = V/v$$

V increases less rapidly than v as p decreases, so V/v becomes smaller until the critical pressure is reached. Past this point V increases more rapidly than v , so V/v (and hence f/G) becomes larger as p decreases, which implies a divergent nozzle.

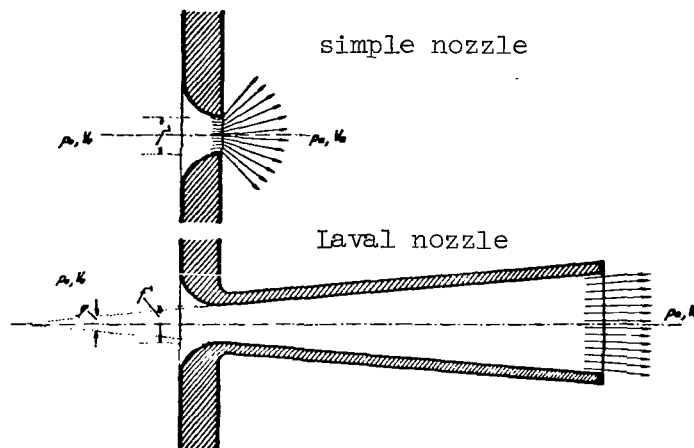


Fig. 3.

Shapes of nozzles.

Only when the exit pressure p_m is larger than the critical pressure p' is there no need for a divergent nozzle in order to produce the highest possible exit velocity. This case is without significance for applications in rocketry.

Provided that the pressure falls below the critical pressure at the narrowest point in the nozzle, the flow speed and nozzle pressure remain independent of the external pressure p_a , so the exit

pressure is in general not equal to the external pressure p_a but is rather solely dependent on the state of the gas in the combustion

chamber and on the cross section ratio f/f'_m for the nozzle.

We have $p_m < p_a$ if the gas pressure in the nozzle falls below the external pressure, so shock waves enter the interior of the nozzle, which raise the gas pressure to the external pressure. These shock waves involve energy losses.

If the excess-pressure ratio is too high (too high a combustion-chamber pressure or too low an external pressure), the external pressure is not attained in the nozzle, so the exit pressure remains larger than the external pressure and the jet spreads out after leaving the exit of the nozzle, which causes appreciable loss of axial momentum on account of the highly divergent bodies of gas. This case has been considered all too little, especially for nozzles having no widening section (Fig. 3).

This means that a given nozzle can operate in the theoretically most favorable fashion only with a specified gas (or n) and for a prescribed pressure ratio p_0/p_a .

The practical relationships in rocketry are such that the rocket always lies at the rear of a fuselage or the like, so the external pressure with respect to the nozzle is governed by the speed. At rest, or at the start, the pressure is therefore the atmospheric pressure; at first it falls slowly as the speed rises (by a few percent before the speed of sound is reached), but thereafter very rapidly, the equivalent of an absolute vacuum being reached a little above twice the speed of sound (see the section on aerodynamic forces). The rocket motor works practically entirely against an external pressure $p_a = 0$, since an appreciable part of the flight (as we

shall see) occurs at speeds well above the speed of sound, and even in part at speeds above the exit velocity of the rocket gas at height, where even the undisturbed external air pressure is only a very small fraction of the ground-level air pressure. This would demand an infinitely large nozzle exit cross section. In fact, the reasonably feasible dimensions force us to accept a certain loss of thrust from the escaping jet.

The pressure must fall steadily from p_0 to p_m , which implies
for the shape of the nozzle that

$$f_x/f_m = c_m/c_x \cdot V_x/V_m = \sqrt{\frac{n-1}{n+1} \left(\frac{2}{n+1} \right)^{2/(n-1)}}$$

$$\sqrt{(p_x/p_0)^{2/\kappa} - (p_x/p_0)^{(\kappa+1)/\kappa}}.$$

The flow speed at the narrowest part of the nozzle, and hence the critical pressure p' , are given by

$$a' = \sqrt{2g \frac{\kappa}{\kappa+1} p_0 v_0} = \sqrt{\frac{2\kappa}{\kappa+1} p_0 / \rho_0} = \sqrt{\frac{2\kappa}{\kappa+1} g R T_0}.$$

This speed is the speed of sound (critical speed) in the critical state of the gas, as we may see by inserting the relation for adiabatic changes of state in the basic equation for the speed of sound in any body, $a = \sqrt{dp/d\rho}$.

The temperature falls as the pressure falls (as the velocity rises) in accordance with

$$T/T_0 = 1 - (\kappa - 1)/(\kappa + 1) \cdot c^2/a'^2 = 1 - (\kappa - 1)/2 \cdot c^2/a_0^2;$$

$$\Delta T = T_0 (\kappa - 1)/2 \cdot c^2/a_0^2$$

and so the critical speed of sound is less than a_0 , the speed of sound for the gas at rest:

$$a_0 = \sqrt{\kappa g R T_0} = \sqrt{\kappa p_0 / \rho_0}.$$

In general, the speed of sound is comparable with the speed c of the flowing gas*

$$a = \sqrt{a_0^2 - c^2 (\kappa - 1)/2}; \quad a' = \sqrt{2/(\kappa + 1)} \sqrt{a^2 + c^2 (\kappa - 1)/2}.$$

The gas can at most attain its own speed of sound at the mouth of a prismatic or convergent nozzle, most of the pressure and heat energies remaining as such unused.

Higher (ultrasonic) speeds occur outside the nozzle (in the escaping jet) or in the divergent part of a Laval nozzle.

For $\kappa = 1$ we have, for example, for diatomic gases that $a' = 3.38 \sqrt{R T_0}$, so for cold air ($R = 29.27$ and $T_0 = 273^\circ$) we have $a' = 302$ m/sec, while for hydrogen ($R = 421.6$ and $T_0 = 273^\circ$) we have $a' = 1150$ m/sec.

Correspondingly higher speeds of sound occur at higher temperatures.

The speed reached on escape into free space is governed by the ratio of cross sections f_m/f' (expansion ratio) for the nozzle but is

independent of the external pressure p_a . This expansion ratio can be

/23

made such as to allow the gas to expand to any arbitrary external pressure. The jet becomes detached from the wall of the nozzle if the latter widens too rapidly, so the angle φ of the cone in Fig. 3 must be kept appropriately small (roughly $\varphi < 10^\circ$). This implies very long nozzles for high degrees of expansion. Friction naturally plays a larger part in such nozzles than it does in simple mouths.

*Hütte I, 26 ed., p. 415.

The limiting velocity on expansion to zero pressure is given by

$$c_{\max} = \sqrt{\frac{2}{\kappa - 1} \frac{\kappa}{\rho_0} p_0}.$$

The ratios of this maximum attainable flow speed to the speeds of sound are

$$c_{\max} : a' : a_0 = \sqrt{(\kappa + 1)/(\kappa - 1)} : 1 : \sqrt{(\kappa + 1)/2}$$

$$\text{or for } \kappa = 1.3 \dots\dots\dots c_{\max} : a' : a_0 = 2.77 : 1 : 1.073$$

$$\text{for } \kappa = 1.4 \dots\dots\dots c_{\max} : a' : a_0 = 2.45 : 1 : 1.095.$$

The theoretical exit velocity given by the heat value E and the exhaust mass m is

$$c_{\text{th}} = \sqrt{2 E/m}.$$

which is related to the pressure and temperature relations in the exhaust gas that occur in the gas used before combustion. If this gas could be expanded or cooled in this initial state (in the limit to zero pressure and to the absolute zero of temperature), considerable amounts of energy could be made available for conversion into exit velocity, in addition to the calorific value of the gas. Under these conditions one could therefore exceed the theoretical

exit velocity c_{th} , as the formula for c_{max} shows. Then p_0 contains the initial heat and pressure energies, apart from the calorific-value energy. In practice, unlimited expansion is restricted by change in the state of aggregation on extensive cooling and by excessive effects of friction, quite apart from constructional difficulties.

Figure 4 shows the state parameters of the exit gas as functions of the cross-section ratio for Laval nozzles and for diatomic gases.

Now we must consider the nozzle efficiency η_d , which indicates how much of the total internal energy of the gas is converted to kinetic energy. It is correspondingly defined as

$$\eta_d = c^2 / c_{max}^2.$$

Dissociation processes occur in the combustion chamber with the propellants of very high energy yield used in rocketry (see section 1123), which give rise to afterburning of the products during the flow in the nozzle. This adds heat to the flowing gas, so the flow should no longer be treated as adiabatic. The scale of the dissociation is primarily related to the gas temperature, which remains approximately constant during the flow of the dissociated gas.

As a rough approximation we may take the flow of the dissociated gas as isothermal. The assumption is only approximately true, on account of the simultaneous (although fairly slight) dependence of the degree of dissociation on the gas pressure.

Isothermal gas flow. The gas-dynamics energy equation

$$A(v^2 - v_0^2)/2g + \Delta J = Q$$

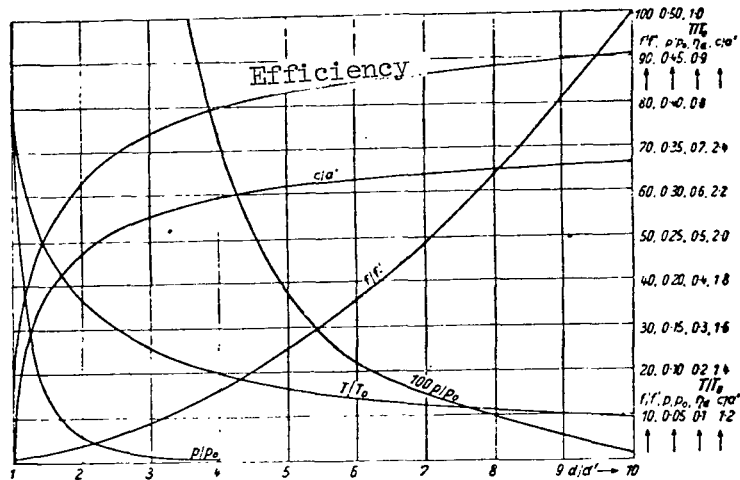


Fig. 4.

Gas parameters in the nozzle for adiabatic flow
and $\gamma = 1.4$

and the relation for isothermal changes of state in a gas

$$Q = A R T \ln p_1/p_2$$

$$\Delta J = 0$$

give us the flow speed c at any point in the nozzle as a function of the gas pressure p at that point and of the initial state $p_0, V_0, v_0 = 0$ in the combustion chamber:

$$c = \sqrt{2g R T_0 \ln p_0 / p}.$$

The actual gas flow resembles an isothermal one more closely than an adiabatic one only so long as the enthalpy of the gas is less than E (the energy available from the calorific value), i.e. as long as the burning consequent on dissociation has not gone to completion. This burning during the flow provides an appreciable additional heat Q to maintain the isothermal temperature. Complete reversal of the dissociation causes this source of heat to vanish; Q becomes zero, and the gas flow becomes adiabatic. The isothermal nozzle flows to be considered here therefore occur particularly in the initial zone of the nozzle.

The condition of continuity for the stability of the motion gives

$$G = f_1 v_1 / V_1 = f_2 v_2 / V_2$$

from which it follows that the cross-section f needed at any point to accommodate the outflowing gas G is

$$f = G / \sqrt{2g p_0 / V_0} \cdot (p/p_0)^2 \ln p_0 / p.$$

Evaluation of this equation gives a minimum in the cross-section at the critical pressure p :

$$p'/p_0 = 0.607$$

so

$$f' = G/0.429 \sqrt{2 g p_0/V_0}.$$

The statements made regarding adiabatic flow apply also here with regard to the nozzle shape. Isothermal flow requires also that the nozzle should first narrow to a throat of cross-section f' and then widen out.

The flow speed at the narrowest point, and hence at the critical pressure p' , is

$$a' = \sqrt{g p_0 V_0} = \sqrt{g R T_0} = \sqrt{p_0/\rho_0}.$$

This speed represents the isothermal speed of sound in the critical state. The temperature is independent of the pressure and gas speed in isothermal flow, so this applies also to the other speeds of sound, which means that here $a' = a_0$, as is readily seen by substituting the relations for the isothermal change of state of a gas into

the basic equation $a = \sqrt{dp/d\rho}$ for the speed of sound.

The critical and, in general, the isothermal flow speeds are somewhat smaller than the corresponding adiabatic speeds under otherwise identical conditions, which implies that the cross-sections appropriate to a given amount of gas are slightly greater than those for adiabatic flow. Table 5 compares the individual quantities for adiabatic and isothermal flows.

Table 2 gives the parameters appearing in these relations for various gases.

The combustion of hydrogen in excess gives rise to an exit gas consisting of a mixture of superheated water vapor with hydrogen. The ratio of the specific heats is then between 1.3 and 1.4; Table 3 gives values calculated by Oberth for various ratios (by weight) of oxygen to hydrogen.

Table 4 gives some of the principal functions of n required in the evaluation of the relations between the gas-state parameters

TABLE 2

Gas	Symbol	Number of atoms	gas constant	Ratio of specific heats
Helium	He	1	212.00	1.66
Argon	Ar	1	21.26	1.66
air	-	-	29.27	1.40
water in gas state	H ₂ O	3	47.20	1.30
oxygen	O	2	26.50	1.40
nitrogen	N	2	30.26	1.40
hydrogen	H	2	420.60	1.407
nitric oxide	NO	2	28.26	1.38
carbon monoxide	CO	2	30.29	1.40
hydrogen chloride	HCl	2	23.25	1.40
carbon dioxide	CO ₂	3	19.27	1.30
nitric oxide	N ₂ O	3	19.26	1.28
sulfur dioxide	SO ₂	3	13.24	1.25
Ammonia	NH ₃	4	49.79	1.29
Acetylene	C ₂ H ₂	4	32.59	1.24
Methyl chloride	CH ₃ Cl	5	16.80	1.28
Methane	CH ₄	5	52.90	1.31
ethylene	C ₂ H ₄	6	30.25	1.25
ethane	C ₂ H ₆	8	28.21	1.20

TABLE 3

O/H (weight)	0.8	0.9	1.0	1.1	1.2	1.3	1.4	1.5	1.6	1.7	1.8	1.9	5.33
$\kappa =$	1.400	1.398	1.396	1.394	1.393	1.391	1.389	1.388	1.386	1.385	1.384	1.383	1.33

for the nozzle.

Table 5 lists the relations between the state parameters for the gases flowing in a nozzle.

The above arguments on processes in nozzles have involved the assumption that ideal gases are concerned in the flow processes, whose motion is thus unaffected by friction on the one hand and by any changes of state apart from those governed by the gas equation:

$$p \cdot V = R \cdot T$$

Both assumptions are only partly complied with, and the resulting effects on the processes will now be briefly considered.

1122. Effects of Friction on Nozzle Processes

The loss of energy caused by friction require that the theoretical relation derived above for the efflux speed must be multiplied by a correction factor ϕ , while the value for the mass passing through must be multiplied by a factor μ , though both of these in general differ little from unity.

The relationships applicable to gases, saturated steam, and superheated steam for the flow speed, absolute temperature, and mass flow are then

TABLE 4

Functions of n	n	$1/n$	$1/(n-1)$	$(n-1)/n$	$\sqrt{(n+1)/2}$	$\sqrt{(n+1)/(n-1)}$	$\left(\frac{2}{n+1}\right)^{n/(n-1)}$
monatomic gases	1.67	0.600	1.5	0.4	1.155	2.000	0.487
-	1.5	0.667	2	0.333	1.118	2.236	0.512
diatomic gases	1.4	0.714	2.5	0.286	1.095	2.449	0.528
superheated steam	1.3	0.769	3.33	0.231	1.072	2.768	0.546
-	1.2	0.833	5	0.167	1.049	3.317	0.564

TABLE 5

47

Relations between parameters of state for gases flowing in a nozzle.

	Adiabatic flow	Isothermal flow
Relation of nozzle cross section to local pressure	$f/f' = 1/\left(\frac{n+1}{2}\right)^{1/(n-1)} (p/p_0)^{1/n} \sqrt{\frac{n+1}{n-1} \left[1 - (p/p_0)^{(n-1)/n}\right]}$	$f/f' = 0.429/\sqrt{(p/p_0)^2 \ln p_0/p}$
Flow speed of gas at any cross section	$c = \sqrt{2 g \frac{n}{n-1} p_0 V_0 \left[1 - (p/p_0)^{(n-1)/n}\right]}$	$c = \sqrt{2 g p_0 V_0 \ln p_0/p}$
Highest possible flow speed for expansion to zero external pressure	$c_{\max} = \sqrt{2 g \frac{n}{n-1} p_0 V_0}$	-
Flow speed of gas at narrowest point of nozzle	$a' = \sqrt{2 g \frac{n}{n+1} p_0 V_0} = \sqrt{\frac{2n}{n+1} p_0/\rho_0}$	$a' = \sqrt{g p_0 V_0} = \sqrt{p_0/\rho_0}$
Speed of sound in gas at any cross section	$a = \sqrt{a_0^2 - c^2 (n-1)/2}$	$a = a'$

[Table 5 cont'd. next page]

[Table 5 continued]

Speed of sound in gas at rest in state in combustion chamber	$a_0 = \sqrt{n g p_0 V_0} = \sqrt{n p_0 / \rho_0}$	$a_0 = a'$
Ratio of flow speed to critical speed of sound	$c/a' = \sqrt{\frac{n+1}{n-1} \left[1 - (p/p_0)^{(n-1)/n} \right]}$	$c/a' = \sqrt{2 \ln p_0 / p}$
Ratio of flow speed to speed of sound at rest	$c/a_0 = \sqrt{\frac{2}{n-1} \left[1 - (p/p_0)^{(n-1)/n} \right]}$	$c/a_0 = \sqrt{2 \ln p_0 / p}$
Absolute temperature of gas	$T/T_0 = (p/p_0)^{(n-1)/n} = 1 - (n-1)/2 \cdot v^2/a_0^2$	$T/T_0 = 1$
Critical pressure	$p'/p_0 = \left(\frac{2}{n+1} \right)^{n/(n-1)}$	$p'/p_0 = 0.607$
Weight of gas flowing through any cross section per second	$G = \gamma' a' f' = \left(\frac{2}{n+1} \right)^{1/(n-1)} f' \sqrt{2g \frac{n}{n+1} p_0 / V_0}$	$G = \gamma' a' f' = 0.607 f' \sqrt{g p_0 / V_0}$

$$c = \varphi \sqrt{2g \frac{\kappa}{\kappa - 1} p_0 V_0 [1 - (p/p_0)^{(\kappa - 1)/\kappa}]}$$

$$T = T_0 \{1 - \varphi^2 [1 - (p/p_0)^{(\kappa - 1)/\kappa}]\}$$

$$G = f\mu \sqrt{2g \frac{\kappa}{\kappa - 1} \frac{p_0}{V_0} [(p/p_0)^{2/\kappa} - (p/p_0)^{(\kappa + 1)/\kappa}]}$$

Zeuner has found that the correction factor φ can be dispensed with if κ is replaced by a somewhat smaller efflux parameter m , in which case the corresponding formulas become*

$$c = \sqrt{2g \frac{\kappa}{\kappa - 1} p_0 V_0 [1 - (p/p_0)^{(m - 1)/m}]}$$

$$G = f \sqrt{2g \frac{\kappa}{\kappa - 1} \frac{p_0}{V_0} [(p/p_0)^{2/m} - (p/p_0)^{(m + 1)/m}]}$$

$$p'/p = \left(\frac{2}{m + 1}\right)^{(m/(m - 1))}$$

*E.g., Hütte I, 26th ed., p. 552.

$$f/f = \left(\frac{m+1}{2}\right)^{1/(m-1)} (p/p_0)^{1/m} \sqrt{\frac{m+1}{m-1} [1 - (p/p_0)^{(m-1)/m}]} \text{ etc.}$$

The relation of m to φ is as follows:

/29

$$m = \kappa (1 + \xi) / (1 + \kappa \xi),$$

in which

$$\xi = 1/\varphi^2 - 1$$

It has been found that φ and μ are very little less than one for nozzles of good shape, being that

$$\mu = 0.97$$

$$\varphi = 0.98$$

The above relation gives m . The effects of friction mean that very long lengths of rocket nozzle with large cross sections could be acceptable, since the ratio of the frictional wall area to the amount of gas passing through would be smaller than in the experimental nozzles so far studied.

1123. Deviations from the Gas Equation

The rocket gases have been taken as ideal in the above (as obeying Boyle's and Charles's laws strictly), which therefore obey the equation of state for a perfect gas:

$$p \cdot V = R \cdot T$$

Real gases obey this law only as a limit, the behavior in general approximating the more closely to this the larger the specific volume, the lower the pressure, and the higher the temperature. On the other hand, fresh deviations become apparent at very high temperatures on account of onset of decomposition in the gas molecules, a point we shall return to later.

Real gases conform to the gas law very well within certain ranges around normal temperature. Table 6 shows the deviation of pV/RT from unity, and hence the deviation from the equation of state, for air and hydrogen.

If it becomes necessary to correct for these small deviations, use is made of the equations for an ideal gas as an approximation, but with somewhat altered values of κ .

Compression of a gas at a suitably low and constant temperature causes the gas to start to become liquid at the saturation pressure, which is governed solely by this temperature. Then further compression leaves not only the temperature but also the pressure constant; the gas laws become completely inapplicable in this region of saturated vapor. The liquefaction proceeds as the pressure rises until the gas is completely converted to a liquid.

For this region (saturated vapor) one uses entropy tables instead of equations of state, which have become inapplicable. These deviations from the gas equation occurring at low temperatures have no real importance for the conditions arising in rockets.

The gas equation ceases to be valid when the compression of the gas is so great that the forces of cohesion between the molecules become appreciable, on account of the small separation between the molecules. The gas equation is then replaced by another equation of state, such as Van der Waals's equation. Figure 4a (the diagram of state) shows that the lower limiting region for the gas equation

/30

/31

TABLE 6

p =		0	20	40	60	80	100 kg/cm ²
Air	0	1	0.9895	0.9812	0.9751	0.9714	0.9699
	+ 100	1	1.0027	1.0065	1.0112	1.0169	1.0235
	+ 200	1	1.0064	1.0132	1.0205	1.0282	1.0364
Hydrogen	Temperature in °C						
	- 150	1	1.0073	1.0180	1.0319	1.0492	1.0699
	- 50	1	1.0130	1.0265	1.0404	1.0548	1.0697
	0	1	1.0122	1.0245	1.0370	1.0496	1.0625
	+ 50	1	1.0111	1.0222	1.0332	1.0443	1.0554
	+ 200	1	1.0078	1.0157	1.0235	1.0313	1.0392

at very high pressures is set by the critical isotherm, and at pressures of the order of the critical pressure also by the general area

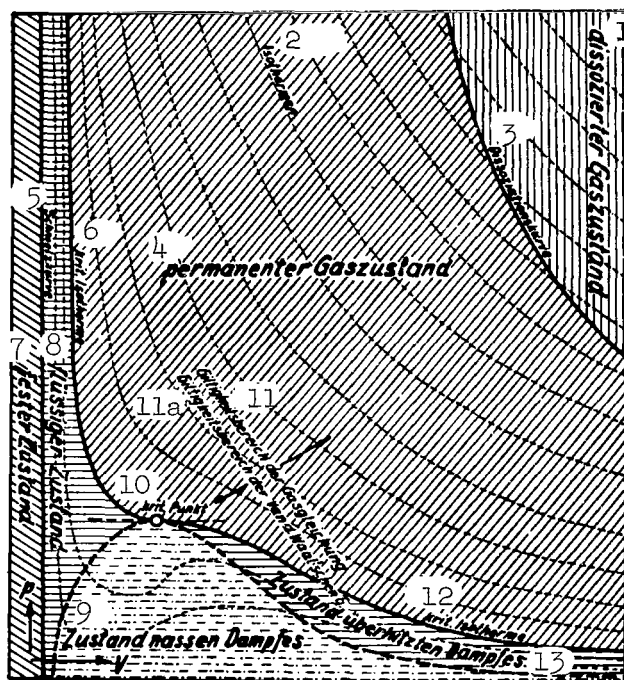


Fig. 4a.

Phase diagram of a substance showing the limiting regions of validity of the gas equation for variation in the state of the substance. 1) Dissociated gas; 2) isotherms; 3) dissociation curve; 4) state of permanent gas; 5) melting point; 6) critical isotherm; 7) solid; 8) liquid; 9) saturated vapor; 10) critical point; 11) region of validity of gas equation; 11a) region of validity of Van der Waals's equation; 12) critical isotherm; 13) superheated vapor.

around the critical point; and in the latter case the gas equation applies considerably above the critical isotherm, as we may see from the deviation of the shapes of the isotherms from rectangular hyperbolas. At lower pressures (larger specific volumes V) the gas equation again applies, by virtue of what was said earlier; this applies also at temperatures below the critical, so the equation is in part usable in the vapor region.

The exhaust gases of a rocket can attain critical or sub-critical temperatures in the nature of things only as the result of extraordinarily continued expansion and so can occur only at very low pressures and very large specific volumes; this means that there is no danger of leaving the region of validity of the gas equation in the direction of low temperatures.

Table 7 gives the critical temperatures T_k (absolute) and critical pressures p_k for some gases that may be involved in rocket motors.

TABLE 7

	T_k^0	$p_k \text{ kg/cm}^2$
H_2O	647	225
CO_2	304	75
O_2	154	51
CO	134	36
N_2	126	34.6
H_2	33	13.2

Dissociation processes in the gas are far more important than the deviations from the gas laws considered above, since they can lead to very substantial deviations from the laws of ideal gases under the conditions arising in rockets*. The energy of a rocket motor is derived by thermochemical means via exothermic reactions (largely oxidation of fuels). Chemical combination of hydrogen and carbon atoms contained in the fuel with oxygen gives the corresponding oxides (CO_2 and H_2O), which makes available the heat energy corresponding

/32

to the calorific value of the propellants; this appears in the form of raised gas pressures and gas temperatures in the combustion chamber. As soon as the temperature reaches certain high levels, the combination of the C and H atoms with the O atoms becomes no longer unrestrictedly stable, and the CO_2 and H_2O already formed dissociate into

the corresponding ions or atoms, whereby the energy already freed is rebound, so the gas pressure and gas temperature tend to fall, until a state of equilibrium is finally attained.

Dissociation thus represents decomposition (here in response to high temperatures) of chemical compounds into their constituent parts; then H_2O in accordance with the equation $2\text{H}_2\text{O} = 2\text{H}_2 + \text{O}_2$ absorbs 1.362,000 kg-m per kg of H_2O , and in general the energy absorbed

is precisely that made available in the forward (association) process, which leads to changes in pressure, temperature, speed, and so on.

The eventual dissociation of the rocket gas can thus alter in a decisive fashion the pressure and temperature already produced as well as the flow speeds.

The dissociation increases with the temperature; the product molecules (e.g., H_2O) decompose ultimately not only to molecules of

the initial substances (to $\text{H} + \text{OH}$ above 2500°) but rather these further decompose into atoms (to $\text{H} + \text{H} + \text{O}$ above 4500°), and by about 5000° there is no molecular state left.

The kinetic theory of gases explains these facts very simply:

*Schüle, Technische Thermodynamik (Technical Thermodynamics), vol. 2, Springer 1923; Schüle, New Tables and Diagrams for Technical Combustion Gases and Their Components for 0 to 4000°C . Springer 1929.

the molecular speeds increase with temperature and finally result in such vigorous collisions between molecules moving in opposite directions that these are broken up if the intramolecular forces are not sufficiently large.

This explanation also shows that the pressure affects the dissociation processes, the effect being that dissociation is reduced by increased pressure, because the dissociated gas has a tendency to take up a larger volume.

The proportion of the total gas dissociated has been measured as a percentage for various gases at given pressure and temperature. Table 8 gives values for some gases of interest here*.

The highest possible exhaust speeds are needed for space travel and rocket flight, but these are subject to very large alterations on account of dissociation resulting from the high temperatures set up by combustion, e.g. those from hydrogen and oxygen in amounts corresponding to the laws of stoichiometry.

/33

TABLE 8

Proportion Dissociated in Percent

Temperature in °C	H ₂ O		CO ₂	
	p = 10 kg/cm ²	p = 1 kg/cm ²	p = 10 kg/cm ²	p = 1 kg/cm ²
1000	$1.39 \cdot 10^{-5}$	$3.00 \cdot 10^{-5}$	$7.31 \cdot 10^{-6}$	$1.58 \cdot 10^{-5}$
1500	$1.03 \cdot 10^{-2}$	$2.21 \cdot 10^{-2}$	$1.88 \cdot 10^{-2}$	$4.06 \cdot 10^{-2}$
2000	0.273	0.588	0.818	1.77
2500	1.98	3.98	7.08	15.80

*See also: Bjerrum, Z. phys. Chemie, 1912; I. Langmuir, The dissociation of hydrogen into atoms, calculation of the degree of dissociation, etc. J. Amer. Chem. Soc., vol. 37; K. Wohl, The dissociation of hydrogen. Zeits. Elektrotechn., 1924.

Dissociation can be reduced:

1. By the use of appropriately high pressure (which causes the temperature to rise somewhat as a result).

2. By alteration of the gas temperature, as by the choice of fuels of suitably low combustion temperature or by the addition of incombustible gases. If instead one adds excess gas (e.g., hydrogen), the specific weight of the exhaust gas falls, and the exit speed for a fixed pressure energy in the combustion chamber increases as the square root of the reciprocal of the density reduction.

3. A very powerful means of suppressing dissociation is available in the shape of the nozzle itself; since this leads to the conversion of pressure and temperature to velocity, the preceding dissociation is reversed in the nozzle, and the bound energy is once more made available. In particular, for the low external pressures ($p_a/p_0 < 1/100$) around a moving rocket the gas temperature in the nozzle is given by

$$T = T_0 \left\{ 1 - \varphi^2 \left[1 - (p/p_0)^{\frac{n-1}{n}} \right] \right\}$$

as so low at the mouth that there is no fear of dissociation at the mouth if this is suitably large.

The gas-kinetic molecular speed is somewhat over 2000 m/sec at the temperature at which the dissociation of water vapor starts to increase rapidly (about 3000°), which in the view of certain investigators represents the highest speed that an undissociated gas can reach. Temperatures of over 3000° are therefore impossible for water vapor, since this completely decomposes at higher temperatures.

Pirquet has divided the burning process of explosion mixture into 10 equal intervals of 10% and has found that after the sixth interval (past 60% combustion) the limiting temperature $T = 3000^\circ$ is reached, at which point about 12% of the already burned gas is dissociated. To suppress further rise in temperature, the expansion must start in this region, so the last 4 intervals in the burning

occur in the nozzle rather than in the combustion chamber. The expansion in the nozzle must be such as to keep the temperature constant in the course of the rest of the combustion. The velocity rises during this isothermal process to 3100 m/sec, apart from frictional losses. Following the completion of this final burning (isothermal expansion) there is the adiabatic process, in which the temperature falls rapidly, so the moderate existing dissociation is reversed and the exit flow speed is further appreciably increased.

In the same place* Pirquet deduced from Zeuner's formula an approximate formula for the ideal exit flow speed c_i in adiabatic expansion as

$$c_i \approx 129 \sqrt{\frac{T_0}{v}} \sqrt{1 - \frac{T_a}{T_0}} \sqrt{\frac{n}{n-1}}$$

or

$$c_{\max} \approx 129 \sqrt{\frac{n}{n-1}} \sqrt{\frac{T}{v}}$$

for expansion to zero pressure, which is valid for not too high temperatures; here T_0 is the temperature at the start of the adiabatic expansion and T_a is that at the end.

Pirquet used this formula to calculate the effects of gases mixed with the combustants to suppress dissociation; he found the following, in particular, for the combustion of explosion mixture with excess hydrogen:

*Ley, Die Möglichkeit der Weltraumfahrt (The Possibility of Space Flight).

For $4 \text{ H}_2 + \text{O}_2 = 2 \text{ H}_2\text{O} + 2 \text{ H}_2$; $v = 10$, $T_0 \approx 3100^\circ$

$$T_a = 1500^\circ; \kappa = 1.24; c_i = 3600 \text{ m/sec}$$

$$T_a = 1000^\circ; \kappa = 1.25; c_i = 4100 \text{ m/sec.}$$

For $6 \text{ H}_2 + \text{O}_2 = 2 \text{ H}_2\text{O} + 4 \text{ H}_2$; $v = 7.3$; $T_0 \approx 2600^\circ$

$$T_a = 1500^\circ; \kappa = 1.26; c_i = 3800 \text{ m/sec}$$

$$T_a = 1000^\circ; \kappa = 1.27; c_i = 4300 \text{ m/sec.}$$

These speeds exceed the molecular speed for the initial state (about 2100 m/sec for H_2O at 3000°), which Pirquet explained in

general as caused by drawing on the velocity of molecular rotation, which he gave as approximately

$$c_r \approx 102 \sqrt{\frac{\kappa}{\kappa - 1}} \sqrt{\frac{T}{v}}.$$

Similarly, he took the molecular translational speed as

$$c_m \approx 78 \sqrt{\frac{\kappa}{\kappa - 1}} \sqrt{\frac{T}{v}}.$$

Then the kinetic energy of the outflowing gas is equal to the calorific value E less the kinetic energy arising from the molecular speed in the end state (after the expansion), so

$$c_1^2 = 2g E - c_{ra}^2 - c_{ma}^2$$

(the molecular speed of the unburnt gas being treated as negligible). Combustion of pure explosion mixture followed by adiabatic expansion and cooling to 1500° absolute then gives, for example,

$$c_1 = 4690 \text{ m/sec.}$$

In the special case of the burning of explosion mixture with excess hydrogen, the high molecular speed of the hydrogen ($c_m = 5650$

m/sec at $T = 3000^\circ$) provides a further explanation for the high exit speed. In addition, we know from the basic relationships of gas dynamics that a gas flows into a vacuum with a speed higher than that corresponding to its translational molecular velocity.

The gas laws are inapplicable in the dissociation region only if the dissociation is partial, as in the case of saturated vapors; they are applicable (naturally, with new gas constants) if the dissociation is complete.

A more precise treatment of isothermal gas flow in the nozzle for a partly dissociated combustion gas is rather troublesome, because the variation in the specific heats with temperature

is important and the dissociation temperature itself is exceptionally dependent on the pressure in the gas flow, the variation moreover being that the dissociation temperature becomes smaller as the mouth of the nozzle is approached. There is also a critical gas speed in isothermal gas flow, which implies an initial narrowing of the nozzle followed by widening, with a throat at the narrowest cross section.

Dissociation has the effect that the efficiency of a given nozzle is less than that for an adiabatic flow free from dissociation, since the isothermal gas flow takes up a very large part of the nozzle, so the cooling consequent on adiabatic expansion is less.

/36

For example, dissociation vanishes for gasoline-oxygen combustion in stoichiometric proportions when the pressure falls to about $1/400$ of that in the combustion chamber, which corresponds to a ratio of nozzle diameters of about $d/d' = 9$.

Higher combustion-chamber pressures and a narrower throat relative to a dissociation-free flow are therefore needed for a given area at the mouth of the nozzle and for a specified thrust if the nozzle efficiency is to be the same.

1124. Shape of the Nozzle

The following principles are of especial importance for the shape of the nozzle:

1. The shape of the cross section should be circular, on the grounds of strength and also as presenting the least surface for a given cross section.
2. The extent of the cross section at the throat is governed by the pressure in the combustion chamber and the thrust required for the rocket. See 141 on the derivation of this.
3. The detailed shape of the nozzle between combustion chamber and throat is not important provided that it is carefully rounded off and that an entirely stable gas flow is set up.
4. The actual nozzle past the throat must comply with the condition of continuity given in 1121.
5. The taper angle of this nozzle should not be larger than about 7° to 10° in order to prevent detachment of the flow from

the wall and hence losses in the flow.

6. Since the rocket motor in a rocket vehicle works virtually against zero external pressure, the expansion ratio, and hence the ratio of diameters for the nozzle, should be made as large as constructional considerations allow in order to cool the gas as far as practicable and thus to keep thermal and thrust losses small. The requirement of point 5 above together with large mouth areas leads to very long nozzles.

7. The nozzle should also be very long in order to allow the combustion process, which persists in the nozzle, time to go to completion.

8. The shape must be chosen with allowance for the various states that the gas has in the nozzle, especially as regards the initial dissociation processes (which see). The theoretically highest work extraction corresponds to a saturated vapor, liquid, or even solid state of the exhaust material at the end of the nozzle, but this is virtually unattainable within the nozzle. In addition, this state is undesirable, on account of the high frictional losses involved. /37

9. To find the parameters of state of the rocket gas as functions of the nozzle cross section, see Fig. 4 in Section 1121.

Moreover, until further experience is gained, a nozzle having the shape of a perfect truncated cone between its mouth and throat would be expedient, if only owing to the simplicity of its construction.

12. Efficiency of a Rocket Motor: General

The efficiency relations of a pure rocket power plant are qualitatively very similar to those of an ordinary aircraft power plant, and so are the other internal relations of a rocket drive with respect to those of other reaction drives.

We may take the internal efficiency of a rocket as the analog of the efficiency of an internal-combustion engine, including the transfer up to the airscrew; this is based on the practical imperfection of the system and represents the ratio of the energy available from the motor to the thermochemical energy of the fuel used.

The airscrew in an aircraft itself operates with a certain external efficiency, which is governed by the mode of conversion of the internal forces into external propelling forces via the reaction principle and which is affected only to a very slight extent by inadequacies of construction; its most important feature is the dependence on the flight speed. This dependence in the case of the airscrew in an aircraft is that the efficiency as regards the power required by the aircraft is zero when the screw is operating with the aircraft at rest; it increases with the flight speed and reaches its maximum (0.7 to 0.8) at a flight speed governed by the shape of the screw, falling at higher speeds.

The much disputed efficiency of a rocket power plant can be treated from this point of view without encountering essentially new conceptual difficulties.

121. Internal Efficiency

The most important causes of the relatively low internal efficiency (η_i of about 0.25 to 0.30) of an ordinary aircraft power plant are as follows:

1. Chemical losses consequent on imperfect burning as a result of poor mixing, lack of oxygen, and so on.
2. Flushing losses: loss of fuel consequent on flushing with fresh gas along with the chemical losses, about 5% of the total chemical energy brought in by the fuel).
3. Loss from the finite time of combustion, which is not restricted to the point of top dead center.
4. Heat losses via the walls (cooling).
5. Losses from gas leaks around pistons and valves (along with 3 and 4, totalling about 15%).
6. Flow losses during mass-exchange processes in pipelines, mixing equipment, pumps, and so on (about 5%).
7. Frictional losses in the entire power plant: pistons, cranks, shafts, valves, gearing, pumps, ignition equipment, and so

on (about 15%).

8. Exhaust losses from incomplete expansion and cooling of the exhaust gas (about 30%).

The total loss is then about 70%, which explains the η_1 of 0.30.

The next point of interest is to determine how far these sources of loss are to be expected for rocket motors also.

Items 1 and 2 occur to a similar extent in rocket motors. These should become the least for well-mixed continuous-burning powder rockets and the greatest for intermittently operating liquid-fueled rockets; they can probably be restricted at suitable combustion-chamber pressures and temperatures. The longest possible nozzle is required to provide complete burning, since the combustion processes extend to the nozzle.

Items, 3, 4, and 5, on the other hand, are not to be expected for rocket motors; this is so from the nature of the engine in the case of 3 and 5. According to Oberth, the cooling losses (item 4) are quite negligible, on the one hand on account of the size of the combustion chamber and of the flow speed, and on the other on account of the use of the propellant itself as coolant, which returns the lost heat to the motor and so makes the heat loss to the coolant minimal or even negative. The last arises on account of the heating of the surface of the aircraft by the airflow or, in any case where liquified gases are used as fuel and coolant, on account of abstraction of heat from the surroundings.

Item 6 does not occur for powder rockets, but for liquid-fueled rockets it is to be expected to much the same extent as for piston engines. Especial relative importance attaches to frictional losses for the gas flow at the nozzle walls, which are particularly prominent in tests on models with small nozzles. These losses become smaller as the nozzle dimensions increase, for the frictional areas increase as the square of the linear dimensions, whereas the gas volumes increase as the cube; they are vanishingly small for large nozzles of proper shape.

Item 7 is restricted to losses in pumps and any ignition equipment; it should be appreciably smaller than for piston engines.

In all, sources 1 to 7 can scarcely account for more than 10 to 15% loss in a rocket motor with liquid fuels.

Item 8 is as highly important for rockets as it is for piston engines, so the internal efficiency is dominated by the pressure by the pressure and temperature of the exhaust gas, i.e., by the energy not converted to kinetic form (see Fig. 4 for the nozzle efficiency).

Tsiolkovskiy estimated a final temperature of 300 to 600°C for an O-H rocket having complete combustion, good cooling, and appropriate length of the exhaust nozzle. The upper limit to the internal temperature is then governed by the dissociation temperature. A maximum taper angle of about 10° for the nozzle makes the expansion (and hence the final temperature) purely a question of nozzle length. Table 9 gives the loss with the exhaust gas as percent of the chemical energy supplied as a function of exhaust gas temperature (after Tsiolkovskiy). This loss may be expected to be least for escape into a vacuum. The size of the mouth of the nozzle is restricted by constructional considerations, so the loss can scarcely be reckoned to be less than 15 to 20% in the range of speeds corresponding to the present rocket vehicle. Then a very rough approximation for the over-all internal efficiency is $\eta_i =$

= 0.70, which is about twice the efficiency of a piston engine.

TABLE 9

Expansion V_m/V_0	Loss in %
1	100
6	50
36	25
216	13
1 300	5
7 800	3
46 800	1.6

The internal efficiency of the rocket motor has a purely mechanical relation to the ratio of the kinetic energy of the exhaust gas to the calorific value E available from the propellant for the acceleration of this gas, so by use of the theoretical exhaust velocity e_{th} we can put that

$$\eta_i = \frac{m c^2/2}{m c_{th}^2/2} = (c/c_{th})^2.$$

The internal efficiency is therefore most clearly defined as the square of the ratio of the actual exhaust velocity to the theoretical velocity.

The actual internal efficiency has been the subject of some measurements, in particular those of Goddard and Oberth. The measurements of the American Goddard relate to intermittently operating powder-rocket models with steel nozzles of good finish having an angle of 8° , a length of 164.5 mm, and a maximum diameter of 26 mm; he considered that considerably more favorable values would be obtained from nozzles of larger size. Table 10 gives some results from Goddard's measurements.

TABLE 10

Propellant	$E, 10^6$ kg-m/kg	c_{th}' , m/sec	Meas. exit speed c , m/sec	η_i , int. eff.
Simple powder from Coston ship's rocket	0.232	2350	1600	0.465
No. 3 pistol powder, Dupont Powder Co.	0.415	2860	2290	0.644
"Infallible" smokeless powder, Hercules Powder Co.	0.528	3220	2434	0.572

These values are very close to that from ballistic tests, which gave a mean internal efficiency of a shot as $\eta_i = 2/3$.

The theoretically predicted improvement in the internal efficiency for escape into a vacuum was also reached in Goddard's experiments.

Oberth's measurements relate to continuously functioning explosion-mixture model rockets, which were conducted on only a rather small budget. Table 11 gives Oberth's results.

TABLE 11

Propellant	$E, 10^6$ kg-m/kg	c_{th}' , m/sec	Meas. exit speed c , m/sec	η_i , int. eff.
Gasoline-air mixture	-	2190	1700	0.604
1 part hydro- gen gas + 2 parts oxygen gas	1.03	4470	4000	0.803

From this we may conclude that the over-all internal efficiency of a good rocket motor, including auxiliary equipment, should be $\eta_i = 0.70$ or so. This will be taken as basis for the subsequent treatment.

/41

122. External Efficiency: General

The nature of the external efficiency will become clear from

the following approach.

Kinetic energy (and hence power) is governed by the speed, but speeds are always relative to the speed of some specified point of reference, so this discussion of power requires that all powers must always be referred to the same point, e.g., the stationary starting point, in order to avoid arriving at valueless false conclusions.

Consider a rocket vehicle moving with a constant speed v (reckoned from the stationary starting point) against air resistance, the thrust P provided by the rocket thus being equal to the air resistance W . The motor works uniformly: it consumes in a specified time the same amount of propellant, whose calorific value is E , and thereby produces a constant amount m of gas, which escapes with a fixed speed c . The power reckoned with respect to a fixed point in the moving rocket is then constant, being $E\eta_1 =$

$$= mc^2/2.$$

The equivalent power reckoned from the fixed starting point and available from the propellant in motion with respect to that point is (see below):

$$L = mc^2/2 + mv^2/2.$$

The fixed rocket thrust P is

$$P = m \cdot c/t,$$

in which t is the time needed for the mass m to escape.

The transport power L' needed to maintain the motion of a body against a resistance W at a constant speed v is given by the principles of mechanics as

$$L' = W \cdot v.$$

Since $W = P$ for steady flight, $mc = L'/v$, and

$$L' = m \cdot c \cdot v.$$

In general, transport power L' and motor power L are not equal, since they are opposed via $W = P$. The ratio of these is defined as the external efficiency η_a , since the difference between the two

/42

powers must represent the lost energy:

$$\eta_a = \frac{L'}{L} = \frac{m \cdot c \cdot v}{mc^2/2 + mv^2/2} = \frac{2v/c}{v^2/c^2 + 1}.$$

This gives us the external efficiency of a reaction drive as dependent on the flight speed, which is entirely foreign to land vehicles; this, as we have already noted, is peculiar to all other reaction drives, such as ships' screws, airscrews, and so on. The deeper significance of this is not of importance, since ships, aircraft, and so on move at constant speed during the major part of the time the drive is operating, so η_a remains practically constant,

as is usual for an efficiency. On the other hand, the flight speed of a rocket vehicle is extremely variable during a large part of the time of functioning of the motor, so the external efficiency of the drive is correspondingly variable.

This variability has a simple physical explanation: the energy consumed by the motor is used to give certain speeds on the one hand to the exhaust gas and on the other to the vehicle; that is, the energy is divided between the kinetic energy lost with the exhaust gas and the kinetic energy gained by the vehicle or the work done against the resistance. The ratio of these parts of the energy varies with the flight speed, and hence the external efficiency

does the same.

We now turn to some relations for the external efficiency in the most important basic states of flight for a rocket vehicle.

1221. External Efficiency for Flight in a Space Free from Gravity and Resistance

No drive power is needed to maintain a state of motion in a space free from gravity and resistance; but if a drive force does act on the vehicle, the motion is accelerated, and uniformly at that for fixed drive force per unit mass. The external efficiency is variable, on account of the varying flight speed.

Following Oberth and Noordung, the situation can be treated somewhat as follows:

The maximum efficiency is attained when the ejected masses have given up the largest possible fraction of their energy to the vehicle. The energy of motion of the gas flow plays the largest part in the energy after the corresponding cooling. If all the energies of motion (and hence the velocities) are reckoned from the state of motion of the starting point, the gas component will then have lost its kinetic energy to the largest extent if it is at rest with respect to the starting point, which means that the flight speed is equal to the exhaust speed. The external efficiency of the reaction process is then unity (100%), since theoretically there is no energy loss. Larger or smaller flight speeds leave the gas component with a part of that speed or part of the exhaust speed, so the associated energy of motion is lost as regards propulsion of the vehicle and the efficiency becomes smaller.

/43

The external efficiency is zero when the rocket is at rest, since the total energy of the gas is carried off. The external efficiency increases as the speed rises until the maximum of one is reached, at which v is equal to c ; the exhaust gases are left at rest behind the rocket, and all the energy is given up. The power apparently increases further at even higher v , but this is merely a result of the kinetic energy previously accumulated in the fuel. The efficiency actually falls, since the fuel does not give up all its energy on escape.

Unit mass of fuel in a moving vehicle can yield the following total energy:

$$L_1 = c^2/2 + v^2/2$$

in which $c^2/2$ is the available thermochemical energy and $v^2/2$ is the kinetic energy.

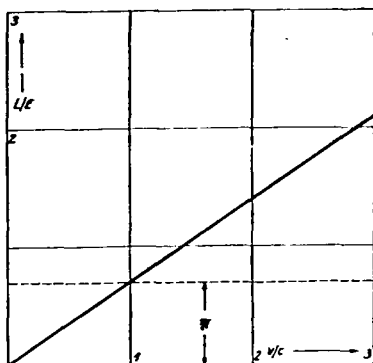


Fig. 5.

Ratio of the energy L received from the fuel to the calorific value E as a function of flight speed v .

The kinetic energy remaining in the gas after escape (apart from the heat energy already allowed for in η_1) is

$$L_2 = (v - c)^2/2.$$

The exhaust gas loses energy, which the rocket gains:

$$L = L_1 - L_2 = v \cdot c.$$

The energy gained thus increases linearly with the flight speed if $c = \text{constant}$; v and c have opposite senses. Fig. 5 shows the relation to the calorific value E of the fuel, which forms the basis of all arguments as to efficiency. Fig. 6 confirms that 1 kg of fuel can yield much more energy than corresponds to its calorific value, at the expense of its kinetic energy. A change of speed of c corresponds to very different changes in kinetic energy at different flight speeds.

/44

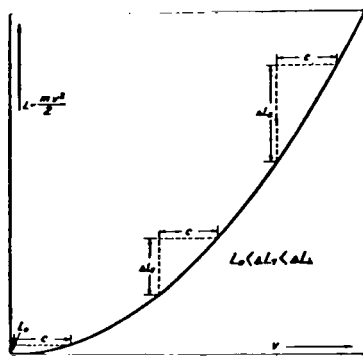


Fig. 6.

Loss of energy consequent
on a change of speed of c .

We define as the instantaneous external efficiency η_a that part of the total kinetic and thermal energy of the fuel which at a given instant is available to the rocket, so we have that

$$\eta_a = \frac{\text{extracted energy}}{\text{energy used}} = \frac{L_1 - L_2}{L_1} = \frac{v \cdot c}{c^2/2 + v^2/2} = \frac{2v/c}{v^2/c^2 + 1}.$$

Fig. 7 shows the behavior of this curve. The efficiency is over 0.8 for the range of speeds represented by $v/c = 0.5$ to $v/c = 2$, so it is in fact higher than that of an airscrew between very wide limits of speed. It approaches zero asymptotically at very high speeds.

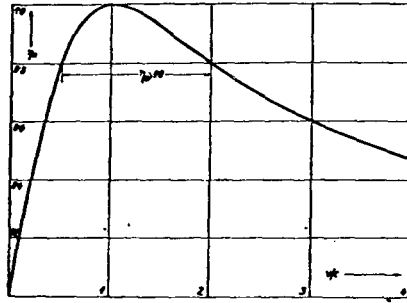


Fig. 7.

Instantaneous external efficiency of a rocket power plant.

Noordung has given rather different results on this point, which is to be ascribed to the use of a less precise definition of external efficiency. This he takes as the ratio of the increase in the kinetic energy of the remaining fuel plus vehicle to the thermochemical energy consumed in the fuel, which gives him negative efficiencies for $v/c > 2$, since the loss in mass of the vehicle via the exhaust at high flight speeds naturally results in a gain in the kinetic energy of the entire system less than the gain in the velocity. The exhaust process then in fact represents a loss of

energy by the vehicle in spite of the increase in flight speed, since part of the mass is lost, taking with it a certain kinetic energy. We may pass over the further consequences of this.

/45

Oberth's external efficiency (the one adopted above) has the disadvantage that the apparently high η_a found at very high speeds

is made available only at the expense of the previously accumulated kinetic energy of the fuel.

The motion of a vehicle in a space free from gravity and resistance is, as we have noted, an accelerated one if the motor is working; the flight speed as reckoned from the fixed starting point is then initially smaller than the exhaust speed, later becomes equal to the latter, and finally exceeds it. Consequently, the external efficiency is initially small, then increases till it reaches unity, and finally falls again.

The mean external efficiency $\eta_a^{(m)}$ for the acceleration period is of interest from the standpoint of economy.

This $\eta_a^{(m)}$ is that part of the energy available at the start of the motion which is present finally in the form of kinetic energy of the moving vehicle. The theorem relating to the center of gravity applies to uniformly accelerated motion in a space completely free from gravity and resistance:

$$c \cdot dm + m \cdot dv = 0,$$

in which dm denotes the mass ejected and dv denotes the change in speed of the residual mass m as a consequence of the exhaust process.

Integration of this equation with respect to m and v shows that the rocket changes from mass m_0 to mass m_1 during the acceleration up to v :

$$c (\ln m_0 - \ln m_1) = v$$

or

$$m_0/m_1 = e^{v/c},$$

which is the basic equation of rocket theory, from which the instantaneous speed of a rocket is calculable in terms of the loss in mass and the exhaust speed, subject to the not precisely correct assumptions as to the motion made in matters of rocket flight. It is assumed here that the rocket motor operates with a variable power such that the increase in speed of the continually lightening rocket during a fixed time is always the same. Then we have:

$$\begin{aligned}\eta_a^{(m)} &= \frac{\text{energy extracted}}{\text{energy expended}} = \\ &= \frac{\text{kinetic energy of final mass } m_1 \text{ at final speed } v_1}{\text{kinetic energy extractable from fuel}} = \\ &= \frac{m_1 v_1^2 / 2}{(m_0 - m_1) c^2 / 2} = \frac{m_1 v_1^2 / 2}{m_1 (e^{v_1/c} - 1) c^2 / 2} = \frac{(v_1/c)^2}{e^{v_1/c} - 1}.\end{aligned}$$

The mean external efficiency then has a maximum of $\eta_a^{(m)} =$
 $= 0.647$ for $v/c = 1.593$, past which point it falls. Fig. 8 shows
the behavior of $\eta_a^{(m)}$ as a function of the final speed; it is rela-
tively high for any final speed in practice available.

1222. External Efficiency for Flight against Gravity in a Space Free from Resistance

Drive power is needed to maintain the state of motion in a

gravitational field in a space free from resistance. A constant drive power then results in an acceleration of the vehicle different from that found for a field-free space. In particular, a constant thrust of appropriate magnitude operating directly against the gravitational field to balance out the acceleration produced by the field, the vehicle then behaving as though without thrust in a gravity-free space. In this case the constant drive power produces no increase in the energy of the vehicle, so the external efficiency is permanently zero. Any excess thrust, on the other hand, produces an effect such as would occur with a vehicle in a gravity-free space subject only to the excess thrust.

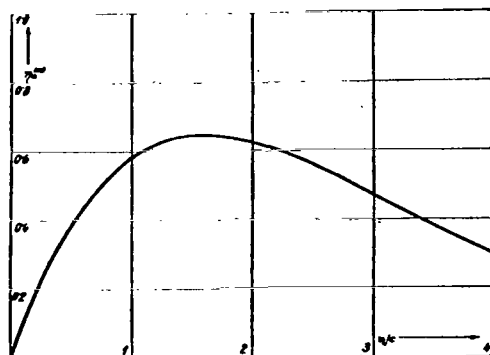


Fig. 8.

Mean external efficiency of a rocket power plant taken over a period of constant acceleration to a final speed v_1 .

The essential correctness of this last position is demonstrated by the following argument:

If the vehicle were suspended at rest in a gravitational field, only the rocket action opposing the gravitational force, then

each second the amount

$$m \cdot c/t = M \cdot g \cdot \cos \bar{\varphi}$$

must be used up, in which $g \cos \bar{\varphi}$ is the acceleration component of the gravitational field in the direction in question. The acceleration component at right angles to this we treat as brought to equilibrium by some other cause of no interest here, so we have no need to be concerned further with it.

/47

The energy converted by the rocket in this process

$$E = mc^2/2$$

is lost completely with the gas; the external efficiency of the process is zero. Now as above we imagine that the rocket action keeps the vehicle in equilibrium in the same way against the gravitational component, but in uniform motion from some cause instead of at rest, the constant velocity v being opposed to the component of the gravitational force. Again we have for each second

$$m \cdot c/t = M \cdot g \cdot \cos \bar{\varphi}.$$

On the other hand, the energy conversion now takes a somewhat different form. The energy available from the gas now consists of the

kinetic component $mv^2/2$ and the thermochemical component $mc^2/2$. The rocket gas after escape possesses kinetic energy

$$L_2 = \frac{m}{2} (v - c)^2.$$

The difference in energy is received by the vehicle:

$$L_1 - L_2 = mv^2/2 + mc^2/2 - m(v - c)^2/2 = + m \cdot c \cdot v.$$

The vehicle each second gains the following potential energy with respect to the gravitational field:

$$L_3 = M \cdot g \cdot \cos \bar{\varphi} \cdot v = + m \cdot c \cdot v.$$

The energy required to perform the work of lifting is in fact transferred from the gas to the vehicle, and the latter moves as though it were suspended in a space free from gravitational fields.

The relations derived in 1221 therefore remain valid if we insert a correction factor given by Scherschefsky in a similar context:

$$\eta_g = \left(1 - \frac{g \cos \bar{\varphi}}{b} \right).$$

Here $g \cos \bar{\varphi}$ is the component of the gravitational acceleration in the flight direction; b is the ideal vehicle acceleration $b = P/M$ resulting from the full thrust P , which differs from the actual vehicle acceleration by the constant gravitational acceleration $g \cos \bar{\varphi}$.

The derivation of this correction factor for resistance-free motion in a gravitational field can be demonstrated somewhat as follows:

The energy taken from the rocket in each second is mcv in all; the mass m_1 ejected to balance the gravitational field gives the rocket an energy m_1cv . The magnitude of this mass m_1 is given by the condition $m_1c/t = Mg \cos \bar{\varphi}$, so $m_1 = tMg \cos \bar{\varphi}/c$. Then from the total energy gained per second we deduct for gravity compensation $m_1cv = (Mg \cos \bar{\varphi}/c) \times cv = vMg \cos \bar{\varphi}$. The second amount ejected to produce the acceleration of the vehicle is $m_2 = m - m_1$, which is given by $m_2c = M(b - g \cos \bar{\varphi})$. Then $M = mc/b$.

The energy available for the acceleration of the vehicle is then $mcv - vMg \cos \bar{\varphi} = mcv(1 - g \cos \bar{\varphi}/b)$.

The necessary acceleration energy as a fraction of the total energy extracted is then

$$\eta_g = \frac{m \cdot c \cdot v (1 - g \cos \bar{\varphi}/b)}{m \cdot c \cdot v} = (1 - g \cos \bar{\varphi}/b),$$

as above.

If this is so for any instant, it applies for the entire acceleration period, if $g \cos \bar{\varphi}/b$ is constant; then η_g is not only the correction factor for η_a but also for $\eta_a^{(m)}$.

Fig. 9 shows this correction factor as a function of b/g and $\cos \bar{\varphi}$. The value is zero for $b/g \cos \bar{\varphi} = 1$, so the rocket motor keeps the vehicle in equilibrium directly against the gravitational force without acceleration in spite of the large energy consumption. Also, η_a increases with $g \cos \bar{\varphi}/b$ and reaches its maximum value of

one when $\cos \bar{\varphi} = 0$, or $\bar{\varphi} = \pi/2$ (flight at right angles to the direction of the gravitational field), while for $\bar{\varphi} = 0$ and $b \doteq 6g$ (a limit set by biological considerations) we have $\eta_g = 0.833$.

Motion at right angles to the axis of the vehicles is of no significance for this treatment.

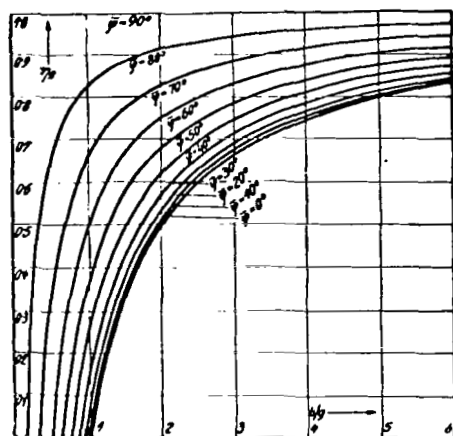


Fig. 9.

Correction factor η_g for the
external efficiency of a rocket
drive unit in flight against
a gravitational force.

1223. External Efficiency for Flight in a Space Free from Gravity Against a Resistance

Here the relationships are to a certain extent similar to those of 1222. Part of the thrust is now needed to overcome the (air) resistance and to maintain the existing state of motion. The excess thrust can be used to accelerate the vehicle, as in 1221. Of especial importance for our further studies is the circumstance that the air resistance W can be treated as a constant quantity independent of the flight speed during the acceleration period, as we

shall see in Section 3, if the flight path is suitably chosen. The thrust needed to overcome the air resistance is therefore also constant.

The mass m ejected per second is divided as regards use into three parts in the most general case:

$$m = m_1 + m_2 + m_3$$

of which m_1 serves to balance out the component of gravity, m_2 provides acceleration of the vehicle, and m_3 is used to overcome the air resistance. In what follows we are concerned only with the part $(m_2 + m_3) = m'$.

While we must treat m_1 (and hence the energy related to it) as power lost to the vehicle, the work of acceleration and that of overcoming resistance are to be taken as work necessary to the task of transport. For these reasons we cannot in general speak of a new efficiency but rather have to consider how the net energy supplied to the vehicle per unit time is divided between work of acceleration and work against the resistance.

The simplest case, and also the most important in practice, is that of uniform flight, which may represent ordinary cruising flight. The speed v remains strictly constant. Then from the instantaneous efficiency

$$\eta_a = \frac{2v/c}{v^2/c^2 + 1}$$

we have from 1221 that the net power received by the vehicle is constant and is entirely utilized in overcoming air resistance.

If $v = \text{constant}$, then $\eta_a = \eta_a^{(m)} = \text{constant}$ also. The work of acceleration is zero, and the total energy needed by the vehicle in accordance with η_a goes to maintain the constant cruising speed by overcoming the air resistance.

Here the external efficiency is directly comparable with that of an ordinary airscrew. The relations given in 122 and 1221 for η_a apply, and in particular we have $\eta_a = 1$ for $v/c = 1$; even in the range $v/c = 0.5$ to $v/c = 2$ it is always greater than $\eta_a = 0.8$ and so is greater than that of a good airscrew, but outside the flight-speed range $v/c = 0.27$ to $v/c = 3.75$ it falls to values of little interest below $\eta_a = 0.5$ (Fig. 7, section 1221).

The practically available exhaust speeds lie roughly between $c = 1000$ m/sec and $c = 4000$ m/sec (on account of the energy E received from unit fuel in an exhaust mass m via the relation $c^2 = (2E\eta_1/m)$, which implies the possibility that a rocket motor could

provide a highly economic long-term drive for flight speeds between about 270 m/sec and 15 000 m/sec, in which the over-all efficiency η of the power plant is greater than $\eta = 0.35$ and hence rather larger than that of an ordinary aircraft power plant ($\eta = 0.25$ roughly).

We may note that it is common at present to consider a flight speed of 270 m/sec (about 1000 km/hr) as the highest speed limit for any ordinary power plant scarcely to be exceeded by racing aircraft, so it is very gratifying and significant that the speed range for good efficiency in a rocket motor begins precisely at this speed.

The second case of practical importance in flight under rocket power is accelerated flight, which is dominant at the start of the flight during the acceleration period before the full cruising speed is reached and for which the highest motor performance is of considerable importance, on account of the very high fuel consumption in this period. The purpose here during the relatively short acceleration period is not to cover a specified distance but to accelerate the vehicle to a specified final speed v_1 , so energy con-

sumed for other purposes (including work against air resistance) must be treated as lost energy in relation to this purpose.

In this respect we must correct the expression given in 1221 for the mean efficiency $\eta_a^{(m)}$ for the acceleration period during ac-

celeration in a space free from gravity by means of a correction factor for the constant resistance W of the medium, whose magnitude is

$$\eta_w = \left(1 - \frac{W}{P'} \right),$$

in which P' represents the thrust of the rocket, $P' = m'c$. The derivation of this correction factor is somewhat as follows:

/51

Of the energy received by the rocket each second, $m'cv$, a part $m_2cv = Wv$ is used to overcome the air resistance.

The remainder is available for the acceleration of the vehicle, being $m'cv - Wv = v(m'c - W)$, the generally available energy.

This acceleration energy as a fraction of the total energy $m'cv$ is

$$\eta_w = \frac{v(m'c - W)}{m' \cdot c \cdot v} = 1 - \frac{W}{m'c} = \left(1 - \frac{W}{P'} \right),$$

in which P' is the thrust of the rocket resulting from m' .

The other flight motions of a rocket vehicle subject to rocket drive are of only minor importance as regards energy.

123. Overall Efficiency

The overall efficiency of the power plant may be split up, as we have seen above, into the internal efficiency η_i and the external efficiency η_a .

The internal efficiency η_i is virtually independent of the

state of motion of the rocket and represents a fixed performance figure for the rocket motor. It is essentially comparable with the efficiency of a piston engine, although it attains considerably more favorable values than the latter. We should take as provisional fixed value for calculations as

$$\eta_i = 0.7$$

The external efficiency is not a constant, for it is very highly dependent on the state of motion of the vehicle, especially on the flight speed. For instance, the external efficiency of transportation for a rocket power unit that provides a fixed speed v against a resistance of the medium of strength W is constant, being

$$\eta_a = \frac{2v/c}{v^2/c^2 + 1}.$$

If the flight at constant speed instead takes place against a gravitational field of strength $g \cos \bar{\varphi}$, the constant efficiency is

$$\eta_{ag} = \eta_a \cdot \eta_g = \frac{2v/c}{v^2/c^2 + 1} (1 - g \cos \bar{\varphi}/b).$$

If the speed v is variable, the efficiency must be so as well so we can speak only of the instantaneous efficiency. A more significant quantity is the mean external efficiency over a larger section of the flight of variable speed v . This mean efficiency is as follows for a constantly accelerated flight in a space free from

resistance and gravitational fields:

$$\eta_a^{(m)} = \frac{(v/c)^2}{e^{v/c} - 1}$$

in which v is the flight speed at the time in question.

Flight of constant acceleration provided by a rocket drive against a gravitational field of strength $g \cos \bar{\varphi}$ involves a mean external efficiency of acceleration of

$$\eta_{ag}^{(m)} = \eta_a^{(m)} \cdot \eta_g = \frac{(v/c)^2}{e^{v/c} - 1} (1 - g \cos \bar{\varphi}/b).$$

If the accelerated flight in addition takes place against a fixed resistance W from the medium, the efficiency of the acceleration becomes

$$\eta_{agw}^{(m)} = \eta_a^{(m)} \cdot \eta_g \cdot \eta_w = \frac{(v/c)^2}{e^{v/c} - 1} (1 - g \cos \bar{\varphi}/b) \left(1 - \frac{W}{P'} \right)$$

To obtain the overall efficiency η corresponding to the calorific value of the fuel we merely multiply the external efficiency for the particular form of flight by η_1 .

The effect of any propulsive mass from the surrounding atmosphere on the overall efficiency is implicitly contained in all equations as a result of the insertion of the appropriate c in accordance with the relation $c = (2E\eta_1/m)^{1/2}$.

To E may be added if necessary the adiabatic compression energy of the mass of air added, but not the kinetic energy of this.

13. Propellants

131. Requirements as to Propellants

Some physical and chemical properties, especially the calorific value, the amount of energy available from 1 kg of propellant, are of basic importance to the requirements imposed on a rocket propellant. The value of the propellant in general increases with the calorific value, especially in aviation, and this applies also to rocketry subject to a certain but purely theoretically significant restriction. The exhaust speed $c \approx (1.4E/m)^{1/2}$ is governed by the calorific value E and the exhaust mass m , and this must be of the order of the projected flight speed in order to ensure a good external efficiency. If only restricted exhaust masses are available, in particular only the mass of the propellant itself, then very high calorific values would imply exhaust speeds so high as to cause the external efficiency to fall greatly; under some circumstances, a propellant of lower calorific value may actually make available to the vehicle a larger net energy. The propellant is therefore to be chosen in accordance with its calorific value in relation to the anticipated flight speed and to the available exhaust mass. Scarcely any practical significance attaches to this restriction, on account of the very high flight speeds aimed at in rocketry and the restricted thermochemical energy from the available propellants normally in question.

A further circumstance is the need for a propellant that can be safely contained and used in the vehicle without resort to costly, heavy, and elaborate equipment. Many propellants are ruled out here, especially on the grounds of the lethal properties of liquefied gases, of chemical attack on the container, pipelines, and nozzle by many propellants and products, and of the danger of explosion.

The notable physical properties include the cooling capacity of the propellant (that is, the capacity to draw a percentage of the heat energy by change of temperature and state of aggregation from that in the tank to that of readiness for use). The heat needed to raise gasoline from 0 to 100°C and then to evaporate it is about 1.4% of the calorific value under normal conditions. The evaporation of 1 kg of liquid hydrogen at -253°C followed by heating to a reduced temperature T_1 at atmospheric pressure in accordance

with $T_1 = T_0 (1/p_0)^{\frac{n-1}{n}}$ is given by Oberth as requiring $3.4 (T_1 + 12)$

kcal. The corresponding figure for liquid oxygen at -183°C is 0.218 ($T_1 + 144$) kcal, while that for liquid nitrogen at -195.7°C is 0.244

($T_1 + 121$). This cooling capacity is thus of significance, since a

rocket motor must employ in place of a special cooling fluid (which transports the heat lost through the walls of combustion chamber and nozzle to the external air) the capacity of the propellant itself to perform cooling. Liquefied gases are quite unsuitable for wall cooling in the usual manner of a coolant, since they are at their boiling points in the state in the tank and so have no capacity to absorb heat prior to evaporation.

Apart from these and other physicochemical properties, which may be taken as fixed and invariable facts, there are several other more variable and economic features that play a part in the requirements as to a rocket fuel. Even in spite of their possible variability, though, they cannot play so dominant a role in the primary choice of propellant as do the previously listed ones.

Here primarily we must reckon the cost of the propellant per unit calorific value, say in reichsmarks per 10,000 kcal. The common commercial propellants gasoline, petroleum, kerosene, and so on naturally at once come out best in this respect and the high-yield liquefied gases the worst. These relations may alter considerably if liquefied gases come to be used extensively. Apart from the national economic importance of replacing, say, gasoline, by hydrogen, the latter may be expected to have a possible outline price from electrolytic production: 11.63 kWh of cheap hydroelectric power per 10 000 kcal (0.34 kg of hydrogen).

Similar circumstances apply to the availability of propellants at the possible landing sites on the Earth, with gasoline, for the time being, coming into primary consideration. Only very few points on the Earth are in question as rocket landing sites, so it should be a simple matter to organize the production of any rocket fuel at these.

132. Independent Propellants

High and low explosives are the principal independent propellants, which require no additional material (oxygen, air, and so on) to produce energy; some particular future propellants (energy of atomic disintegration, energy of atomic hydrogen, and so on) belong rather to some extent to the 'electron-rocket plane', which largely relies on the ejection of small masses by electrical means with speeds approaching that of light. The energy needed for this is in most projects in some way to be derived directly from the Sun's rays, so this is irrelevant to the purposes of rocketry to be considered here. The fantastic exhaust speeds associated with such energy-rich propellants are, in addition, scarcely worthy of consideration, since a maximum possible rocket-flight speed of about 8000 m/sec together with an exit speed such as that of cathode rays or α -rays gives a hardly encouraging external efficiency of $\eta_a =$

/55

$= 0.00016$ for the rocket drive. Such profligate energy expenditure would still not be justified even if inexhaustible energy sources became available from solar sources or atomic disintegration. If one could use the high energy to eject appropriately large exhaust masses with rather lower speeds (as Oberth proposed with his electron rocket operating on the principle of the electric wind), one would obtain under such circumstances relationships entirely worthy of discussion.

Atomic hydrogen, on the other hand, is a propellant ideally and directly suited to rocket flight; this combines to form molecular hydrogen, the energy thereby made available is quoted* as 52,500 kcal/kg, which without the addition of any other mass gives an exhaust speed of somewhat in excess of 20,000 m/sec, which would provide very good external efficiencies and which would allow of close control by the addition of trifling amounts of additional mass. At present the provision of energy from atomic hydrogen is an unsolved problem.

Low and high explosives hold out real promise for our purpose, since they are independent of the availability of any accessory material containing oxygen, for the oxygen needed for the combustion of the fuel (e.g., carbon, sulfur) is either mixed with the latter

*F. R. Bichowsky and L. C. Capeland. J. Amer. Chem. Soc., 50, 315, 1928.

in the form of an oxygen carrier (such as saltpeter) or is present within highly complicated synthetic molecules, as in nitroglycerine, nitrocellulose, and so on. On the other hand, the calorific value is relatively low, and most such materials, particularly those of high yield, have a pronounced tendency to explode spontaneously. For the latter reason they have no real importance for manned rockets.

To sum up, we may say that the independent propellants (which are listed in Table 14) under present circumstances are not to be considered for the propulsion of rocket aircraft.

133. Dependent Propellants (Combustants)

The dependent propellants are ones that by themselves are not in a state to provide energy; to do this they need a further accessory material, which is usually oxygen. The energy production in this case is a consequence of oxidation.

The dependent propellants to be considered are almost exclusively hydrogen, carbon, and chemical compounds of these, which collectively are distinguished by a very high calorific value. This is controlled by the constituents, carbon and hydrogen, and it varies

from 12.20×10^6 to 3.48×10^6 kg-m/kg (Table 15) in accordance with the proportion by weight of hydrogen or carbon. The hydrogen-rich fuels (such as CH_4) have higher calorific values than the carbon-

rich ones (such as C_6H_6).

Accordingly, hydrogen itself takes first place, which rocket technologists for the most part consider to be the best fuel. On the other hand, it has some disadvantages that should not be underrated. These appear in essence as the complete impossibility of using it in gas (even compressed) form, on account of the size of

the tanks, so the liquid form (density 0.07 ton/m^3) must be employed. The boiling point of liquid hydrogen at atmospheric pressure is about -253°C , so very rapid evaporation at normal body temperatures can be prevented only by the most careful and painstaking heat insulation (latent heat of evaporation 123 kcal/kg as against 539 kcal/kg for water). Other troublesome disadvantages are particularly that the hydrogen cools all the equipment and pipelines to its own temperature, at which most constructional materials acquire a brittleness resembling that of glass, the result being, according to Oberth,

that its handling is as troublesome and dangerous as that of boiling water.

Liquid hydrogen is a colorless, extremely light, and very mobile liquid with the following parameters: boiling point under normal conditions -253°C , melting point -257°C , critical temperature -240°C , critical pressure 13.2 kg/cm^2 , latent heat of evaporation 123 kcal/kg , density 0.070 ton/m^3 .

Methane comes next in the fuel table; it has its boiling point at -161.4°C and a latent heat of evaporation of 125 kcal/kg , and its smaller calorific value makes it somewhat less dangerous than liquid hydrogen.

Following these there are the usual liquid fuels, headed by gasoline, petroleum, and benzene, whose favorable properties are well known. The importance of these liquid fuels leads us to detail their more important parameters and properties below.

Gasoline: From mineral oil, brown-coal tar, and coal; minimum calorific value about $10,200 \text{ kcal/kg}$, boiling point 60 to 120°C , density 0.7 to 0.74 ton/m^3 , viscosity 1°E , flash point -55 to -25°C , spontaneous ignition at 475 to 530°C , usually consisting of members of the aliphatic series C_5H_{12} , C_6H_{14} , C_7H_{16} , C_8H_{18} , and so on. /5.

Colorless transparent fluid.

Petroleum (gas oil): From mineral oil, minimum calorific value about $10,250 \text{ kcal/kg}$, boiling point 250 to 350°C , density 0.865 to 0.895 ton/m^3 , viscosity 1.5 to 2.5°E at 20°C , flash point 65 to 85°C , spontaneous ignition at about 350°C , pour point -20°C , in essence consisting of hydrocarbons. Bright yellow to yellow-brown fluid.

Benzene: From coal tar or lighting gas ('coal benzine'), minimum calorific value about 9600 kcal/kg , boiling point about 100°C , density 0.887 ton/m^3 , flash point -15°C , spontaneous ignition at about 730°C , freezing point when pure $+5.5^{\circ}\text{C}$, falling with the usual impurities. Consists mainly of C_6H_6 with traces of C_7H_8 , C_8H_{10} , and so on. Mobile colorless liquid.

The other fuels listed in Table 15, carbon and alcohol, are of no significance as rocket fuels on account of their low calorific values.

134. Liquid Oxygen Carriers

The dependent fuels need oxygen in order to develop their heat energy. The simplest method, and the only one presently usable way to procure this oxygen for aviation, is to take it from the atmosphere, so only the fuel itself must be carried in the aircraft. The currently accepted view is that the oxygen content of the air falls roughly linearly to zero at a height of about 100 km, so in the overall range of rocket flight envisaged we can reckon to find an atmosphere containing oxygen. It is therefore exceptionally tempting to consider taking the oxygen needed for rocket flight from the atmosphere also, since the other gases in the air (nitrogen, helium, and so on) may be very welcome as additional mass and as a means of minimizing dissociation. The special feature of the flight paths considered here (that over most of the flight path at full motor power the dynamic pressure is constant in spite of the fall in density with height) makes this view tenable.

The pronounced effect of added mass is evident from Tables 19 and 20.

On the other hand, this way of ensuring the oxygen need not be considered more closely for the following reasons:

1. The atmospheric pressure at the heights in question is so extremely low that it can be neglected in relation to the dynamic pressure even at, say, a flight speed of 360 km/hr near the ground. The raising of the air pressure consequent on this initial compression as a result of the dynamic pressure from about 625

kg/m² to the injection pressure for the combustion chamber, which even for a variable-pressure rocket is about 30,000 to 40,000 kg/m², would appear virtually impossible in the foreseeable future with conceivable superchargers, as would the provision of the vast amounts of air needed.

2. The oxygen must in any case be carried in the vehicle for the highest parts of the flight path, where the dynamic pressure falls rapidly on account of increasing inertial effects arising from curvature of the path.

3. The injection of liquid propellant into the combustion chamber of the rocket is considerably simpler than that of partly gaseous material and allows the use of constant pressure motors, which have higher internal efficiency and produce no pulsation effects.

Again, there is no need for special ignition equipment and similar auxiliary gear which can cause trouble.

4. Further, the complete autonomy and uniformity of the rocket vehicle up to the greatest heights envisaged, which correspond to orbital speeds, is assured only by complete carriage of the oxygen and deserves the necessary development to conform with the work already done by space-travel theorists.

5. Finally, it is at present merely an unverified hypothesis that the higher layers of the stratosphere contain adequate oxygen.

This means that the oxygen needed for the combustion must be carried in full in the rocket.

The possible forms in which this can be achieved are as follows:

1. Several chemical oxygen carriers (for instance, salt-peter has been used in black-powder rockets since ancient times); these are listed in Table 12.

TABLE 12

Oxygen carrier	Oxygen content, wt. %	Heat of dissociation in oxygen release, 10^6 kg-m/kg
KClO_4	46.2	- 0.427
KNO_3	48.5	- 0.505
HClO_4	64.0	- 0.080
N_2O_5	74.2	+ 0.005
HNO_3	76.3	- 0.233
H_2O_2	94.2 (47.2)	+ 0.295
O_3	100.0	+ 0.303

All these carriers contain, in addition to oxygen, more or less valueless ballast. Some of these compounds are largely ruled out on account of their chemical properties (e.g., HNO_3) or those

of their decomposition products (e.g., HCl). Potassium perchlorate, saltpeter, and nitric acid are also largely ruled out on account of the appreciable energy demand on decomposition (negative energies of dissociation). The apparently promising nitrogen pentoxide (nitric acid anhydride) is expensive, explosive, and poisonous. At 0°C it takes the form of hard rhombic crystals, which melt even at 3°C and boil at about 50°C . The substance is very unstable and often explodes without any apparent cause, decomposing to nitrogen dioxide and oxygen.

2. Hydrogen peroxide has a special place among the oxygen carriers. Only part of its oxygen content is available under the conditions in question, so the effectively usable oxygen content is 47.2% of the total weight. On the other hand, it is noteworthy that the release of oxygen also sets free the substantial energy of 1323 kcal/kg, which substantially increases its value in combination with a dependent propellant. Table 17 gives values. Hydrogen peroxide is an odorless and colorless liquid (blue in large depths) of specific gravity 1.458 having its melting point at -2°C . It evaporates slowly at ordinary temperatures. The decomposition in accordance with the equation $2\text{H}_2\text{O}_2 = 2\text{H}_2\text{O} + \text{O}_2$ is sometimes explosive in the undiluted state or in concentrated solution in the presence of the slightest traces of catalysts (alkalis or heavy metals), though it can be delayed by certain stabilizers. H_2O_2 is very expensive in the pure state.

3. Liquid ozone is a peculiar and in some respects even more valuable oxygen carrier. Not only is it entirely free from ballast mass; its decomposition preceding combustion in accordance with the equation $2\text{O}_3 = 3\text{O}_2$ sets free 0.303×10^6 kg-m per kg of ozone, which is added to the calorific value of the fuel.

Liquid ozone is an oily dark-blue liquid with the following parameters: boiling point under normal conditions -112°C , melting point -251.4°C , critical temperature -5°C , critical pressure 67 kg/cm², latent heat of evaporation 73 kcal/kg, and density 1.71 ton/m³.

The relatively high boiling point imposes much less demand on the properties of the constructional materials and on the heat insulation than does liquid oxygen. The very high density allows the insulated tanks to be of rather smaller size.

Disadvantages are that it oxidizes most metals, that its vapor is injurious to health at high concentrations, and (especially) that it is extremely explosive in the form of its gaseous evaporation product. Careful research is needed to establish whether this disadvantage can be overcome by suitable measures, such as the use of gas diluents or the like, which in view of its other notable advantages is very much to be hoped.

4. For the present there remains on purely kinetic and partly constructional grounds:

Liquid oxygen itself as the best oxygen carrier. This is a bright blue liquid of mobility comparable with water having the following parameters: boiling point at normal pressure -183°C , melting point -219°C , critical pressure 51 kg/cm^2 , latent heat of evaporation 51 kcal/kg , density 1.143 ton/m^3 .

The boiling point and density are rather less favorable than those of liquid ozone, and the advantageous dissociation energy of the latter is entirely lacking.

135. Liquefied Gases*

Liquefied gases play a considerable part in rocket projects and have to be considered seriously for our purposes, in accordance with the above evidence; but their properties are in general not familiar, so they are given in condensed form here.

*Hardin-Traube, Die Verflüssigung der Gase (Liquefaction of Gases). Emke, Stuttgart, 1900;

Luhmann, Die Industrie der verdichteten und verflüssigten Gase (The Compressed and Liquefied Gas Industries). Hartleben, Vienna and Leipzig, 1904;

Müller-Pouillet, Lehrbuch der Physik und Meteorologie (Textbook of Physics and Meteorology). Vieweg und Sohn, Braunschweig, 1906;

Teichmann, Komprimierte und verflüssigte Gase (Compressed and Liquefied Gases). Knapp, Halle, 1908;

Urban, Laboratoriumsbuch für die Industrie der verflüssigten und verdichteten Gase (Laboratory Manual for Liquefied and Compressed

The state of aggregation of a body is dependent on the temperature and pressure; the denser states of aggregation tend to arise if the pressure is raised or the temperature is lowered, and the changes occur in the sequence gas-liquid-solid. Both factors are themselves not independent, since the temperature range in which a given substance takes the form of gas, liquid, or solid is dependent on the pressure, and vice versa. Fig. 4a illustrates this.

Here particular interest attaches to any values that divide the liquid state from the gaseous one, especially any temperature above which the substance cannot exist in liquid form. The critical temperature is the highest temperature at which the liquid and gaseous states can coexist (highest boiling point), and no pressure variation is possible. The gas parameters corresponding to this highest possible temperature are called critical parameters (in particular, the pressure is called the critical pressure). Lower pressures require lower temperatures for boiling; normal atmospheric pressure corresponds to the normal boiling point.

If we consider for clarity the relationships for a normal atmospheric pressure of 760 mm Hg (which is in fact the one commonly encountered with liquefied gases), the normal boiling points of certain materials are found to be as follows:

Aluminum, 1800°C; mercury, 357°C; water, 100°C; carbon dioxide, -78.5°C; methane, -164°C; oxygen, -183°C; nitrogen, -196°C; and hydrogen, -253°C.

The corresponding melting points (temperatures at which the liquid and solid states can coexist at normal air pressure) are as follows:

Aluminum, 658°C; water, 0°C; mercury, -38.9°C; carbon dioxide, -79°C; ether, -118°C; methane, -184°C; nitrogen, -219°C; hydrogen, -257°C.

These series show directly which substances are found under the conditions of daily life as solids, which as liquids, and which

/61

Gas Industries). Knapp, Halle, 1909;
 Schall, Herstellung und Verwendung der verflüssigten und verdichteten Gase (Production and Use of Liquefied and Compressed Gases). Jaenecke, Leipzig, 1910;
 Claude-Kolbe, Flüssige Luft (Liquid Air). 1920;
 Drows, Komprimierte und verflüssigte Gase (Compressed and Liquefied Gases). Knapp, Halle, 1928;
 Laschin, Der flüssige Sauerstoff (Liquid Oxygen). Halle, 1929;
 Drows, Kältetechnik (Refrigeration Technique). Halle, 1930.

as gases. A substance exists only as a gas above its boiling point, while it cannot exist as a solid above its melting point.

The liquefied gases of primary interest to us, oxygen and hydrogen, have extremely low boiling points, and their temperatures must be kept below these during storage. Heat flows in from the surroundings very rapidly under normal conditions, on account of the very large temperature difference, which leads to very rapid evaporation, since the latent heats of evaporation are only 51 and 109 kcal/kg; this can be kept within acceptable limits only by storage with the greatest possible degree of heat insulation. Double-walled (Dewar) vessels are required, in which the space between the walls is carefully evacuated in order to minimize heat conduction; in addition, the walls in contact with the vacuum are mirror-silvered, in order to suppress heat radiation as far as possible. On the other hand, the vessels must remain open, since the vapor pressure would otherwise very soon cause fracture. Any metal directly in contact with the liquefied gas acquires the same temperature, which causes extreme reduction in strength and elastic range, together with reduction in plasticity of a similar order; for instance, steel becomes as sensitive to shock as glass.

/62

The liquid is apparently harmless if spilt on the skin, because the local evaporation prevents direct contact. Liquid actually contacting the skin produces severe burns.

136. Choice of the Most Suitable Propellant

If the independent propellants are ruled out on the grounds dealt with above, the choice is virtually restricted to liquid hydrogen and the usual liquid fuels.

The choice must fall on liquid hydrogen if the requirements are for the absolute minimum weight for a given energy yield and for the attainment of the highest exhaust velocity, and with it better external efficiency. The view of authoritative cosmonauts is that the stoichiometric ratio of hydrogen to oxygen does not give the highest exhaust speed, but rather about 2.6 parts by weight of oxygen to one part of hydrogen, on account of dissociation effects. The favorable effects of the excess hydrogen provide exhaust speeds in excess of 4000 m/sec from such a mixture. Table 21 gives numerical results for the combustion of explosion mixture with excess hydrogen.

Some very troublesome disadvantages, however, go with the slightly larger calorific value of liquefied explosion mixture

relative to, say, gasoline with oxygen; examples are:

1. Introduction of a fresh uncertainty into experimental rocket motors, on account of the use of a fuel of unknown characteristics in place of gasoline.

2. A tank volume of about 1 dm^3 is needed to accommodate 10^6 kg-m of energy in the form of gasoline and liquid oxygen, whereas this same energy in the form of the most favorable mixture of

liquefied explosion gases requires about 4.2 dm^3 in tank volume, or about 4.2 times as much, which gives rise to difficulties of space, such as increase in dimensions of the vehicle, greater weight, increased air resistance, and so on.

3. Apart from the 4 times greater volume, the tanks for liquefied explosion mixture must take the form of heavy, inconvenient, and expensive Dewar vessels, which involves weight considerably in excess of that for normal gasoline tanks made of light alloy; this may very easily result in loss of the weight advantage per unit energy for explosion mixture.

4. Filling with liquefied explosion gas must involve considerable loss by evaporation.

/63

5. Considerable difficulties arise in the choice of material and design for the tank, on account of the very unfavorably altered properties of materials at the temperature of liquid hydrogen, which may require the use of copper or lead for the double-walled tank in place of light alloy.

6. Difficulties of design in the control of temperature differences of -250°C to $+3000^\circ\text{C}$, especially as regards the behavior of materials.

7. Unacceptability of joints involving accidental frictional contact for the handling and use of the liquid in the vehicle, on account of the constant danger of fire.

8. Danger of tank explosion as a result of vigorous evaporation consequent on heating.

9. Troublesome and tedious tank operations (precooling with auxiliary liquefied gas and so on).

10. Danger of icing on fuselage if constructed as a flying boat, hence endangering the take-off.

11. Considerably higher price of hydrogen relative to, say, gasoline.

12. Impossibility of storage at landing fields and hence expensive ground installations.

These and other reasons make it clear that we must bear in mind the possible use of other fuel combinations, whose calorific values are not so widely different that a compromise on weight for secondary reasons becomes inconceivable.

Table 13 collects from the tables of section 137 some combinations on which a closer choice may be made.

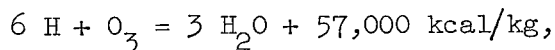
The actual best combination can be found only from detailed consideration and (especially) tests.

/64

The combinations involving hydrogen are to be rejected, on account of the very considerable demand for tank space, especially insulated tank space. If, in addition, we rule out ozone and nitrogen pentoxide on the grounds given above, the choice narrows finally to combinations 6 and 7.

If we assume that the difficulties associated with the provision of liquid oxygen can be overcome, in which case the higher calorific value of combination 6 may be taken as available, we may say that the choice falls finally on combination 6, especially in view of the inconvenient secondary features of pure hydrogen peroxide.

Since the practical evaluation of the chemical reaction of highest known energy



(with ice as final product and the exceptional energy yield of

24.3×10^6 kg-m per kg, equivalent to $c_{th} = 21,800$ m/sec) is the

least available, we may take as the best combination available under present conditions as that of a stoichiometric mixture of gasoline with liquid oxygen, which will be used as the basis for later calculations.

TABLE 13

No.	Combination	cal. value, 10^6 kg-m/kg	c_{th} , m/sec	ins. tank vol., dm^3 per 10^6 kg-m
1	1 kg H_2 + 2.6 kg O_3	1.32	5080	3.35
2	1 kg H_2 + 2.6 kg O_2	1.10	4680	4.20
3	1 kg H_2 + 17 kg H_2O_2	0.96	4330	0.84
4	1 kg H_2 + 10.8 kg N_2O_5	1.03	4500	1.18
5	1 kg gasoline + 3.5 kg O_3	1.25	4960	0.36
6	1 kg gasoline + 3.5 kg O_2	1.01	4450	0.67
7	1 kg gasoline + 7.4 kg H_2O_2	0.80	3940	-
8	1 kg gasoline + 4.7 kg N_2O_5	0.80	3940	-

Subject to appropriate experimental verification, gasoline might be replaced by mineral oil or coal-tar distillates of higher boiling point (such as gas oil, heavy oil, and so on), which have the advantages over gasoline of being cheaper and of having greater capacity to absorb heat without boiling.

137. Propellant Tables

The calorific values given in the tables all relate to the case of substances at +15°C and atmospheric pressure before and after the combustion. Part of the heat made available by combustion goes to heat the fuel and oxygen from 15°C, while another is released by cooling of the product gas to the temperature $T_1 =$

$T_0 (1/p_0)^{\frac{n-1}{n}}$ corresponding to a normal pressure of 1 atm. Then

the theoretical exhaust speed c_{th} of the product relative to the motor is calculated from the available energy E per kilogram in relation to the exhaust mass m in accordance with the mechanical relation $mc^2/2 = E$ as

/65

$$c_{th} = \sqrt{2 E/m} = \sqrt{2gE}.$$

The theoretical specific thrust is defined in an obvious fashion as the force in kg available to the vehicle for a second from the use in that second of 1 kg of the propellant carried in the vehicle.

On this basis the I_{th} given in Tables 14, 16, 17, 18, and 21 have been calculated in accordance with

$$I_{th} = m \cdot c_{th} = \sqrt{2E/g}.$$

TABLE 14

86

Independent propellant (ready to produce energy without auxiliary material)	(minimum) E, 10^6 kg-m/kg	c_{th} , m/sec	I_{th} , kg-sec/kg
Disintegration of radium	~ 200,000	-	-
Association of atomic hydrogen ($H + H = H_2$)	22.40	21 000	2140
Nitroglycerine $C_3H_5(ONO_2)_3$	0.768	3 880	396
Explosive gelatine	0.700	3 710	379
Nitrocellulose, $C_6H_{10}O_5 + 4NO_3$	0.683	3 660	373
Cordite (smokeless nitroglycerine powder)	0.535	3 240	330
Guhr dynamite	0.555	3 300	337
Picric Acid $C_6H_2(NO_2)_3OH$	0.346	2 600	265
Black powder	0.299	2 420	247
Solar constant, kg-m/sec-m ² at Earth's orbit	~ 175	-	-
Condensation of water vapor	0.230	2 120	216
Freezing of condensed water vapor	0.034	667	68

TABLE 15

Dependant propellants (fuels, not capable of producing energy without oxygen)	$E, 10^6$ kg-m/kg	$c_{th},$ m/sec	$I_{th},$ kg-sec/kg
H_2	12.20	-	-
CH_4	5.13	-	-
C_8H_{18} (~ Gasoline)	4.55	-	-
Petroleum	4.40	-	-
Benzene (C_6H_6)	4.10	-	-
Carbon (C)	3.48	-	-
Alcohol (C_2H_5OH)	2.73	-	-

TABLE 16

Dependent fuels, with oxygen needed for combustion	$E, 10^6$ kg-m/kg	$c_{th},$ m/sec	$I_{th},$ kg-sec/kg
Hydrogen (1 kg H_2 + 8 kg O_2 = 9 kg H_2O)	1.36	5170	527
Methane (1 kg CH_4 + 4 kg O_2 = 5 kg CO_2 H_2O)	1.03	4490	458
Gasoline (1 kg C_8H_{18} + 3.5 kg O_2 = 4.5 kg CO_2 H_2O)	1.01	4450	453
Petroleum (1 kg Petrol. + 3.46 kg O_2 = 4.46 kg gas)	0.99	4410	449
Benzene (1 kg C_6H_6 + 3.4 kg O_2 = 4.4 kg CO_2 H_2O)	0.93	4270	435
Carbon (1 kg C + 2.67 kg O_2 = 3.67 kg CO_2)	0.95	4320	440
Alcohol (1 kg C_2H_6O + 2.08 kg O_2 = 3.08 kg CO_2 H_2O)	0.89	4180	427

TABLE 17

Dependent fuels, with nitrogen peroxide as carrier of the oxygen needed for combustion	$E, 10^6$ kg-m/kg	$c_{th},$ m/sec	$I_{th},$ kg-sec/kg
Hydrogen (1 kg H_2 + 10.8 kg N_2O_5)	1.034	4500	459
Methane (1 kg CH_4 + 5.4 kg N_2O_5)	0.802	3970	405
Gasoline (1 kg C_8H_{18} + 4.73 kg N_2O_5)	0.794	3940	402
Petroleum (1 kg Petrol. + 4.67 kg N_2O_5)	0.777	3900	398
Benzene (1 kg C_6H_6 + 4.59 kg N_2O_5)	0.733	3660	373
Carbon (1 kg C + 3.61 kg N_2O_5)	0.755	3850	393
Alcohol (1 kg C_2H_6O + 2.81 kg N_2O_5)	0.717	3750	383

TABLE 18

Dependent fuels, with ozone as carrier of the oxygen needed for combustion	E, 10 ⁶ kg-m/kg	c _{th} , m/sec	I _{th} , kg-sec/kg
Hydrogen (1 kg H ₂ + 8 kg O ₃ = 9 kg H ₂ O)	1.63	5670	578
Methane (1 kg CH ₄ + 4 kg O ₃ = 5 kg CO ₂ H ₂ O)	1.27	5000	510
Gasoline (1 kg C ₈ H ₁₈ + 3.5 kg O ₃ = 4.5 kg CO ₂ H ₂ O)	1.25	4960	506
Petroleum (1 kg Petrol. + 3.46 kg O ₃ = 4.46 kg gas)	1.22	4900	500
Benzene (1 kg C ₆ H ₆ + 3.4 kg O ₃ = 4.4 kg CO ₂ H ₂ O)	1.17	4800	490
Carbon (1 kg C + 2.67 kg O ₃ = 3.67 kg CO ₂)	1.17	4800	490
Alcohol (1 kg C ₂ H ₆ O + 2.08 kg O ₃ = 3.08 kg CO ₂ H ₂ O)	1.09	4630	473

TABLE 19

Dependent propellants, with the air needed for combustion for points near the Earth	$E, 10^6$ kg-m/kg	c_{th}' m/sec	I_{th} (per kg of fuel) in kg-sec/kg
Hydrogen (1 kg H_2 + 40 kg air)	0.298	2420	10,120
Methane (1 kg CH_4 + 20 kg air)	0.244	2190	4,680
Gasoline (1 kg C_8H_{18} + 17.5 kg air)	0.246	2200	4,150
Petroleum (1 kg Petrol. + 17.3 kg air)	0.240	2170	4,050
Benzene (1 kg C_6H_6 + 17 kg air)	0.228	2120	3,890
Carbon (1 kg C + 13.35 kg air)	0.242	2180	3,190
Alcohol (1 kg C_2H_6O + 10.4 kg air)	0.239	2170	2,520

TABLE 20

Dependent propellants, with the air needed for combustion for a height of about 50 km	$E, 10^6$ kg-m/kg	c_{th}' , m/sec	I_{th} (per kg of fuel) in kg-sec/kg
Hydrogen (1 kg H_2 + 80 kg upper air)	0.151	1720	14,200
Methane (1 kg CH_4 + 40 kg upper air)	0.125	1565	6,550
Gasoline (1 kg C_8H_{18} + 35 kg upper air)	0.126	1570	5,770
Petroleum (1 kg Petrol. + 34.6 kg upper air)	0.124	1560	5,660
Benzene (1 kg C_6H_6 + 34 kg upper air)	0.117	1515	5,400
Carbon (1 kg C + 26.7 kg upper air)	0.126	1570	4,430
Alcohol (1 kg C_2H_6O + 20.8 kg upper air)	0.125	1565	3,420

TABLE 21

Explosion mixture with excess hydrogen	$E, 10^6$ kg-m/kg	c_{th}' , m/sec	I_{th}' , kg-sec/kg
1 kg Hydrogen + 8 kg Oxygen + 0.0 kg Hydrogen	1.36	5170	527
1 kg " + 8 kg " + 0.5 kg "	1.29	5030	513
1 kg " + 8 kg " + 1.0 kg "	1.22	4890	499
1 kg " + 8 kg " + 1.5 kg "	1.16	4770	487
1 kg " + 8 kg " + 2.0 kg "	1.11	4680	478
1 kg " + 8 kg " + 2.5 kg "	1.06	4570	465
1 kg " + 8 kg " + 3.0 kg "	1.02	4470	455

On the other hand, in Tables 19 and 20 it has been assumed that the oxygen and the neutral added mass are derived from the atmosphere (are not carried in the vehicle). The theoretical specific thrust (theoretical exhaust speed c_{th} multiplied by the effective

exhaust mass m) is then to be reckoned not relative to unit exhaust mass but relative to unit weight of the fuel carried in the vehicle and drawn from the tank in one second.

The great advantage of drawing additional mass from the atmosphere is thereby made abundantly clear.

14. Power of Rocket Motor: General

The power of a rocket motor can be divided into an internal power and an external, by exact analogy with rocket efficiency. /67

The internal power is accordingly the kinetic energy of the exhaust gas reckoned in a coordinate system attached to the motor, which provides the external power required by the vehicle via the external efficiency, which is dependent on the current state of motion of the vehicle, and via the kinetic energy of the propellant.

Here we do not have to consider the internal power, which is a quantity entirely analogous to that for a piston engine. The analogy is so close that the internal power of a rocket motor can be specified in horsepower, exactly as for a piston engine; this horsepower is dependent on the type and size of the rocket motor, can be controlled with a gas throttle, and so on, so it is an unambiguous motor parameter.

However, a quantity more characteristic of the rocket motor and also more obvious is the rocket second-thrust, which equals the momentum of the exhaust mass and which thus is calculated from the quantities m and c that govern the internal power; this is now not relative to a specified coordinate system but is absolute and independent of the state of motion provided that the motor performance remains constant. /68

This thrust equally contains the magnitude of the fuel consumption, which as regards calculation is a consequence of the definition of power and which represents a directly measurable quantity, in accordance with the fulfillment of the task of a rocket motor, namely the production of a drive force.

The thrust itself, on the other hand, is only an accessory calculated quantity as regards the internal or external power; its significance lies in economic considerations rather than in power ones.

141. The Second-Thrust

This is governed by the momentum of the exhaust gas in accordance with the relation

$$P \text{ [kg sec]} = m \text{ [kg sec}^2/\text{m]} \cdot c \text{ [m/sec]}; P = m \cdot c.$$

The energy E from the fuel delivered up by unit weight of the exhaust gas gives the thrust as

$$P = \sqrt{2\eta_i E/g}.$$

This is then primarily a function of the energy content of the mass ejected per second.

The exhaust velocity corresponding to this energy content E

$$c_{th} = \sqrt{2gE}$$

theoretically corresponds (section 111) to a combustion-chamber pressure of

$$p_0 = \frac{\kappa - 1}{\kappa} \frac{E}{V_0}.$$

The size of the combustion chamber is affected also by its relation to V_0 apart from that to the combustion-chamber pressure prescribed by E and hence can be calculated in that way, or it can conversely be found from the permissible combustion-chamber pressure specified on technical grounds together with the mass of gas required.

We have seen already in section 111 that the amount of gas that can be introduced into the combustion chamber is given by

$$G = \frac{p_0 V_{\text{combustion chamber}}}{E} \frac{\kappa}{\kappa - 1}.$$

If now the time t is specified for reasons of combustion technique, this being the time that the gas must stay in the chamber in order to burn fully, then the chamber volume required is found as follows as a function of the four specified quantities G' , E , p_0 , and t ,

/69

$G' = G/t$ being the mass of gas handled per second:

$$V_{\text{combustion chamber}} = \frac{G' \cdot E \cdot t}{p_0} \frac{\kappa - 1}{\kappa}.$$

Fig. 10 shows the combustion-chamber volume needed for 1 kg of gas as a function of E and p_0 for the case of this kilogram of

gas remaining in the chamber for 1 sec. Volumes required for other values of G or t may be found simply by multiplication by G or t .

The actual exhaust velocity c is less than that implied by p_0

on account of the loss corresponding to the internal efficiency of the rocket motor η_1 , namely

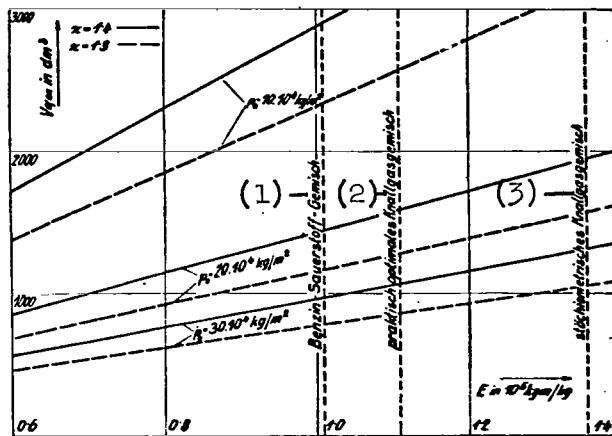


Fig. 10.

Combustion-chamber volume needed for 1 kg of gas as a function of E , p_0 and κ for $t = 1$ sec.

(1) - Gasoline-oxygen mixture; (2) - best practical explosion mixture; (3) - stoichiometric explosion mixture.

$$c = \sqrt{2g\eta_1 E} = \sqrt{19.62 \eta_1 E},$$

so the actual thrust per kilogram of gas comes out as

$$P/G = c/g = \sqrt{2\eta_1 E/g} = \sqrt{0.204 \eta_1 E},$$

and hence is controlled solely by the energy content of the fresh gas provided that the shapes of chamber and nozzle are correct; it is not dependent on the size of the combustion chamber, state of the gas in the chamber, and so on.

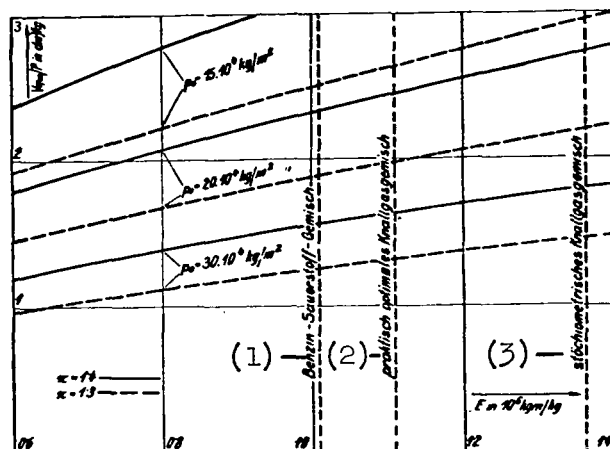


Fig. 11.

Chamber volume needed per kg of thrust as a function of E , p_0 , and κ for $t = 1$ sec.

(1) - Gasoline-oxygen mixture; (2) - best practical explosion mixture; (3) - stoichiometric explosion mixture.

The weight of gas G needed per kg of thrust is then

$$G/P = \frac{1}{\sqrt{2\eta_1 E/g}} = \frac{1}{\sqrt{0.204 \eta_1 E}}.$$

Fig. 11 shows the chamber volume needed per kg of thrust as a function of E and p_0 (the permissible pressure) for $t = 1$ sec as calculated from this relation in conjunction with Fig. 10, the relation used being

/70

$$V_{\text{combustion chamber}}/P = \frac{\kappa - 1}{\kappa} \cdot \frac{1}{p_0} \sqrt{Eg/2\eta_i}.$$

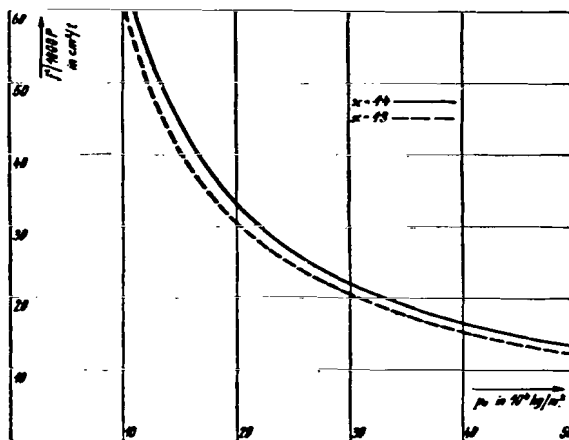


Fig. 12.

Throat area needed per ton of thrust
as a function of p_0 and κ .

The values given by Fig. 11 for the volume must be multiplied by t if other t are to be used.

If the combustion-chamber gas is extensively dissociated, which is always the case for the high-yield propellants involved, we must take as our E not the total heat energy yield but only the

part not taken up by the dissociation.

After the chamber size required for a specified thrust has been found in this way, the next point to be considered is the cross section of the throat (the narrowest cross section of the nozzle).

From section 112 we have the relation of this narrowest cross section to the weight of the gas flowing through as

$$f' = G / \left(\frac{2}{\kappa + 1} \right)^{\frac{1}{\kappa - 1}} \sqrt{2g \frac{p_0}{V_0} \frac{\kappa}{\kappa + 1}}.$$

The relation for the mass of gas needed to produce 1 kg of thrust gives us, together with the chamber-pressure relation $p_0 V_0 = (\kappa - 1)E/\kappa$, that the least cross section per kg of thrust is

/71

$$f'/P = \left(\frac{2}{\kappa + 1} \right)^{\frac{1}{1 - \kappa}} / 2p_0 \sqrt{\frac{\kappa^2 \eta_1}{\kappa^2 - 1}}.$$

This can be kept small primarily by the use of high chamber pressure; it is essentially controlled by the latter. Fig. 12 gives the throat area needed per ton of thrust as a function of p_0 for κ of 1.3 and 1.4, for which purpose $\eta_1 = 0.70$ has been assumed. The numerical relationships in the two cases are as follows:

$$f'/P = 0.607/p_0 \quad \text{for} \quad \kappa = 1.3$$

or $f'/P = 0.658/p_0$ for $n = 1.4$.

Let the maximum thrust needed for an aircraft of 21 tons all-up weight be 15 tons; a chamber pressure of 30 atm in an equal-pressure motor then implies a throat area of about 315 cm^2 , the circle diameter thus being about 20 cm.

The available energy is present mainly as heat in the throat and is then to an increasing extent converted to kinetic energy corresponding to the thrust.

The extent of this further conversion is related in a known way to the cross section ratio of the nozzle. If we allow a loss of 15% of the total energy as heat in the exhaust gas (Fig. 4), we have from section 121 that this corresponds to a ratio of cross sections $f_a/f_m = 36$, which means that the diameter at the exit of the nozzle

/72

must be 6 times that at the throat. Finally, the maximum permissible angle for the nozzle gives us that the length of the nozzle must be about 36 times the diameter at the throat. The principal nozzle dimensions are therefore derivable from Fig. 12 for any prolonged thrust. The speed of efflux is virtually independent of the chamber pressure, provided that this is not above the critical pressure, but the rocket thrust increases with the pressure, since the gas density increases. High chamber pressures must therefore be envisaged in the production of small rocket motors, especially ones with small nozzle dimension, which have constructional advantages.

The above example of a 15-ton rocket motor implies a mouth diameter for the nozzle of 1.20 m together with a nozzle length of 7.20 m.

It is a very different matter whether such dimensions can be accommodated in an aircraft. In any case, we know that the rocket power is principally governed by the outside dimensions of the nozzle.

In fact, the heat loss associated with the above nozzle dimensions is somewhat less than that quoted, because the jet emerging from the nozzle has converted almost all its energy to motion, of which a certain component is available to the rocket as net axial thrust. The loss therefore should be taken as about 30% overall at most, as was assumed in the calculation of $\eta_1 = 0.7$.

In the case of dissociation we may assume as rough approximation isothermal flow through the throat, whereupon we have similarly

$$f'/P = 1.65 \sqrt{gRT_0} / p_0 \sqrt{2g\eta_1 E},$$

in which $v' = (gRT_0)^{1/2}$ and $p' = p_0/1.65$ are the critical speed and the critical pressure of an isothermal flow. The throat cross section needed in this case is somewhat smaller for the same η_1 .

We have mentioned at some points above that the efficiency of a rocket could be kept high at low flight speeds by the addition of mass taken in from the surrounding atmosphere, which would substantially reduce the exhaust velocity and hence would increase the thrust available from a given amount of energy. Gorokhov's project (use of air as oxygen carrier for the combustion and augmentation of the mass by the balance) is not in that form directly usable for our purpose.

/73

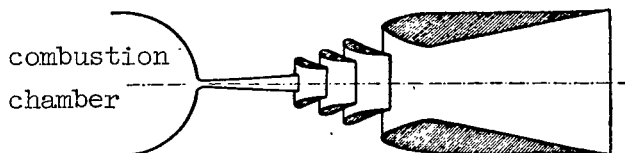


Fig. 13.

Melot's nozzle system for increasing the external efficiency of a rocket at low flight speeds.

Melot has proposed another method, in which the utilization of atmospheric oxygen is abandoned but which has the advantage of greater simplicity of design.

Fig. 13 shows Melot's nozzle schematically*; this is shaped to cause the nozzle pressure to fall below the external pressure, air being allowed to enter via lateral apertures in the nozzle. After leaving the exit nozzle proper the gas jet enters a series of Venturi nozzles, into which air is drawn by injection, this being accelerated by the jet to give finally a gas flow of lower speed but increased mass, which serves to raise the thrust. Provided that there are no losses, the conservation of energy gives us the speed from

$$c_2 = c_1 \sqrt{m_1/m_2}$$

(decrease), whereas the thrust is shown by

$$P_2 = P_1 \sqrt{m_2/m_1}$$

to increase; this provides a considerable increase in the propulsive force. Here we should not overlook the fact that Melot's nozzle merely represents a means of keeping η_a high at low flight speeds

by reducing c . Research by official French and American bodies (Conservatoire des Arts et Métiers, Paris; National Advisory Committee for Aeronautics, USA) between 1918 and 1927 would show however that no decisive advantage is to be had, at least for the usual speeds of tropospheric aircraft. In any case, it is worthy

*Anon., Ein Strahlantreibsmittel für Flugzeuge (A Jet-Propulsion Device for Aircraft). Flugsport, No. 8, 1926;
Kort, Raketen mit Strahlapparaten (Rockets with Jet Equipment). ZFM, 1932, No. 16;
Eastman, Jacobs, and Shoemaker, Tests on Thrust Augmentors for Jet Propulsion. NACA Technical Notes No. 431, September 1932, Washington.

of note that the steering fins of a rocket aircraft could be arranged to operate very much the way of Melot's nozzle within the atmosphere.

Finally, possible thrust control for a given rocket motor is of interest.

74

The theoretical maximum thrust is related to G (the amount of propellant used per second) by $P = G(2E/g)^{1/2}$, and the latter is entirely susceptible to throttling. A reduction in G causes a fall in chamber pressure in accordance with

$$p_0 = G \cdot \frac{\kappa - 1}{\kappa} \frac{Et}{V_{\text{combustion chamber}}},$$

while the specific volume V_0 of the gas in the chamber increases in the same ratio:

$$V_0 = \frac{V_{\text{combustion chamber}}}{G \cdot t},$$

the result being $p_0 V_0 = \text{constant}$. The flow speeds in the nozzle re-

main unaltered provided that the pressure ratio does not fall below the critical value, which cannot occur if $p_a = 0$. The thrust from

the gas flow in the nozzle then varies in direct proportion to the amount of gas; otherwise, the nozzle operates under equally favorable conditions. The rocket power may thus be controlled in a very simple fashion via the flow of propellant, which theoretically is without effect on the internal efficiency.

142. Internal Power

By definition, the kinetic energy of the gas emerging per second, which is available for the rocket thrust, is the internal power, which also implies that it is measured in a coordinate system attached to the rocket.

Its numerical value is given by the rocket-thrust equation $P = mc$ as

$$L_i = P \cdot c/2 = mc \cdot c/2 = P \sqrt{E\eta_i g/2}.$$

On the other hand, it is naturally related to the fuel G consumer per second:

$$L_i = G \cdot E \cdot \eta_i.$$

Figs. 10, 11, and 12 (for the thrust) readily give the internal power as a function of the dimensions of the rocket motor; this thrust has merely to be multiplied by the instantaneous value of c , the exhaust velocity.

If the 15-ton rocket above is driven by gasoline and liquid oxygen ($c = 3700$ m/sec), the internal power in horsepower comes out as:

$$L_i^{[PS]} = \frac{P \cdot c}{2 \cdot 75} = 370,000 \text{ PS.}$$

The fuel consumed per second is calculated from the internal power

and the thrust P provided as:

$$G = \frac{L_i}{E\eta_i} = P \sqrt{\frac{2g}{E\eta_i}}.$$

In this example $G = 77$ kg (of gasoline + liquid oxygen).

The experimental measurement of internal power for a given rocket motor is best performed by direct measurement of the thrust and the propellant consumed per second.

The internal power is of no particular importance apart from estimation of the fuel consumption.

143. External Power

By definition, the external power is the net energy received by the vehicle in a second. Section 1221 gives this numerically as

$$L_a = m \cdot c \cdot v.$$

The external power is then not a quantity inherent in the motor, being dependent on the flight speed.

The most notable point is that this is actually larger than the internal power $L_i = mc^2/2$ if the flight speed v is larger than $c/2$; but this does not make the rocket a perpetuum mobile, since in addition to the heat energy of the fuel represented in L_i there is the kinetic energy $mv^2/2$ consequent on the flight speed, as we have

shown in detail in section 1221.

The external power may then be calculated from the internal power in accordance with

$$L_a = (L_i + mv^2/2) \eta_a.$$

This is thus only a very conditional index of the performance of the motor. The external power of the above 15-ton rocket is 11,100, 111,000, and 1,600,000 horsepower at flight speeds v respectively of 200, 2000, and 29,000 km/hr, in accordance with the relation

$$L_a^{[PS]} = P \cdot v/75.$$

The conception of drive power in terms of horsepower is of exceptional importance for all existing means of transport, but for rocket vehicles this becomes a meaningless and purely formal calculated quantity, the thrust itself replacing it as a measure of the performance.

2. AIR FORCES

LITERATURE FOR THE AIR FORCE SECTION

A. Books: In particular, in addition to the known aerodynamics textbooks:

/76

Handwörterbuch der Naturwissenschaften (Dictionary of the Natural Sciences) vol. 4, 1913 (Prandtl, Gasbewegung (Gas Movement)).

Geiger-Scheel, Handbuch der Physik (Handbook of Physics), vol. 7, 1927 (Betz, Aerodynamik (Aerodynamics); Ackeret, Gasdynamik (Gas Dynamics)).

Wien-Harms, Handbuch der Experimentalphysik (Handbook of Experimental Physics), Vol. 4, 1931 (Eberhardt, Ballistik (Ballistics); Prandtl, Strömungslehre (Fluid Dynamics); Busemann, Gasdynamik (Gas Dynamics)).

Cranz-Becker, Lehrbuch der Ballistik (Textbook of Ballistics) 1927.

Hütte, des Ingenieurs Taschenbuch (Engineers Handbook), vol. 1, 1931 (Betz Aerodynamik (Aerodynamics); Betz, Gasdynamik (Gas Dynamics)).

Prandtl, Abriss der Strömungslehre (Outline of Fluid Dynamics) 1931.

B. Articles in periodicals and books of which only a few passages in the field covered are pertinent are introduced as footnotes at the proper places.

MEANING OF THE MOST IMPORTANT REGULARLY USED SYMBOLS

[UNITS]

a velocity of sound in gas at velocity v ;

$$a = \sqrt{a_0^2 - v^2 (\kappa - 1)/2} \quad [\text{m/sec}].$$

a' velocity of sound in gas at the critical state;

$$a' = \sqrt{2/(\kappa + 1)} \cdot \sqrt{a^2 + v^2 (\kappa - 1)/2} \quad [\text{m/sec}].$$

a_0 velocity of sound in gas at rest; $a_0 = \sqrt{\kappa g R T}$ [m/sec].

b span of a wing, greatest distance perpendicular to direction of movement [m].

c_p general coefficient for air force; $c_p = P/qF = p/q$ [-].

c_a lift coefficient; $c_a = A/qF$ [-].

c_w drag coefficient; $c_w = W/qF$ [-].

c_m moment coefficient; $c_m = M/qFt$ (moment referred to the intersection of the profile chord and the tangent perpendicular to the profile chord at the profile nose) [-].

d profile thickness, greatest frame diameter, gauge, wing thickness (maximum height of profile perpendicular to the wing chord) etc. [m].

g acceleration of gravity near the earth; $g = 9.81$ [m/sec²].

m Mach angle; $\sin m = a/v$ [°].

p air pressure [kg/m²].

q dynamic pressure $q = \frac{\gamma}{2g} v^2$ [kg/m²].

t profile depth (length of a surface in the direction of flow) wing chord (maximum extent of wing profile) [m].

/77

v flying speed [m/sec].

α profile attack angle, angle between undisturbed wind direc-

- tion (direction of flight) and profile chord, half the ogival angle [$^{\circ}$].
- γ weight of a unit volume of air [kg/m^3].
- γ_0 weight of a unit volume of air near the earth; $\gamma_0 = 1.222$ [kg/m^3].
- κ adiabatic exponent, for air: $\kappa = 1.405$.
- ϵ gliding coefficient, reciprocal of wing efficiency;
 $\epsilon = c_w/c_a$ [-].
- ϱ air density [$\text{kg}\cdot\text{sec}^2/\text{m}^4$].
- ϱ_0 air density near the earth; $\varrho_0 = 0.128$ [$\text{kg}\cdot\text{sec}^2/\text{m}^4$].
- A lift [kg], or the value of 1 mkg in kcal (mechanical heat equivalent, $A = 1/427$ [mkg/kcal]).
- F frame area, wing area (maximum projection of wing) etc. [m^2].
- R Reynolds number [-].
- R gas constant [m/deg].
- T absolute temperature (centigrade temperature + 273 $^{\circ}$) [$^{\circ}$].
- W drag [kg].

Wing profile: cross section of the wing perpendicular to the wing span.

Profile chord: for profiles with concave bottom camber it is the tangent through the profile trailing edge; otherwise, it is an especially designated reference line (generally through the trailing edge and the profile nose point farthest removed from the trailing edge).

20. AIR FORCES. GENERAL.

The force P acting on a body moving through the air at any speed is calculated according to the equation

$$P = c_p \cdot \frac{\gamma}{2g} \cdot F \cdot v^2.$$

For practical reasons this generally directed force is resolved into two component forces, lift and drag, perpendicular and parallel to the direction of movement, and correspondingly calculated from

$$A = c_a \cdot \frac{\gamma}{2g} \cdot F \cdot v^2.$$

and

$$W = c_w \cdot \frac{\gamma}{2g} \cdot F \cdot v^2.$$

The coefficients c_p , c_a , and c_w depend to a great degree upon speed; at very low speeds, without significance in aviation, they have relatively high values which rapidly decrease as speed increases; in the region of customary flying speeds they have a very flat minimum so that there they may be considered to be practically constant, increasing again as the sonic velocity is approached. In the region of the speed of sound the coefficients have a pronounced maximum, and as flying speed further increases above the speed of sound they decrease asymptotically to very low values according to a monotonous function without known limit.

Because quantitative comprehension of lift is generally somewhat simpler than that of drag, we will take up the former first.

Because flow phenomena differ basically at flying speeds below and above the speed of sound in air, and in addition air forces in the subsonic and supersonic regions of flying speed are very different, the treatment of both lift and drag in each of the two regions must be done separately.

The "Air Forces" section is therefore subdivided into the topics:

1. Lift in the subsonic region,
2. Lift in the supersonic region,
3. Drag in the subsonic region,
4. Drag in the supersonic region.

The necessity for treatment of air forces in the supersonic region follows from the fact made known in the section on "Propulsive Forces," that the external efficiency of the rocket assumes favorable values only at very high flying speeds which at times are several times the speed of sound. The configuration of fuselage and especially the wings of the rocket plane must thus be such that the plane structure completely fulfills its purposes at speeds far above the sonic. On the other hand, the air forces must also be adequate at the low speeds of takeoff and landing, although at these speeds the aerodynamic airplane efficiency, that is, the most favorable ratio c_a/c_w , is of less importance than it is to have c_a as large as

possible. It is thus necessary to evaluate the findings of each of the above cited topics 1 to 4 for a further important topic, namely determination of the most favorable

5. Fuselage and wing form of the rocket plane.

The proper understanding of air forces at all flying speeds is of basic importance for the calculation of flying performances to be made later, but here we must emphasize that the aerodynamic quality of the rocket plane, if we understand this to be as usual the most operationally favorable ratio of c_a/c_w , does not play anywhere

near the role for performance and economy that it does for the presently common tropospheric airplane.

It thus should not cause anxiety to anyone if in the course of further investigations it is found that the ratio of supporting lift forces to the power-consuming drag forces above the speed of sound is not anywhere near as favorable, because of aerodynamic, or expressed better, gas-dynamic reasons, as that which we shall come to expect in the near future of high-performance tropospheric airplanes.

21. LIFT IN THE SUBSONIC REGION. GENERAL.

If a body moves at given speed v through the air, then there is always an air force component W counter to the direction of movement; it is called drag, and to overcome it a secondary effort of magnitude $W \cdot v$ must be exerted. This drag is discussed in Sections 23 and 24. In addition, an air force component perpendicular to the direction of movement can appear; this is called lift in aeronautics and requires no expenditure of work. This component will concern us in Sections 21 and 22.

When the lift for a body is high in comparison with the energy-consuming drag, the body is called a wing, and its efficiency is indicated by the ratio of lift to drag.

211. TWO-DIMENSIONAL THEORY OF LIFT ON A SINGLE WING IN INCOMPRESSIBLE FLOW.

At flying speeds up to about 0.2 speed of sound the pressure differences in flow around a body are so small compared with the

atmospheric pressure of still air ($10,330 \text{ kg/m}^2$) that the air can be approximately considered as an incompressible medium, like water; the laws of hydrodynamics then are valid for air.

The air pressure on the upper surface of a body experiencing lift must on average be less than that on the undersurface. If we consider the flow around the body to be steady-state then there is the following relationship between p_x and local speed v_x :

$$p_x + \frac{\gamma}{2g} \cdot v_x^2 = \text{const.},$$

i.e., where the pressure is low the velocity must be high and vice versa.

If the line integral of velocities is taken along an arbitrary line enveloping the wing we obtain a finite circulation Γ , because the high velocities of the wing's upper surface outweigh the lower ones on the undersurface.

This circulation Γ is related to lift on a wing element of

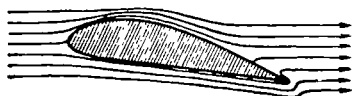


Fig. 14a. Subsonic flow around a wing profile; pure translation flow.

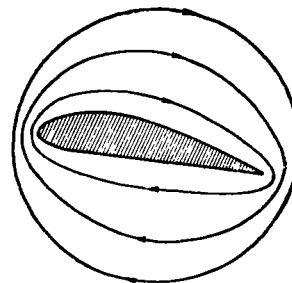


Fig. 14b. Subsonic flow around a wing profile; pure circulation flow.

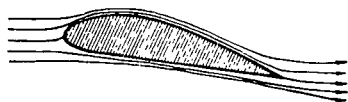


Fig. 14c. Subsonic flow around a wing profile; superimposed translation and circulation flow.



Fig. 14d. Subsonic flow around a wing profile; actual profile flow with region of dead space.

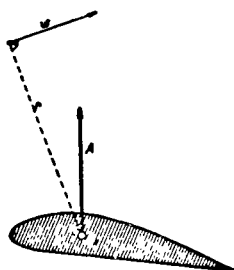


Fig. 15. Flow phenomena at great distances from the profile.

width b of the wing conceived to be infinitely wide by means of the Kutta-Joukowski equation:

$$A = \frac{\gamma}{g} v \Gamma b.$$

The lift coefficient then becomes:

$$c_a = 2\Gamma/vt.$$

Flow around the profile itself consists of pure translation flow without circulation (Fig. 14a) at a given translation v and of pure circulation about the wing (Fig. 14b) without translation. The value of this circulation flow determining the lift results from the experiential fact that in the actual flow around the profile, which is occasioned by superposition of the two sketched potential flows, there is neither a flow around the sharp profile trailing edge from above downward (predominantly circulation) or from below upward (predominantly translation). Fig. 14c shows the resultant flow. In actuality, of course, the circulation is somewhat smaller because the high pressure gradient on the suction side of the profile results in considerable boundary layer separation, in turn causing a dead-air region on the suction side (Fig. 14d). This pushes the streamlines upward, and this corresponds again to a lesser circulation. The dead space therefore results in a reduction in lift and an increase in drag, thus reducing the wing efficiency.

Because circulation can not occur in practically frictionless free air flow, a viscous boundary layer on the body surface must be drawn upon to explain its origin; this then readily leads to the fact that with every acceleration of the wing a "starting vortex" is released from the entire length of the wing's trailing edge; in circulation amount it equals the circulation change on the wing corresponding to the lift change and is directed oppositely.

When the attack angle of a wing is increased, circulation and thus lift immediately increase. This further increases the suction side pressure drop and this again increases boundary layer separation, so that dead air space and drag increase with angle of attack until finally the boundary layer can no longer follow the body surface and the flow completely separates from the suction side. An irregular decrease in lift coefficients and increase in drag coefficients then occur. These phenomena limit lift coefficients for normal profiles to $c_{a \max}$ of 1.2 to 1.4 maximum. With highly cam-

bered profiles $c_{a \max}$ can reach approximately 2.0.

By special effects on the boundary layer, such as use of slotted wings (acceleration of the boundary layer by mixing of high energy flow from the pressure side), suction wings (partial suction of the endangered boundary layer into the interior of the wing) or rotor wings (artificial transport of the boundary layer against the suction side pressure increase by a moving wing surface, the Magnus effect), even higher lift coefficients may be obtained although the wing efficiency always suffers.

To calculate disturbance phenomena at some distance from the wing it is advantageous to make use of the previously described resolution of flow into translation and circulation.

If it is noted that the disturbance caused by translation decays according to the square of the distance from the wing but the disturbance from circulation only linearly, then it is readily seen that at a distance from the wing greater than half the wing chord only circulation flow need be considered, so that the disturbance movement w at distance r from the point of application has the magnitude:

$$w = \Gamma / 2r\pi$$

and is perpendicular to vector r (Fig. 15).

The wing form must be taken into consideration when the potential flow in the immediate vicinity of the wing is investigated.

The conformal mapping method of Kutta-Joukowski-Blasius, or the replacement of the wing by vortices, sources, and sinks according to Prandtl-Birnbaum, is used.

With the aid of these methods, lift can be theoretically determined in magnitude, direction, and point of application for various profiles.

For certain simple, analytically comprehensible, thin profiles the well-known definite equations for lift and moment coefficients (see Hütte), which also agree for moderately thick profiles whose center line coincides with the thin profile, are valid.

Recently * definite equations have been published for general profiles too. If the abscissa axis is placed in the wind direction

* Munk, "Fundamentals of Fluid Dynamics for Aircraft Designers." Ronald Press, New York, 1929.

through the wing trailing edge and the coordinates of the trailing edge are chosen as: $x = t/2$, $y = 0$ then according to Munk:

$$c_a = 2 \int \frac{y}{(t/2 - x)\sqrt{(t/2)^2 - x^2}} dx,$$

$$c_m = \int \left[\frac{1}{t/2-x} - \frac{4x}{t^2} \right] \frac{y}{\sqrt{(t/2)^2 - x^2}} dx.$$

212. THREE-DIMENSIONAL THEORY OF LIFT ON THE SINGLE WING IN INCOMPRESSIBLE FLOW.

The previously discussed two-dimensional lift theory assumes wings of infinite span.

In reality, the suction-side negative pressure and pressure-side positive pressure can equalize by flow around the lateral wing edge so that on the pressure side there is a pressure gradient toward the lateral wing edge and on the suction side a pressure gradient from this edge.

This pressure gradient transverse to the direction of movement results on one hand in a decrease in lift for a given angle of attack in comparison with the two-dimensional problem, and this must be balanced by increasing the angle of attack by

$$\Delta\alpha = 57.3^0 \cdot (c_a/\pi)(F/b^2)$$

and on the other hand the streamlines, especially near the wing tips, are directed out of the principal flow direction on the pressure side toward the tip and on the suction side away from the tip (Fig. 16). Flow around the wing tip causes the so-called induced drag here, which we will study further in 233, and in addition the distribution of lift over the longitudinal extent of the wing ceases

to be a constant, decreasing instead to zero at the wing tips. For the elliptic and similar wing plan forms (closely approximated also by rectangular wing forms) most favorable in regard to induced drag, the longitudinal distribution assumes the form of an ellipse with major axis coinciding with the longitudinal axis of the wing. If it is assumed for narrow wings that the lift in the wing center coincides reasonably closely with that of an infinitely long wing, then the lift loss ΔA resulting from the decrease at the wing tips for a wing with rectangular plan from the difference in rectangular and elliptical lift distribution amounts to about 20% of the total lift.

/83

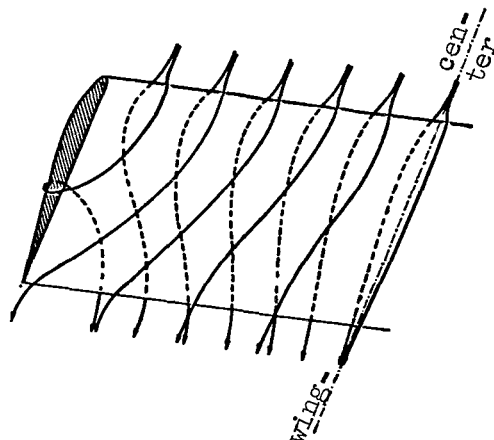


Fig. 16.

Three-dimensional flow around the wing at subsonic speed.

The longitudinal component of the streamlines, so fateful but yet unavoidable for our usual wings because of this lift loss and the considerable induced drag, is directed on the pressure side toward the wing tip; it appears to have been used advantageously by nature for the better flyers among the birds. By use of concave profiles on the pressure side, the formation of longitudinal flow has been powerfully promoted, and this flow has been directed along the wing toward the downwardly bent wing tip with a speed that can considerably exceed that of the actual flying speed. The tip

directs it downwardly and then allows it to shoot forth beneath the wing tip, producing a considerable additional lift that results in no new drag because the drag component arising from this lift is in the longitudinal direction of the wing and thus perpendicular to the flying direction; it finds its reaction in the equal force of the other wing tip. In addition, through the overshooting of the wing tip in the longitudinal direction of the wing the conditions for formation of tip vortex and thus induced drag are favorably influenced (Fig. 17)* .

/84

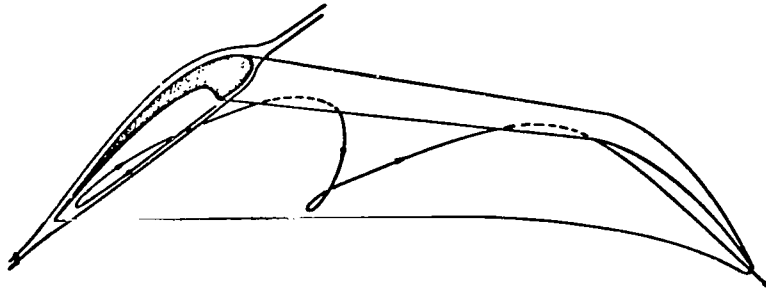


Fig. 17.

Three-dimensional flow on a bird's wing, according to G. Lilienthal.

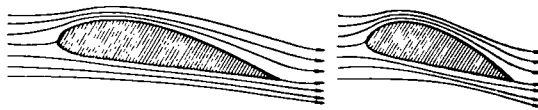


Fig. 18.

Streamline analogy for understanding compressible flow past a profile.

* For further details, see: Lilienthal, G., "Die Biotechnik des Fliegens" (The Biotechnics of Flight), 1925; Sanger, E., "Über Flügel hoher Güte" (High Efficiency Wings) Flugsport, April 1931.

213. TWO-DIMENSIONAL THEORY OF LIFT FOR A SINGLE WING IN A COMPRESSIBLE FLOW *

At flying speeds v above 0.2 sonic velocity in air, the pressure differences in flow around a body in comparison with absolute atmospheric pressure manifest themselves to such a degree that the compressibility of the air may no longer be neglected. Since pressures and velocities are related by the Bernoulli equation, velocities may be used as a scale instead of pressures.

As a result of rigorous theoretical considerations, Glauert concludes that as long as flow velocity v_x does not exceed sonic

velocity a at any point on the profile, lift in a compressible

medium equals $(1 - v^2/a^2)^{-1/2}$ times lift in an incompressible medium. The highest local surface velocities v_x occur at the profile shoulder,

but according to Glauert, v_x for profiles of medium thickness hardly

exceeds $2v$, so for these profiles the theoretical equation gives a good approximation up to about $v = 0.5$ to $0.6a$. The validity limit is correspondingly lower with thick profiles, and for very thin profiles it increases to nearly $v = a$ in the limiting case. At $v = 0.6a$, lift in the compressible medium has increased by 25% over lift in the incompressible medium. As soon as local surface velocity at the profile shoulder exceeds sonic velocity, compression waves occur, leading to rapid decrease in lift and increase in profile resistance. The limit of validity of the equation and thus of favorable profile behavior depends not only on profile shape, being attained more readily at high lift values than at lower.

Summing up, Glauert reaches the following general conclusions:

/85

* Bryan, "The Effect of Compressibility of Stream Line Motions." Techn. Rep. of the Advisory Comm. for Aeronautics, Rep. 55 (1918), Rep. 640 (1919) London; Glauert, "The Effect of the Compressibility on the Lift of an Aerofoil." Trans. Roy. Soc. London (A) 118, 113, 1928; Busemann, "Profilmessungen bei Geschwindigkeiten nahe der Schallgeschwindigkeit." (Profile Measurements at Speeds Near Sonic Velocity) Yearbook of the WGL (Wissenschaftliche Gesellschaft für Luftfahrt = Scientific Society for Aeronautics), 1928.

1. When speed increases from zero to $0.6 a$, lift coefficient increases by the factor $(1-v^2/a^2)^{-1/2}$, and the zero-lift angle of attack remains unchanged.

2. Lift decreases between $v = 0.6 a$ and $v = a$, but the critical velocity at which lift begins to decrease rapidly, depends upon the profile shape. The rapid decrease probably appears sooner at the higher lift coefficients.

Busemann reaches similar conclusions with the aid of so-called "streamline analogy." According to him, a useful picture is obtained if the streamlines of incompressible flow are imagined materialized of sheets between which the compressible flow occurs, with its pressures established by the streamline sheets. The negative and positive pressure referred to dynamic pressure are greater

by $(1-v^2/a^2)^{-1}$ in compressible flow than in incompressible. In compressible flow therefore the centrifugal forces are not enough to preserve the balances between the increased positive and negative pressures, as is the case in incompressible flow. If, however, the entire flow pattern including the profile is shortened in the flow

direction by $(1-v^2/a^2)^{1/2}$, then all radii of curvature and thus centrifugal forces increase by the required amount (Fig. 18). If the course of flow is known in the incompressible case, then the flow patterns for compressible flow can be found in the same case for all v/a values. Thus it is found for the flat plate and for an arc with exact slightly bent thin profiles that lift is increased by

the factor $(1-v^2/a^2)^{-1/2}$; this has approximate validity. The method assumes streamlines of low curvature and absence of pronounced flow around edges.

The so-called "potential line analogy" reaches the same conclusions in another way. It proceeds from the conversion of potential lines, instead of the streamlines above, from the incompressible to the compressible case. To keep the streamlines that are orthogonal to the potential lines less convergent and divergent, the curvature of the potential lines must be reduced by the distortion described in the streamline analogy but extending only to the potential lines. The delimitation of the body in the flow results as a streamline orthogonal to the potential lines after the distortion. The connecting line of the leading and trailing branch points of the streamline on the body is chosen as principal distortion direction, because otherwise the distorted body contour would not form a closed

line. The body thereby has its thickness decreased by the factor

$(1-v^2/a^2)^{1/2}$ and the angle of attack is analogously reduced; this is exactly opposite to the streamline analogy. In addition it is seen here too that the course of compressible flow is qualitatively similar to that of incompressible flow, but with increasing speed the density decreases, so that at points of higher speed the streamline interval is relatively larger than with incompressible flow. However, since speed is higher for convex curvatures and lower for concave curvatures, compressibility has the effect of an intensification of streamline curvature.

The potential line analogy finds practical expression in the Prandtl rule*, which is valid to about $v/a \approx 0.8$ for slender bodies with surface elements inclined at small angles to the undisturbed flow:

"If flow of an elastic 'compressible' liquid with a velocity $v < a$ occurs around a flat body, then the pressures acting on the body are the same as for a corresponding body in inelastic fluid at the same velocity and density when the ordinates y of the body in

the elastic fluid are related to the corresponding ordinates y' of the body in the inelastic fluid by:

$$y/y' = \sqrt{1 - (v/a)^2}.$$

"Because of the same pressure distribution, the requirements for vortex separation are approximately the same in both cases."

Thus a flat plate in a compressible medium, for example, at angle of attack α , is found to have the same lift as in the incompressible medium at angle of attack $\alpha' = \alpha/\sqrt{1 - v^2/a^2}$.

According to the Prandtl rule, wing profiles in compressible

* Ackeret, "Über Luftkräfte bei sehr grosser Geschwindigkeiten, insbesondere bei ebenen Strömungen." (Air Forces at Very High Speeds, Especially for Two-Dimensional Flows) Helvetica Physica, Acta I.

media have the same properties as in incompressible media if profile thickness, camber rise, and angle of attack are reduced in the ratio

$$\sqrt{1 - v^2/a^2}.$$

The relationships for the case that sonic velocity is exceeded in part, while flying speed itself is still below or barely above sonic velocity (the region from about $v = 0.8 a$ to $v = 1.2 a$ for thin profiles), have scarcely been investigated theoretically as yet.*

/87

214. THREE-DIMENSIONAL THEORY OF LIFT FOR A SINGLE WING IN A COMPRESSIBLE FLOW **

The relationships found in three-dimensional theory of lift for the individual wing in incompressible flow can be transferred in simple fashion to compressible flow conditions if use is made, as Busemann did, of a three-dimensional extension of the streamline analogy or the potential line analogy.

In the streamline analogy the wingspan b is distorted in the same degree as the wing thickness d .

In the potential surface analogy, the wing chord t is unchanged and the wing span b is lengthened in the same degree as the wing thickness d and the angle of attack α are reduced. (It follows that the wing plan with the potential surfaces, defined by the stagnation points, is distorted, while the wing profile is only supplementarily shown as a streamline orthogonal to the distorted potential surfaces.) The three-dimensional application of the potential surface analogy is limited to the case of approximately developable potential surfaces.

In the compressible case the lift distribution at the lowest induced drag is elliptical over the wing span, and the induced drag is correspondingly calculated.

* Bateman, Proc. Roy. Soc. London (A) 125, 598 (1929); Taylor, Z. f. angew. Math. u. Mech., Vol. 10, 334 (1930).

** Busemann, in Wien-Harms "Handbuch der Experimentalphysik" (Handbook of Experimental Physics), Vol. IV, p. 441, 1931.

215. RESULTS OF EXPERIMENTS ON WING PROFILES AT LOW SPEED

The results of wing profile experiments in ordinary wind tunnels at about 20 to 60 m/sec undisturbed flow velocity have only indirect value for our purposes.

In addition, the results of systematic test series in the reports of the various institutes (Göttingen, Eiffel, etc.) are so detailed and so well known that we may dispense with them here.

The influences of systematic change of mean camber, chord thickness, shaping of the profile leading and trailing edges, properties of stationary pressure point profiles, slotted profiles, etc., can be studied there.

216. RESULTS OF EXPERIMENTS ON WING PROFILES AT HIGH SPEED

Tests on wing profiles with approach velocities of 150 to 350 m/sec, although very important for our purposes, are very rare.

The most complete series of experiments has been carried out by Briggs * at the instance of the American government. Fig. 19 and the following summary are a brief excerpt from those results.

1. Lift Coefficients as a Function of Speed v .

For the thickest profile ($t/d = 5$), c_a is constant only for angles of attack of about 0° and $v/a < 0.65$; at higher speeds it increases with negative angles of attack and decreases with positive ones. With thinner profiles, c_a does not change up to higher v/a

values, but after reaching a critical value it suddenly decreases for all angles. This decrease can be observed for negative angles of attack too. The angle for $c_a = 0$ becomes increasingly negative

* Briggs, Hull, Dryden, "Aerodynamic Characteristics of Airfoils at High Speeds." N.A.C.A., U.S.A., Rep. 207, 465 (1924); Briggs, Dryden, "Pressure Distribution over Airfoils at High Speeds." Ibid., Rep. 255, 555 (1926).

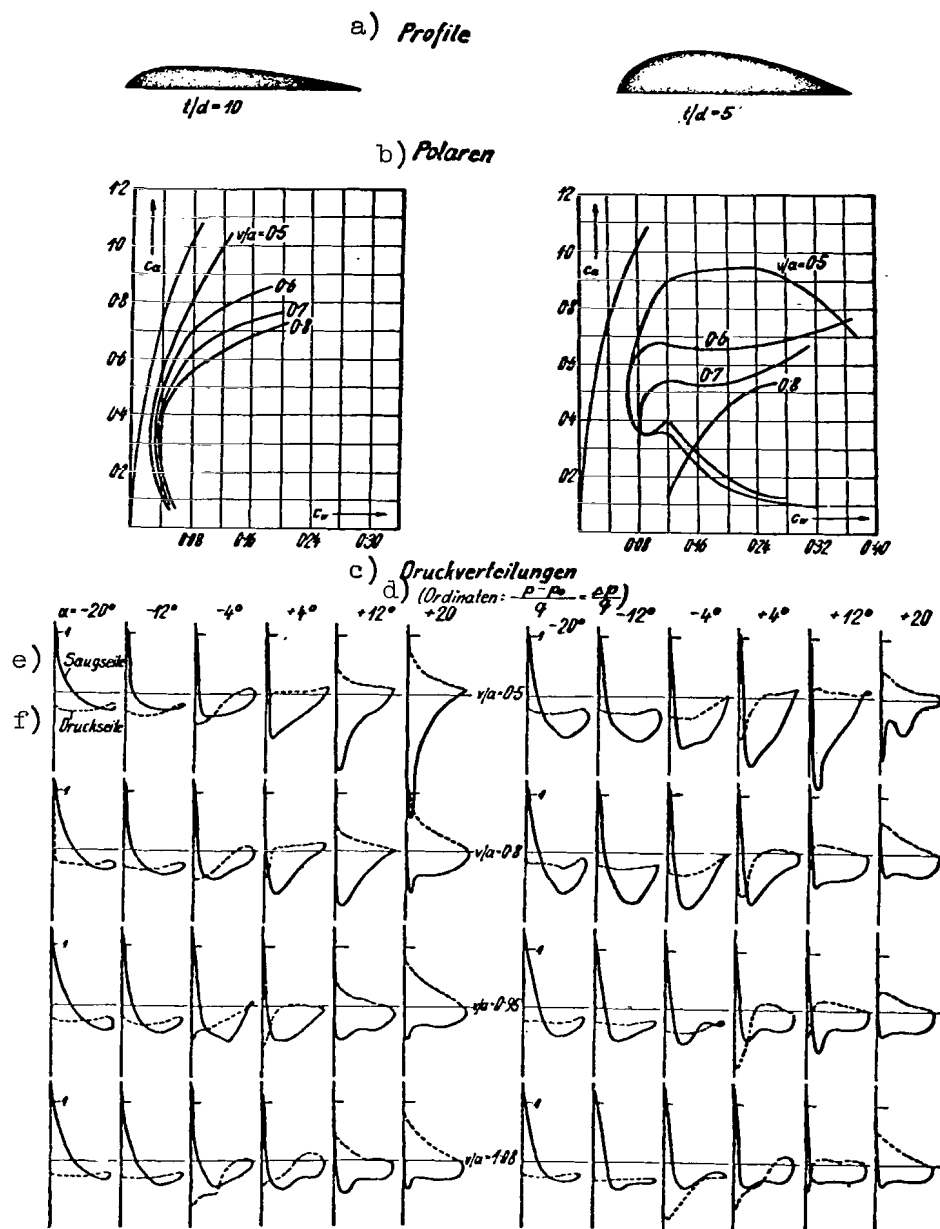


Fig. 19.

Excerpt from Briggs' test results on air forces on wing profiles at high speed.

a) profiles; b) polar curves; c) pressure distribution; d) ordinates; e) suction side; f) pressure side

as speed increases.

2. Polar Curves for Lift and Drag Coefficients c_a and c_w .

Induced drag is plotted from the usual equations $c_{wi} = (c_a^2/\pi)(F/b^2)$ with $F/b^2 = 0.24$. The remaining profile drag itself is not constant at low speeds. At $c_a < 0.4$, and thus negative α , it is fairly obscure. At higher speeds it increases more and more for a given c_a , and $c_{a \max}$ becomes smaller. Thin profiles behave much better than thick ones.

3. Pressure Distribution Curves.

The pressure distribution curves show characteristic zones of flow separation, characterized by a sharp peak followed by constant drop, such as is also observable on cylinders or spheres after flow separation. For each profile there is a critical angle of attack and a critical speed at which flow separation occurs. Localization of separation is made easy by the fact that for turbulent flow the pressure at the trailing edge is less than the static pressure, while the opposite is true in laminar flow. The separation appears to occur suddenly in a narrow region, increasing very rapidly with speed or α . The fact that separation begins at the maximum ordinate of the thin profile is not entirely clearly explainable from the pressure curves alone, although indications for this can be observed. The sudden separation is the cause of the drop of c_a and shows

clearly therein. For thin profiles it appears between 0.8 a and 0.95 a at small angles, and for thick profiles between 0.65 a and 0.80 a. Separation seems to depend more upon compressibility (v/a) than upon Reynolds number, and in addition, higher wing fineness seems to promote separation. The highest observable pressure drop on the suction side is 37 cm Hg or $p/p_0 = 0.51$. The similarity to

the critical air ratio $p/p_0 = 0.53$ warrants the conclusion that this

drop can not be exceeded in Bernoulli flow. Lower pressures (down to 0.25 atm) have been observed only in turbulent flow. Observations of flow near the profile, made with the aid of a soot film dissolved in oil, showed at $v/a = 1.08$ and $\alpha = 0$ degrees on the thinnest ($t/d = 10$) and the thickest ($t/d = 5$) profiles that the

flow separates from the upper surface at 0.43 and 0.29, respectively, chord length from the profile leading edge, and that the resulting vacuum is filled by an air flow from the underside of the wing around the profile trailing edge upward and forward. A readily visible flow region, oppositely directed to the principal flow, forms on the upper surface. The turbulent region for thinner profiles begins directly behind the maximum ordinate, and for thick profiles at the trailing edge. Experiments with filaments showed the same results. The counterflow, initially very thin, rapidly increases as angle of attack increases. At low speeds the reverse flow begins at relatively high angles of attack and is identical with the familiar flow separation. At high speeds it begins at low angles of attack and is accompanied by rapid decrease in c_a and rapid increase in c_w .

In summary, Briggs' extensive experiments show:

1. The value of c_a decreases very rapidly for increase in speed at a given angle of attack. The cause is probably separation phenomena on the suction side and filling of the resulting vacuum by flow around the trailing edge.
2. The value of c_w increases rapidly under the same conditions, probably because of the increased energy used in wave formation when the sonic velocity is exceeded locally at the profile shoulder.
3. The pressure center moves toward the trailing edge.
4. The critical speed at which the coefficients begin to change rapidly decreases with increasing angle of attack and increasing profile thickness.
5. The angle of attack for $c_a = 0$ increases to high negative values and then suddenly becomes zero.
6. The critical velocity is indicated by the inception of flow separation on the suction side.

22. LIFT IN THE SUPERSONIC REGION. GENERAL.

Although the transition of flying speed from subsonic speed to supersonic speed does not involve discontinuous changes in flow conditions on the wing profile, since even at flying speeds far below sonic velocity the latter is exceeded at various regions on the surface and these regions are merely extended as flying speed increases, nevertheless this transition considerably facilitates theoretical treatment, because if sonic velocity is sufficiently exceeded it is necessary to investigate only supersonic flow patterns; they are to some extent simpler to study quantitatively than those of pure subsonic flow, not to mention the speed region in which both types of flow exist.

Of course, here too, some more or less valid assumptions must be made. First of all, frictional forces are completely neglected, as in the treatment of subsonic lift; they are hardly significant. In addition, however, no account may be taken of the suction-side separation phenomena, which are very significant here. Finally, the flow is assumed free of external forces, vortices, and heat transfer.

Although the forces can scarcely be calculated with complete certainty for a given profile, nevertheless the limits within which they are to be expected are fairly well determinable.

Some properties of supersonic flow may be alluded to here.

Although the air flowing around a body at subsonic speed is accelerated in flow past the body because the space is narrow, it is decelerated when it flows past at supersonic speed.

Furthermore, in supersonic flow, waves are formed that resemble the surface waves of water, especially those accompanying a moving vessel.

Finally, supersonic flow shows the characteristic, entirely foreign to subsonic flow, that disturbances in it are never felt upstream but only downstream within a cone of very definite aperture angle with peak at the center of disturbance.

/92

221. TWO-DIMENSIONAL THEORY OF LIFT ON THE SINGLE WING IN PURELY SUPERSONIC FLOW

2211. FLOW AROUND A PROJECTING EDGE.

The first fundamental analytic solution of this three-dimen-

sional problem comes from Prandtl-Meyer *. We first consider a gas flow at supersonic velocity parallel to a wall A-B (Fig. 20). A small obstacle at C is assumed to cause a slight disturbance in the uniform gas flow. The disturbance propagates itself in cylindrical waves relative to the moving gas with the sonic velocity for the gas temperature. The position of such a cylindrical wave at various times is shown by the circles drawn. The circle radius increases with elapsed time, $r = a \cdot t$. The circle's center displaces at velocity v , so that $s = v \cdot t$. All positions therefore have an envelope C-D, which makes angle m with the flow direction and is known as the Mach angle.

$$\sin m = r/s = a/v.$$

The envelope is therefore present only when $v > a$.

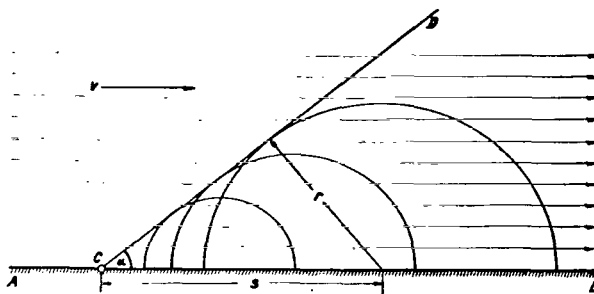


Fig. 20.

Two-dimensional supersonic flow parallel to a plane wall.

* Meyer, "Über zweidimensionale Bewegungsvorgänge in einem Gas, das mit Überschallgeschwindigkeit strömt." (Two-Dimensional Motion Phenomena in a Gas Flowing at Supersonic Velocity) Mitt. Forschungsarbeiten VDI, No. 62, 1908. Part of this is according to Ackeret's presentation in Scheel's "Handbuch der Physik" (Handbook of Physics).

The waves which continuously newly form at point C give a noticeable disturbance only where they are thickest, which is along the Mach line C-D. After sonic velocity is exceeded, a disturbance in the gas can therefore not be propagated against the flow but is carried along by the flow, being propagated in it at the Mach angle.

/93

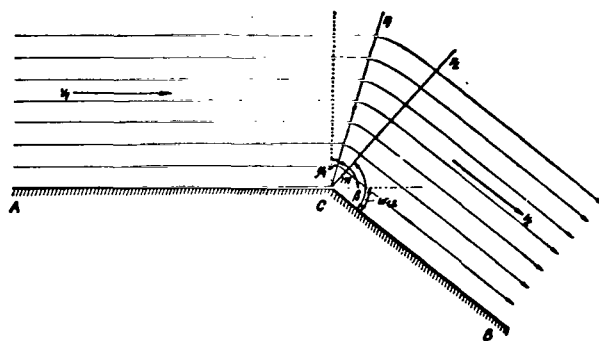


Fig. 21.

Two-dimensional supersonic flow around a projecting edge.

Next, the special case of flow around a corner will be discussed (Fig. 21); here the gas state along a radius is constant. The disturbance in the supersonically moving gas at the corner propagates itself into the gas at the Mach angle. The streamlines parallel to the wall A-C experience a deflection along this radius r_1 because the expansion begins there. After sufficient expansion

the streamlines continue parallel to wall C-B along the second Mach angle β . The expansion can be conceived of as a phenomenon produced by an infinite number of elemental disturbances penetrating the interior gas flow at the Mach angle from the corner. The phenomenon is in essence the same as that accompanying emergence of a gas expanding into the open air. Since a separating layer forms between the emerging gas and the outer still air, the solid wall C-B can be

replaced by quiet external gas masses into which the jet expands. In this case the gas expands until the pressure obtaining in the gas stream equals the pressure of the gas masses into which it flows and then continues in parallel streamlines. If the blunt corner is straightened out, the limiting case of Fig. 20 results. Compression appears if wall C-B is rotated further. Treatment analogous to the previous would result in self-penetration of the flow. However, since this is not possible, a discontinuity arises; this is the compressive pulse causing sudden pressure increase; we shall treat this separately.

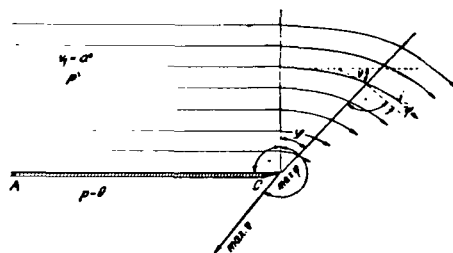


Fig. 22.

Two-dimensional supersonic flow
around the end of a plane wall.

If we therefore imagine for expansion that wall A-C stops at C and wall C-B is thus entirely removed, and, in addition, that the pressure on the under side of A-C is lower than on the upper side, then the pressure drop in the flow around C in the region A-C- r_1

94

again does not manifest itself until radius r_1 , which is determined

by the Mach angle $\sin \mu = a/v$, is reached. The pressure drop causes flow deflection just as with the blunt corner. Under the assumption of frictionless and forceless flow, adiabatic change of state, and absence of turbulence, it is found that again all variables of state and velocity are independent of r , the beginning of the deflection is at radius r_1 , the end is at radius r_2 , and the streamlines are

curved inside $r_1 r_2$ and straight outside. In addition they are geo-

metrically similar with the similarity center at C.

In further reasoning it is first assumed for simplification that the gas approaching along A-C has exactly sonic velocity a' and that expansion occurs to zero pressure, so that on the other side of the wall the pressure $p = 0$ (Fig. 22). The pressure drop then begins along the Mach wave going outward from C at 90° to A-C, and extends through angle φ .

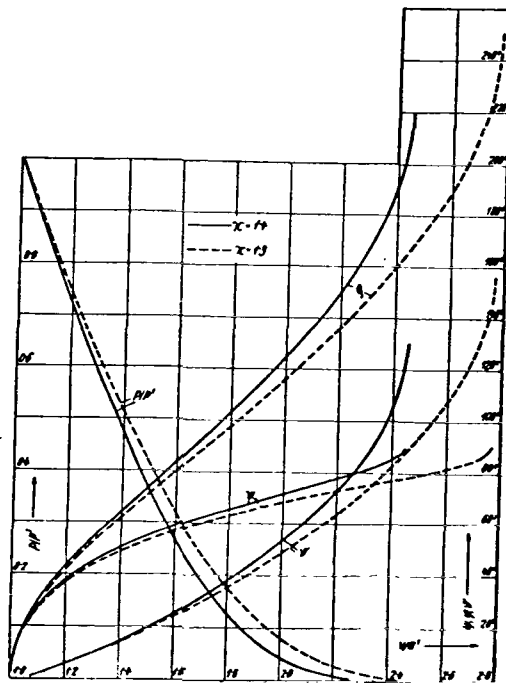


Fig. 23.

Graph of relationship between gas quantities of state and the deflection angle in expansion around an edge for air ($\kappa = 1.4$) and superheated water vapor ($\kappa = 1.3$), according to the Betz representation.

The velocity potential in this case is:

$$\Phi = \sqrt{2 i_0/A} \cdot r \sin \left(\sqrt{\frac{\kappa - 1}{\kappa + 1}} \varphi \right),$$

in which A is the mechanical equivalent of heat, i.e., i_0 is the heat content of the gas per unit of mass in the state before beginning of movement, and therefore

$$\sqrt{2 i_0/A} = v_{\max} = a' \sqrt{(\kappa + 1)/(\kappa - 1)},$$

i.e., the maximum speed at adiabatic expansion to zero pressure.

The velocity components resulting from the velocity potential are:

radial:

$$v_r = \frac{\partial \Phi}{\partial r} = \sqrt{2 i_0/A} \sin \left(\sqrt{\frac{\kappa - 1}{\kappa + 1}} \varphi \right),$$

tangential:

$$v_t = \frac{\partial \Phi}{r \partial \varphi} = \sqrt{2 i_0/A} \sqrt{\frac{\kappa - 1}{\kappa + 1}} \cos \left(\sqrt{\frac{\kappa - 1}{\kappa + 1}} \varphi \right),$$

both independent of r .

The parameters of state, also independent of r , follow from

$$(i_0 - i)/A = (v_r^2 + v_t^2)/2 \text{ and in addition } v_t = a'.$$

Pressure as a function of φ is:

$$\varphi = \frac{1}{2} \sqrt{\frac{\kappa + 1}{\kappa - 1}} \arccos [(\kappa + 1)(p/p_0)^{\frac{\kappa - 1}{\kappa}} - 1],$$

in which p_0 is the initial pressure when the gas is still.

Upon expansion in perfect vacuum p becomes equal to zero, and

$$\varphi_{\max} = \frac{\pi}{2} \sqrt{\frac{\kappa + 1}{\kappa - 1}}, \text{ i.e., the entire lower half-space will not be}$$

filled by the curving flow. For φ_{\max} , $v_t = a' = 0$, and the velocity therefore becomes purely radial, with all streamlines approximating this direction. For air ($\kappa = 1.405$), φ_{\max} becomes $219^\circ 19'$.

The polar equation of the streamlines is

$$r = r_0 \left[\cos \left(\varphi \sqrt{\frac{\kappa - 1}{\kappa + 1}} \right) \right] - \frac{\kappa + 1}{\kappa - 1}$$

For practical application of the method the angles $\psi = \pi/2 - \varphi$ shown in Fig. 22 and the deflection angle $\gamma = \varphi - \psi$ are of interest. The equation:

$$\tan \psi = \sqrt{\frac{\kappa + 1}{\kappa - 1}} \tan \left[\varphi \sqrt{\frac{\kappa - 1}{\kappa + 1}} \right] \quad \cos \psi = a/v.$$

relates φ and ψ .

Because all the parameters of state, pressures, flow velocities, etc. depend upon only one variable, but ψ , φ and γ are related uniquely, each of the three angles can be chosen as independent variable. In Fig. 23 and Table 22 the relationships calculated by Meyer from the above equations are shown for air in the region of $p/p_0 = 0$ to

$$p/p_0 = \left(\frac{2}{\kappa + 1} \right)^{\frac{\kappa}{\kappa - 1}}$$

For $p/p_0 = 0$ we obtain the function values for flow into perfect vacuum, and for $p/p_0 = 0.527$ with $\kappa = 1.405$ (air), the

TABLE 22

p/p_0	φ		ψ		$v = \varphi - \psi$		v/a	v/a'	Pressure factor, according to Busemann
	0	'	0	'	0	'			
0	219	19	90	00	129	19	∞	2.44	--
0.01	135	33	74	19	61	14	3.70	2.089	--
0.02	125	23	71	51	53	32	--	--	946.50
0.03	118	23	70	06	48	17	2.935	1.942	951.50
0.04	113	05	68	40	44	25	--	--	955.50
0.05	108	39	67	24	41	15	2.600	1.850	958.66
0.06	104	51	66	16	38	35	--	--	961.50
0.07	101	26	65	13	36	13	--	--	963.75
0.08	98	21	64	14	34	07	2.300	1.749	965.80
0.09	95	30	63	17	32	13	--	--	967.80
0.10	92	51	62	23	30	28	2.153	1.695	969.50
0.11	90	22	61	30	28	52	--	--	971.14
0.12	88	00	60	39	27	21	2.040	1.649	972.57
0.13	85	45	59	48	25	57	--	--	974.00
0.14	83	37	58	59	24	38	--	--	975.37
0.15	81	33	58	10	23	23	1.895	1.576	976.63

[Table 22 continued next page]

[Table 22 continued]

p/p_0	ϕ		ψ		$v = \phi - \psi$		v/a	v/a'	Pressure factor, according to Busemann
	0	'	0	'	0	'			
0.16	79	33	57	21	22	12	--	--	977.78
0.17	77	37	56	33	21	04	--	--	978.89
0.18	75	44	55	45	19	59	--	--	980.00
0.19	73	54	54	57	18	57	--	--	981.00
0.20	72	07	54	09	17	58	1.707	1.480	982.00
0.21	70	21	53	21	17	00	--	--	983.00
0.22	68	38	52	32	16	06	--	--	983.91
0.23	66	56	51	43	15	13	--	--	984.75
0.24	65	16	50	53	14	23	--	--	985.58
0.25	63	37	50	03	13	34	1.558	1.400	986.42
0.26	61	59	49	13	12	46	--	--	987.23
0.27	60	22	48	21	12	01	--	--	988.00
0.28	58	45	47	29	11	16	--	--	988.72
0.29	57	09	46	35	10	34	--	--	989.43
0.30	55	33	45	41	9	52	1.430	1.319	990.13
0.31	53	57	44	45	9	12	--	--	990.80
0.32	52	22	43	48	8	34	--	--	991.44

[Table 22 continued next page]

[Table 22 continued]

p/p_0	ϕ		ψ		$v = \phi - \psi$		v/a	v/a'	Pressure factor, according to Busemann
	0	'	0	'	0	'			
0.33	50	46	42	50	7	56	--	--	992.06
0.34	49	09	41	50	7	19	--	--	993.69
0.35	47	32	40	48	6	44	1.320	1.240	993.28
0.36	45	54	39	44	6	10	--	--	993.83
0.37	44	15	38	38	5	37	--	--	994.37
0.38	42	35	37	30	5	05	--	--	994.90
0.39	40	53	36	18	4	35	--	--	995.40
0.40	39	10	35	04	4	06	1.221	1.168	995.90
0.41	37	24	33	46	3	38	--	--	996.36
0.42	35	35	32	24	3	11	--	--	996.82
0.43	33	43	30	58	2	45	--	--	997.24
0.44	31	46	29	26	2	20	--	--	997.64

[Table 22 continued next page]

[Table 22 continued]

p/p_0	φ ° ' "		ψ ° ' "		$v = \varphi - \psi$ ° ' "		v/a	v/a'	Pressure factor, according to Busemann
0.45	29	45	27	48	1	57	1.130	1.100	998.04
0.46	27	38	26	03	1	35	--	--	998.41
0.47	25	23	24	08	1	15	--	--	998.78
0.48	22	58	22	01	0	57	--	--	999.08
0.49	20	18	19	38	0	40	--	--	999.27
0.50	17	18	16	53	0	25	1.045	1.037	999.47
0.51	13	44	13	31	0	13	--	--	999.67
0.52	8	56	8	52	0	04	--	--	999.86
0.527	0	00	0	00	0	00	1	1	1000.00

values for a flow region in which flow velocity is equal to sonic velocity. Therefore p/p_0 must always equal or be less than 0.527,

/97

or otherwise non-turbulent supersonic flow can not be maintained and separation phenomena will occur.

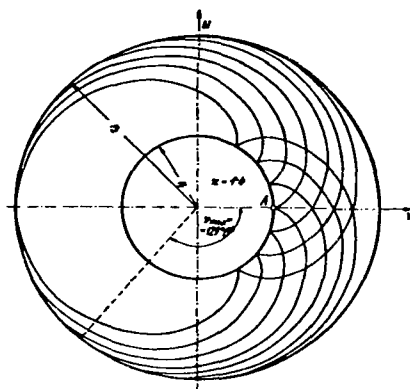


Fig. 24.

Characteristic curves,
according to Ackeret.

Since the phenomena at a given point in supersonic flow are independent of events downstream, arbitrary sectors limited by two rays drawn through the edge can be taken out of the basic flow (Fig. 22), and other suitable flows can be inserted therein. This makes possible the transition from the basic solution described to the previously mentioned general problem of flow around a projecting edge with arbitrary deflection $w_{1,2}$ at given approach velocity v_1^* .

In Fig. 23 a given point v_1/a' of the abscissa axis corres-

* According to the Betz representation in: Hütte I, 420 (1931).

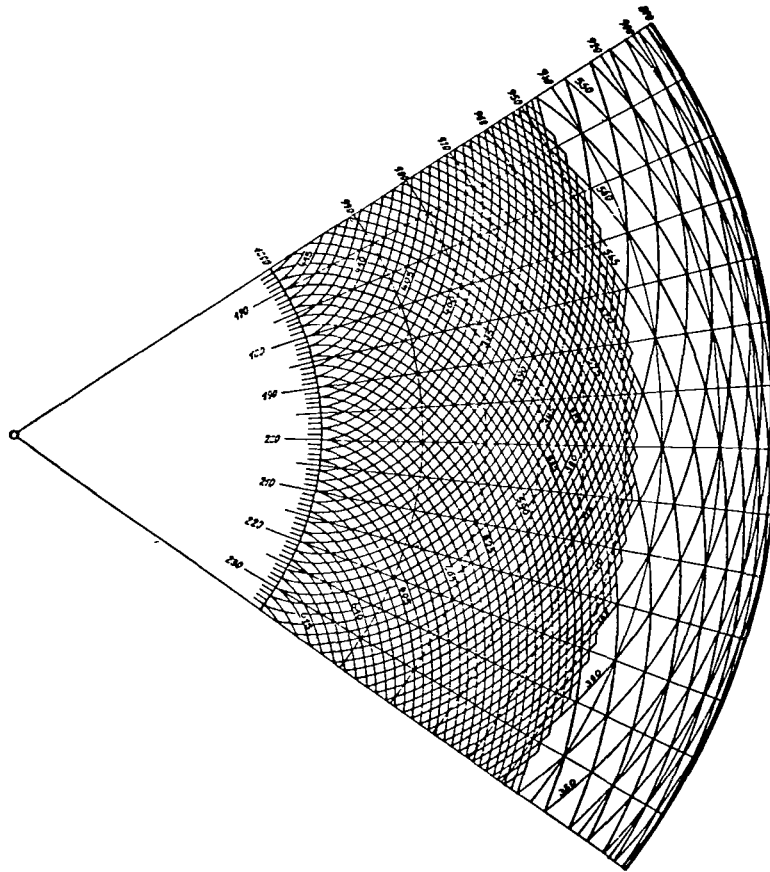


Fig. 25.

Characteristic-curve chart according to Busemann's representation.

ponds to v_1 , and the corresponding ν represents that deflection angle ν_1 necessary to reach velocity v_1 starting from sonic velocity in accordance with the basic solution. Simultaneously, angles φ_1 and ψ_1 , determining the position of the Mach disturbance line r_1

and the initial direction of the disturbance, are found. A further deviation by angle $w_{1,2}$ to $v_2 = v_1 + w_{1,2}$ occurs; the values v_2/a' , ψ_2 , and ϕ_2 belonging to v_2 are also to be taken from the diagram. Velocity v_2 , Mach angle $\beta = 90 - \psi_2$ of radius r_2 , and angle ϕ_2 of ray r_2 are thus obtained. The flow in the transition region between r_1 and r_2 is identical with the flow in the sector between ϕ_1 and ϕ_2 of the basic solution.

Another, chiefly graphic, solution of the problem of supersonic flow around a projecting edge was evolved by Steichen *, Busemann **, and Prandtl ***. Ackeret **** gives a clear picture of the fundamentals of the method that we follow in part here. He concludes that the differential equation of the flow potential Φ for two-dimensional, frictionless, steady state, potential flow without

-
- * Steichen, "Beiträge zur Theorie der zweidimensionalen Bewegungsvorgänge in einem Gas, das mit Überschallgeschwindigkeit strömt." (Contributions to the Theory of Two-Dimensional Flow Phenomena in a Gas Flowing at Supersonic Velocity) Thesis, Göttingen, 1909.
 - ** Busemann, "Zeichnerische Ermittlung von ebenen Strömungen mit Überschallgeschwindigkeit." (Graphic Determination of Two-Dimensional Flows at Supersonic Velocity) Z. f. angew. Math. u. Mech., 1928; Busemann, Zeichnerische Verfolgung von Überschallströmungen" (Graphic Plot of Supersonic Flows) in the Gas Dynamics section of Wien-Harms, "Handbuch der Experimentalphysik" (Handbook of Experimental Physics), vol. IV, 1931.
 - *** Prandtl-Busemann, "Näherungsverfahren zur zeichnerischen Ermittlung von ebenen Strömungen mit Überschallgeschwindigkeit" (Approximation Method for Graphic Determination of Two-Dimensional Flows at Supersonic Velocity) Stodola honorary publication, Zürich, 1929.
 - **** Ackeret, "Gasdynamik" (Gas Dynamics) In Geiger-Scheele, "Handbuch der Physik" (Handbook of Physics), vol. VII, 1927.

heat transfer or turbulence is:

$$\phi_{xx} \left(1 - \frac{\phi_x^2}{a^2}\right) + \phi_{yy} \left(1 - \frac{\phi_y^2}{a^2}\right) - 2 \frac{\phi_x \phi_y}{a^2} \phi_{xy} = 0,$$

in which the two velocity components are:

98

$$u = \frac{\partial \phi}{\partial x} = \phi_x; \quad v = \frac{\partial \phi}{\partial y} = \phi_y.$$

If a new and unknown potential $\chi(u,v) = ux + vy - \phi(xy)$ is assumed therein, with u and v the independent variables, then the potential equation becomes:

$$\frac{\partial^2 \chi}{\partial u^2} (1 - v^2/a^2) + \frac{\partial^2 \chi}{\partial v^2} (1 - u^2/a^2) + 2 \frac{\partial^2 \chi}{\partial u \partial v} uv/a^2 = 0.$$

If the outlines of the characteristic curves of the transformed potential equation are now chosen as curved coordinates in the u - v plane, then the definite and integrable differential equation of these "characteristic curves" is:

$$\left(\frac{dv}{du}\right)^2 (1 - v^2/a^2) - 2dv/du \cdot uv/a^2 + (1 - u^2/a^2) = 0.$$

This result has a simple geometric explanation: Two concentric circles of $r_1 = a'$ and $r_2 = a' \sqrt{(\kappa + 1)/(\kappa - 1)}$ are drawn; a' is the critical sonic velocity, r_2 the maximum velocity. If a circle

of $r = (r_2 - r_1)/2$ is rolled between the drawn circles, the points

obtained lie on the characteristic curves. Busemann finds a basic property of the characteristic curves for the graphic treatment of the problem at hand. Namely, if a hodograph for a supersonic flow is drawn so that all speeds occurring in the plane emanate from one pole, then all points with supersonic velocity that can occur on the same wave form a unique characteristic curve which runs in the direction of the wave normals at every point.

The "characteristic-curve method" can be put to practical use in the following manner *:

For every point in the flow plot there is a point in the velocity plot related by its velocity direction.

/99

Since the points along a stationary wave in the flow plot correspond to the points along a characteristic curve in the velocity plot, the characteristic curves represent the figures of the waves in the velocity plot. Various flows can thus be shown superimposed by a single characteristic-curve chart. Since the wave directions at corresponding points are retained in this type of depiction, the flows can differ only in the intervals of wave groups. These intervals are determinable graphically from the boundary conditions.

A characteristic-curve chart like that in Fig. 25 can be used for practical depiction; only those waves corresponding to the characteristic curves in the chart need be shown.

/100

To facilitate plotting, the characteristic curves are designated oppositely by the numbers 318 to 417 and 518 to 617. On circles of constant velocity (and thus constant pressure) the intersecting characteristic curves have constant sums with "pressure factors" 870 to 1000 (their actual values can be taken from Table 22). Velocity directions are designated by the differences of intersecting characteristic curves, using "direction factors" 165 to 235. If only every n -th one of these characteristic curves in both groups is used for the figure, then the mean velocities and directions lie at the intersection points of the characteristic curves, displaced by $n/2$, of both groups. Busemann also recommends that in indicating the state the numbers of these two averaged characteristic curves be written in each zone of the flow plot with the larger one above and the smaller underneath, when the flow is from left to

* See the thorough description by Busemann in the "Handbuch der Experimentalphysik."

right. If the flow over a wave coming from below enters a new zone, then only the lower number changes, by n units, with respect to the zone just left, and analogously the upper zone number changes for a wave coming from above. Depending upon whether the change manifests itself as increase or decrease in zone number, a solid "compression line" or a broken "rarefaction line" occurs. The type of line then accompanies the wave to the edge. The direction of a wave element is perpendicular to the line connecting those points in the velocity chart that are determined by the zone numbers of the two zones separated by the wave element.

In the initial zones the factors result from the initial conditions, and at the solid jet boundaries, from the boundary conditions. This establishes the direction and therefore the difference in zone numbers, and care must be taken that these actually appear as differences in the zone numbers.

2212. Flow Around a Convex Surface*

The extraordinary significance of the Prandtl-Meyer treatment of supersonic airfoils lies in the fact that it remains valid, as does the graphical Prandtl-Busemann treatment, not only for an isolated deflection of the flow around a corner, but also for deflections of the flow around various types of convex corners and, hence also for deflection of the flow around a continuous convex curve.

Specifically we can break off the Prandtl-Meyer flow on any given radius vector, say A -- C in Fig. 26, and instead apply a segment of rectilinear flow without the flow in A -- B -- C

/101

*According to Ackeret's representation in the Geiger-Scheele Handbuch der Physik, Bd VII (Handbook of Physics, Vol. VII, 1927).

being in any way altered. As already mentioned, the real reason behind this fact, so alien to subsonic flow, is the fact that all disturbances are felt not upstream, but downstream within the confines of the Mach angle.

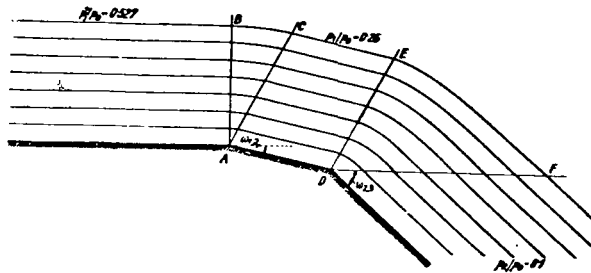


Fig. 26.

Plane supersonic flow around several leading edges.

If, for example, a gas is flowing along a wall to A (Fig. 26) with the critical pressure $p'_0 = 0.527 p_0$, where p_0 is the pressure of the gas at rest, and if we place a second wall A -- D at A, to form the angle $w_{1,2}$ with the extension of the first wall, then we can calculate from the ratio p'/p_0 and the angle $w_{1,2}$ with the extension of the first wall, then we can calculate, from the ratio p'/p_0 and the angle $w_{1,2}$ the pressure ratio

p_1/p_0 , in the usual way, with p_1 being the constant pressure along the new wall A -- D. The gas expands in this process on the curve v in Fig. 23 to the point where the deflection angle $w_{1,2}$ is attained.

We then have $v_2 = w_{1,2} + v_1$ and, by interpolation in Table 22 or

directly from the diagram in Fig. 23, we can find the appropriate p_1/p_0 ratio for the argument of v_2 . If we place several such walls

in succession, we will end up with a pressure along the last wall in the series corresponding to the total deflection $w_{1,n}$, where $2_{1,n}$

will be the angle between the last wall and the extension of the first wall.

Further, we shall have $v_n = w_{1,n} + v_1$. All the walls must

present obtuse angles to the ray, since all of the calculations up to this point are valid solely for the case of expansion.

If we now reduce the individual segments in size infinitely, the polygonal longitudinal section of the wall will go over into a continuous curve in the limit.

For the total deflection up to a certain point P on the curve $w_{1,p}$, we shall mean the angle between the tangent to the curve at

that point and the initial direction. We thereby obtain the pressure ratio corresponding to that point, as mentioned earlier. The continuous curve must present its convex side to the flow consistently, and the shape of the curve will in other respects be a matter of indifference.

In Fig. 27, the stream arrives at A at a supersonic velocity. The φ -, ψ -, v - values at A are φ_a , ψ_a , v_a . The expansion process

/102

setting in above the surface is determined by the inclination of the upper surface to the original direction of flow. If this is equal to $w_{1,p}$ at point P, then we will have $v_p = v_a + w_{1,p}$, with ψ_p

and φ_p specified once v_p is given, so that the disturbance lines along which the disturbance state remains constant become known. The Mach disturbance lines form the angle ψ with the normal to the wall. The streamlines can be constructed quite simply since the direction of the tangent coincides at any point p' with the direction of the tangent at that point on the wall lying on the same disturbance line.

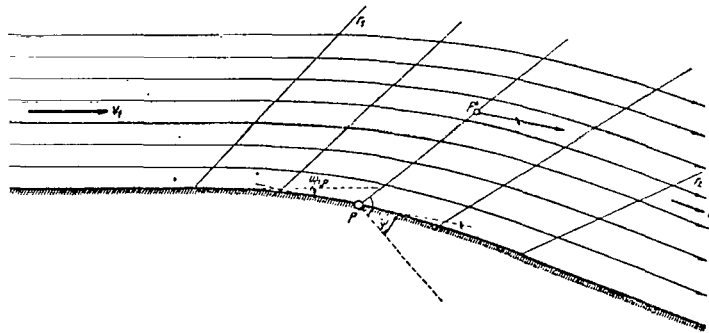


Fig. 27.

Plane supersonic flow around
a convex surface.

The application of the more recent Prandtl-Meyer graphical treatment to the case of supersonic flow about a convex surface is inferred directly from the explanation of that treatment, and can be skipped here.

2213. Flow Around a Leading Edge

The first analytic solution of this problem in the plane is

again traceable to Prandtl-Meyer*. Since it appears to be slightly less amenable to practical application than the shock polar technique developed by Busemann for this case, we might deal with it more briefly by concentrating on an elucidation of the qualitative process involved.

Suppose a discontinuous deflection about an angle $w_{1,2}$ is imposed on a stream of gas flowing at supersonic speed in the direction A--B, whereby no transition region occurs as in the case where the flow is around a leading edge, since the flow processes assumed for the given ratios would lead to self-mixing of the flow. Instead, a surface of discontinuity (Fig. 28) will occur between the two Mach lines at certain angles $w_{1,2}$, with the surface proceeding from the

bend B and forming an angle with the initial direction of flow which will lie somewhere between the Mach angle r_1 and the right angle.

The required change in pressure and velocity will occur discontinuously across this surface, by means of an oblique compression shock.

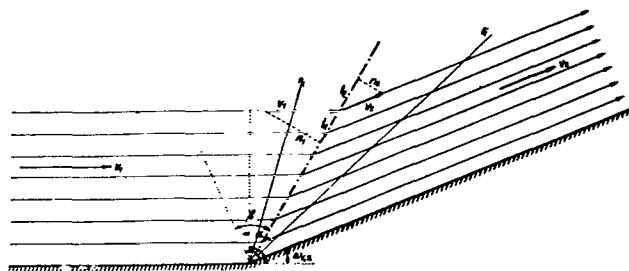


Fig. 28.

Plane supersonic flow about a leading edge.

*Meyer. Mitt. Forschungsarb. VDI, No. 62, 1908; partially according to the Ackeret approach in the Geiger-Scheele Handbuch der Physik 1927, and partially according to the Betz approach in Hütte, I, 1931.

The gas will flow on at a lower velocity ($v_2 < v_1$) after the pressure increase. The compression shock itself is not an adiabatic process, since the entropy is increased.

While the gas must have a stagnation pressure

$$p_0 = p_1 [1 - (v_1/a_0)^2 (n-1)/2]^{-n/(n-1)}$$

at pressure p_1 in an adiabatic change of state, in order to generate a velocity v_1 , the direct generation of the velocity v_2 will require a lower stagnation pressure p_0^* . This pressure loss is calculated using the equation:

$$\frac{p_0^*}{p_0} = \left(\frac{v_1}{a'} \right)^2 \left(\frac{1 - (v_1/a')^2 (n-1)/(n+1)}{1 - (a'/v_1)^2 (n-1)/(n+1)} \right)^{1/(n-1)}$$

The discontinuous reduction in the velocity v_1 to v_2 proceeds in such a way that the components parallel to the surface of the shock remain unaltered, i.e. $t_1 = t_2$, as ensues from arguments based on momentum, while the components n_1 normal to the surface of the shock decreases to n_2 in accord with the formula

$$n_1 n_2 + \frac{n-1}{n+1} t^2 = a'^2.$$

The angles α and β , with $\tan \alpha = t/v_1$ and $\tan \beta = t/v_2$ taken into account, result in

/10

$$\cos^2 \alpha = \frac{[(n-1) + (n+1)p_2/p_1](n-1)}{4n[(p_0/p_1)(n-1)/n - 1]}$$

$$\text{and } \tan \beta = \frac{(n-1)p_1 + (n+1)p_2}{(n-1)p_2 + (n+1)p_1} \tan \alpha$$

The angle of deflection w itself follows from $w = \beta \rightarrow \alpha$. The relationships between w , p_1/p_0 , and p_2/p_0 are plotted in Fig. 29 and in

Fig. 30 for $n = 1.405$.

We infer from Fig. 29 that the compression shock is possible only between the limits $p_1/p_0 = p_2/p_0$ and $p_2/p_0 = p_1/p_0$.

$$\frac{1}{n^2 - 1} [4n(p_1/p_2)^{(n-1)/n} - (n+1)^2].$$

$$p_2 > p_1, \cos^2 \alpha \leq 1, p_1/p_0 < \left(\frac{2}{n+1} \right)^{n/(n-1)}.$$

The straight limiting line signifies the compression shock under the Mach angle, whereas the curved limiting line signifies the straight compression shock $\alpha = \beta = 0$. The curved limiting curve

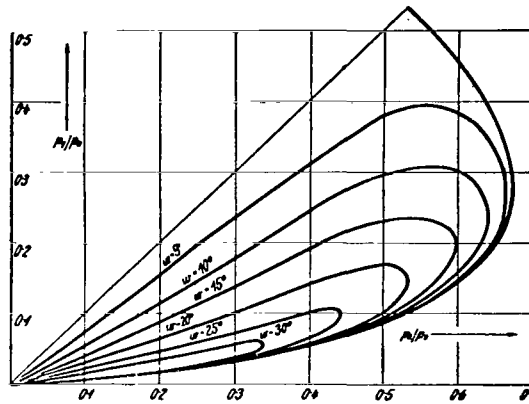


Fig. 29.

w-surface, according to Meyer..

contacts the x-axis at the origin. The ratio p_2/p_0 is maximized at the point $p_2/p_0 = 0.669$, $p_1/p_0 = 0.278$ on the limit curve. The limiting lines intersect at right angles. The highest possible pressure difference turns out to be 0.456, from the maximum of $(p_1 - p_2/p_0)$, at $p_1/p_0 = 0.126$ and $p_2/p_0 = 0.618$.

Another treatment of supersonic flow around a leading corner, which appears to have advantages for practical applications, is the Busemann shock polar approach*. On the basis of given general pressure, velocity, and angle relations in the Prandtl-Meyer approach, the variables of the final state, and in particular the velocity component of the velocity parallel to the surface of discontinuity, t , and v_2 , appearing in response to a discontinuous deflection through

the angle w , can be calculated for any initial state v_1 . These var-

iables can be used to plot a velocity diagram (Fig. 31). The connecting line of all possible final states v_2 which can come about

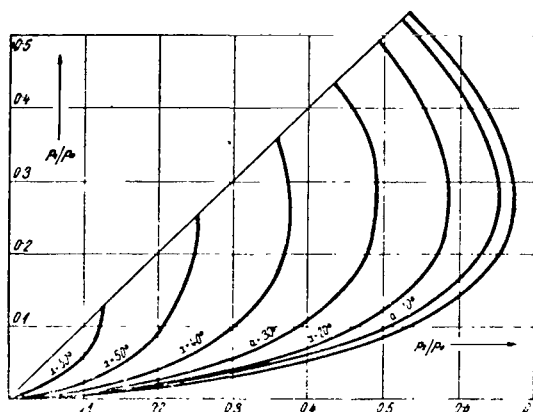


Fig. 30.

α -surfaces, according to Meyer.

via different discontinuous deflections w from the state v , is drawn in Fig. 31, and was termed the "shock polar" by Busemann. A shock

*Busemann, "Verdichtungsstöße (Compression shocks), section on "Gasdynamik" (Gas dynamics) in the Handbuch der Experimentalphysik.

polar can be drawn for any initial state v_1 of the gas which includes the angle $(90-m)$ made with the direction of the abscissa, m here referring to the Mach angle belonging to the state v_1 . The shock polar also makes it possible to ascertain the lowest possible velocity value $v_{2 \min}$ corresponding to the straight compression shock. Furthermore, the maximum possible angle of deflection $w_{1,2 \max}$ belonging

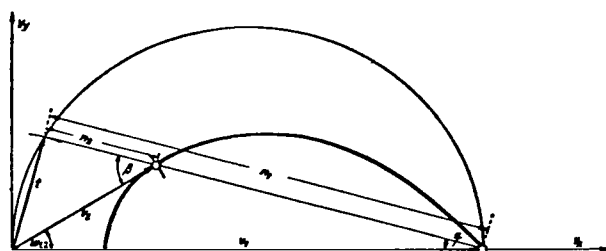


Fig. 31.

The shock polar.

to the initial state v_1 can be found. As smaller angles of deflection two states distinguished by the final velocity v_2 and the final pressure p_2 are always explicitly possible. Experience shows the state belonging to the greater v_2 to occur in reality. At angles of deflection greater than $w_{1,2 \max}$, say upstream of a blunt obstacle, the compression shock begins upstream of the obstacle in a manner such that $v_{2 \min}$ will occur at the foremost point of the compression shock wave whose surface lies normal to the flow, and from there

onward all points of the shock polar will be traversed at a decreasing inclination of the shock surface, until the Mach angle is reached. At the same time, this is the sole case of supersonic flow where the disturbance is felt upstream. Subsonic velocity also occurs here, by the way, at the point $v_{2 \min}$, and this point is passed by when $w_{1,2 \max}$ is attained in the course of the variable inclination of the shock surface.

Actually, the shock polar need not be ascertained point by point, since its closed equation can be derived in a straightforward manner.

Busemann finds it to be:

/106

$$v_y^2 = (v_1 - v_x)^2 \frac{v_x - a'^2/v_1}{[a'^2/v_1 + 2v_1/(\kappa + 1)] - v_\kappa}$$

That is the equation of the ordinary strophoids whose three constants signify that

1. the double point for $v_1 > a'$ or the singular point such that $v_1 < a'$ at $v_x = v_1$, lies at $v_x = v_1$,
2. the simple intersection point with the v_x -axis lies at $v_x = a'^2/v_1$,
3. the asymptote lies at $v_x = a'^2/v + 2 v_1/(\kappa + 1)$.

We can then construct the strophoids in the usual manner (Fig. 32).

In Fig. 33, the shock polar is drawn for air, in such a manner, to the extent that the strophoid branches have physical significance.

When the compression shock is intersected, or even contacted, by the Mach lines, the shock strength does not remain constant over

the entire length, but rather we find a change in the entropy increment. That is why the isentropic curves (curves of equal shock strength here) are drawn explicitly, and designated with the ratios p_0'/p_0 , which give the pressure drop at individual velocities.

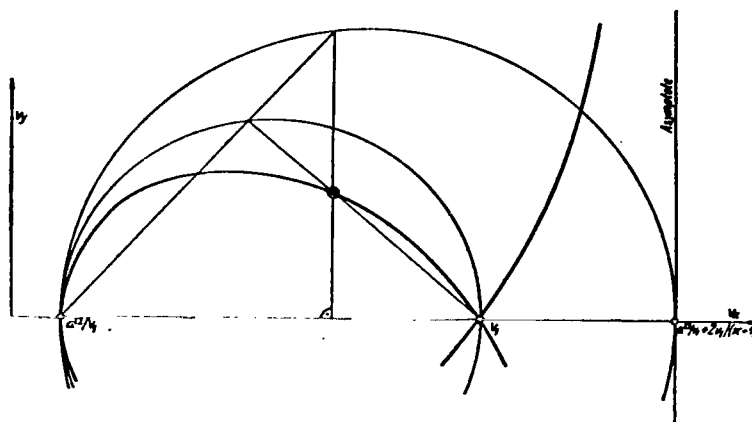


Fig. 32.

Plotting shock polar as strophoids.

While the plotting of flow patterns with constant compression shocks presents no fundamental difficulties, in the picture after the compression shock, with the corresponding new diagram of characteristics, the stream filaments which cross the variable compression shocks no longer form any kind of potential flow. Busemann recommends the procedure of breaking down the flow through some streamlines into strips of approximating potential and treating each strip separately, but it is important in that case to see to it that the adjacent strips on both sides agree at the boundary with respect to both pressure and direction. In flow around bodies, special difficulties are brought about by the fact that the discontinuous changes of state on the two boundaries no longer agree, so that we have to deal with a variable "jump" in order to attain the corresponding exactness.

In order to find the final velocity v_2 and the throttling loss p_0^*/p_0 from the initial velocity v_1 and the deflection angle $w_{1,2}$ accompanying an oblique compression shock of the air, we proceed in

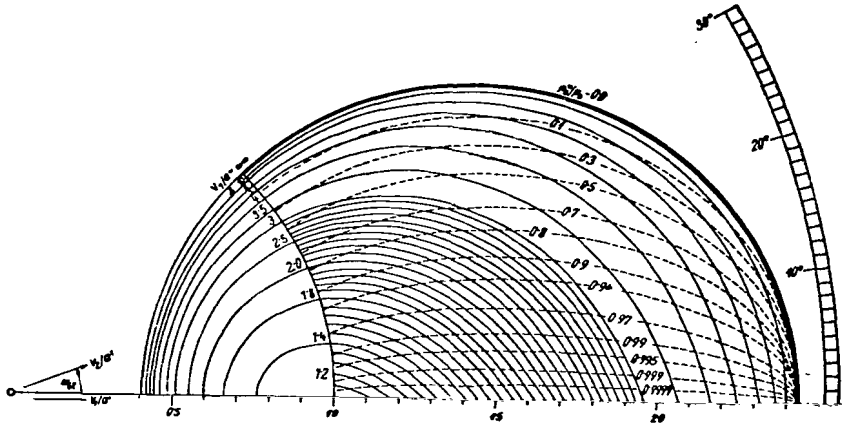


Fig. 33.

The Busemann shock polar diagram as a relationship between the initial velocity v_1 , the final velocity v_2 , the deflection angle $w_{1,2}$, and throttling loss p_0^*/p_0 (hatched) in the case of an oblique compression shock in air ($\gamma = 1.4$).

actual practice with the aid of the Busemann shock polar diagram in such a manner as to calculate the ratio v_1/a at the state v_1 , and then to calculate v_1/a' . Once v_1/a' has been found, we resort to

the above diagram (see the horizontal scale), choose the corresponding shock polar curves, and determine their intersection with the ray through the pole inclined at the angle $w_{1,2}$ to the horizontal.

The distance of this point of intersection from the pole directly represents the v_2/a' to be found, while the shock loss p^*/p_0 is read off from the broken-line pressure curve passing through the point.

2214. Flow around a concave surface

If, with Ackeret*, we assume that in Fig. 34 the streamline segment B--C of the ordinary Meyer expansion is realized in material form and the direction of motion reversed in the sense of the arrow, without any change in pressure (an accepted procedure in the case of supersonic flow), we get the typical case of a supersonic flow along a concave surface. At the same time, it is clear that the converging Mach interference lines meet in the point A. Such intersections of interference lines, which are generally distributed over a fairly large area, represent more than a simple crossing without mutual interaction; they lead to compression shocks in the same sense as in a Meyer compression. If, as in most of the practical cases with which we are concerned, the slope of the concave surface is correspondingly flat (Fig. 35), the Mach waves meet at such a distance from the body that the interference waves propagated by the compression shock itself, again at Mach angles, now miss the body, so that its pressure distribution must be computed in the same way as for flow around a convex surface. If the slope of the surface A--B is steeper, the compression shock approaches closer and closer to the point A, which it finally reaches when the entering angle at A assumes a finite value. As the angle increases further, the compression shock, in a manner familiar from the case of a Meyer compression, at first remains at the point A, until the entering angle reaches the maximum value $w_{1,2 \max}$, whereupon the compression shock migrates forward in the familiar manner, away

/108

*Ackeret, Gasdynamik in Geiger-Scheele (Gas Dynamics in Geiger-Scheele), Handbuch d. Physik, 1927.

from the tip and against the direction of flow.

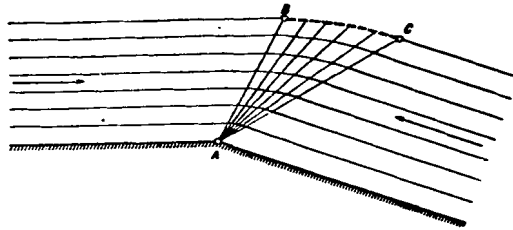


Fig. 34.

Plane supersonic flow around
a concave surface.

2215. Air forces on supersonic profiles

A foundation for the treatment of supersonic flows around thin airfoils was provided by Ackeret* in 1925 on the basis of Meyer flow about a convex angle. The method has been generalized by Busemann**, and it is essentially the latter's version that we shall follow.

/109

On the basis of his method of characteristics, Busemann finds the overpressure Δp , as compared with the static pressure in the flow, for thin profiles at small angular deflections to be:

*Ackeret, Luftkräfte auf Flügel die mit grösserer als Schallgeschwindigkeit bewegt werden (Air Forces Acting on Airfoils Moving at Speeds Greater Than Sound), ZFM, 1925.

**Busemann, Gasdynamik, Handbuch Exp. Phys., 1931, vol. 4.

Busemann-Walchner, Profileigenschaften bei Überschallgeschwindigkeit (Profile Features at Supersonic Speed), Forsch. Arb. Ing. Wesen, 1933.

$$\Delta p = \pm 2 q \beta \tan m = \frac{2q\beta}{\sqrt{v^2/a^2 - 1}},$$

if β is the angular deviation of the streamline from the direction of flow and $q = \gamma/2g \cdot v^2$ is the stagnation pressure of the flow.

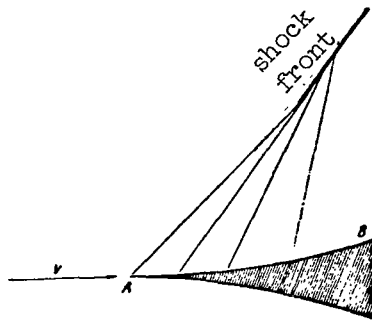


Fig. 35.

Development of compression shock.

From this we can find the lift and drag for thin profiles with a low angle of attack (Fig. 36) referred to a unit of length of the wing, which is assumed to be infinitely long (plane problem)

$$A = \int_0^t (\Delta p_u - \Delta p_0) dt = \frac{2q}{\sqrt{v^2/a^2 - 1}} \int_0^t (\beta_u + \beta_0) dt = \frac{4qt}{\sqrt{v^2/a^2 - 1}} \bar{\beta},$$

$$\begin{aligned} W &= \int_0^t (\Delta p_u \beta_u - \Delta p_0 \beta_0) dt = \frac{2q}{\sqrt{v^2/a^2 - 1}} \int_0^t (\beta_u^2 + \beta_0^2) dt = \\ &= \frac{2q}{\sqrt{v^2/a^2 - 1}} \int_0^t (\beta_u'^2 + \beta_0'^2) dt + \frac{4qt}{\sqrt{v^2/a^2 - 1}} \bar{\beta}^2. \end{aligned}$$

Thus the profile drag, calculated in this way, can be broken down into a part that vanishes with the angle of attack and is always equal to $\bar{\beta}$ times the lift and another part which, as distinct from the first, depends on the shape of the profile, especially on its thickness, but not on the angle of attack. The latter part vanishes for a thin, flat plate, which accordingly must be regarded as the ideal supersonic profile. The first component of the drag is, in the same sense as the still to be discussed induced drag of a subsonic airfoil of finite length, a direct consequence of the lift and represents the induced subsonic drag in the supersonic region, where a true induced drag is not found. It is a consequence of the fact that the resultant air force must be perpendicular to the plate, if, as we have assumed, tangential friction forces are disregarded. The energy consumed by the drag is contained in the air waves produced. The eventual compression waves combine as a result of convergence at a corresponding distance from the profile to form a compression shock, into which the rarefaction waves also finally flow (Fig. 37). If the cross section of the air jet is correspondingly large, the air waves are damped out at a great distance from the body. Energy and momentum are then expended in heating part of the gas medium and forming a wake. Busemann's explanation

for the fact that the drag is proportional to the square of the deflection angle times the wing chord is that the increase in entropy

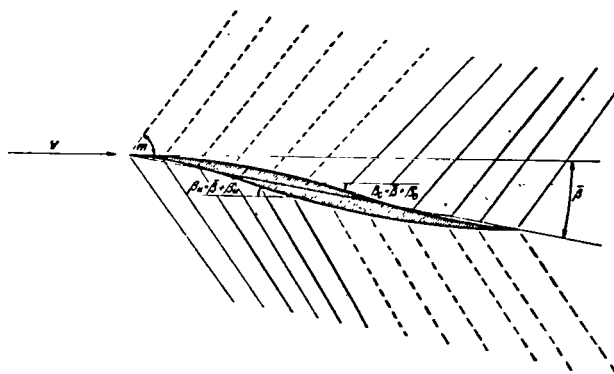


Fig. 36.

Supersonic profile.

is proportional to the third power of the angular deflection, whereas the length of a compression front is proportional to the chord divided by the angular deflection.

The drag due to the compression shocks, or the impact wave resistance, is more pronounced if the profile is thick, so that the Ackeret method is particularly suitable for good profiles.

It is of particular interest that at very high supersonic velocities the initially linear dependence of the excess pressure Δp on the deflection vanishes, to be replaced by an increasingly quadratic one, such as is given by the Newtonian drag theory. We shall return to this point later.

If we relate the lift forces to the stagnation pressure in the usual way, we find that the dependence of the lift coefficient on the speed is at first very strong but later much less:

/111

$$c_a = A/q F = \frac{4 \bar{\beta}}{\sqrt{v^2/a^2 - 1}} .$$

This dependence is illustrated in Fig. 38.

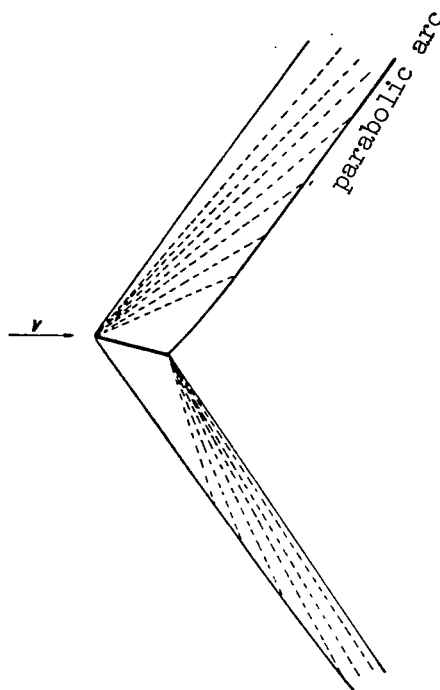


Fig. 37.

Damping of air waves at some distance from profile.

Similarly, for the drag:

$$c_w = W/q F = \frac{2k}{t \sqrt{v^2/a^2 - 1}},$$

where k is the profile constant:

$$k = \int_0^t (\beta_u'^2 + \beta_0'^2) dt + 2t \bar{\beta}^2.$$

We shall henceforth refer to these simple formulas as "A. B. formulas," borrowing the initial letters of the names of their discoverers. The quality of a good supersonic profile can be characterized by the lift-drag ratio:

$$c_a/c_w = 2 \bar{\beta} t/k = \frac{2 \bar{\beta} t}{\int_0^t (\beta_u'^2 + \beta_0'^2) dt + 2t \bar{\beta}^2},$$

i.e., is independent of the air speed. This quality criterion relates to the impact wave resistance alone, and thus, in this form, is still infinitely large with respect to the subsonic airfoil. In connection with the further discussion of quality, it should be borne in mind that the reciprocal of the over-all quality characteristic is equal to the sum of the reciprocals of the individual values. The correctness of the Ackeret supersonic airfoil theory

has been experimentally confirmed by the English*.

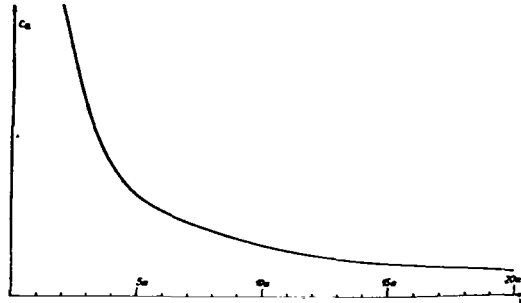


Fig. 38.

Variation of lift coefficients in supersonic region.

2216. The Flat Plate

In the last few pages we have arrived at the important result that, in principle, the thin, flat plate constitutes the best supersonic profile. Since, moreover, in this case the phenomena occur in their simplest form, the flat plate seems particularly well-suited and promising from the point of view of a theoretical study of the properties of supersonic airfoils.

First, in order to free ourselves of the restrictive assumptions of the A. B. formulas for lift and drag, we shall calculate these forces directly from the plane elementary flows of several angles of attack and velocities in air at a pressure $p = 10^4 \text{ kg/m}^2$

/112

*Taylor, Applications to Aeronautics of 'Ackeret's Theory of Aerofoils, Moving at Speeds Greater than that of Sound. Aeron. Res. Comm. R. & M. Nr. 1467, London, April, 1932.

and a temperature of 15°C . ($T = 288^{\circ}$, $a = 340$ m/sec, $\rho = 0.128$ kg \cdot sec²/m⁴.)

For example:

$$\alpha = 3^{\circ}, v = 2a = 680 \text{ m/sec.}$$

$$v/a = 2, a' = \sqrt{2/(n+1)} \sqrt{a^2 + v^2} (n-1)/2 = 418 \text{ m/sec}; v/a' = 1.625;$$

for v/a' it follows from Fig. 23 that $p/p' = 0.225$, $p' = p/0.225 = 4.45 \cdot 10^4$ kg/m².

Suction side: Corresponding to $v/a' = 1.625$ Fig. 23 gives a fictitious pre-deflection angle of: $v_0 = 28^{\circ}$; therefore the total deflection $v = v_0 + \alpha = 28 + 3 = 31^{\circ}$, whence again from Fig. 23 it follows that:

$$v_s/a' = 1.645; v_s = 418 \cdot 1.645 = 688 \text{ m/sec}; p_s/p' = 0.195;$$

$$p_s = 0.195 \cdot 4.45 \cdot 10^4 = 0.870 \cdot 10^4 \text{ kg/m}^2.$$

Pressure side: At the leading edge we first get an oblique compression shock with the discontinuous deflection $w_{1,2} = \alpha = 3^{\circ}$.

From Fig. 33 for $v/a = 2$ and $w = 3^{\circ}$ we get a $v_d/a' = 1.585$ and a

$p_0^*/p_0 = 0.999$ (i.e., completely negligible, but included here for

the sake of a general demonstration of the method). For $v_d/a' =$

$= 1.585$ Fig. 23 gives:

$(p_d)/p' = 0.278$, hence $p_d/p' = 0.278 \cdot 0.999 = 0.278$; therefore

$$p_d = 0.278 p' = 0.278 \cdot 4.45 \cdot 10^4 = 1.235 \cdot 10^4 \text{ kg/m}^2.$$

The force P on the area F will thus be: $P = F(p_d - p_s)$;

the lift and drag are given by $A = P \cos \alpha$ and $W = P \sin \alpha$; and finally the lift and drag coefficients referred to the stagnation pressure are:

$$c_a = (p_d - p_s) \cos 3^\circ / q = (1.235 - 0.870) 10^4 \cdot 0.999 / (0.064 \cdot 680^2) \\ = 0.1235.$$

$$c_w = c_a \tan 3^\circ = 0.1235 \cdot 0.0524 = 0.00647.$$

(To this should be added the drag due to skin friction !)

The lift-drag ratio is thus $\cot \alpha: 1/\epsilon = c_a/c_w = 19.08$.

$$\alpha = 6^\circ, v = 2a = 680 \text{ m/sec.}$$

p' remains the same as above: $p' = 4.45 \cdot 10^4 \text{ kg/m}^2$.

$$v_0 = 28^\circ, v = 34^\circ, v_s/a' = 1.74, v_s = 728 \text{ m/sec}, p_s/p' = 0.166,$$

$$p_s = 0.740 \cdot 10^4 \text{ kg/m}^2.$$

$$\alpha = 6^\circ, v_d/a' = 1.52, p_d/p' = 0.333, p_d = 1.48 \cdot 10^4 \text{ kg/m}^2.$$

$$c_a = (1.48 - 0.74)/2.955 = 0.250.$$

$$c_w = 0.250 \cdot 0.1051 = 0.0263.$$

$$1/\epsilon = 9.51.$$

$$\alpha = 9^\circ, v = 2a = 680 \text{ m/sec.}$$

$$p' = 4.45 \cdot 10^4 \text{ kg/m}^2, p_s = 0.615 \cdot 10^4 \text{ kg/m}^2, p_d = 1.720 \cdot 10^4 \text{ kg/m}^2,$$

$$c_a = 0.379, c_w = 0.0598,$$

$$\alpha = 12^\circ, v = 2a = 680 \text{ m/sec.}$$

$$p' = 4.45 \cdot 10^4 \text{ kg/m}^2, p_s = 0.49 \cdot 10^4 \text{ kg/m}^2, p_d = 1.96 \cdot 10^4 \text{ kg/m}^2,$$

$$c_a = 0.487, c_w = 0.1036.$$

This manner of calculation, though the most accurate, is clearly laborious, and becomes even more so at higher speeds, where the specially prepared primary flow diagrams become useless.

Accordingly, it is worth finding out up to what angles of attack the A. B. formulas for c_a and c_w , which are only valid for

very small angles, can still be used in practice.

In 2215 we found:

$$c_a = \frac{4\alpha}{\sqrt{v^2/a^2 - 1}}; \quad c_w = \frac{2k}{t \sqrt{v^2/a^2 - 1}}; \quad \epsilon = 2\bar{\alpha} t/k.$$

For the case of a flat plate the formulas reduce to:

/114

$$c_a = \frac{4 \alpha}{\sqrt{v^2/a^2 - 1}}; \quad c_w = \frac{4 \alpha^2}{\sqrt{v^2/a^2 - 1}}; \quad \epsilon = \alpha.$$

In the cases previously calculated by the exact method the formulas give the values presented in Table 23.

TABLE 23

Calculated according to	$v = 2a = 680 \text{ m/sec}$											
	$\alpha = 3^\circ$			$\alpha = 6^\circ$			$\alpha = 9^\circ$			$\alpha = 12^\circ$		
	c_a	c_w	$1/\epsilon$	c_a	c_w	$1/\epsilon$	c_a	c_w	$1/\epsilon$	c_a	c_w	$1/\epsilon$
Exact method	0.123	0.0065	19.08	0.25	0.0263	39.51	0.37	0.0598	6.31	0.48	0.104	4.70
A. B. formulas	0.121	0.0063	19.10	0.242	0.0259	39.55	0.363	0.0570	6.37	0.484	0.1012	4.78

In the practical region of airfoil qualities and angles of attack the agreement is completely satisfactory, so that henceforth we shall reckon with the simple A. B. formulas.

In Figs. 40 and 41 we have plotted the lift coefficients as a function of the angle of attack and flying speed and the polar curves at different speeds in accordance with the A. B. equations. Fig. 40 shows that for a flat plate the lift coefficients -- and with them the drag coefficients -- decrease rapidly with increasing speed, so that the lift-drag ratio remains constant. The qualitative resemblance to known ballistic drag curves is evident. Fig. 41 shows that there is a certain qualitative similarity between the polar curves obtained purely by calculation and those obtained experimentally by Briggs, and furthermore that all the polar curves are geometrically similar, with the center of similarity at the origin

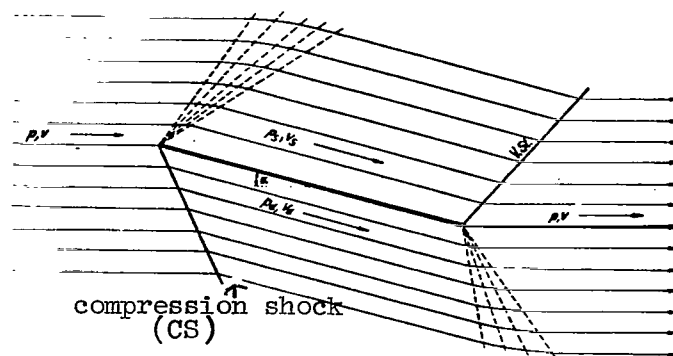


Fig. 39.

Plane supersonic flow around a flat plate.

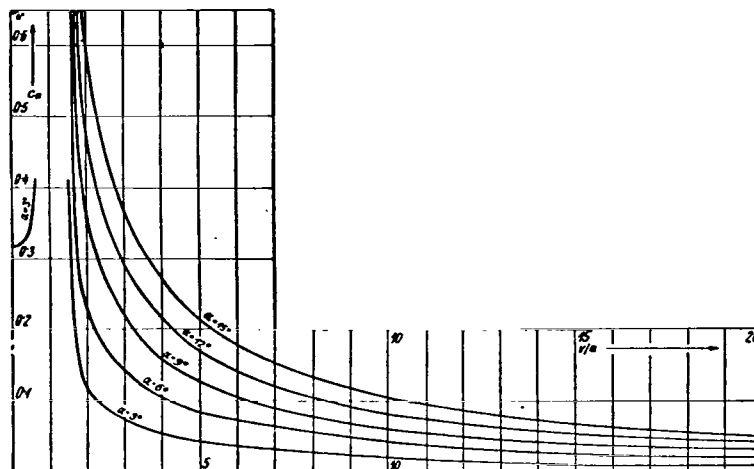


Fig. 40.

Lift coefficients for a flat plate.

of the coordinates.

In the present case the A. B. method employed is subject to a certain limitation, of no practical importance, insofar as in the region from $v = a$ to about $v = 1.3 a$ the critical impact angles w_{\max} are so small that they approach the angles of attack

employed, with the result that in this region of speeds the compression shock, neglected as very small, was actually incorrectly calculated. On the other hand, another discrepancy occurs in connection with the compression shock at very high speeds of the order of $v = 10 a$, when the Mach angle is smaller than the angle of attack.

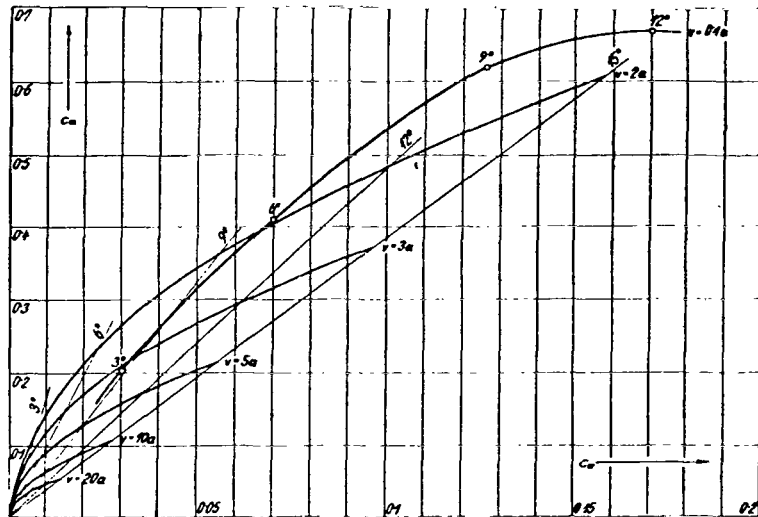


Fig. 41.

Polar curves for a flat plate.

The absolute magnitude of the air forces in the vicinity of the ground itself is also worth noting. The currently customary lift-drag ratio of about 10 roughly corresponds to an angle of attack α of 6° . From the polar diagrams for $v = 2a$ we get a coefficient c_a of about 0.25.

The unit load on such an airfoil is thus:

$$A/F = c_a \cdot q = 0.25 \cdot 2.9 \cdot 10^4 = 7200 \text{ kg/m}^2.$$

2217. The curved plate*

If the entering tangent is parallel to or makes only a small angle with the direction of flight, the effect of the compression shock can be neglected and the flow represents simple Meyer expansions, continuously distributed over the entire chord. The extent of the deflection is again determined by the respective slope of the wing surface. Along the top edge of the profile we always get expansion, on the pressure side compression. In the latter case a gentle pressure rise is necessary if the converging Mach compression waves are not to meet in the immediate vicinity of the profile, undergo reflection, and interfere with the pressure distribution over the profile itself. In accordance with 2215, the lift coefficient

/116

$$c_a = \frac{\frac{4}{\pi} \alpha}{\sqrt{v^2/a^2 - 1}},$$

*Ackeret, Luftkräfte auf Flügel, die mit grösserer als Schallgeschwindigkeit bewegt werden, (Air Forces Acting on Airfoils Moving at Speeds Greater Than Sound), AFM, 1925.

and hence is completely independent of the shape of the profile.

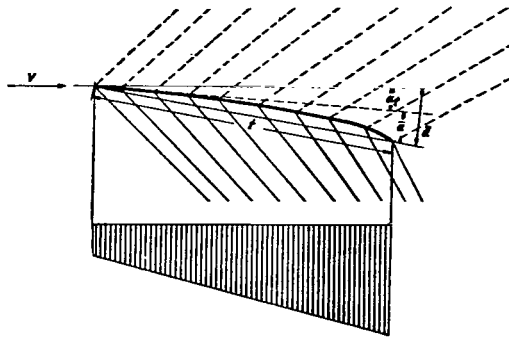


Fig. 42.

Plane supersonic flow around a curved plate.

The drag coefficient

$$c_w = \frac{2 \int_0^t (\alpha_u'^2 + \alpha_0'^2) dt}{t \sqrt{v^2/a^2 - 1}} + \frac{4\alpha^2}{\sqrt{v^2/a^2 - 1}}$$

Now, however, definite assumptions must be made concerning the

geometry of the airfoil, for example $y = -ax^2$, i.e., a parabolic form, with the entering tangent parallel to the direction of flow. In this case

$$\alpha'_0 = \frac{dy}{dx} - \bar{\alpha}; \quad \alpha'_u = -\frac{dy}{dx} + \bar{\alpha}.$$

If the angle made by the entering tangent is a small nonzero angle α_t , it is simply added to the designated angles:

$$\alpha'_0 = \frac{dy}{dx} - \bar{\alpha} + \alpha_t = -2ax - \bar{\alpha} + \alpha_t = -2ax + \bar{\bar{\alpha}} - \bar{\alpha}$$

$$\alpha'_u = -\frac{dy}{dx} + \bar{\alpha} + \alpha_t = 2ax + \bar{\alpha} + \alpha_t = -2ax + \bar{\bar{\alpha}}.$$

Hence:

/117

$$c_w = \frac{2}{t \sqrt{v^2/a^2 - 1}} \left[\int_0^t (\alpha'^2_0 + \alpha'^2_u) dx + 2 \bar{\bar{\alpha}}^2 t \right].$$

Thus, the drag is greater than for a flat plate, while the lift remains the same.

The pressure distribution consists in a linear rise or fall in pressure towards the trailing edge. Leakage around the trailing edge necessarily following from the pressure distribution can not interfere with the pressure distribution itself.

2218. Separation Effects in the Supersonic Region

None of the previous profile analyses have taken into account the separation effects at certain angles of attack, although these are familiar in connection with subsonic profiles. In principle, conditions on the suction side of a supersonic airfoil are also more favorable in that the pressure rise from the shoulder of the profile to the trailing edge, so fateful for the subsonic airfoil in view of its decisive contribution to boundary-layer separation, is avoided; in fact, as a rule, it is even possible to produce a fall in pressure in this direction, so that instead of being retarded the boundary-layer flow can even be accelerated.

Briggs' experimental results, however, would appear to be directly opposed to these satisfying conclusions, and Briggs states flatly that on the suction side flow detachment occurs at the latest when the local pressure has fallen to 0.51 times the external pressure. Briggs links this figure with the critical air pressure ratio $p'/p_0 = 0.527$.

It is perfectly clear that owing to the discontinuous flow conditions and the compression shocks the moment of transition from subsonic to supersonic flow could give rise to boundary-layer separation.

Whether such separation is no longer to be feared under conditions of pure supersonic flow remains uncertain. At any rate, it will be very difficult to avoid compression shocks on the suction side of a profile, since the latter can easily take the place of the otherwise lacking pressure rise and hence lead to flow separation.

2219. Boundary and Sum Curves for Lift on the Suction and Pressure Sides from $v = 0$ to $v = 8000$ m/sec

From what has been said so far it follows that in the supersonic region the lift on the pressure side of a profile, even if it is flat or only slightly curved, can be calculated in advance with a good degree of accuracy. However, in view of the friction and separation phenomena, which are not amenable to calculation, the theoretical treatment of the suction side presents serious difficulties. For practical purposes, therefore, a simpler and more summary treatment, capable of providing a rough estimate of the anticipated errors, would appear to be desirable.

Accordingly, we shall plot the lift coefficient c_a against the speed, taking the components for the suction side (c_{as}) and pressure side (c_{ad}) separately and allowing the speed to vary over the entire range in which we are interested, namely from $v = 0$ to $v = 8000$ m/sec.

In the subsonic region, c_{as} , the lift coefficient relative to the suction side, can not be so sharply separated from the total lift, but in this region the need for separating it is also less. Therefore, in line with ordinary approximation assumptions, we shall assume that approximately $c_{as} = 2/3 c_a$. If the practical maximum for $c_a : c_{a_{max}} = 1.2$, the greatest possible c_{as} will be $c_{as} = 0.8$. Actually, the airfoil will mostly be used with the angle of attack of the best gliding angle, for which c_a will amount to only about half its maximum value, so that at low speeds the c_{as} of most practical interest will be about 0.4. From this value, derived from the conditions of incompressible flow and strictly valid only at very low v , the lift coefficient increases with increasing speed, under the growing influence of the compressibility, in accordance with the previously discussed Prandtl-Glauert relation:

$$c_{as_{comp.}} = c_{as_{incomp.}} (1 - v^2/a^2)^{-1/2},$$

until at a certain point on the profile surface the local flow velocity reaches the speed of sound. This usually occurs at the shoulder of the profile, i.e., the point on the suction side with the largest ordinate, and, in the case of the thin ($t/d = 10$) to very thin profiles in which we are exclusively interested, at about $v = 0.8a$. Beyond this limit, therefore, both subsonic and supersonic flows may be observed over the profile, so that the theoretical treatment encounters insuperable difficulties. However, from empirical investigations, especially those of Briggs, we know that from this moment

on the lift declines fairly sharply with increasing v .

Conditions amenable to theoretical treatment are only re-established when the flying speed exceeds the speed of sound. On the suction side the underpressure of the vortex-free supersonic flow can be theoretically stated in accordance with 2215, and, apart from the speed, also depends on the shape of the profile and the angle of attack. At the same time, the separation effects, which, as the speed increases, develop at ever smaller angles of attack, interfere with these underpressure conditions in such a way that according to Briggs' experimental results higher pressures are observed in the vortex region than in a vortex-free supersonic flow. The vacuum which first arises as a result of the separation of the flow from the surface of the suction side (this vacuum would correspond to the maximum c_{as}) is quickly filled with turbulent air as a result of

leakage around the trailing edge, inflow from the ends of the wings, and break-up of the separated laminar flow, so that the pressure again increases from zero, and according to Briggs' experimental results in the vicinity of the sonic limit reaches higher mean values than before the break-away of the laminar flow, so that c_{as} becomes

smaller as a result of separation. Whether this filling of the vacuum on the suction side takes place to the same extent at very high speeds or whether in this case the vacuum pressure with its high c_{as} is better maintained is at present outside the scope of our

knowledge. In relation to very high speeds ($v = 3a$ and more) it is sufficient for practical purposes to state that at most the pressure on the suction side can fall to zero, in which case the limiting value of the lift coefficient on the suction side may be found from:

$$\begin{aligned}
 A &= F p_a \cos \alpha = c_{as_{\max}} \cdot \gamma / 2g \cdot F v^2; \\
 c_{as_{\max}} &= \Delta p / q = \frac{p_a \cos \alpha}{\gamma / 2g \cdot v^2} = \frac{\rho_a RT_a g \cos \alpha}{\rho / 2 \cdot v^2} = \\
 &= \frac{2}{\kappa} \cos \alpha \frac{a^2}{v^2} \doteq 165 \, 300 \cos \alpha / v^2,
 \end{aligned}$$

if we bear in mind that $p_a/\rho_a = RT_a/g$ and $a_a = \sqrt{\kappa g RT_a}$. The subscript "a" always refers to the value in the outer stationary air.

In accordance with the discussion of c_{as} , in the subsonic region, c_{ad} , the lift coefficient relating to the pressure side, has a maximum value of about $c_{ad_{max}} = 0.4$ for $v = 0$, becoming $c_{ad} = 0.2$ in the region of the usual angles of attack. As the speed increases, it also increases under the influence of the compressibility in accordance with the relation:

$$c_{ad_{comp.}} = c_{ad_{incomp.}} (1 - v^2/a^2)^{-1/2}$$

up to the limits applicable to c_{as} . On the pressure side the following region up to $v = a$ should also be characterized by a decrease in lift as a result of the reduction in circulation due to supersonic and separation effects on the suction side. From the point $v = a$ the lift on the pressure side can be satisfactorily established by the Ackeret-Meyer method. In the supersonic region the variation of c_{ad}

/120

is also susceptible to a simple mechanical interpretation, which has the advantage of unusual clarity and gives information on the (lower) limiting value of c_{ad} . Thus, we may imagine the lift on the pressure

side as being produced, in accordance with Fig. 43, by the completely loss-free isothermal deflection of a gas jet of cross section $k \cdot F \cdot \sin \alpha$ and velocity v through the angle α . In the course of a second the momentum component of the flow at right angles to the direction of the plate $k \cdot m \cdot v \cdot \sin \alpha = k \cdot F \cdot \sin \alpha \cdot v \cdot \gamma/g \cdot v \cdot \sin \alpha =$

$= k \cdot \gamma/g \cdot F \cdot v^2 \cdot \sin^2 \alpha$ decreases continuously to zero and hence has

a mean value of $k \cdot \gamma/2g \cdot F \cdot v^2 \cdot \sin^2 \alpha$. According to the theorem of momentum, this average loss of momentum is equal to the external force P at right angles to the plate

$$P = k \cdot \sin^2 \alpha \cdot \gamma / 2g \cdot F \cdot v^2,$$

hence

$$A_d = k \cdot \sin^2 \alpha \cdot \cos \alpha \cdot \gamma / 2g \cdot F \cdot v^2$$

and

$$c_{ad} = k \sin^2 \alpha \cos \alpha.$$

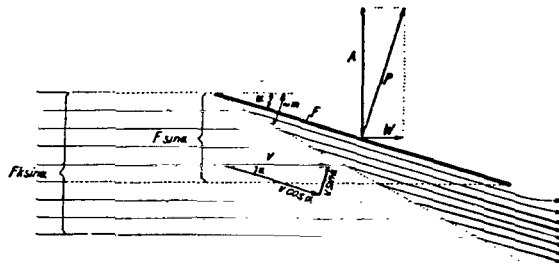


Fig. 43.

Limiting values of lift on the pressure side.

Here k represents how many times greater than the projected area of the airfoil in the direction of flight is the cross section of the gas jet fully affected by the loss of momentum. It is conceivable that this "region of influence" will become smaller with increasing speed, so that c_{ad} diminishes with increasing v , as the exact theory

requires; however, it is difficult to imagine k becoming less than one. It also seems plausible that k may become equal to unity (i.e., only the mass of air flowing through the cross section $F \cdot \sin \alpha$ in the direction of motion in front of the airfoil succeeds in imparting momentum to the airfoil), if the flying speed becomes so great

that the compression shock and Mach interference waves attach themselves to the pressure side, i.e., if the angle of attack and the Mach angle are approximately the same. From the condition $\alpha = m$ it follows that this speed limit will be about:

$$v \doteq a/\sin \alpha.$$

Above this speed there will be some justification for reverting to the original form of the old Newtonian expression:

$$c_{ad} = \sin^2 \alpha \cdot \cos \alpha$$

or for very small angles simply: $c_{ad} \doteq \alpha^2$.

If, in view of the large free paths of the air molecules at altitudes in question, the air is regarded not as a continuous medium but, with Newton, as an incoherent collection of small material par-

ticles, the total loss of momentum, i.e., $P = 2k \cdot \sin^2 \alpha \cdot \gamma/2g \cdot F \cdot v^2$, would have to be treated as a force effect on the body. Given this assumption, in the rest of the discussion it will be necessary to double the lift and drag forces derived from the limiting relation for the excess pressure.

If we consider that under the conditions in question the air is not an incompressible body, then, assuming an adiabatic change of state, instead of the old expression for the excess pressure Δp on the pressure side in terms of the pressure of the air at rest

$$\Delta p = q \sin^2 \alpha = \gamma/2g \cdot v^2 \sin^2 \alpha = p_a \cdot \kappa/2 \cdot v^2/a^2 \cdot \sin^2 \alpha$$

we get the new value

$$\Delta p_{ad} = q_{ad} \sin^2 \alpha = p_a \left[\left(\frac{n-1}{2} \frac{v^2}{a^2} + 1 \right)^{n/(n-1)} - 1 \right] \sin^2 \alpha.$$

Thus for c_{ad} we would have:

$$c_{ad} = \Delta p_{ad} / q_{ad} \cdot \alpha^2 = \frac{\left[(n-1)/2 \cdot v^2/a^2 + 1 \right]^{n/(n-1)} - 1}{n/2 \cdot v^2/a^2} \alpha^2.$$

The total lift coefficient c_a is obtained by adding c_{as} and c_{ad} .

In Fig. 44 we have tried to represent these relations graphically.

Thus, for speeds above $v = a/\sin \alpha$ the limiting relation

$$c_a = 165,300 \cos \alpha / v^2 + \sin^2 \alpha \cos \alpha \text{ should give sufficiently}$$

accurate values for all angles of attack.

For speeds between $v = a/\sin \alpha$ and about $v = 1.5 a$ the A. B. formulas or better the exact calculations from the primary flows certainly come closer to the truth.

In the range of speeds between about $v = 0.8 a$ and $v = 1.5 a$ the circumstances are quite obscure, but on the basis of empirical investigations this region is known well enough to make any serious surprises unlikely.

The range of speeds between $v = 0$ and $v = 0.8 a$ has been satisfactorily explored by means of a combination of simple wind tunnel experiments and theoretical analysis, especially along the lines laid down by Prandtl-Glauert.

In the subsequent theoretical study of flight paths the calculations will be further simplified by assuming that up to the speed of sound the value of c_a determined in the wind tunnel

is constant, while at higher speeds the simple boundary value formulas can be immediately employed. The boundary between the two regions is fixed by the point of intersection of the two curves.

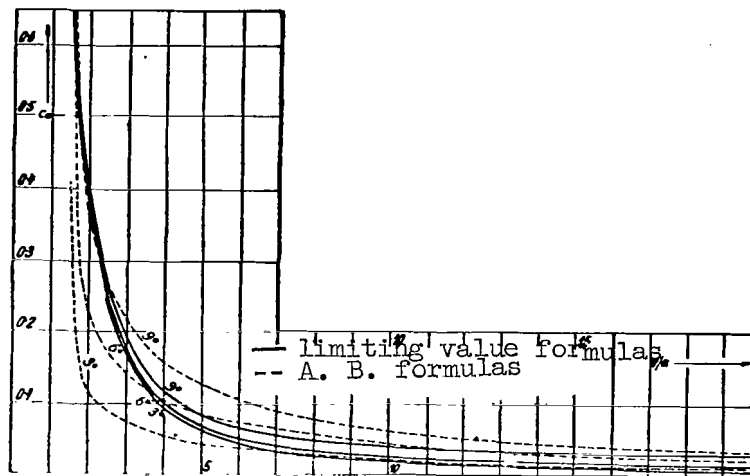


Fig. 44.

Lift coefficients for a flat plate from limiting value formulas.

222. The three-dimensional theory of airfoil lift under conditions of pure supersonic flow

At the ends of a supersonic airfoil of finite length there is a drop in the lift forces, and, according to Busemann, in the drag forces too, such that, together with reduced lift, we get a gliding angle the same as that of an airfoil of unlimited span. This statement is exactly true of the flat plate and approximately true of moderately thick profiles.

Thus, the supersonic airfoil is not actually susceptible to

induced drag.

No information is available concerning the magnitude of the decrease in lift associated with the ends of the airfoil. From the nature of supersonic flow we may assume that in connection with airfoils of ordinary slenderness it is inconsiderable and can make itself felt at most at the Mach angle.

223. Principles of airfoil design in the supersonic region

The basic principle governing the design of supersonic airfoils is as follows: theoretically the best supersonic airfoil is a flat, infinitely thin plate and in practice an airfoil of finite thickness will perform the better the more closely it approaches this shape. In relation to a thin plate the quality is equal to the reciprocal of the angle of attack and in the case of profiles of finite thickness deteriorates with the slenderness ratio t/d . From the point of view of airfoil design, the theoretical requirement for the thinnest possible cross section is opposed by the fact that

owing to the lack of induced drag the ratio b^2/F is to some extent without influence on the quality of the airfoil, so that the use of a very short, broad wing with low static spar root moments would appear advisable.

In the case of profiles of finite thickness, the nose should in any case be made sharp-edged, so that the angle between the entering tangents is at most equal to the operational angle of attack and only underpressure develops on the suction side.

In view of the superior subsonic properties of a profile with a mean curvature convex upward and in order to avoid the intersection and subsequent reflection and interference effects of pressure-side compression waves, it is advisable to make the pressure side completely flat.

The contour of the suction side of the profile is broadly fixed by the requirement of minimum thickness imposed by design considerations and by the direction of the entering tangent. In the

interests of high quality, the condition that $\int p \cos \alpha_x / \int p \sin \alpha_x$

be a maximum should be observed, to the extent that this is feasible.

With regard to the use of these airfoils, they should not be flown at an angle of attack so small that overpressures develop on the suction side of the profile nose.

/12

It would appear to be theoretically correct to make the nose of the profile so slim that the angle between the entering tangents approaches zero and to bend this edge forward in the direction of flight to achieve a smooth entry. In practice, however, the losses due to the compression shock on the pressure side are so small that there is no point in taking them into account in the design.

23. Resistance in the Subsonic Region. General.

Now we consider the component of the aerodynamic force on a body of general shape that acts in opposition to the motion along this direction and that requires each second an amount of work Wv to overcome it. The last feature is the cause of the great design interest attaching to the resistance, since it governs the propulsive power needed.

In classical hydrodynamics we assume an ideal medium whose pressure at a given point is the same in all directions and which is incompressible. On this basis we arrive at d'Alembert's paradox for a body moving in such a medium, for the processes of motion and hence the pressure distributions on the front and rear sides of a sphere are completely symmetrical, which implies for this (or any other) body that the air exerts no resistance to the motion.

/124

Therefore we discard the first condition; an ideal frictionless fluid is no longer considered, and we assume a capacity to exert a tangential frictional force on the surface. This leads to the assumption of a boundary layer at this surface, thence to consideration of the detachment of this layer, and finally consideration of the form resistance.

Speeds of the order of those presently common for aircraft give rise in this way to consistent theoretical results.

The second assumption (incompressibility of an ideal medium) also becomes invalid even for practical purposes if the speed is raised further. There are some usable principles for a detailed consideration of the calculated results for the range of speeds between normal flight speeds and the speed of sound; these will be considered below.

The induced resistance of a bearing surface of finite span occupies a special position; this will consequently be considered separately.

231. Frictional Resistance

This resistance is directly of major significance for the subsonic region, because c_{wr} (the frictional resistance coefficient)

for the usual streamlined bodies used in aircraft accounts for the major part of the total resistance. It is also indirectly of considerable importance to the form resistance on account of its effects on onset of boundary-layer detachment and further on the breakaway on the upper surface of wings of large angle of attack, on blunt-ended bodies, and so on.

The need to assume internal friction (viscosity) of the air in motion processes for finite speeds v leads to shear stresses between adjacent parallel layers of air having a separation dy , these being proportional to the velocity difference:

$$\tau = \eta \cdot \frac{dv}{dy}.$$

Here η is the viscosity in $\text{kg}\cdot\text{sec}/\text{m}^2$.

Reynolds number indicates the mechanical similarity in the treatment of frictional forces on bodies differing in size relation; this gives the ratio of the inertial to the frictional force, being a dimensionless number:

$$R = v \cdot t / \nu.$$

Here v is the undisturbed flow speed relative to the wall, t is the length of the wall in the flow direction, and $\nu = \eta/\rho$ is the kinematic viscosity (m^2/sec).

Practical aerodynamics employs in place of the actual Reynolds number a parameter of about the same magnitude:

125

$$R = 70 \cdot v \text{ [m/sec]} \cdot d \text{ [mm]}.$$

Reynolds number takes no account of the compressibility, so a further conversion factor v^2/a^2 must be included. The viscosity of air is very dependent on the temperature t , being

$$10^6 \eta = 1.712 \sqrt{1 + 0.003665 t} (1 + 0.00080 t)^2.$$

For example, the shearing force between parallel layers of air of area 1 m^2 and separation 1 mm moving with a relative speed of 1 m/sec at 0°C is

$$\tau = 1.712 \cdot 10^{-3} = 0.001712 \text{ kg/m}^2.$$

This shows that the frictional coefficient for air is very small, so the frictional forces are very small in relation to the mass and pressure forces, which causes Reynolds number to be large; the ideas derived from the theory of ideal media (such as potential flow around a body) apply closely to real air if solid boundaries are not present, for which their validity completely fails, since they do not assist in the understanding of adhesion to the surface.

The shear stress between a rigid wall and air in motion relative thereto is deduced from the molecular theory, which gives an infinite stress; this means that the air directly in contact with the wall adheres to it, the tangential component of the motion being zero.

Prandtl's boundary-layer theory enables one to overcome these difficulties. The boundary layer is in essence such that the flow processes in the free air are dominated by the inertial forces (and

so correspond closely to the laws of ideal fluids), while viscosity is dominant in a thin boundary layer near a solid wall, the inertial forces here playing a subordinate role. The flow speed is reduced by the friction at the wall in this thin transition region; the speed directly at the wall is taken as zero. The thickness of a laminar

/126

boundary layer is found to be proportional to $1/R^{1/2}$. The flow within the boundary layer itself is laminar at small Reynolds numbers;

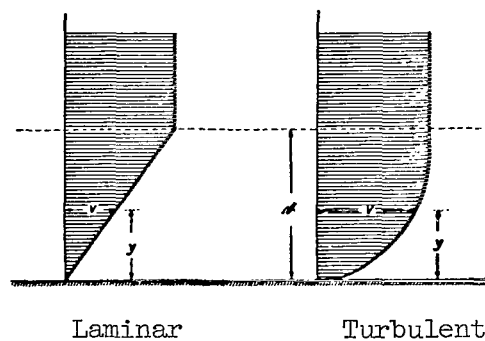


Fig. 45.

Boundary layers.

the speed increases linearly with distance from the wall until the full flow speed is reached. The laminar flow gives way to turbulent above a certain critical Reynolds number, in which case the speed as

a function of distance from the wall follows the law $y^{1/7}$ (Fig. 45). The thickness of the boundary layer on a planar plate having laminar

flow is given by $\delta = 5.83 (\nu/v)^{1/2} x^{-1/2}$, in which x is the distance from the leading edge.

The resistance of a plate of surface area O and thickness t exposed on one side to a flow of speed v outside the boundary layer is

$$W_f = c_f \cdot \gamma / 2g \cdot 0 \cdot v^2,$$

in which

$$c_f = 1.327/R^{1/2}.$$

A planar plate having a turbulent boundary layer has a boundary layer thickness that increases rather more rapidly in accordance with

$$\delta = 0.370 (x/v)^{1/5} x^{4/5}.$$

The resistance is calculated as previously, except that $c_f = 0.072/R^{1/5}$. In fact, a planar plate usually shows both types of flow, there being a laminary boundary layer behind the leading edge, which gives way to a turbulent one at a critical Reynolds number ($R \approx 10^5$). The Prandtl-Geber treatment is applicable with $c_f = 0.073/R^{1/5} - 1600/R$ only so long as the formula for laminar flow does not give larger values.

These frictional coefficients represent lower limiting values for very smooth surfaces (metal, heavily lacquered fabric, and so on). Rougher surfaces having projections of the order of the thickness of the boundary layer give larger frictional coefficients, which are largely independent of Reynolds number.

Slightly curved surfaces (wings, fuselage, etc.) give laminar flow up to the point of least pressure, with turbulent past this. The resistance agrees fairly closely with that of a planar plate of the same area. The pressure distribution can be deduced as for potential flow, since this is not affected by the thin boundary layer.

No detailed examination has been made of how far these results can be applied to speeds above about $0.2a$; qualitatively

speaking, we would expect the compressibility to have no effect on the boundary layer whereas Reynolds number is affected in the ratio v^2/a^2 , so c_{wr} is not independent of the speed.

It is certain that the frictional resistance remains basically proportional to the first power of v as long as the pressure differences are very small relative to the external air pressure; though it is affected by the type and thickness of the boundary layer, and hence increases more rapidly, the dependence is scarcely that of the second power. For thinner laminar boundary layers we have $W = k_1 v^{1.5}$; for thicker turbulent ones, $W = k_2 v^{1.8}$

Momentum transfer plays the dominant part in turbulent boundary layers; this leads to larger energy losses, so the shearing stress increases more rapidly than as the first power of v (hydraulic studies give the increase as almost in accordance with the second power). In any case, a resistance coefficient corresponding to a quadratic law relating resistance to speed must be assumed if the resistance is dominated by friction. This result is commonly known.

232. Form Resistance

Frictional resistance accounts for the major part of the overall resistance of a streamlined body at low (ordinary) flight speeds; the form resistance is then scarcely significant. The picture is rather different for bodies of poor shape even at low speeds and even for bodies of the best shape at higher speeds, even ones still far from the speed of sound.

Vortex motion occurs in any part of a fluid that comes near the surface of a solid body and hence into the region of the boundary layer as a result of a free effectively frictionless potential flow.

Such parts of the fluid showing vortex motion may enter the free flow later on behind the body, in which case they cannot lose this motion (by virtue of the laws of frictionless fluids); the vortex layers develop into vortex 'streets' and continually carry off energy, which is maintained by continuous fresh production of vortices within the boundary layer. The resulting resistance to relative motion between body and fluid is termed the form resistance, which can be substantially affected by choice of the shape and hence of the corresponding boundary-layer detachment.

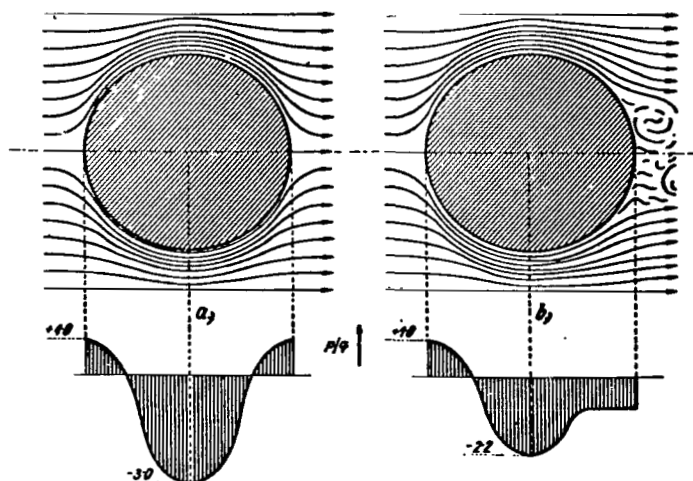


Fig. 46.

Origin of form resistance in the subsonic region.

The causes of the last may be summarized (according to Betz) briefly as follows:

1. Larger pressure increase along the wall in the flow direction (principally from highly convex surfaces and, especially, sharp edges). The slowly moving boundary layer has low kinetic energy and cannot flow into a region of higher pressure; it accumulates and eventually becomes detached.
2. Accelerated nonstationary flow reduces the tendency to breakaway, whereas retarded flow accentuates it.
3. Thick boundary layers (e.g., ones caused by a long surface in front of the point) become detached more readily than thin ones.
4. Turbulent boundary layers become detached later than laminar ones.

5. Rough surfaces generally favor detachment, but can hinder it under some circumstances if they cause laminar layers to become turbulent in accordance with 4.

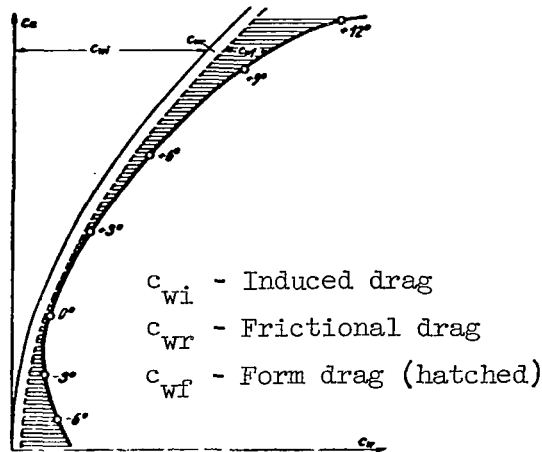


Fig. 47.

Form resistance of a wing.

The pressure distribution thus determines the occurrence of the form resistance to be expected. The symmetrical flow predicted by potential theory for a frictionless fluid (e.g., that around a cylinder) corresponds to a similarly symmetrical pressure distribution (Fig. 46a), which means that there is no shape resistance. In fact, air friction gives rise to a boundary layer of reduced flow speed near the surface, which (as Fig. 46a shows) must flow against a rapidly increasing pressure after passing the midline. This gives rise to case 1 of the above causes of detachment; the thickness of the boundary layer increases rapidly, the speed falls, the layer becomes stalled, at a certain point susceptible of calculation under some circumstances detachment occurs, and the layer mixes with the free potential flow far from the surface, which is accompanied by vortex production, which causes an appreciable change in the

pressure distribution (Fig. 46b). The site of detachment is closely governed by the ratio of the inertial force to the frictional force and hence by Reynolds number. The resultant of the pressures on the leading and trailing sides is no longer zero but leaves a residual resistance force acting against the flow direction, which must be balanced by an external force (e.g., as in a motor vehicle).

These causes of flow detachment further imply that detachment and hence the resulting force in the flow direction are smaller if the part of the body behind the principal section is tapered ("streamlined") toward the meridian with large radii of curvature.

The pressure distribution approaches the theoretical one for potential flow as Reynolds number increases. Above the critical Reynolds number, the region of the slipstream extends behind the body as a narrow band.

The form resistance is very variable along the wing profile as the angle of attack increases. The induced drag and the frictional drag are readily calculated for ordinary speeds, and the form resistance may be deduced as a function of angle of attack from experimental polar curves (Fig. 47). The profile drag consists almost entirely of surface-friction drag for small angles of attack, but the boundary-layer thickness on the upper surface increases rapidly with α , which leads to onset of detachment ('dead water'), which ultimately extends to the whole of the rear part of the reduced-pressure surface (flow breakaway).

/130

At higher speeds (above about 0.2a) the ratio of the inertial force to the static pressure (i.e., the compressibility) becomes important in addition to Reynolds number. A good method is available* for the graphical representation of compressible potential flow for the cases of planar and rotational symmetry, but such treatments are naturally of rather less value for the deduction of drag forces than is, say, Fig. 46a.

The relation of inertial force to static pressure comes to dominate the breakaway effects as the speed increases; the viscous forces become of secondary importance. The increasing inertial forces naturally favor breakaway very greatly, so the reduced-pressure area on the lee side of a body exposed to a fast flow rapidly increases in size; the drag coefficient increases very greatly. A good example of this is given by Brigg's measurements on wing profiles at high speeds. Fig. 48a shows the polar curves for a single

*Bryan, The Effect of Compressibility of Streamline Motions. Tech. Rep. Advis. Comm. for Aeronautics, London, No. 55, 1918, and No. 640, 1919.

profile at various speeds, for comparison with Fig. 47. Fig. 48b shows the effects somewhat more clearly in terms of the drag coefficient of a profile as a function of v for various angles of attack.

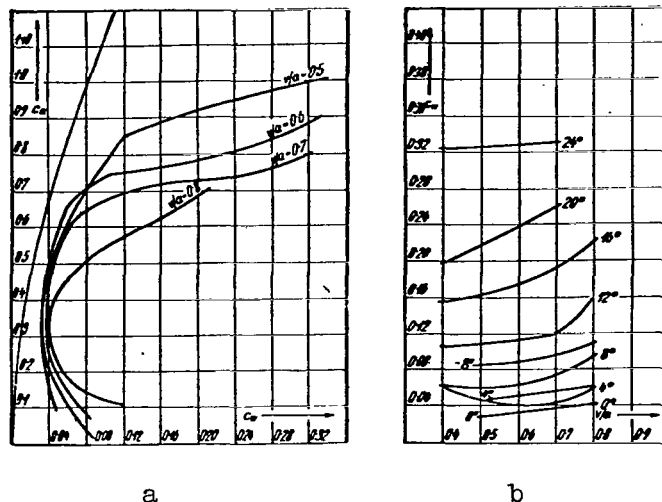


Fig. 48.

Form drag of a wing at high subsonic speeds.

The form drag in essence consists of the difference of the resultant pressures on the leading and trailing sides; it attains high values particularly on account of the reduced pressure (relative to the static pressure) on the lee surface, which is caused by breakaway of the flow from the surface. This breakaway is slight at low speeds, for which the ratio of viscosity to inertia exceeds that of pressure to inertia, if the viscosity is small relative to inertia (Reynolds number large). The ratio of inertia to pressure is appreciable at high speeds, and the breakaway becomes rapidly larger; the turbulent wake area encompasses an increasing proportion of the lee side. The pressure deficit on the upper surface (suction) can equal the air pressure p_a at the limit, but it falls well below

this limit in the subsonic region. Little is known about the relation of this mean suction to the speed, shape of body, etc.; only a few general indications are available from test results on the overall drag.

233. Induced Drag

We have so far considered the resistance to motion for bodies moving in a medium without giving rise to a force component normal to the direction of (transverse force, lift). This restriction does not apply to wings, so we must consider the induced drag arising from the lift effect. The origin of the induced drag of a wing is as follows (see also section 212). The excess pressure arising on the underside in the middle of a long wing balances the pressure deficit on the upper side at the ends of the wing by flow around the tips. The extremely vigorous circulation from the underside around the end to the upper side is superimposed on the main flow parallel to the profile and gives rise to a spiral vortex, whose axis may coincide with the flight direction. This peripheral vortex arises at any wingtip and remains in the virtually friction-free slipstream; it thus stretches from the starting point along the entire path to the landing point and is kept unbroken during the flight by a continuous supply of energy. The resulting end resistance from the wingtips usually exceeds the residual flight resistance by a large factor and therefore deserves special consideration. It is least when the lift is distributed over the span b in the form of a half ellipse, which occurs when the wing plan is elliptical. Prandtl gave an exact expression for this case. He found* that

/132

$$W_i = A^2 / \pi q b^2.$$

The drag coefficient c_{wi} for the induced drag is then $c_{wi} = (c_a^2 / \pi)$

*Hütte, I. 26th edition, p. 402.

(F/b^2) , in which b^2/F denotes the chord ratio of the wing.

This formula applies only as an approximation for a contour other than elliptical, but appreciable deviations are to be expected only for any wing with a discontinuity at the middle. The induced drag can then be appreciably larger.

A practicable value of the aspect ratio is $b^2/F = 5$, in which case the induced drag of a good profile is 2 or 3 times the other drag of the profile; this is primarily the factor preventing an improvement in the wing performance $1/\epsilon = A/W$. This quantity governs the economics and range of an ordinary aircraft, so designers' attempts to reduce it are understandable. The best method is clear from the structure of the formula for the drag coefficient itself (use of wings of very high aspect ratio).

Abundant use has been made of this simple method where the high static bending moments that result from the use of such wings (sailplanes). In regard to load-carrying aircraft, some scope was found at first for improvement in the performance by reduction of the parasitic drag (of cabin, fuselage, etc.), so long wings should come into use with the more general utilization of integral wing assemblies.

The change in the coefficient of a wing in response to change in aspect ratio is governed solely by the induced drag, as (following Betz*) we may show for a wing of parameter b_1^2/F_1 . The lift and drag coefficients for another wing of the same profile but a different aspect ratio b_2^2/F_2 at the corresponding point are simply

$$c_a = c_{a1} = c_{a2}$$

$$c_{w2} = c_{w1} + \frac{c_a^2}{\pi} (F_2/b_2^2 - F_1/b_1^2)$$

*Hutten, I. 26th edition, p. 402.

$$\alpha_2 = \alpha_1 + c_a/\pi \cdot (F_2/b_2^2 - F_1/b_1^2)$$

(angle of attack in radians). Another and apparently ready means of reducing the induced drag is to prevent flow around the ends of the wings by means of thin end plates. No success has been obtained with this.

A distinctive and effective method would appear to be used in nature by the large soaring birds, which has not been imitated as yet. The underside of the wing has a concave shape and a periphery that tapers outward, which gives rise to the underside lift-yielding flow considered in section 212 along the length of the wing, which (according to observations by Hankin and G. Lilienthal) appears to extend beyond the end of the wing and so has a marked effect on the production of tip vortices. No practical success has been obtained with this, though.

/133

In other respects these relationships are of secondary importance for our purpose, as has already been mentioned and which will later be demonstrated, for the aerodynamic performance of a rocket aircraft and with it of a rocket wing have relatively less effect on the economics and load capacity than they do for ordinary aircraft.

The behavior of the induced drag at higher speeds is of interest; no study in depth has been published, though Briggs has suggested that it should behave as demonstrated here for low speeds up to the speed of sound and that sufficiently precise results should be obtained by calculation from the lift. Adequate methods of calculation are available for the lift itself. The relationships become completely different for purely supersonic flow; according to Busemann, induced drag in general does not appear.

234. Overall Resistance

Frictional and form components make up the overall drag for a body moving with a subsonic speed in air in such a way as not to give rise to a force component at right angles to the direction of motion. General statements can be made about both drag components, especially via Prandtl's boundary-layer theory. The purely computational derivation of the drag of a body moving through the air by reference to the geometry is feasible in only a very few cases of no practical sig-

nificance. In most cases the calculation is performed by a combination of theoretical relationships with tests made subject to certain verified assumptions, particularly tests on models, which provide adequate precision for the purposes of the engineer as regards the forces to be expected. The values derived from tests in artificial airstreams or from experimental firings do not in general enable one to distinguish the two drag components, but this is usually no disadvantage for the engineer. It is always possible to derive one of the components separately when this is necessary by measuring the pressure distribution on a model constructed with small holes, though this is troublesome.

In general, we can only say that a body with a blunt rear side (plates at right angles to a flow, wings of high angle of attack, projectiles, and so on) has the form resistance as the main component of the overall drag, whereas a body with a suitably chosen shape (tapered rear) will not show breakaway, in which case the very small overall drag is essentially frictional.

We know that tests in the subsonic region do not agree with Newton's assumption (air resistance proportional to the square of the speed). But, for reasons of expediency we retain Newton's resistance formula

$$W = c_w \cdot \gamma / 2g \cdot F \cdot v^2$$

in aircraft engineering and take account of the deviations from the very roughly quadratic relation actually found by saying that the drag coefficient c_w is also a function of speed. We may say quite

generally that at very low speeds (up to about 0.05a), for which frictional forces exceed all other sources of drag, the drag is proportional to the speed to the power 1.5 to 1.8 for all bodies, as it is for bodies of excellent streamline shape at higher speeds; this means that c_w must fall correspondingly rapidly as the speed increases.

Inertial forces become dominant over viscous ones as the speed increases, which causes c_w to become more independent of the speed, but

at higher speeds the inertial forces become appreciable relative to the static pressure, whereupon this coefficient rises again. The range of the first, very considerable fall in c_w is insignificant

for the regions of interest here, since it covers the range $R = 10$ to $R = 10^5$, which itself corresponds to very low flight speeds (mostly less than the minimum flying speed) for the aircraft dimensions involved. Diagrams for c_w (such as Fig. 49) indicate this range clearly.

Much greater interest attaches to the range from 0.2 sonic speed upward, in which c_w increases rapidly. From about 0.2a upward the

/135

hydrodynamic treatment is replaced by the gas-dynamic one. This

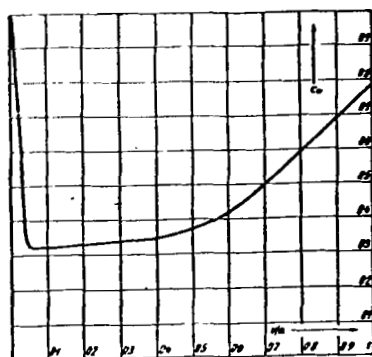


Fig. 49.

Drag coefficient of a sphere in the subsonic region.

rise itself was already known in 1790; Bashforth made the first detailed study for spheres in 1870. Lorenz's experiment was designed to explain the rise as a resonance effect* and is now viewed as in-

*H. Lorenz. Phys. Z., 18, 209, 1917.

correct especially since the maximum in c_w is attained not at the speed of sound but appreciably above it. Sommerfeld* pointed out some similarities with the older electron theory. The rise is very considerable below the speed of sound, which must have its origin in the very pronounced boundary-layer breakaway, which occurs even when the body moves relative to the undisturbed air with a speed well below that of sound if the local flow speeds on many parts of the surface have already reached or exceeded the speed of sound (this occurs, for instance, when $v = 0.4a$ when a compressible medium flows at right angles to the axis of a circular cylinder); this gives rise to wave resistance, which we shall deal with in detail later.

This view is confirmed by the circumstance that tapered bodies cause a much later and smoother rise than do short thick ones, because the local rises in flow speed are smaller.

A formal method of calculating the increase has been given by Lechner**, which requires a knowledge of c_{w0} (for low speeds), c_{wa} (for the speed of sound), and for c_{wmax} (for speed v_m). He found that

$$c_w = c_{w0} \frac{(a + bv) a}{(a + bv) a - v},$$

in which

$$a = 2c_{w0} \frac{v^2}{a^2} \frac{c_{wm} - c_{wa}}{(c_{w0} - c_{wa})^2 (1 - a^2/v_m^2)};$$

*Klein-Sommerfeld, Theorie des Kreisels (Theory of the Gyroscope), 1898.

**Lechner, Über den Einfluss der Wellenbewegung auf den Bewegungswiderstand (Effects of Wave Motion on Resistance to Motion).
Österr. Flugzeitschrift, 1918.

$$b = 2c_{w0} \frac{v_m^2}{a^3} \frac{c_{wa} - c_{wm}}{(c_{w0} - c_{wa})^2 (1 - a^2/v_m^2)} -$$

$$- \frac{c_{wa}}{a (c_{w0} - c_{wa})}.$$

Fig. 49 shows the drag coefficient of a sphere as a function of v , which in part derives from Hélie's ballistic tests. Similar curves can be derived for any body, as Fig. 48 shows.

/136

Section 24 deals with more detailed relations, in part derived from theory, for this region.

24. Resistance in the Supersonic Region. General.

The assumption used before for subsonic flight, that air drag is proportional to:

1. a coefficient c_w dependent upon the shape of the body,
2. air density γ/g ,
3. greatest spar cross section perpendicular to the longitudinal axis or to wing surface F ,
4. a particular function of flying speed $f(v)$,

and that these factors are practically independent of each other, is retained here. This assumption led us to the resistance equation

$$W = c_w \cdot \gamma/2g \cdot F \cdot f(v).$$

We included a certain dependence upon v for resistance coefficient c_w and thus obtained the usual form:

$$W = c_w \cdot \gamma / 2g \cdot F \cdot v^2,$$

that we will retain in the supersonic region as well.

Here, too, all investigations stem from determination of the resistance coefficient c_w , which is dependent upon body shape and flying speed.

The two resistance components found in the subsonic region for a body moved through air without transverse force, namely frictional resistance and form resistance, appear again here. In the supersonic region, frictional resistance, increasing at less than the second power of flying speed, constitutes a very minor part which will be treated only briefly. Form resistance is divided here into two clearly separate components: The form pressure resistance at the forward end, increasing at about the square of speed and whose c_{wfd} is therefore nearly a constant, and the rear suction. The

latter soon increases to its limit after the sound barrier is exceeded; this limit is equivalent to an absolute vacuum on the entire

body surface behind the main frame and is thus about 1 kg/cm^2 under standard atmospheric conditions. Air flows into the rarefied space formed behind the body and creates friction vortices; the energy required occurs partly as heat in the wake of the body, according to Cranz, and partly as outwardly directed kinetic energy, sensible as the whistling of projectiles, for example. This component of resistance depends upon the shape of the body's tail; its resistance coefficient c_{wfs} asymptotically approaches zero. After the sound

barrier is passed, wave resistance is added; its coefficient c_{ww} in-

creases to considerable values shortly above the sound barrier and then drops again for well-shaped bodies and also asymptotically approaches zero. It appears at all projecting parts, especially the head; the energy consumed by the latter goes out as wave energy and is audible as the crack of a projectile. The shape of the body's

head is of decisive importance for the magnitude of this resistance.*

241. Frictional Resistance

Some considerations from the molecular kinetic theory will serve to show the nature of tangential friction forces, especially in the supersonic region.**

The theory explains pressure against a restraining wall by gas at rest as the resultant impact force of the impinging gas molecules in strong thermal motion. If c_i is the component of the mean value of molecular velocities in a given direction i , then the gas pressure of the impinging and elastically rebounding molecules is:

$$p_i = \rho c_i^2.$$

The resultant mean molecular velocity c itself is shown by a simple consideration of the equality of its three components to be:

$$c = \sqrt{3RT},$$

(for example, at 0°C, c is 485 m/sec for air, 1844 m/sec for hydrogen,

*See also: Karman-Moore, "Resistance of Slender Bodies Moving with Supersonic Velocities, with Special Reference to Projectiles," Trans. Am. Soc. Mech. Eng. (Appl. Mech.) No. 23, 1932.

**See, among others, Jaeger, Kinetische Theorie der Gase (Kinetic Theory of Gases) in Geiger-Scheel, "Handbuch der Physik" (Physics Handbook), vol. 9, Springer, 1926.

396 m/sec for carbon dioxide, and 621 m/sec for water in permanent gaseous state.)

In addition, the free path l that a molecule covers on the average before colliding with another molecule is calculated from the number of molecules per unit of mass N and molecule diameter d as:

$$l = \frac{0.677}{\rho N \pi d^2}.$$

(For example, $l = 0.96 \cdot 10^{-5}$ cm for air at standard pressure and temperature.)

From the molecular kinetics standpoint, friction of a gas stream flowing past a solid wall is explained as the continuous movement of molecules, because of their thermal motion, transverse to the flow direction out of the flow layers of lower flow speed into those of higher speed and vice versa, and out of the stream to the wall, there experiencing changes in motion magnitude, and thus accelerating or decelerating because of collisions with other air and wall molecules.

According to Jaeger, the gas viscosity η already known from subsonic friction depends upon free path length in the relationship*:

$$\eta = 0.419 \rho c l.$$

From the molecular properties of the gas η is therefore calculated

as $\eta = 0.09 c / N d^2$. Friction phenomena themselves play a very similar part qualitatively in the supersonic region to the part played in the subsonic region in the boundary layer between the solid surface and the free flow. The flow speed in the boundary layer is partly

*Jaeger, G. Wiener Berichte (2a), vol. 108, p. 452, 1899.

below and partly above the sound barrier, so that the relationships of subsonic flow are partially valid, and the occurrence of turbulent boundary layer friction is particularly to be expected.

Little is known of the quantitative relationships of supersonic flow. A basis for their estimation can be formed from the viscosity of air and the fact that the boundary layer is very thin at high speeds, so that high shear stresses must be expected from the high velocity gradients.

According to a letter from Dr. Busemann to the author, these shear stresses can be taken as 0.3% of the dynamic pressure, so that the friction coefficient of a flat plate due to friction on both sides will be $c_{wr} = 0.006$, for example. Of course, a fixed value

of this type would mean a preponderance of frictional resistance over all other drag components at very high supersonic speeds, assuming slender shapes.

This is improbable. Frictional resistance has been shown to drop at speeds not too far above sonic to very low values compared to the other resistances, and extrapolation of known test values to higher speeds gives fairly continuous curves only under this assumption (see, for example, Fig. 70).

The conditions described are furthermore valid for standard gas pressures and, according to experiments of Kundt-Warburg*, down to pressures of about 0.017 atm, corresponding to a flight altitude of about 30 km. At lower air densities and thus longer free paths of molecules an appreciable layer appears on the solid wall where the molecules strike the wall before they have passed through their mean free path, so that the gas behaves differently there from the way it does in its free interior.

As the free path increases further, the air's friction coefficient accordingly decreases. The free path becomes similar in magnitude to the calculated boundary layer thickness or the unavoidable roughness of the airplane's surface so that the usual boundary layer formation is disturbed and the air can no longer be considered a continuous medium in this respect.

If the mean free path at very low air densities finally becomes comparable to the magnitude of the body's dimensions, so that molecular collisions with one another are less important than molecular collisions with the wall, then the friction stress obeys the simple law**:

*Kundt-Warburg, Pogg. Annalen, vol. 155, p. 337, 525, 1875.

**"Handbuch d. Physik" (Handbook of Physics), vol. 9, p. 442.

$$\tau = \rho c v / 4 = p / 4 \cdot \sqrt{3/RT} v.$$

At 60 km flight altitude, where this law of very rarefied gases is perhaps still not fully valid, the friction coefficient at corresponding flying speeds for a surface not inclined to the flight direction would be several thousand times less than 0.003.

According to the above equation, friction in highly rarefied gases depends upon gas pressure p , so that the angle of attack α of surface to the air stream is of similar influence, as it is in form pressure resistance; therefore surfaces at higher angles of attack experience higher friction forces than do surfaces inclined less or not at all to the air flow.

Finally, if the body surface is not completely rough in the sense of molecular kinetics, i.e., if the impinging air molecules are only partly given the speed v of the flying wall, then not even the assumed and extremely small friction force will come into full play.

It may be concluded from all these considerations that in subsequent studies we can completely neglect, under the conditions that we have, frictional resistance in comparison with the other drag components.

Frictional resistance is nevertheless of very great interest from another standpoint.

In the Prandtl boundary layer between the solid body's surface and the free flow of adequately dense gas, frictional heat continually occurs, being taken away in the wake and clearly visible as highly heated wake region in the schlieren photographs of moving projectiles.

Busemann* states in regard to the magnitude of temperatures resulting from frictional heat that the innermost layer of the boundary layers that adheres directly to the wall has the temperature that would result from adiabatic compression at the point of stagnation (see Section 242). This temperature drops within the extremely thin boundary layer of the supersonic region to the temperature outside the boundary layer. Because of actual thermal conduction losses and radiation losses to the outer air in the very small and slowly moving gas region, this theoretical temperature peak at high

/140

*Handbuch der Experimentalphysik" (Handbook of Experimental Physics), vol. 4, p. 365/366.

supersonic speeds should be very much flattened. In particular, at higher temperatures the deviations from adiabatic behavior, known from the nozzle, and especially dissociation conditions, will manifest themselves.

At the high flight altitudes necessary for rocket flight at high supersonic speeds the long free path has the above-described effect of scarcely allowing an appreciably heated boundary layer to appear.

The extent to which the wall of the airplane warms up to whatever the maximum air friction will be depends largely upon its thermal capacity and the duration of the temperature, since the amounts of heat available are extremely small, especially at the very low air densities at the flight altitudes in question.

This hardly need be considered a danger to the development of rocket flight.

In conclusion, we can ignore to a first approximation both the force effects and the thermal effects of frictional resistance in further investigations.

242. Form Resistance

Form resistance was defined in Section 232 as the difference between the resultant of pressure distribution on the front and rear, with the front and rear sides separated by the line connecting those surface points at which the pressure, decreasing from the front-side positive pressure down to the rear-side negative pressure, reaches the zero value. Form resistance thus is separated into the front excess pressure (form pressure resistance) and the rear suction.

The excess pressure can be simply imagined as the gradual loss, by a certain air mass $\gamma/g \cdot K \cdot F \cdot v$ striking k times the main frame area F per unit of time, of the air mass's total momentum

$\gamma/g \cdot k \cdot F \cdot v^2$ during a unit of time. This mean momentum loss

/141

$\gamma/2g \cdot k \cdot F \cdot v^2$ is directly equal to the drag force W_{fd} , according to the momentum theorem, and therefore:

$$W_{fd} = k \cdot \frac{\gamma}{2g} \cdot F \cdot v^2,$$

so that consequently:

$$c_{wfd} = k.$$

Of course the air mass involved can under certain circumstances retain a part of the impulse it has in the direction of flight and can flow sideways around the body. The amount by which c_{wfd} is smaller

than k depends chiefly upon the shape of the body's front side. For purely cylindrical bodies, whose leading surface is equal to the main frame area and perpendicular to the direction of flight, the value $c_{wfd} = k = 1$ is fairly appropriate as long as no stagnation

cone forms ahead of it to assist flow around it. For a conical tip (Fig. 50) with half-aperture angle α it may be assumed as an approximation that in the direction of flight only the momentum component

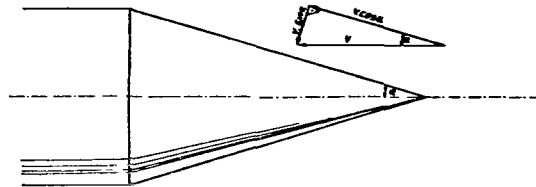


Fig. 50.

Maximum supersonic flow at cone tip.

$k \cdot \gamma/g \cdot F \cdot v \cdot v \cdot \sin^2 \alpha$ is lost, so that here the pressure resistance is:

$$W_{fd} = k \cdot \sin^2 \alpha \cdot \gamma/2g \cdot F \cdot v^2$$

and $c_{wfd} = k \cdot \sin^2 \alpha$. At $\alpha = 90^\circ$ we again arrive at the limiting value determined previously. At $\alpha = 22.5^\circ$, a mean angle occurring on well-formed projectiles, $C_{wfd} \doteq 0.15$, assuming $k = 1$. These con-

siderations have limited application in the subsonic region and also in the region just above the sonic, of course. If flying speed reaches values where the Mach angle equals or is less than the half-aperture angle α , so that the entire tip enters completely undisturbed air (a phenomenon that according to Cranz has already been indicated for very fast ogival projectiles), then the assumption $k = 1$ can re-

quire a correction and the value $c_{wfd} \doteq \sin^2 \alpha$ may represent a useful approximation.

In any case it is known that the shape of the leading side of a body has a decisive influence upon profile pressure drag.

It is highly probable that at flying speeds below $v = a/\sin \alpha$ air masses outside the cross section area F undergo momentum losses, too, so that $k > 1$. Above this region there are fairly accurate studies by Prandtl and Busemann, which will be referred to in Section 243.

/142

If it is also noted here that the air is elastically compressible, and again assuming adiabatic change of state of ideal gases, the positive pressure Δp at the leading side in comparison with the pressure of still air is found to be, not

$$\Delta p = q = \gamma/2g \cdot v^2 = p_a \cdot \kappa/2 \cdot v^2/a^2$$

but the new value:

$$\Delta p_{ad} = q_{ad} = p_a \left[\left(\frac{\kappa - 1}{2} v^2/a^2 + 1 \right)^{\kappa/(\kappa-1)} - 1 \right].$$

The form pressure coefficient thus changes according to the equation:

$$c_{wfd} = k \Delta p_{ad} / q = k \frac{[(\kappa - 1)/2 \cdot v^2/a^2 + 1]^{\kappa/(\kappa-1)} - 1}{\kappa/2 \cdot v^2/a^2}.$$

The air heating ΔT corresponding to adiabatic air stagnation of Δp is:

$$\Delta T = T_a \frac{\kappa - 1}{2} v^2/a^2.$$

The coefficient a again is the quantity in the external still air.

The form pressure drag takes on other very vital significance, in addition to its numerically large magnitude, because it causes the head of the moving body to be heated, and this heating, as we know from the example of glowing and vaporizing meteors, can increase to extraordinary temperatures at very high speeds.

All known methods for calculating this heating involve very great uncertainties.* The most unfavorable limiting case comes from an assumption based on the heat of compression of air in the region of the pressure-side stagnation; according to this the loss of

kinetic energy per unit of air mass of $v^2 \sin^2 \alpha/2$, contained in the study of Fig. 20, is completely converted into a corresponding increase in heat of the stagnated gas, whose temperature is then higher than the body temperature, so that a heat transfer takes place between body and air; this raises the body temperature until this heat absorption is in equilibrium with the heat given off by the body.

These stagnation temperatures of air thus appear much more unpleasant than the previously discussed friction temperatures,

*See Oberth, H. "Wege zur Raumschiffahrt" (Methods of Space Travel), 1929.

because they involve much greater amounts of heat.

From the energy equation of gas dynamics for adiabatic flow:

/143

$$A v^2/2g - J = 0$$

there follows:

$$A v^2/2g - c_p T = 0.$$

At stagnation of the velocity component ($v \sin \alpha$) the air thus experiences a temperature increase:

$$\Delta T = A v^2 \sin^2 \alpha / 2gc_p \doteq v^2 \sin^2 \alpha / 2000.$$

The known equations $a = \sqrt{\kappa gRT_a}$ and $c_p - c_v = AR$ make it possible to write:

$$\Delta T = T_a (\kappa - 1)/2 \cdot v^2 \sin^2 \alpha / a^2,$$

when T_a is the absolute temperature of the undisturbed outer air.

It is difficult to assess the extent to which these temperatures are reached in view of the strong radiation of the highly compressed gas, and the extent to which the heat in the compressed gas is imparted to the body itself.

For a conical tip of $\sin \alpha = 0.1$, at $v = 6000$ m/sec in the boundary regions of the atmosphere ($T_0 = 270^\circ$), the total stagnation temperature of the air would be about $T = 450^\circ$, for example.

With the aid of some rather uncertain assumptions on heat transfer conditions between body wall and stagnated air and also with the help of the Stefan-Boltzmann law for the emission of compression heat, assumed to be solely by radiation, Oberth arrives at an equation for wall temperature ϑ :

$$\vartheta \doteq (\gamma/\gamma_0)^{1/6} \cdot v \cdot \sin^{1/3} \left(\alpha + \frac{19000}{v} \right),$$

valid for α between 45° and 90° and v between 5000 and 15000 m/sec, conditions that fairly well cover those known for meteors. Deviation from this formula can be $\pm 1000\%$, according to Oberth himself. The temperatures theoretically derived by P. Vieille* are of the same order of magnitude. Table 51 shows some of the values calculated by

/144

TABLE 51

v [m/sec]	Temperature [$^\circ\text{C}$]
1 200	680
2 000	1 741
4 000	7 751
10 000	48 490

*Cranz, "Ballistik" (Ballistics), vol. 1.

him for blunt-nosed projectiles and air density near the earth. It should be noted that for other air densities the heat transfer is proportional to the square root of air density. In summary it may be said that with the very slender nose shapes of bodies in question and the low angles of attack of wings it is not necessary to fear questionable wall temperatures because of stagnation temperature.

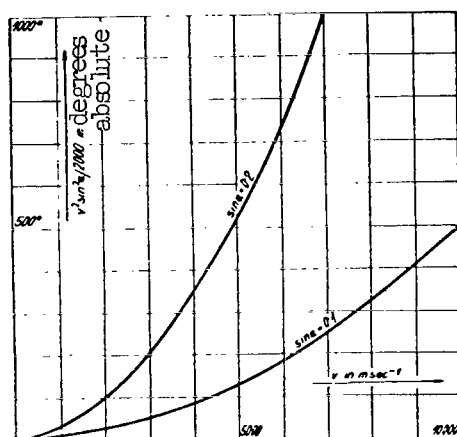


Fig. 51.

Upper limits of stagnation temperature at body wall.

Fig. 51, showing the dependence of stagnation temperature $v^2 \cdot \sin^2 \alpha / 2000$ upon flying speed v and half-aperture angle or angle of attack α , also shows that only the unfavorable blunt heads are in danger at high speeds.

A fundamentally more accurate determination of stagnation temperature as a function of flying speed is given by the combination of the equations for adiabatic air compression with the pressure equations of Busemann (see Sections 2215 and 243).

For example, the adiabatic stagnation temperature of the perfectly blunt point ($\alpha = \pi/2$) is found to be

$$T = T_0 \left(\frac{n-1}{2} v^2/a^2 + 1 \right),$$

when T_0 is the temperature of the undisturbed outer air. This

temperature value would be the same as the theoretical peak value of friction temperature mentioned in Section 241.

It should be especially noted that the friction temperature appears only in the boundary layer, but the stagnation temperature appears in the entire stagnated air space, so that the temperatures are superimposed only in the boundary layer; in some cases the previously stagnated velocity at the outer limit of the boundary layer must be taken into account when calculating friction temperature. This means that the stagnation temperature at the blunt point is in each case theoretically the highest possible temperature appearing on the entire body surface. The extent to which high air temperatures also occur in the outer boundary layer zones and outside the boundary layer depends upon the ratio of the actual stagnation temperature to the maximum friction temperature at the given point.

The second component of profile drag is the resultant of the trailing-side underpressure, the form suction resistance, called suction for short. Thus while the form pressure resistance increases without known limits as speed increases, suction reaches a limit at the absolute absence of air at the rear of the body; thus each frame area unit can be equal at most to the external air pressure,

which is $10,330 \text{ kg/m}^2$ near the earth. The upper limit of c_{wfs} is

therefore readily calculated

$$c_{wfs} = p_a/q = \frac{\rho_a RT_a g n}{\rho_a / 2 \cdot v^2 n} = \frac{2}{n} \cdot \frac{a^2}{v^2} \doteq 165,300/v^2$$

independent of air pressure.

For bodies with concave rear (for example, projectiles with hollow base, nozzle mouths of rockets) this absolute vacuum is

attained when the flying speed v equals that speed v_{\max} at which the air enters the empty space. As is well known, v_{\max} can be calculated from the basic general gas-dynamic relationship for adiabatic phenomena:

$$v^2 = \frac{2\kappa}{\kappa - 1} \cdot \frac{p_0}{\rho_0} \left[1 - (p/p_0)^{(\kappa-1)/\kappa} \right]$$

and is

$$v_{\max} = a_0 \sqrt{2/(\kappa - 1)} = 2.23 a_0.$$

As already emphasized, this simple relationship is valid only in the rear part of more or less cylindrical bodies with hollow, i.e., concave base.

It is, for example, a ballistic experimental fact that a concave projectile base of this type exerts a higher suction than a flat base or one curved outwardly.

According to the Meyers calculations, valid to be sure only for two-dimensional flows, we must assume that with body cross sections that continuously taper to the rear the absolute air vacuum is either attained at much higher speeds, or not at all. Probably however the lee side pressure approaches the zero value closely at high speeds. In Section 243, we introduce a more exact calculation of pressure conditions for this flow, using Meyer's method for compression flow as modified by Busemann for the three-dimensional case; the result of this is that with a very favorable shape of the body nose a poorly formed tail can cause very considerable additions to overall resistance, so that the form of the body end is of great importance in the supersonic region as well. With the relatively compact head of the German S-bullet [spitzer bullet], the overall

resistance at 800 m/sec is about 5 kg/cm², and thus suction is about 20% of overall resistance. Between $v = 0$ and $v = 2.23 a$, or the correspondingly higher range of validity of the limiting value

equation, the suction increases in a manner only partly amenable to calculation, but probably continuously from $c_{wfs} = 0$ to $c_{wfs} = 165,300/v^2$.

243. Wave Resistance

So far no workable theory of impact wave resistance at $v > a$ has been established for the three-dimensional case. However, numerous theoretical expressions have been proposed, of which only a few actually lead to results that can be applied in practice.

A body moving through air at subsonic velocity develops ahead of it spherical compression waves propagated at the speed of sound, which means that the compression precedes the body in the familiar way. However, when the speed of the body exceeds the speed of sound, the compression waves lag behind the point that produces them, and all the interference waves have a conical envelope with its apex at the nose of the body, the so-called Mach cone, the half angle m of which can be computed from the equation $\sin m = a/v$ discussed in Section 221. Figs. 52 and 53 show Schlieren pictures, made by Cranz, of the waves produced by projectiles in flight.

/147

In the case of a real body the shock waves are always more or less flattened in front because of the finite width of the nose cross section. The compression ahead of a plane perpendicular to the direction of flight is propagated at $v = a$ ($a \neq a_0$); here m is 90° .

With increasing distance from this bluff nose the air density, and hence the speed of sound, drops; the shock wave follows a curved course with decreasing m until the normal speed of sound is reached, whereupon it continues in a straight line. The higher the speed at which the body travels, the closer the apex of the shock wave to the nose. According to Cranz, in the case of a very sharp nose and a high supersonic speed the shock wave even begins somewhat behind the nose, so that the latter advances in completely undisturbed air. At low speeds approaching the speed of sound, the apex of the wave moves away from the nose, and the angle of the cone approaches π (see Fig. 52d). The eddies visible in the wake of the bodies consist of the flow-off of boundary-layer particles strongly heated by friction. The pictures are taken in such a way that dark areas represents overpressure while light areas represent underpressure. They illustrate the advantage of a sharp, pointed nose which eliminates the plane shock front. By its nature impact wave resistance has nothing in common with frictional resistance or form drag; as Ackeret says, it

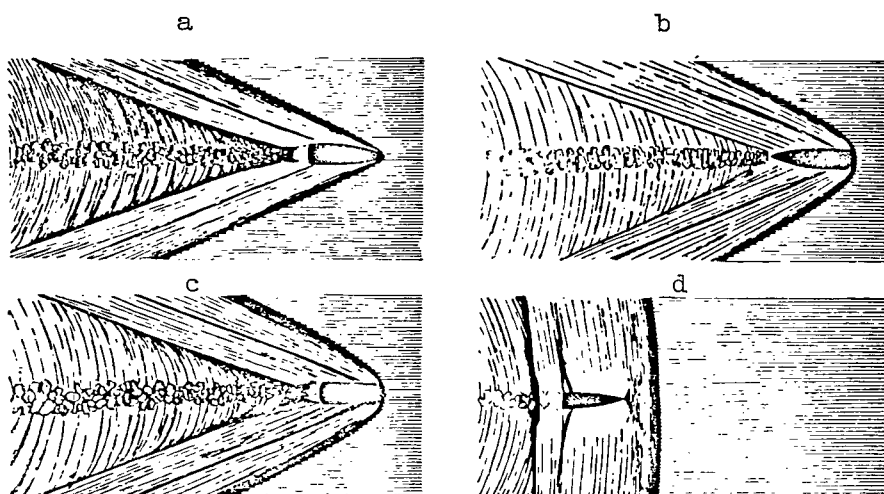


Fig. 52.

Line drawings from schlieren pictures of the pressure distribution around projectiles in flight (dark areas represent excess pressure, light areas underpressure).

- a) Air waves and turbulent air around a pointed projectile traveling at a speed of about $v = 880$ m/sec.
- b) Same projectile in reversed configuration traveling at same speed.
- c) Cylindrical projectile traveling at about $v = 880$ m/sec.
- d) Pointed projectile traveling at about $v = 340$ m/sec (about the speed of sound) [After Cranz: Ballistics].

is rather to be compared with the induced drag of airfoils of finite length. It is a pure compression resistance. There are many parallels between the phenomena of supersonic waves in air and the wave phenomena characterizing a ship traveling through water of limited depth t . The rate of propagation of waves in water, a function of the depth, corresponds to the speed of sound, at high speeds the bow may be observed to penetrate the undisturbed region, the drag coefficient plotted as a function of v shows a peak at the wave speed, just as with bodies moving through air, etc.

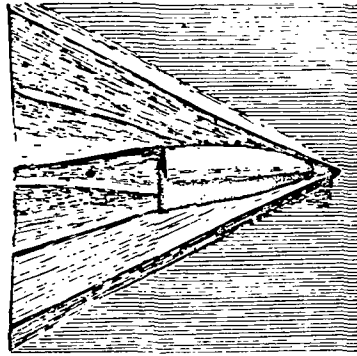


Fig. 53.

Drawing of a plaster model after Cranz, in which the air pressures prevailing in the vicinity of a projectile in flight are plotted vertically from a plane passing through the projectile axis. The resulting surface is parallel to this plane and assumed to be illuminated from above in a direction perpendicular to the projectile axis.

From these similarities Cranz draws the conclusion that, just as with ships, more attention should be paid to the design of the rear end of supersonic bodies.

On these analogies Lorenz has based his aerodynamic drag formula*:

/148

$$W = k_1 \cdot F \cdot v^2 + k_2 \cdot l \cdot v + \frac{k_3 \cdot F \cdot v^4 + k_4 \cdot l \cdot v^3}{\sqrt{(a^2 - v^2)^2 + k_5 \cdot l^2 \cdot v^2}},$$

where l is the length of the body and $k, k_1, k_2, k_3, k_4, k_5$ are constants, of which k_1 and k_3 depend only on the shape of the body

while the rest are also functions of the surface. The above-mentioned individual drag components -- form drag, frictional resistance, impact wave resistance -- are easily recognizable. The formula shows correctly that the specific drag W/F increases as the cross section diminishes and that in the vicinity of the speed of sound the factor

W/v^2 has a peak. Moreover, it resembles the experimental curves. The five constants must be determined by experiment in each case.

Sommerfeld** pursues a basically different course. He compares a body moving at supersonic speed with an electron moving at a velocity greater than that of light, and applies formulas for the electrical energy losses due to radiation to the supersonic drag, insofar as the latter constitutes an impact wave resistance. He finds that

$$W_w = k_1 (1 - a^2/v^2),$$

*Lorenz, Z. VDI 1916, S. 625; 1907, S. 1824. - Lorenz, Ballistik (Ballistics).

**Klein-Sommerfeld, Die Theorie des Kreisels (Theory of the Gyroscope), Vol. IV, 1910.

when $v > a$, currently the best impact wave resistance formula. Fig. 54 shows W/v^2 as a function of v .

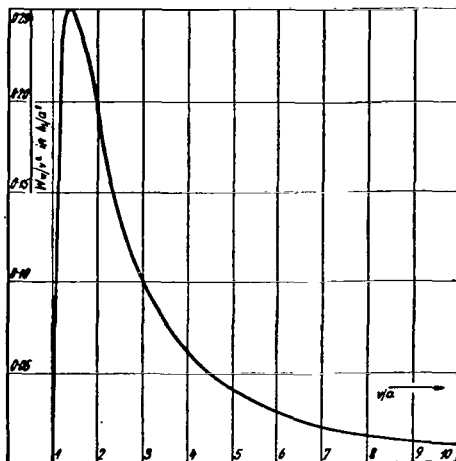


Fig. 54.

Impact wave resistance according to Sommerfeld.

Lechner* gives the following mechanical derivation of Sommerfeld's formula:

The wave motion involves energy which must be supplied by the kinetic energy of the body or a driving motor. This wave energy is concentrated on the surface of the Mach cone. Assuming the mean

/149

*Lechner, Über den Einfluss der Wellenbewegung auf den Wellenwiderstand (Effect of Wave Motion on Wave Resistance). Österr. Flugzeitschrift 1918.

energy density of the surface is e , then the total energy released per unit of time is $L = l \cdot \pi \cdot r \cdot e$, where r is the radius of the base circle referred to a unit of time and l is the length of the generator of the cone (see Fig. 55). Since $O - A = a$ and $\sin m = a/v$, we get:

$$L = e\pi av \cos^2 m = e\pi av (1 - \sin^2 m) = e\pi av (1 - a^2/v^2).$$

From $W_w = L/v$ it follows that

$$W_w = e\pi a (1 - a^2/v^2),$$

that is, the Sommerfeld formula with $k_1 = e\pi a$. Furthermore:

$$c_{ww} = W_w/q = k_1/v^2 \cdot (1 - a^2/v^2),$$

which is plotted in Fig. 56.

If with Sommerfeld we make all the other resistances $W_r = k_2 \cdot v^2$, then for the total resistance we get:

$$y = W/v^2 = k_2 + \frac{e\pi a}{v^2} (1 - a^2/v^2).$$

From $dy/dv = 0$ it follows that this curve has a maximum at $v = a\sqrt{2}$, i.e., when $a = 340$ m/sec at $v = 479$ m/sec which is in excellent agreement with experiment. Beyond this point y decreases

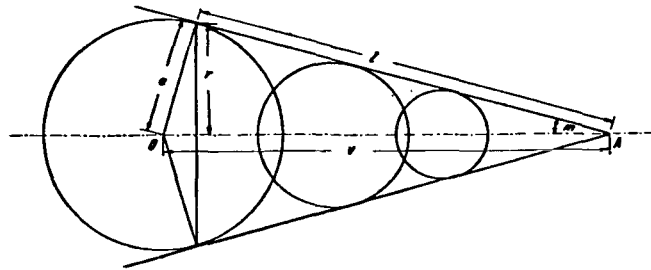


Fig. 55.

Lechner's derivation of the Sommerfeld law of impact wave resistance.

again and at $v = \infty$ approaches the value $y = k_2$. If we take the ordinate $y = 350$ corresponding to $v = 480$ m/sec from Siacci's empirical curve, then $e = 34,500$, $k = 306,000$, and

$$c_{ww} = 306,000/v^2 \cdot (1 - a^2/v^2).$$

The values given by the equation then show a certain agreement with the Siacci curve indicated by the solid line in Fig. 56. The impact wave resistance is assumed to be zero when $v = a$ and approaches a fixed limiting value when $v = \infty$.

The Sommerfeld law, however, still does not take the shape of the body directly into account. At the same time we must keep in mind the fact that there is often a considerable interval, depending on the body shape, between the flying speed v and the local maximum

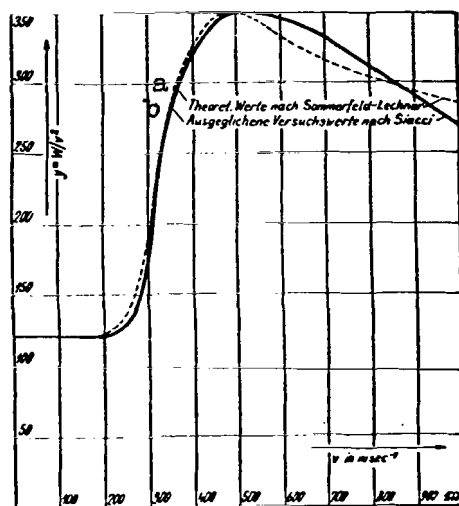


Fig. 56.

Agreement between the Sommerfeld-Lechner theoretical curve for aerodynamic drag and Siacchi's empirical curve.

- a) Theoretical values according to Sommerfeld-Lechner; b) Adjusted experimental values according to Siacchi.

flow velocities of the body surface, so that wave resistance occurs even at flying speeds much lower than the speed of sound, as indicated by the plain rising trend of the c-curve that starts even below the speed of sound. As a matter of fact, this first obvious rise can be

regarded as a sign of incipient wave resistance and the corresponding pronounced flow separation effects.

An earlier relation between the specific aerodynamic drag p and the flying speed v , which, however, claims to be valid for cosmic speeds as well, has been derived by P. Vieille from the propagation of plane waves for bodies with a flat front boundary surface at right angles to the axis:

$$v = \sqrt{\frac{gp_0}{2\gamma} \left[2n + (n+1) \frac{p - p_0}{p_0} \right]}.$$

In Table 25 observed values are compared with those computed from Vieille's formula.

TABLE 25

v [m/sec]	W_{computed} [kg/cm ²]	W_{observed} [kg/cm ²]
400	1.58	1.25
800	6.85	6.23
1,200	15.64	15.01
2,000	43.80	-
4,000	175.6	-
10,000	1098	-

The compression processes in the vicinity of the forward stagnation point and therefore the pressure rise in front of the body can be computed by Prandtl's method. The compression itself takes place in two stages, first the discontinuous compression shock, which leads to the impact wave resistance, follows a nonadiabatic course,

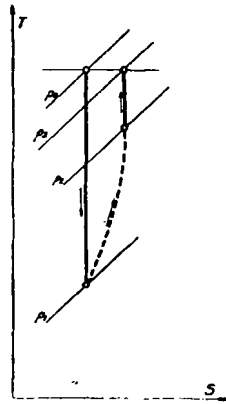


Fig. 57.

Compression process in the entropy diagram.

and finds its expression in the entropy diagram (Fig. 57) as the pressure rise from p_1 to p_2 , after the gas has previously expanded from the rest state p_0, θ_0 to the state of undisturbed motion p_1, v_1, θ_1 . The second stage consists in the subsequent adiabatic compression from p_2 to p_3 which leads back to the original enthalpy $i_3 = i_0$ (moreover, for ideal gases $T_3 = T_0$).

The second stage corresponds to the form pressure drag. Be-

cause of the irreversibility of the process as a whole, however, p_3 is smaller than p_0 . The pressure rise is now computed from the expression:

$$p_3 - p_1 = c \cdot \gamma_1 / 2g \cdot v_1^2 = (c_1 + c_2) \gamma_1 / 2g \cdot v_1^2,$$

where c_1 represents the discontinuous process (impact wave resistance) and c_2 the continuous process (form pressure drag). For these two quantities Prandtl gives the equations:

$$c_1 = \frac{2}{n+1} (1 - a^2/v_1^2)$$

$$c_2 = \frac{(n-1 + 2 a^2/v_1^2)[9n-1 + (6-4n) a^2/v_1^2]}{[2n - (n-1) a^2/v_1^2] 4(n+1)}.$$

Since by definition c_1 and c_2 are very closely related to the corresponding drag coefficients (they would be identical if the overpressure $p_3 - p_1$ were uniformly present over the total area F , whereas in fact they represent a definite multiple of c_{ww} and c_{wfd} which, however, varies with the speed), their graphs show the characteristic variation of c_{ww} and c_{wfd} as a function of v . At subsonic velocities,

of course, only c_{wfd} occurs (Fig. 58). The Prandtl calculations relate to a flat plate at right angles to the direction of flight; therefore the results bear the closest resemblance to the experimental results obtained with bluff, cylindrical projectiles.

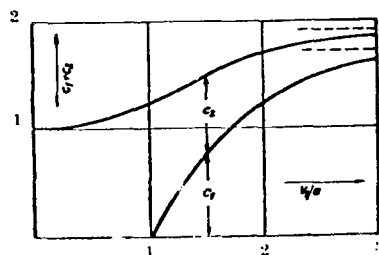


Fig. 58.

Theoretical coefficients
 c_1 and c_2 after Prandtl.

Bairstow, Fowler and Hartree* have measured the pressure distribution over the noses of projectiles in flight by means of burning fuses. Fig. 59 shows the results obtained for various velocities. Δp represents the excess pressure or underpressure relative to still air.

/152

Busemann** has developed the Meyer method of computing a plane supersonic flow to determine the pressures on a conical nose. Under supersonic flow conditions all coaxial cones with the same apex are surfaces of constant pressure. The pressure change is concentrated in the Mach cone in the form of a compression shock. In the corresponding plane problem (Fig. 60) the Mach cone becomes a Mach

*Bairstow, Fowler, Hartree. Proc. Roy. Soc. London (A), vol. 97, p. 202.

**Busemann. Drücke auf kegelförmige Spitzen bei Bewegung mit Überschallgeschwindigkeit (Pressures on Conical Noses at Motion with Supersonic Speed). Z. a. M. u. M. 1929.

plane, in which lie the velocity reduction and, at right angles, the pressure rise and the direction of velocity change. The half angle α of the Mach cone in which for the same velocity v a compression shock of the same intensity is produced can be determined.

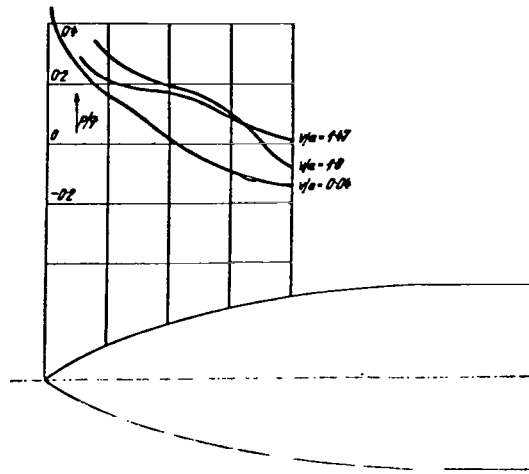


Fig. 59.

Measured pressure distribution
over the nose of a projectile.

Immediately behind the shock the streamlines on the cone form the same angle $w_{1,2}$ with the axis as with a wedge. In the course of the sub-

sequent flow, however, they must crowd together, in order to maintain a finite stream tube cross section with increasing distance from the cone axis. This bending of the streamlines results in adiabatic compression, with cones as surfaces of equal pressure.

In the velocity diagram the change in velocity dv must in each case lie at right angles to the corresponding conical surface of equal pressure with the half angle φ . With the aid of the continuity condition, Busemann finds a relation between dv and $d\varphi$ and as the

quotient of these two quantities the radius of curvature R of the streamline pattern in the velocity diagram (characteristic):

$$\frac{dv}{d\varphi} = R = - \frac{v \sin \beta / \sin \varphi}{\sin^2 (\varphi - \beta)}.$$

$$1 = \frac{(\kappa + 1)/2 \cdot v'^2/v^2 - (\kappa - 1)/2}{\sin^2 (\varphi - \beta)}$$

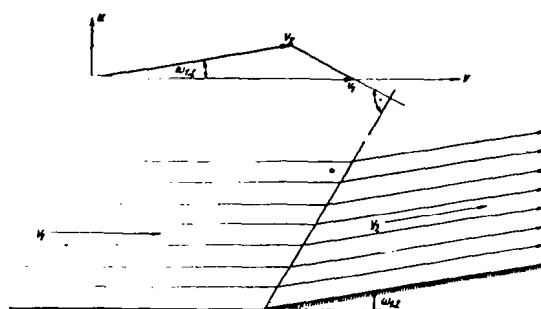


Fig. 60.

Velocity diagram.

With the aid of this relation the streamline can be drawn in the velocity diagram to the point where the angle β between velocity direction and cone axis is equal to the corresponding φ . Here $\beta = \alpha$. From the corresponding v_3 we obtain the pressure, constant over the

/153

entire conical surface. If $v_3 > a$ the cone can be interrupted at any point, without a change in the flow up to that point. This also

makes it possible to investigate any other body of revolution with a continuous or discontinuous meridian, as long as it does not require compression. The practical application of the method then takes roughly the following form:

To draw the velocity diagram for a given α select on the α -line an arbitrary velocity v_3 (corresponding in order of magnitude

to the velocity range it is intended to investigate), drop a perpendicular at the end point of v_3 , and mark off on it a small Δv ,

through the end point of Δv and 0 draw the line $\alpha - \Delta\beta$, then compute $\Delta\varphi$ from the equation for R, and draw the line $\alpha - \Delta\varphi$ also from the end point of Δv . At right angles to the latter select a new Δv , again draw the two lines, etc., until φ equals the α , the Mach angle, of v_1 , which, however, must first be accurately determined, where-

upon v_2 and $w_{1,2}$ can be found. Finally, v_1 is computed from the

latter using the Meyer method. The pressure rise associated with the shock wave from v_1 to v_2 is also computed according to Meyer; the

pressure rise associated with compression from v_2 to v_3 is obtained from the adiabatic equation.

To draw the flow diagram take α and β from the velocity diagram, assuming the latter itself to be given. All the computed φ lines are drawn in from the apex of the cone; an arbitrary, still undisturbed streamline is picked out and drawn as a polygon from line to line, the corresponding direction being taken from the velocity diagram.

The writer is obliged to Dr. Busemann for a friendly letter giving a formula that embraces both the form pressure drag and the impact wave resistance*. According to this formula, the excess pressure Δp on a conical nose with a small angle 2α is:

$$\Delta p = q\alpha^2 \ln \frac{4}{\alpha^2 (v^2/a^2 - 1)}.$$

* See also: Handbuch der Naturwissenschaften, 2nd edition, article on "Motion of Liquids and Gases."

Hence the drag coefficient:

/154

$$c_w = \alpha^2 \ln \frac{4}{\alpha^2 (v^2/a^2 - 1)}.$$

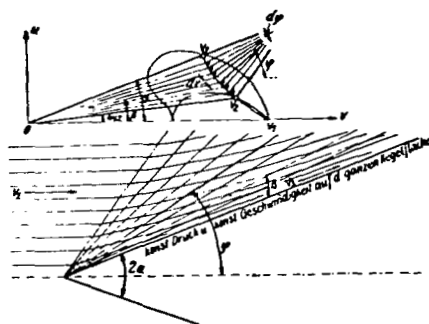


Fig. 61.

Pressures on a conical nose
at supersonic speeds after
Busemann.

244. Overall Resistance

The above-mentioned Busemann method of determining the theoretical pressures on conical noses is of basic importance in computing the total supersonic drag of a body of revolution in an axial flow where the friction may be neglected.

Its extension to bodies of the shape shown in Fig. 62 appears feasible and since by means of such shapes any body of revolution can be represented with any degree of accuracy, within certain limits it can be used to determine the total drag of any body of revolution.

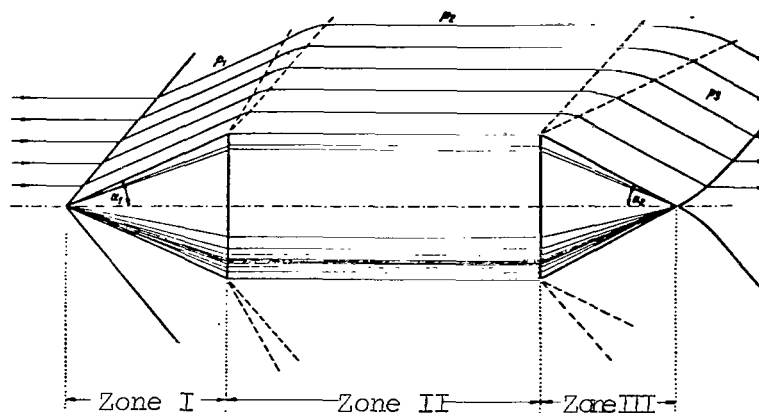


Fig. 62

Supersonic flow around a body of revolution.

The processes associated with flow around the simple basic shape illustrated, which remain unchanged in the case of more complex meridians can be divided into three zones:

Zone I: Shock wave and adiabatic compression to pressure p_1 in the familiar manner.

Zone II: At the start of the zone expansion to pressure p_2 which is then maintained over the rest of the zone. This expansion can be approximately treated as a plane process and is covered by the theory of the first Meyer case (flow around a convex edge with the deflection angle α_1). However,

the condition that the arriving flow is purely parallel is not fully satisfied.

Zone III: Initially further Meyer expansion about the angle α_2 , computable as an approximately plane problem. However, the angle of deflection of the streamlines must again

become smaller with decreasing distance from the axis, in a manner analogous but opposite to that of zone I. Hence additional adiabatic expansion and finally, at the end of zone III, a shock wave that re-establishes the direction of flow and pressure of the undisturbed air, but does not affect the pressure distribution under investigation.

The flow processes in zone III could be analyzed with the aid of the Busemann method for zone I by simply reversing it, which is compatible with the principles of supersonic flow. Again, the velocity v_3 and the pressure p_3 are con-

stant over the whole of zone III. But such a computation of the pressure conditions in zone III is only of very problematic value, since given the assumed discontinuous meridian transition from II to III we certainly, and even with the optimum continuous transition most probably, get separation of the flow, which completely upsets the pressure conditions and makes them impossible to calculate. Finally, the whole method becomes completely invalid, for the other zones too, as soon as the Mach wave attaches itself to the surface of the body, that is when $m = \alpha_1$.

2441. Boundary and Sum Curves for the Total Drag

For practical purposes it is convenient to derive boundary and sum curves for the individual drag components just as we did for the lift in section 2219.

In accordance with the previous discussion, the total aerodynamic drag of a body flying at supersonic speed consists of the four components:

1. Frictional resistance,
2. Form pressure drag,
3. Form suction drag,
4. Impact wave resistance.

The frictional component is assumed to be excluded, that is $c_{wr} = 0$. The form pressure drag coefficient at velocities below and

only slightly in excess of the speed of sound proved to be a function of the velocity, whereas at extremely high velocities, where most of the nose dips into the undisturbed flow, it can be assumed to be ap-

proximately $c_{wfd} \doteq \sin^2 \alpha = k_1$. This is possible from about $v = a/\sin \alpha$ on. At lower velocities c_{wfd} can be established approximately by means of this limiting value combined with Prandtl's formula for c_2 (see Section 243).

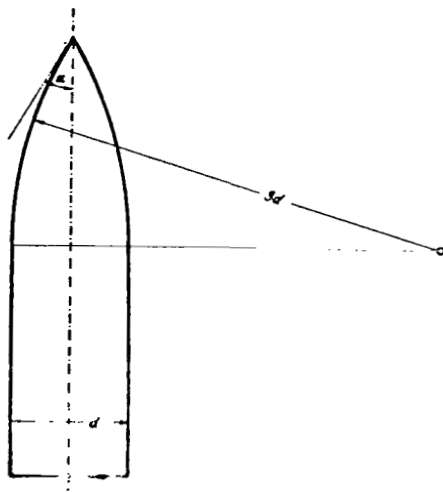


Fig. 63.

Projectile with ogival head having a radius of curvature equal to three times the caliber and a sharp nose.

The suction drag coefficient was found to be $c_{wfs} = 165,300/v^2$, from a velocity $v > 2.23a_0$ for bodies with concave tail ends, and

from a correspondingly higher velocity for bodies with well-shaped ends. With respect to lower velocities it is only possible to say that $c_{wfs} < 165,300/v^2$.

According to Sommerfeld, the impact wave resistance coefficient is

$$c_{ww} = k_2/v^2 \cdot (1 - a^2/v^2).$$

In this connection it must be borne in mind that in the case of a good, extremely slender nose configuration the impact wave resistance can shrink to a negligibly small quantity.

This means that the overall resistance is again best estimated for extremely high velocities ($v \geq a/\sin \alpha$) at about:

$$c_w \doteq k_1 + 165,300/v^2 + k_2/v^2 \cdot (1 - a^2/v^2).$$

For example, for a projectile with an ogival head having a radius of curvature equal to three times the caliber and a sharp

nose (Fig. 63) $k_1 = \sin^2 \bar{\alpha} = 0.23$, if we put $\bar{\alpha} = 0.85\alpha$. A more accurate determination of the correct $\bar{\alpha}$ is difficult because the pressure distribution over the nose of the projectile varies with the velocity. If we finally determine k_2 so that for $v = 1300$ m/sec the sum curve

of the drag agrees with the known experimental curve for this projectile, then we get the curves for the total drag and its individual components shown in Fig. 64.

Thus, by combining experiments, possible over a limited range of velocities, with the sum curves for the drag, we are in a position to predict with some degree of probability the entire course of the

drag curve and to obtain some idea of its probable form for other body shapes.

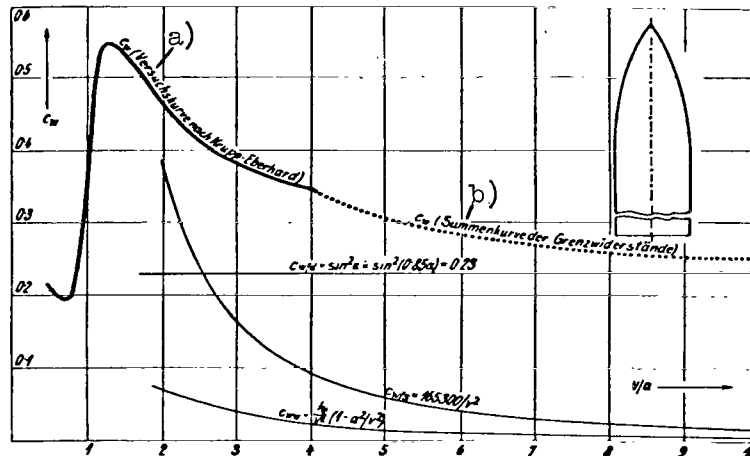


Fig. 64.

Drag coefficients of a projectile with an ogival head having a radius of curvature equal to three times the caliber and a sharp nose.

- a) c_w (experimental curve after Krupp-Eberhardt); b) c_w (sum curve of the limiting drags).

In introducing experimental results it should be noted that c_w is not independent of d as assumed. For example, Eberhardt reports the following decrease in the specific drag with increasing caliber for the above-mentioned ogival projectile with a radius of curvature three times the caliber:

$v = 850 \text{ m/sec}$; caliber 6 cm $W/F = 1.94 \text{ kg/cm}^2$,

" 10 " " = 1.85 "

" 28 " " = 1.25 "

" 30 " " = 1.06 "

$v = 550 \text{ m/sec}$; caliber 6 cm $W/F = 1.00 \text{ kg/cm}^2$,

" 10 " " = 0.98 "

" 28 " " = 0.62 "

" 30 " " = - "

Below we shall discuss the most important results obtained from supersonic drag experiments.

2442. Siacci's Mean Value Curve

In 1896 Siacci reduced the results of all previously conducted aerodynamic drag tests to a universal law, which contains the mean values of the experimental results and is valid for velocities ranging from $v = 0$ to 1200 m/sec .

Siacci's drag formula is as follows:

/158

$$W = 107.5 \cdot i \cdot \gamma \cdot F \cdot f(v),$$

where

$$f(v) = 0.2002v - 48.05 +$$

$$+ \sqrt{(0.1648v - 47.95)^2 + 9.6} + \frac{0.0442v (v - 300)}{371 - (v/200)^{10}}.$$

TABLE 26

Values of c_w After Siacci

v [m/sec]	c_w	v [m/sec]	c_w	v [m/sec]	c_w
20	0.193	420	0.533	820	0.485
40	0.194	440	0.545	840	0.480
60	0.194	460	0.552	860	0.473
80	0.194	480	0.557	880	0.468
100	0.194	500	0.558	900	0.462
120	0.194	520	0.560	920	0.455
140	0.194	540	0.558	940	0.450
160	0.196	560	0.557	960	0.443
180	0.196	580	0.554	980	0.437
200	0.197	600	0.549	1000	0.432
220	0.199	620	0.544	1020	0.427
240	0.202	640	0.540	1040	0.420
260	0.209	660	0.535	1060	0.417
280	0.225	680	0.528	1080	0.411
300	0.276	700	0.523	1100	0.405
320	0.350	720	0.517	1120	0.400
340	0.412	740	0.511	1140	0.395
360	0.460	760	0.504	1160	0.390
380	0.493	780	0.498	1180	0.386
400	0.519	800	0.492	1200	0.382

Table 26 gives $f(v)$ for a series of v . The curve of $c_w = 1720 \cdot i \cdot f(v)/v^2$, defined in the usual way, is shown in Fig. 65. The curve has a point of inflection at $v = 340$ m/sec and a maximum at $v = 480$ m/sec.

$i = 1$ for ogival projectiles with a nose length between 0.9 and 1.1 times the caliber.

$i = 0.865$ for standard projectiles with a radius of curvature of twice the caliber or a nose length of 1.3 times the caliber.

2443. Krupp's Aerodynamic Drag Tables

At present, the most accurate measurements of the drag of bodies moving at very high velocities are the ballistic tests with rifle bullets and artillery shells conducted by Krupp, Cranz, Becker, and Eberhardt.

In aeronautic notation the Krupp drag law may be written:

$$W = c_w \cdot \gamma/2g \cdot F \cdot v^2.$$

It appears that -- by contrast with ordinary subsonic computations -- each body configuration is governed by its own aerodynamic drag law, that is, there is no form factor independent of the velocity. Eberhardt has split the drag coefficient c_w into two factors, of which

/159

one (l) is a function of velocity and shape, and the second (k) a function of the velocity alone.

Consequently, $c_w = i \cdot k$.

Values of i for a series of projectile geometries:

$1/i = 1$ for Krupp standard projectiles with a 2-cal. radius of curvature of the ogival head and a 0.36-cal. flattening at

the nose.

$1/i = 1.3206 - 58.2/v - 0.0001024 v$ for projectiles with a 3-cal. radius of curvature and a 0.36-cal. flattening.

$1/i = 1.4362 - 73.4/v - 0.0001128 v$ for projectiles with a 5.5-cal. radius of curvature and a 0.36-cal. flattening.

$1/i = 1.1959 - 40.6/v + 0.0001467 v$ for projectiles with a 3-cal. radius of curvature and a 0.26-cal. flattening.

$1/i = 1.1311 - 47.7/v - 0.0003166 v$ for projectiles with a 3-cal. radius of curvature and a sharp nose.

$1/i = 1.410 - 122.68/v + 0.0005915 v$ for S-projectiles (cf. Fig. 65).

Values of k are grouped in Table 27.

The c_w - v curve has a peak at about $v = 480$ m/sec and at high

velocities approaches the horizontal asymptotically, so that the square law again applies.

More recent experiments have been conducted by the French*.

/160

245. Shapes with Favorable Supersonic Drag

In the velocity range in which frictional forces predominate, that is, at Reynolds numbers up to about $R = 10^6$ ($v \doteq 0.05a$) bodies with the minimum surface area may be expected to have the least drag. In relation to a fixed volume, therefore, spherical shapes will encounter the least amount of frictional resistance.

In the velocity range in which static pressure forces predominate, that is, from the previously mentioned limit to about $0.6a$ for bluff and $0.8a$ for slender forms, experiments have shown that the bodies with the least aerodynamic drag are spindle-shaped with a round head and a slender, tapering tail. In this case the overall slenderness is a function of the velocity such that the sum of frictional resistance and form drag becomes a minimum. That is slenderness

*Dubuis. Mém. de l'art. française VII, 3, 613, 1928.

increases with the velocity from the most favorable frictional form (sphere). As is known, at $v = 30$ m/sec the optimal slenderness for large airships is about 5. At higher velocities even more.

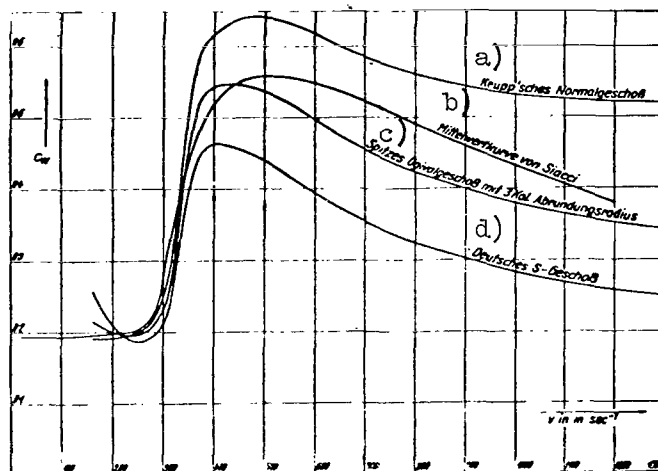


Fig. 65.

Experimental data on the aerodynamic drag of projectiles at high velocities.

a) Krupp standard projectile; b) Siacci mean value curve; c) Pointed ogival projectile with a 3-cal. radius of curvature; d) German S-projectiles.

In the velocity range in which inertial forces predominate and the speed of sound begins to be locally exceeded ($v = 0.8$ to $1.2a$), the best configuration is a pointed nose, a high degree of slenderness, and a tapering tail.

Accordingly, in the purely supersonic range ($v = 1.2a$) the measures needed to minimize the drag are already predictable.

TABLE 27
Values of k After Krupp

v	k	v	k	v	k	v	k
40	-	360	0.550	680	0.592	1000	0.533
60	-	380	0.598	700	0.585	1020	0.532
80	-	400	0.618	720	0.580	1040	0.529
100	-	420	0.628	740	0.576	1060	0.528
120	-	440	0.637	760	0.570	1080	0.526
140	-	460	0.641	780	0.567	1100	0.525
160	0.191	480	0.642	800	0.562	1120	0.523
180	0.191	500	0.642	820	0.558	1140	0.522
200	0.192	520	0.640	840	0.555	1160	0.522
220	0.193	540	0.635	860	0.552	1180	0.521
240	0.197	560	0.630	880	0.548	1200	0.521
260	0.204	580	0.625	900	0.546	1220	0.521
280	0.219	600	0.618	920	0.543	1240	0.521
300	0.250	620	0.612	940	0.540	1260	0.520
320	0.323	640	0.604	960	0.538	1280	0.520
340	0.453	660	0.597	980	0.535	1300	0.520

The problem is to design a body of revolution with a central section which for practical reasons is usually cylindrical or slightly barrel-shaped and an aerodynamically optimal front (nose) and rear (tail) section. Thus the problem falls automatically into two parts: the design of the nose and tail sections.

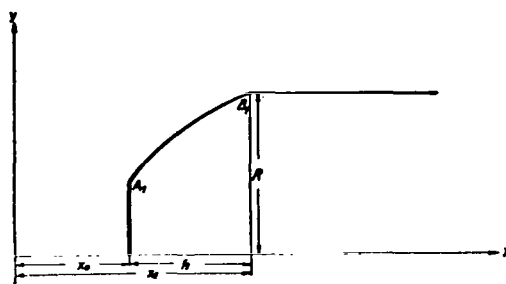


Fig. 66.

Design of nose.

I. In the supersonic range the design of the nose is generally considered much the more important, because of the decisive effect of the shape of the nose on wave resistance and form pressure drag. The problem itself, to select the nose design that minimizes the drag in the direction of the longitudinal axis, goes back to Newton and is essentially a problem in the calculus of variations.

The problem has been solved by August* taking into account exclusively the Newtonian form pressure drag; for the meridian curve $A_1 - B_1$ (Fig. 66) this leads to:

$$x = c \left[\frac{3}{4} \cdot \left(\frac{dx}{dy} \right)^4 + \left(\frac{dx}{dy} \right)^2 - \ln \left(\frac{dx}{dy} \right) + c_1 \right],$$

*Cranz. Ballistik (Ballistics).

$$y = c \cdot dy/dx \cdot [1 + (dx/dy)^2]^2,$$

where c and c_1 follow from the boundary conditions:

$$x = x_1, y = R,$$

$$x = x_0, dy/dx = 1.$$

For a number of reasons and particularly because the normal pressure is assumed to be independent of y , the above solution is of little practical importance.

The direct calculations for the coefficients i for ogival and conical noses are based on similar assumptions.

According to Hélie* the coefficient i for ogival projectiles is proportional to $\sin \alpha$, which is supposed to have been confirmed by numerous experiments.

According to Hamilton, the mean slope of the meridian with respect to the longitudinal axis is critical, so that the i behaved like the reciprocals of the nose surface areas.

If we take $i = 1$ for an ogival with $n = 4$, then:

/162

$n =$	4	6	8	10	12	14
$i =$	1.00	0.82	0.71	0.64	0.58	0.54.

With the same assumptions for $i = 1$ on the basis of the elementary Newtonian law for the form pressure drag alone we get:

*Cranz. Ballistik (Ballistics), Vol. 1, 2nd edition, p. 81.

$$\begin{array}{cccccc}
 n = & 1 & 2 & 3 & 4 & 5 \\
 i = & 4 & 2 & 1.34 & 1 & 0.8.
 \end{array}$$

Under the same conditions H  lie's assumption gives:

$$\begin{array}{ccccccccc}
 n = & 4 & 5 & 6 & 8 & 10 & 12 & 14 \\
 i = & 1 & 0.91 & 0.84 & 0.73 & 0.66 & 0.60 & 0.56.
 \end{array}$$

Heydenreich gives similar series based on German ballistic tests:

$$\begin{array}{cccccccccc}
 n = & 1 & 1.4 & 2 & 3 & 4 & 6 & 8 & 12 & 16 \\
 i = & 1.42 & 1.26 & 1.16 & 1.05 & 1 & 0.89 & 0.84 & 0.73 & 0.68,
 \end{array}$$

the accuracy of which, however, is rather questionable.

Thus, for slender bodies the discrepancies between the various assumptions are quite unimportant, so that c_w can be converted to

ogival noses of different slenderness with some degree of probability, as long as the slenderness is great.

According to H  lie, the conversion can be based on the relation:

$$i_1/i_2 = \frac{n_2 \sqrt{2n_1 - 1}}{n_1 \sqrt{2n_2 - 1}} \quad \text{if } n \geq 4.$$

A nose design of maximum slenderness is for all that the basic requirement for low drag. We already know that the smallest possible average inclination of the meridian with respect to the axis leads to low form pressure drags. The fact that a sharp nose, which is perfectly compatible with the above requirement, and the avoidance of all shoulders, reentrant angles, and other irregular features leads to a minimum impact wave resistance is demonstrated by experiment and particularly clearly by the Mach flow patterns.

Accordingly, the requirement of minimum pressure drag for a given nose height is best satisfied by a cone attached coaxially to

the central cylinder. However, the discontinuity in the meridian at the junction of cone and cylinder might lead to vigorous wave formation, that is increased impact wave resistance. Furthermore, the resulting shape would neither permit optimal utilization of the interior space nor constitute an esthetically satisfying design. For these reasons the conventional shape of a projectile nose would seem to be the best for our purposes. Furthermore, the ogival provides for economical utilization of the interior space, since the useful zone extends from the cylindrical central section deep into the nose, which is also a factor in favor of the required very slender nose design.

/163

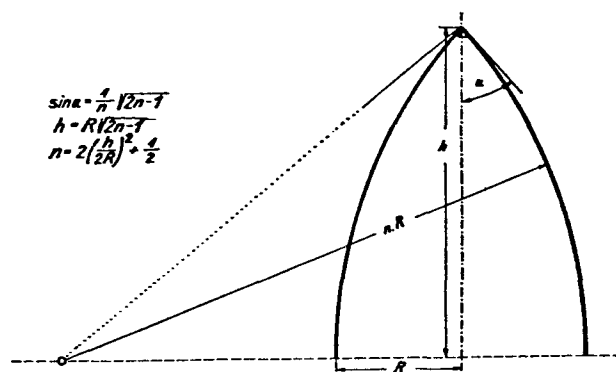


Fig. 67.

Geometric properties of the ogival nose.

II. So far, with some justification, the design of the tail end of supersonic bodies has received little attention, since compared with the nose drags of the relatively badly shaped projectile noses the suction played hardly any part. In connection with the body shapes under investigation the conditions are different, insofar as in this case such nose slendernesses still appear thoroughly debatable and the nose drag is a small fraction of the suction to be expected from a bluff end, as long as the velocity remains less than about $v = a / \sin \alpha$.

This automatically creates the requirement that the tail should also have an elongated, tapered shape, while the radius of curvature of the meridian should be large, in order to prolong flow separation as much as possible.

In this way, at least in the region $v = a$ to about $v = a/\sin \bar{\alpha}$, where $\bar{\alpha}$ is the mean angle of inclination of the tail meridian with respect to the axis, the c_{wfS} , which is particularly significant in

this region, can be largely saved, especially as here the frictional resistance, which increases with the length of the tail, does not play a part.

Some idea of the effect of the angle of inclination of the tail meridian with respect to the axis on the corresponding under-pressure conditions can be derived from Briggs' experiments on the pressure distribution over air foils at supersonic speeds and various angles of attack. At very high supersonic speeds ($v > a/\sin \alpha$) the picture changes to the extent that in any case the suction coefficient begins to fall below the c_{wfd} , which means that

/164

the tail configuration becomes less important.

Thus, at very high supersonic speeds we can state with the same degree of generality as for supersonic airfoils, that for a given slenderness the most favorable body shape is probably a straight circular cone with the apex pointing forward.

Thus we arrive, purely theoretically, by way of the optimal air forces at very high supersonic speeds at the exaggerated version a superhigh-speed aircraft with a conical fuselage and flat wings shown schematically in Fig. 68.

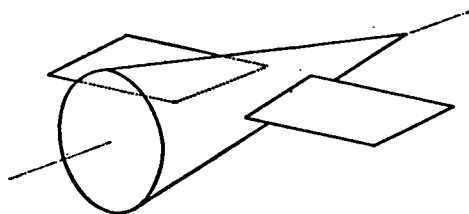


Fig. 68.

Schematic representation of the gasdynamically optimal shape for a superhigh-speed aircraft.

25. Fuselage and Wing Design for a Rocket Aircraft

We must now consider the detailed design of two bodies with basically different functions:

1. Bodies with a utilizable interior space of definite dimensions and minimum aerodynamic drag. These will simply be called the "fuselage" and divided into nose, middle, and tail sections.

2. Bodies that need not have any utilizable interior space and, apart from minimum drag, are intended to provide maximum lift. These we shall continue to call "airfoils" or "wings."

251. Design of Fuselage

If the cross section of the middle of the fuselage is given, the principles derived in Section 24, require the slenderest possible nose and tail. However, since the overall slenderness of the fuselage has an upper limit primarily for static reasons, but also to keep down the weight, and finally because the frictional resistance increases with the slenderness of the fuselage, establishing its optimal size is quite a complicated problem.

Without going into too much theoretical detail, we shall assume a fuselage with a slenderness ratio $l/d = 10$ as being structurally feasible.

If we further assume a fuselage with an ogival nose, in accordance with the arguments of the previous section, we note that for the ogival shapes in question the rear part of the ogival is so spacious that the cylindrical central section of the fuselage can be dispensed without prejudice to the useful volume.

Accordingly, the nose can be followed immediately and continuously by the tail, also initially assumed to be ogival. In the decision about where along the length of the fuselage (l_0d) the boundary between nose and tail should fall considerations of space and statics play only a minor role. Nor does the location of the main frame have much effect on the intensity of the frictional forces, so that initially the siting of this boundary seems to be determined only by the need to minimize the work done in overcoming the drag over the entire flight path. In this connection it should be borne in mind that as the flying speed varies the drag components corresponding to nose and tail are very strongly displaced in the sense that as

the speed increases the suction, relatively speaking, forms an ever smaller part of the total drag, so that at these high speeds it is important to have the main frame set as far to the rear as possible.

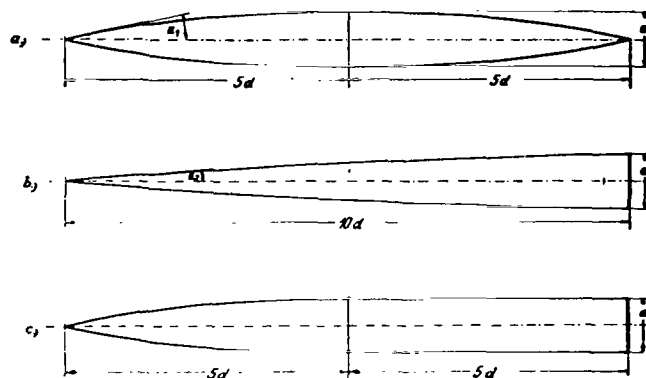


Fig. 69.

Design of fuselage.

In practice, the choice obviously lies in the range between approximately midlength (Fig. 69a) and the rear end (Fig. 69b). At extremely high supersonic speeds the second configuration will at any rate give the lowest total drag.

The sine ratio of the two ogival angles:

$$\sin \alpha_1 / \sin \alpha_2 = 1.98,$$

that is, if we can still trust the Hélie relation under these extreme

conditions, the sum of form pressure drag and impact wave resistance is twice as great in the first case as in the second.

Since, in the case of the latter shape, we must reckon with almost total vacuum suction from about $v = 2.3a$ on and since, given the very favorable nose design, $(c_{wfd} + c_{ww})$ remains smaller than

this c_{wfs} even at high speeds (up to about $v = 4a$), and further since

the fuselage should have favorable drag coefficients even at subsonic speeds, one might consider, quite apart from the question of appearance, adding a slender tail to obtain a shape intermediate between Figs. 69a and b.

However, as far as the general energy balance of a rocket flight is concerned, the work done in overcoming drag is generally less important than a possibly reduced internal efficiency of the rocket motor. But according to Section 14 a high internal efficiency depends on a maximum nozzle exit section, which, of course, can only be accommodated in fuselages of the type shown in Fig. 69b.

Since the ratio of the drags due to nose and tail depends on the speed, that is, since, if both parts could be accurately computed, the location of the main frame would have to be determined in relation to the internal efficiency of the rocket on the basis of minimum power consumption over the entire flight path, we shall again refrain from entering into detailed, numerical design calculations and, without any strict mathematical justification, consider a projectile-like body of revolution of the type shown in Fig. 69c.

The nose is a pure ogival with a height of $5d$; the main frame is located at the center of the fuselage; the tail, which is directly and continuously attached to the nose, consists of a straight circular cylinder, the height of which is also $5d$, so that the tail has a blunt termination suitable for accommodating an adequate nozzle exit section.

The drags affecting this fuselage can be estimated with the aid of the familiar ballistic relations.

The ogival angle of the nose:

$$n = 2 (h/d)^2 + 1/2 = 50.5,$$

$$\sin \alpha = 1/n \cdot \sqrt{2n - 1} = 0.198.$$

After conversion to the present nose design by way of the Eberhardt and Hélie relations, for $v = 1300$ m/sec. = 3.83a the Krupp drag tables give:

$$c_w = i \cdot k,$$

$$k = 0.520 \text{ (from the table).}$$

According to Eberhardt for an ogival projectile with $n = 6$:

$$1/i = 1.1311 - 47 \cdot 7/v + 0.0003166 v,$$

and if $v = 1300$ m/sec $i = 0.664$.

According to Hélie this form factor must be reduced in the ratio of the sines of the ogival angles.

/167

$$\sin \alpha_{\text{krupp}} = 1/6 \cdot \sqrt{11} = 0.555,$$

$$\sin \alpha = 0.198.$$

Therefore

$$i = 0.664 \cdot 0.198 / 0.555 = 0.237,$$

hence

$$c_w = i \cdot k = 0.237 \cdot 0.520 = 0.123.$$

By using the limiting value formula, which is probably already fairly accurate in the velocity range in question, we obtain a similar value:

$$c_{wfs} \doteq 165,300/v^2 = 0.098.$$

For a characteristic ogival angle $\sin \alpha' = \sin (0.85 \alpha) = 0.171$

$$c_{wfd} \doteq \sin^2 \alpha' = 0.029,$$

whence

$$c_w = c_{wfs} + c_{wfd} = 0.127,$$

that is, if we neglect the impact wave resistance as compared with the sources of drag at the speed in question, in view of the theoretically very favorable and structurally sound design of the nose.

We shall continue to calculate with this somewhat less favorable value. The general behavior of the drag coefficient is represented approximately in Fig. 70. The fact that the neglected impact wave resistance becomes more pronounced just above the speed of sound may be compensated by the reduced suction, which in this area certainly no longer corresponds to the limiting value formula. Moreover, it plays no part in the type of design illustrated in Fig. 70.

For $v > 4a$ the c_w -curve was obtained by adding the c_{wfs} and

c_{wfd} limiting value curves. For $v < 4a$ the Krupp-Eberhardt experimental curve was used and the c_w -curve constructed by the proportional reduction of this curve. Naturally, this part of the curve should only be used with great caution, as the discontinuous junction with the limiting value curve indicates.

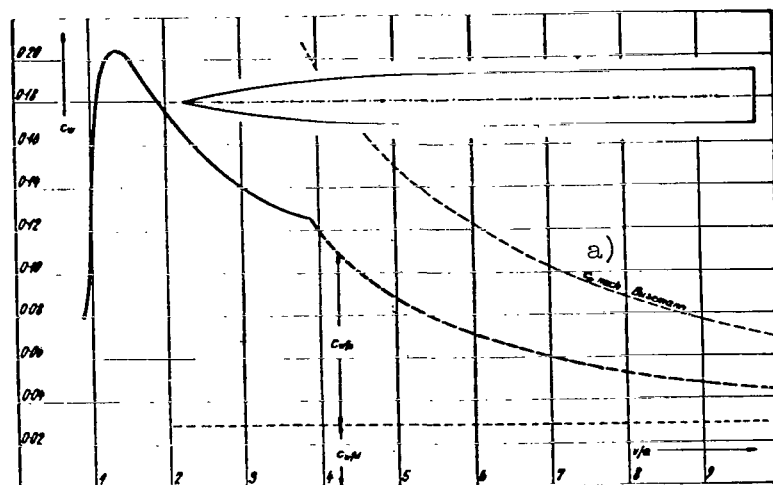


Fig. 70.

Probable curve of fuselage drag coefficients.

a) c_w after Busemann

Thus, the drag characteristics of the body of revolution selected for use as a fuselage may be reduced to some kind of order, and, furthermore, the quality of the design can be estimated.

The key significance of the c_{wfd} and hence the slenderest possible nose at very high supersonic speeds is again made clear regardless of the highly unfavorable configuration of the tail.

The possibility of a reduction of the suction in the region of the sound barrier, where the speed has an important influence on the power consumption, achieved at the expense of the nozzle cross section, calls for a thorough study of competitive designs.

Here we shall continue to calculate with the values thus far determined. In particular, we shall use the constant drag coefficient $c = \text{constant} \pm 0.08$ obtained from Fig. 70 or more accurate wind tunnel experiments at moderate velocities for speeds up to just above the speed of sound, whereas for higher speeds we shall go directly to the limiting value formula

$$c_w \doteq 165,300/v^2 + \sin^2 \alpha.$$

The boundary between the two regions lies where both formulas give the same value of c_w .

Finally, Fig. 70 also includes the c_w -curve that would follow from Busemann's assumptions concerning friction, pressure, and suction:

$$c_w \doteq 0.003 M/F + \alpha^2 \ln \frac{4}{\alpha^2 (v^2/a^2 - 1)} + \frac{2}{\pi} a^2/v^2,$$

where M is the surface area of the fuselage. For the geometry in question this would give approximately:

$$c_w \doteq 0.045 + 0.17^2 \ln \frac{4}{0.17^2 (v^2/a^2 - 1)} + 1.4 a^2/v^2.$$

This curve is very similar to that obtained from our limiting value formula, except for the effect of the high value attributed to the fixed coefficient of friction.

/169

252. Design of Wings

The wing design is primarily conditioned by the fact that the rocket plane, like ordinary aircraft, must land and take off at very low subsonic speeds (about $v = 0.1a$), whereas it normally flies at very high supersonic speeds.

The profile and contours of the wing must be designed so as to reconcile as far as possible these two contradictory requirements.

2521. Design of Wing Profile

According to aerodynamic experiments, high lift coefficients can be obtained at moderate speeds by means of strongly curved profiles with a thickened nose.

According to the findings of Section 22, quality at very high supersonic speeds is achieved by a wing in the shape of a flat, infinitely thin plate, that is, with a profile in the form of geometric straight line.

Thus, at first sight, the two ideal profiles display a rather discouraging dissimilarity. However, for structural reasons a purely "straight-line" profile is impossible, and the extreme slenderness ratio t/d of the profile will be about 20, which under the present special conditions (especially with regard to wing slenderness) enables us to accommodate the structural framework inside the wing. If the pressure side of the resulting profile is made flat (see Section 223) and the suction side convex, the profile as a whole will have a moderate mean curvature corresponding to the subsonic requirements.

On the other hand, though plates make poor subsonic wings given even the slightest curvature they achieve lift coefficients not much inferior to those of good subsonic profiles.

Thus, the groundwork for the design of the profile would appear to have been laid.

On the basis of the further design requirements, developed in Section 223 (sharp leading edge, minimum angle between entering tangents) and structural considerations we arrive almost inevitably

at the profile shown in Fig. 71. By neglecting the subsonic requirement (moderate profile curvature) we would arrive, somewhat as with the optimal supersonic-drag body (fuselage), at a wedge-shaped segment with a bluff rear end as the best practical supersonic wing.

/170

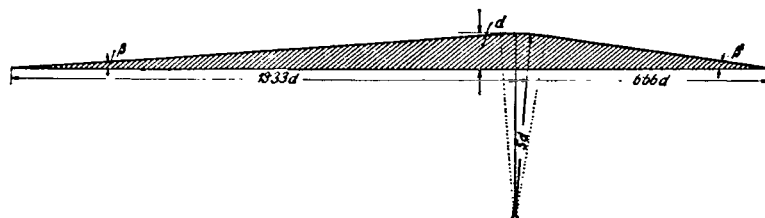


Fig. 71.

Wing profile of rocket plane
(supersonic profile).

However, even with a profile of this shape, some of the available spar depth would again have had to be sacrificed. Yet it seems unjustifiable to imperil the already uncertain take-off and landing properties just for the sake of a minor improvement in cruising characteristics.

Essentially, the profile constitutes a triangle, the altitude of which is $1/20$ of the length of the longest side, which it meets at its third point. The obtuse angle corresponding to this altitude is rounded off with a radius of curvature of $5d$. The entering and exit angles, which have an important influence on the gas-dynamic properties are:

$$\tan \beta = 1/13.33 = 0.075, \text{ hence } \beta = 4^{\circ}17',$$

$$\tan \beta' = 1/6.66 = 0.150, \text{ hence } \beta' = 8^{\circ}32'.$$

Below we turn our attention to the aerodynamic and gasdynamic characteristics of this supersonic profile, which is essentially that proposed by Tsiolkovskiy-Kaluga. We shall investigate the profile to determine the coefficients c_a , c_w , and c_m for all the speeds in

question, that is from $v = 0$ to 8000 m/sec, namely:

1. In the subsonic range by means of wind tunnel experiments.
2. At speeds ranging from $v = a$ to $5a$ by the Meyer-Ackeret method.
3. At speeds exceeding $v = 5a$ by means of the limiting value equations.

Finally, the results obtained will be presented in several comprehensive graphs.

25211. Study of Supersonic Profiles in the Subsonic Region

Thanks to the friendly cooperation of the head of the Aero-Mechanical Institute of the Vienna Technical University, Oberbaurat Doz. Ing. Katzmayer, the profile characteristics in the aerodynamic region could be determined by means of the Institute's wind tunnel facilities. A wooden model with the dimensions $900/180/9$ mm was used for the measurements. The results are presented in the form of polar curves in Fig. 72. As the figure shows, the best gliding angle $1/\epsilon \doteq 5.5$ occurs at an angle of attack of about 3° . In view of the shortness of the distance to be covered in this region and the high available take-off power, the poor quality at subsonic speeds is of no significance and in fact may even be favorable for landing. The largest measured lift coefficient, $c_{a \max} = 0.82$ at an angle of attack $\alpha = 15^\circ$, can be considered satisfactory.

/171

25212. Study of Supersonic Profiles in the Supersonic Region

We shall conduct this investigation systematically for speeds ranging from $v = a$ to $5a$ by the Ackeret-Meyer method. Since we can

regard the whole profile as consisting of flat plates on both suction and pressure sides, we are able to apply the method discussed in Section 2216 directly. Furthermore, since in each case we only need either the suction- or the pressure-side component of the lift or drag, we cannot make use of the A. B. equations, but must have

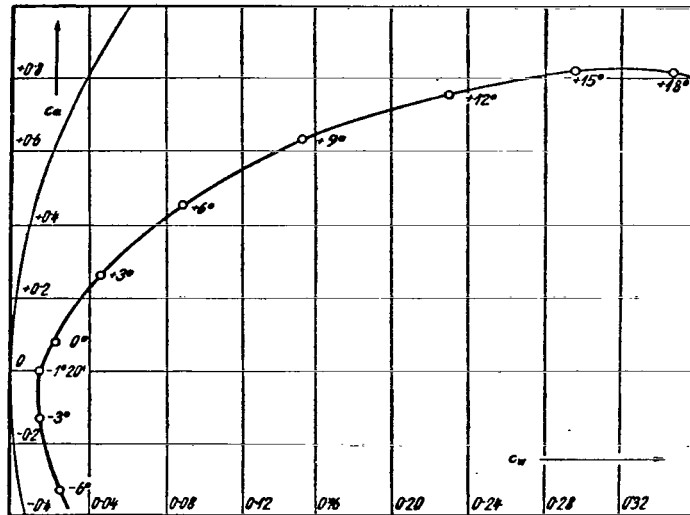


Fig. 72.

Subsonic polar curves for
supersonic profile.

resort to computations based on the primary flows, which, moreover, have the advantage of being more accurate. The numerical application is as described in Section 2216; the results are presented in Figs.

73 and 74. Here c_p^s and c_p^d are the usual coefficients of the total

air forces (at right angles to the plate) on the suction and pressure sides, that is:

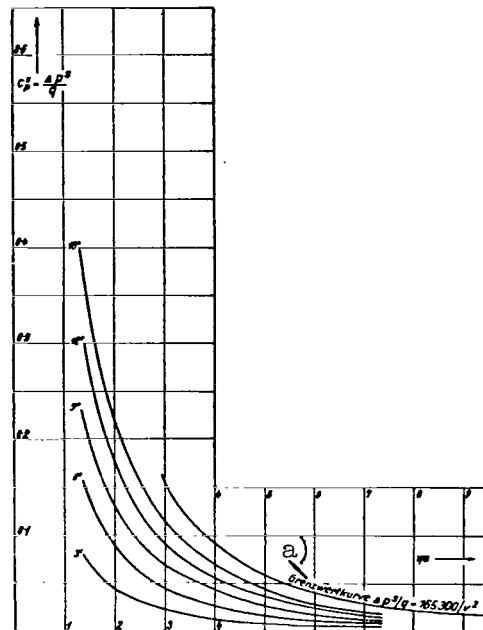


Fig. 73.

Coefficients of the suction-side

air force P^s acting on a flat plate moving through air at the velocity v and the angle of attack α assuming a frictionless supersonic potential flow

$$c_p^s = P^s / q F = 1 p^s / q.$$

a) Boundary value curve

$$\Delta p^s / q = 165,300 / v^2$$

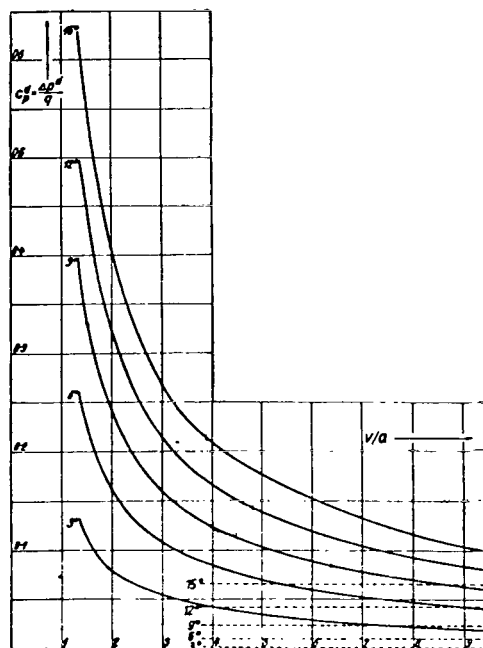


Fig. 74.

Coefficients of the pressure-side

air force P^d acting on a flat plate moving through air at velocity v and the angle of attack α assuming a frictionless supersonic potential flow

$$c_p^d = P^d/q = \Delta p^d/q$$

[Broken lines represent values according to the Newtonian relation

$$c_p^d = \sin^2 \alpha].$$

$$c_p^s = P^s / Fq = \Delta p^s / q$$

and

$$c_p^d = P^d / Fq = \Delta p^d / q,$$

where P^s and P^d are the total air forces themselves, and Δp^s and Δp^d the specific under- and overpressure with respect to the corresponding atmospheric pressure.

The two figures confirm the well-known fact that at very high supersonic speeds the air forces of the underpressure regions (suction side) recede in importance as compared with those of the overpressure regions (pressure side). Fig. 74 reveals the velocities at which the Mach angle is equal to the angle of attack, that is, where the assumptions of the Meyer method are partially fulfilled.

Finally, Fig. 75 shows the values c_p of the total (suction and pressure sided) air forces at right angles to the flat plate plane. Though these c_p values may have no direct significance for

the present profile investigations, they suitably supplement what was said in Section 2216.

Now we can easily derive the characteristics of our profile from Figs. 73 and 74.

If we designate the three surface planes (pressure side, front and rear suction sides) as F_1 , F_2 and F_3 , respectively, then

for a specific velocity v/a and a specific angle of attack α (the latter always referred to the pressure side) we have:

$$c_a = c_p^d(\alpha) \cos \alpha + \\ + c_p^s(\alpha - \beta) \cos (\alpha - \beta) F_2 / F_1 +$$

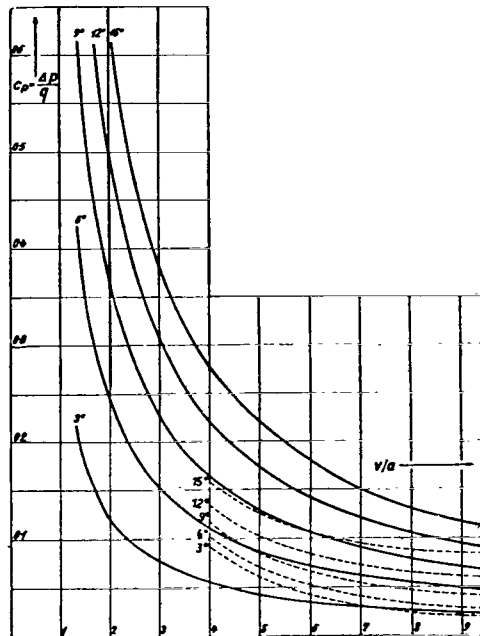


Fig. 75.

Coefficients of the total air force P acting on a flat plate moving through air at the velocity v and the angle of attack α assuming a frictionless supersonic potential flow

$$c_p = P/q F = \Delta p/q$$

[Broken lines indicate values according to the relations

$$c_p = 165,300/v^2 + \sin^2 \alpha].$$

$$+ c_{p(\alpha+\beta')}^s \cos (\alpha + \beta') F_3/F_1,$$

$$c_w = c_{p(\alpha)}^d \sin \alpha +$$

$$+ c_{p(\alpha-\beta)}^s \sin (\alpha - \beta) F_2/F_1 + c_{p(\alpha+\beta')}^s \sin (\alpha + \beta') F_3/F_1,$$

$$c_m = c_{p(\alpha)}^d \cdot 1/2 + c_{p(\alpha-\beta)}^s F_2^2/2F_1^2 +$$

$$+ c_{p(\alpha+\beta')}^s \cdot F_3 [F_2 \cos (\beta + \beta') + F_3/2]/F_1^2$$

or in relation to the geometry of our chosen profile:

$$c_a = c_{p(\alpha)}^d \cos \alpha + 0.666 c_{p(\alpha-\beta)}^s \cos (\alpha - \beta) +$$

$$+ 0.334 c_{p(\alpha+\beta')}^s \cos (\alpha + \beta'),$$

$$c_w = c_{p(\alpha)}^d \sin \alpha + 0.666 c_{p(\alpha-\beta)}^s \sin (\alpha - \beta) +$$

$$+ 0.334 c_{p(\alpha+\beta')}^s \sin (\alpha + \beta'),$$

$$c_m = 0.500 c_{p(\alpha)}^d + 0.222 c_{p(\alpha-\beta)}^s + 0.272 c_{p(\alpha+\beta')}^s.$$

The angles to which the individual c_p^d and c_p^s relate, are added in parentheses.

The numerical values of the formulas are plotted directly in the characteristic curves of Section 25214.

When using the formulas for angles of attack smaller than $\alpha = 4^\circ 17'$ note the change of sign.

25213. Study of Supersonic Profiles in the Hypersonic Region

In the practical case of angles of attack of about up to $\alpha = 9^\circ$, the Ackeret method becomes cumbersome and unreliable at speeds above about $v = a/\sin \alpha$, since it provides neither for the anticipated suction-side separation effects nor for the adherence of the Mach wave to the pressure side of the wing.

In this range of high supersonic speeds, the treatment can again be approximately based on the limiting value formulas.

Since the angle of attack of the suction side is not involved, the lift and drag coefficients may be expressed simply as:

$$c_a = 165,300 \cos \alpha / v^2 + \sin^2 \alpha \cos \alpha,$$

$$c_w = c_a \tan \alpha,$$

$$c_m = 0.5 c_a.$$

/174

Of course, the above equations are only valid for $\alpha > 4^\circ 17'$.

Polar curves based on these equations are shown in Fig. 76.

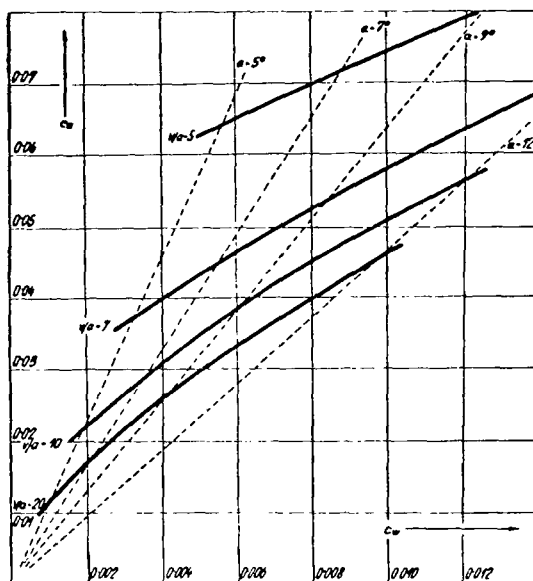


Fig. 76

Polar curves of a supersonic profile in the extreme supersonic range.

25214. Characteristic Curves of the Supersonic Profile

The properties of a supersonic profile are broadly indicated by the polar curves in Fig. 77.

In order to be able to use a simple mathematical expression for the anticipated lift forces in flight path studies, as previously noted in Section 2219, in the velocity range up to just above the

speed of sound we employ the wind-tunnel lift coefficient

$$c_a = f(\alpha),$$

while at higher speeds the limiting value equation

$$c_a = 165,300 \cos \alpha / v^2 + \sin^2 \alpha \cos \alpha$$

immediately comes into play.

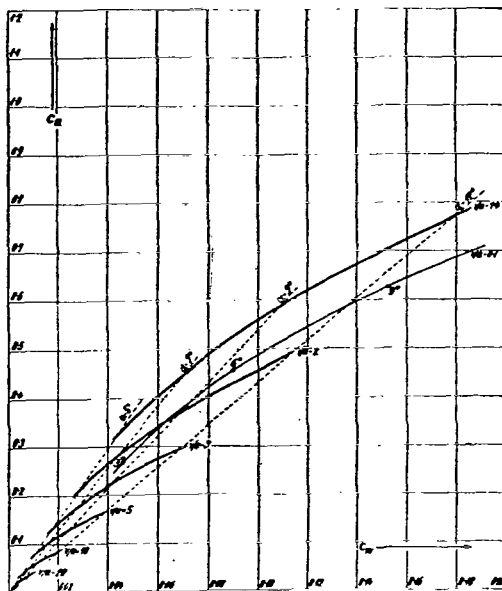


Fig. 77.

Polar curves of a supersonic profile (rocket profile).

The boundary between these two regions is determined by the value of v obtained from the equation:

/175

$$165,300 \cos \alpha / v^2 + \sin^2 \alpha \cos \alpha = f(\alpha).$$

This value is further understood to represent the lower limit of the "pure supersonic region."

We should again emphasize that all these investigations have been carried out without allowance for the frictional resistance.

2522. Design of Wing Contour

The theoretical relations for the supersonic wing initially leave the design of the wing contour completely free, since the induced drag exerts no influence in the supersonic range.

Indirectly, however, these relations require a reduced wing span, insofar as they call for the thinnest possible wing profile, which for structural reasons is feasible only if the wing is stubby.

Because of the key requirement for suitable take-off and landing characteristics, the subsonic properties of the wing also affect the contour design. These also require maximum slenderness.

Actually, therefore, it is most convenient to retain the wing slenderness ratio $b^2/F \doteq 5$ usually adopted for subsonic aircraft, since in this case the edge lift losses, an unknown factor in the supersonic range, probably also remain within reasonable limits.

With regard to the geometry of the contour, unless experiment indicates otherwise, a simple rectangular shape should be preferred.

Further considerations, such as those relating to arrow and Vee shapes, décalage, etc., involve only the safety (stability) of the aircraft, and will not be discussed here, since we are primarily concerned with performance.

At any rate, the wing construction will probably be of the multispar type, and theoretical expressions for a fairly accurate

/176

design are available.*

253. External Design of Rocket Aircraft

There is a widespread belief that the only practical design for a rocket plane is the all-wing type, which is desirable in tropospheric aircraft to achieve maximum aerodynamic quality.

A number of objections can be brought against this view. First, the all-wing aircraft, the "flying wing," presupposes a very thick profile, which has been expressly created for this purpose by Professor Junkers. However, we are acquainted with the extremely unfavorable supersonic characteristics of thick profiles. At any rate, they cannot give the required high aerodynamic quality. If, however, we select the profile discussed here, with its probably still feasible thickness of $t/20$, for a minimum practical thickness of 1.50 m we get a wing chord of 30 m and a span of 150 m, that is, dimensions that are out of the question for any experimental model and probably for any series-production model of a rocket plane. Another circumstance, which perhaps still receives too little attention, is the fact that at high altitudes the cabin of a rocket

/177

plane is subjected to an internal overpressure of $10,000 \text{ kg/m}^2$ while the tanks are subjected to even higher pressures, which it would be economically impossible to handle with other than cylindrical (tank-like) shapes.

For these and a number of other reasons the conventional arrangement with a special fuselage and wings would appear to be the best design at least for an experimental model and probably for the final production version.

* See, among others: E. Sänger: "On the exact calculation of multispar parallel-web wing skeletons with indirect and direct stress of full- and semi-cantilever types" ZFM 1931, no. 20; E. Sänger: "On the approximate calculation of multispar parallel-web wing skeletons with indirect and direct stress of full- and semi-cantilever types" ZFM 1932, no. 9.

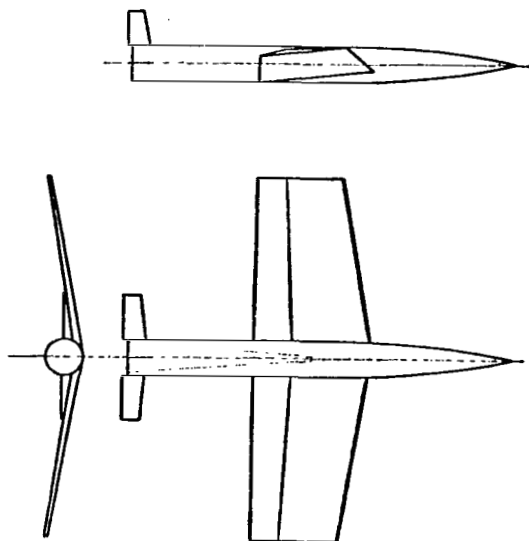


Fig. 78.

External configuration of the rocket plane used as a basis for flight path computations.

Without intending to make any definite structural proposals, which would exceed the scope of this book, further theoretical study might well be based on an external geometry of the type shown schematically in Fig. 78.

3. FLIGHT PATHS

Literature on this section

To the extent that more complete reference literature is available on the topic, the reader may seek such references in the appendix to Section 1.

A few additional literature references appear as footnotes.

/178

Meanings of the most important symbols regularly used in this section [units in brackets]

$\rho_h, \gamma_h, p_h, R_h, \kappa_h, c_h$, etc... are the density, specific weight, pressure, gas constant, absolute temperature, adiabatic exponent, speed of sound in air at altitude h , in the respective units $[\text{kg sec}^2/\text{m}^4]$, $[\text{kg}/\text{m}^3]$, $[\text{kg}/\text{m}^2]$, $[\text{m}^\circ]$, $[\circ]$, $[-]$, $[\text{m}/\text{sec}]$.
 $\rho_0, \gamma_0, p_0, R_0, T_0, \kappa_0, c_0$, ... are the same variables in the air at altitude zero (standard air).

- A aerodynamic (gas-dynamic) lift [kg]
- W aerodynamic (gas-dynamic) drag, air resistance [kg].
- F wing area, area of lifting surface, as in section 2, or inertial force normal to trajectory (centrifugal force) [kg].
- G flying weight [kg].
- G_0 initial flying weight, weight at take-off [kg].
- P rocket thrust [kg].
- R Radius of the earth (average value reported: $6.37755 \cdot 10^6$ meters) [m].

- T forces of inertia (mostly in direction tangential to trajectory) [kg]
- c_a lift coefficient, as in section 2 [--].
- c_{a0} lift coefficient, for flight speed at zero altitude.
- g acceleration due to gravity [m/sec^2], average value:
9.81 m/sec^2
- g_0 acceleration due to gravity at the earth's surface [m/sec^2].
- g_h acceleration due to gravity at altitude h [m/sec^2].
- h altitude [m].
- M mass of airplane [$\text{kg sec}^2/\text{m}$].
- r radius of curvature of the flight trajectory (usually $r \doteq R$) [m].
- s flight path [m, or km].
- t flight duration [sec].
- v flight speed [m/sec].
- v_0 flight speed at altitude zero [m/sec].
- v_a critical flight speed, at borderline between subsonic and supersonic regions [m/sec].
- ϵ lift/drag ratio, L/D ratio of airplane, as in section 2 [--].
- ρ at some points, the radius of curvature of the flight path [m].

30. FLIGHT PATHS. GENERAL

The flight of the rocket-boosted airplanes discussed here follows more or less the following general outline:

The aircraft takes off from land or water in the usual manner (more or less with a rocket propulsion thrust equal to half the take-off weight, and thus very rapidly) into the wind, then traverses a curve in the desired flight direction and proceeds to climb with a fairly constant rocket propulsion force, with the thrust eventually overtaking and surpassing the gross aircraft weight.

The aircraft climbing under its engine propulsion travels along an ascending trajectory dependent on the air density decreasing upwards and on the rapidly increasing flight velocity in such a way that the lift force on the wings remains almost constant.

With the increasing flight velocity, the curvature of the flight trajectory becomes gradually more significant (principally because of the osculation of the trajectory with the curve of the earth's surface) to the extent that the resulting inertial forces (centrifugal forces) act in the same sense as the lift on the wings, thereby reducing the loading on the wings.

The flight trajectory continues in this range essentially in a manner such that the sum of the centrifugal force, increasing rapidly with velocity, and the lift force on the wings will be consistently equal to the gross flying weight, which decreases with the passage of time because of the high fuel consumption rate. The aerodynamic wing forces should decrease even more rapidly as a result, and this can be brought about only by climbing to greater altitudes with thinner air because of the prescribed velocity. The dynamic pressure decreases in equal measure, and likewise the air drag to be overcome by a portion of the engine power, up to the point when the airplane weight carried by the wings amounts to only a very small percentage of the remaining actual flying weight. At that instant, the required flight velocity and flight altitude will have been attained, the engine is throttled, and the climbing phase comes to an end.

The high-altitude flight phase following thereupon is an almost purely gravitational motion about the center of the earth, and as such requires no propulsive power to cover any length of its route. Actually, however, at this point the aircraft is traveling in what is still an atmosphere, albeit an extraordinarily tenuous one, so that there is still a very slight air drag which must be continually overcome by an ever so modest rocket thrust. The fuel consumption required for this purpose is, as we shall see, almost negligibly small.

At the same time, the wings still retain a slight lift action,

which is expressed inside the aircraft as a still perceptible, but slight weight on the part of objects and persons, and which maintains the altitude of the aircraft with respect to the earth's surface constant, together with the far more predominant centrifugal force associated with the curvature of the trajectory.

At some appropriate distance from the termination of the flight, the engine is completely throttled and the descent phase is initiated. The descent phase is carried out as a pure gliding flight over very long intervals, since the quite considerable potential and kinetic energy of the aircraft must be dissipated in overcoming the air drag, which will be very slight at first.

/180

If the low thrust of the motor were to be cut off completely in high-altitude flight, the very low drag presented by the air at that altitude would in turn exert a delaying effect on the flight speed. As the flight speed declines, the wing lift, in itself low, will decline to a slight extent, and the centrifugal force will decline even faster, whereupon the aircraft will begin to lose altitude since the two forces are no longer able to balance out the craft's weight.

The descending airplane will reach the more dense layers of air, whereupon the delaying effect of the air drag will be enhanced and the flight speed will decline more precipitously. As a result, the load on the wings will increase steadily, and the centrifugal force will virtually vanish altogether, with the aircraft recovering its complete maneuverability at about 30 km altitude and will finally land at its destination much in the manner of the modern-day tropospheric aircraft.

Both take-off distance and landing distance will be short, the first because of the high motor thrust available on take-off, and the latter because of the slight loading on the wings at landing, after much fuel has been consumed, and because of the poor L/D ratio of the aircraft in the subsonic range.

The subsequent sections will be mainly devoted to the computational study of these flight trajectories in terms of their generating functions, the forces operating on the aircraft.

Special emphasis should be placed on the fact that the numerical results cited in what follows provide at most a graphic idea of the relationships to be anticipated, but are actually of limited value because of the extreme vagueness of the principles underlying the calculations.

The findings arrived at in the reasoning below are therefore qualitative, in the first instance, and should be appraised quantitatively only with caution. Similarly, the phenomena described will be observed in actuality in each case only to the extent that the numerical values arrived at approximate the reality, which can be learned only through experience.

For that reason, much greater weight was placed on the overall picture, in developing the rather complex relationships involved, than on mathematically exact computational approaches.

31. STRUCTURE OF THE ATMOSPHERE. GENERAL *

The boundaries of the range of rocket flight are specified on the one hand by the solid or fluid surface of the earth, and on the other hand by that altitude in the atmosphere at which the air pressure descends to such a low value that the flight speed required to attain the aerodynamic lift needed in the limiting case at that point will become equal to the angular velocity of a body gravitating freely about the earth and passing through that point. The range of rocket flight consequently covers an enormous portion of the atmosphere, the composition of which we are now about to deal with.

311. Composition and General Properties of the Atmosphere

If we assume the known composition of the atmosphere at the bottom of the air mass, with its principal components nitrogen and oxygen, to apply to all altitudes throughout the atmosphere, then, according to Wegener, we shall arrive at the following figures for the air pressure at various atmospheric heights, in mm mercury column:

Table 28

Flight altitude, km	0	20	40	60	80	100	120	140
Air pressure, mm Hg	760	41.7	1.9	0.087	0.0042	0.0001	-	-

*Hann-Süring. Lehrbuch der Meteorologie, 4. Aufl. 1923 (Course on Meteorology, 4th edition). Geiger-Scheel, Handbuch der Physik, Vol. XI, 1926.

The atmosphere would have thinned out to its practical limit at about 100 km altitude, as we see. This view is not reconcilable with a large body of observational evidence. For example, meteor flare-ups have been observed at altitudes up to 600 and even 1000 km, and polar aurorae have been measured up to 750 km altitude, while twilight phenomena have revealed the atmosphere to be capable of reflecting light up to 600 km altitude, etc., so that we have to reckon with the existence of an atmosphere, however tenuous, at those heights.

In fact, the atmosphere also consists, even near the earth's surface, of slight quantities of lighter gases such as hydrogen, helium, etc. By Dalton's law, each gas behaves as if no other gases were present. Whenever diffusional equilibrium prevails between the various gases present, and this can be safely assumed for the continually intermixed troposphere, the partial pressure of each gas will diminish in accord with its own particular law. The pressure drop with height will be the smaller, however, the lighter the gas. At great altitudes, then, the partial pressure of the lighter gases would have to predominate, so that these would become the predominant constituents of the atmosphere at heights from 70 to 80 km.

Enrichment of the lighter gases has in fact been successfully established in the higher-lying layers of the troposphere.

Agreement is still lacking on the nature of these light gases which must be present. The prevailing view holds that hydrogen primarily is involved, with slight quantities of helium, but the Wegener hypothesis to the effect that a substantially lighter "electron gas: consisting of residues of atoms, similar to the coronium in the external solar atmosphere, constitutes the upper layers of the earth's atmosphere, has gained much favor. This geocoronium is believed to have already demonstrated its presence conclusively in terms of its spectral lines. Under this assumption, Wegener calculated the composition of the atmosphere in the manner reflected in Table 29. If we limit our inquiry to the known gases hydrogen and helium, the composition will agree with the figures in Table 30 as stated by Hann and Humphreys.

In the latter table, the hydrogen column contains what is approximately the sum of the volume percentage of hydrogen and geocoronium listed in Table 29. Finally, we note the existence of still other views on the nature of the high-altitude gas, e.g., the hypothesis of a nitrogen crystal atmosphere, and others.

The air pressure values corresponding to the assumptions underlying Tables 29 and 30 may be found in Table 31.

At 100 km altitude, these values turn out to be 100 % higher than indicated in Table 28.

Table 29

Constituents of the Atmosphere in Volume Percent,
According to Wegener

Flight altitude km	Geocoronium	Hydrogen	Helium	Nitrogen	Oxygen	Argon
0	0.00058	0.0033	0.0005	78.1	20.9	0.94
20	0	0	0	85	15	0
40	0	1	0	88	10	0
60	4	12	1	77	6	0
80	19	55	4	21	1	0
100	29	67	4	1	0	0
120	32	65	3	0	0	0
140	36	62	2	0	0	0

In addition to the air pressure and the composition of the air, the air temperature also varies measurably with height, and to be specific it decreases at a constant rate of about 5.5°C per km difference in height upward, starting from the earth's surface, and continuing on up to about 11 km height, whereupon it remains constant at about -55° to -60°C . This discontinuity in the temperature decline constitutes the boundary between the lower layer, the troposphere, where meteorological processes and continuous vertical movements occur, and the stratosphere, which is free from effects of meteorological processes and vertical air movements. The height of the lower stratospheric boundary, however, not only varies from locality to locality, as Table 32 shows, in that it lies at about 9 km over the poles and at about 17 km over the equator, but also fluctuates in time over the same locality, e.g. between 9.4 km in March and 11.3 km in August, in central Europe. Furthermore, it rises about 2 km over the normal height in the front of cyclones, and sinks to

3 or 4 km below the normal height in the wake of cyclones.

Table 30

Constituents of the Atmosphere in Volume Percent,
According to Hann and Humphreys

Flight altitude, km	Hydrogen	Helium	Nitrogen	Oxygen	Argon
0	0.003	0.0005	78.1	20.9	0.94
15	0	-	79.5	19.7	0.8
20	0	-	81.2	18.1	0.6
30	0.2	-	84.2	15.2	0.3
40	0.7	-	86.5	12.6	0.2
50	2.9	0.03	87.5	10.3	0.1
100	96.4	0.6	3.0	0.0	0.0

Table 31

Air Pressure at Various Altitudes, in mm Hg

Flight altitude, in km	0	20	40	60	80	100	120	140
According to Hann-Humphreys	760	41.7	1.9	0.101	0.0175	0.0091	0.0072	0.0058
According to Wegener	760	41.7	1.92	0.106	0.0192	0.0128	0.0106	0.0090

Table 32

Height of Stratospheric Boundary at Various Points
Around the Earth, According to Wegener

Locality	Batavia	Sub-tropics	Canada	N. Italy	Central Europe	North Lapp-land	Spitz-bergen
Geographical latitude	7° S	30° N	43° N	45° N	50° N	68° N	77° N
Height of boundary, km	17	14	11.7	11.1	10.5	10.4	10-11
Temperature at boundary	-85	-63	-61	-59	-56	-57	-

The constant stratospheric temperature from about -55° to -60°C has been definitely established at 30 km altitude by measurements. For still higher layers, recent assumptions based on sound propagation phenomena and meteor observations hold, partially in opposition to the opinion prevailing until recently, that the atmosphere again becomes warmer above 30 km, to reach 0°C at 40 km, $+15^{\circ}\text{C}$ at 50 km, and 30°C at 60 km altitude. At present, this hypothesis has not gained general acceptance. Between 20 and 40 km, an ozone atmosphere is partially suspected, one which could account for the abrupt cut-off of the solar spectrum at 2950 Å. The upper limits of the stratosphere lie at about 60 to 70 km, at which point the composition of the atmosphere undergoes a drastic change.

The last atmospheric layer, filled with a still-unknown gas, extends still further out, probably thinning out into the gaseous matter of outer space without any clearly defined boundary. Some equilibrium height between the earth's attraction and the repulsion effect of the centrifugal force established by the earth's rotation, which would set in at about 35,000 km height if the angular velocity of all layers of the atmosphere were constant, cannot exist in reality, since the upper-lying layers of the atmosphere would not be able to partake of the earth's rotation on account of the frictional resistance presented by the matter in outer space, as demonstrated by the regular and powerful easterly wind which makes itself felt at about 30 km height. There is thus no practical point in talking about an upper limit to the atmosphere.

312. Air Density as a Function of Flight Altitude

Since a rocket-powered airplane would carry its own supply of oxygen needed to drive its motors, and since the crew would be housed in a pressure-tight cabin, the composition of the air and the air pressure would be of little interest compared to the air density, which would exert decisive effects on the air forces operating on and around the rocketplane. The magnitude of the air density can be found readily, if the air pressure is known, from the sea-level value with the aid of the gas equation of state, using the formulas:

$$\frac{\rho}{\rho_0} = \frac{\gamma}{\gamma_0} = \frac{p}{p_0} \frac{R T_0}{R T},$$

so that the air pressure, air temperature, and the composition of the air at the height in question must be known. For that region, in which these quantities are completely specified, the air density has been standardized, in terms of the international standard atmosphere of the Convention Internationale de Navigation Aerienne (CINA), as a basis of calculations, to the following values:

Standard value at sea level:

1. $p_0 = 10,332 \text{ kg/m}^2$
2. $T_0 = 288^\circ$,
3. and hence, $\gamma_0 = 1.2249 \text{ kg/m}^3$.

Temperature drop τ per 1000 m height:

1. $\tau = -6.5^\circ \text{ C}$ when $0 < h < 11,000 \text{ km}$,

2. $T = -56.5^{\circ}\text{C}$, when $11,000 < h < 22,000$ m,
and hence $T = 56.5^{\circ}\text{C}$

Constant on earth's gravitation, $g = 9.80 \text{ m/sec}^2$.

For the standard weights of air, we have:

$$\gamma/\gamma_0 = [(2.88 - 0.0065 h)/288]^{4.253}, \text{ when}$$

$$0 < h < 11,000 \text{ m (troposphere),}$$

$$\log \gamma/\gamma_0 = (h - 11,000)/14,600 \quad \text{when}$$

$$11,000 < h < 22,000 \text{ m (stratosphere)}$$

The air weights arrived at on the basis of these formulas appear in Table 33, column 1, for certain altitudes.

TABLE 33

Standard Weight γ [kg/m^3] of Air at Various
Flight Altitudes h [km]

Flight altitude	CINA standard atmosphere	According to Hann-Humphreys	According to Hohmann's formula
0	1.2249	1.293	1.293
1	1.1116		1.15
2	1.0064		1.00

[Table 33 cont'd. next page]

[Table 33 continued]

3	0.9091		0.90
4	0.8191		0.80
5	0.7361		0.70
6	0.6597		0.62
7	0.5895		0.54
8	0.5252		0.48
9	0.4664		0.424
10	0.4127		0.375
12	0.3108		0.290
14	0.2267		0.225
16	0.1640		0.175
18	0.1208		0.135
20	0.0878	0.0885	0.105
22	0.0638		0.081
25			0.055
30			0.0283
35			0.01464
40		0.00403	0.0074
45			0.00376
50			0.00187
55			0.000915
60		0.00018	0.000448
65			0.000217

[Table 33 cont'd. next page]

[Table 33 continued]

70			0.0001025
75			0.0000497
80		0.0000103	0.0000230
85			0.0000106
90			0.0000049
95			0.0000022
100		0.0000019	0.00000098

Column 2 of this table presents the standard weights arrived at by using the earlier relationships, for a few high altitudes.

Hohmann, in his Die Erreichbarkeit der Himmelskörper (The Attainability of Celestial Bodies), derives a formula, closed and standard for all flight altitudes for the air which yields the familiar values, specified to exactness on theoretical grounds, with satisfactory accuracy despite the ease with which the formula can be handled:

/186

$$\gamma/\gamma_0 = (1 - h/400\,000)^{49}.$$

In Table 33, column 3, we present the values based on the use of this simple formula for a series of flight altitudes.

Because of its simple structure, and because of its accuracy which is entirely satisfactory for our purposes, we shall use the Hohmann air density formula exclusively in our subsequent flight trajectory calculations, even though there is no apparent justification for the numerical agreement it affords with the actual em-

pirical findings. Further improvements in the relation between the formula and reality could be attained by altering the fixed values.

313. Speed of Sound as a Function of the Flight Altitude*

Since the speed of sound is of enormous importance to the aerodynamic forces, as we have learned in section 2, we are interested here in the variability of the speed of sound in air with flight altitude. From the general formula for the speed of sound in a gas

$$c = \sqrt{\kappa p / \rho}$$

we find in a first approximation that the speed of sound has the same value at each height, since pressure and density are proportional by the Boyle-Mariotte law, so that the ratio p/ρ is constant. At each height, then, we presuppose the same air temperature T , the same adiabatic exponent κ , and the same gas constant R .

In actuality, as we learned in section 311, the temperature and the gas constant vary with height.

If the speed of sound at sea level is:

$$c_0 = \sqrt{\kappa p_0 / \rho_0},$$

*E. g. : B. Gutenberg. Die Geschwindigkeit des Schalles in der Atmosphäre (The Speed of Sound in the Atmosphere). Physik. Zeitschrift, 1926.

then we have, from the equation of state for a gas, the following formula for the speed of sound at any height h at temperature T , and where the gas constant of the gas mixture prevailing at that point is R :

$$c_h = \sqrt{\kappa p/\rho} = c_0 \sqrt{R T/R_0 T_0},$$

since

$$p/\rho = p_0/\rho_0 \cdot R T/R_0 T_0.$$

Now, since we may put $R = R_0$ within the troposphere, the temperature

however falling from the normal sea-level value $T = 273^\circ$ to the normal stratosphere temperature $T = 218^\circ$, we find that the speed of sound will drop in the stratosphere, as against the sea-level

/187

value, by a factor of $\sqrt{218/273} = 0.894$, for those reasons: thus a rather unimportant change.

The information at hand tells us no more about the temperature relationships at very great stratospheric heights, so that we could hardly expect any considerable influences on the speed of sound. It is only beyond the upper stratosphere limits that the gas constant undergoes a significant change, and rises, if we assume a hydrogen atmosphere, to 14 times the sea-level value, so

that the speed of sound will increase by a factor of $\sqrt{14} = 3.7$ at those heights, if we ignore temperature effects.

Things stand much the same with the possible variability of the second factor, the adiabatic exponent κ . The nature of the gas constituents of the atmosphere varies basically with height, according to Section 311, but even so the determining components are still diatomic gases such that $\kappa = 1.40$, so that we can anticipate a constant κ at each height. A certain change would be

possible only because of abnormal gas states, for instance oxygen condensed to ozone, or possibly completely dissociated gases in the higher layers of the stratosphere. Leaving the geocoronium aside, which would play no substantial role even in the light of Wegener's own findings at a stratospheric altitude used for rocket flight purposes, the value of μ could drop to 1.3 or rise to 1.6, respectively, and the speed of sound would experience slight changes in the process, by a factor of 0.96 or 1.07 of the sea-level value, respectively.

For practical purposes, we can treat the speed of sound as a constant and as independent of the flight altitude, in our subsequent discussion.

314. Acceleration due to Gravity as a Function of Flight Altitude

Given $5.98 \cdot 10^{27}$ g as the mass of the earth, and $\Gamma = 6.67 \cdot 10^{-8}$ cm³ g⁻¹ sec⁻² as the universal gravitational constant, the acceleration due to gravity acting on a mass m_1 at the earth's surface (average radius of earth: 6,378,000 m) will be, in accord with the Newtonian law of gravitation $K = \Gamma \cdot m_1 \cdot m_2 / r^2$:

$$g = k/m_1 = 980,665 \text{ cm/sec}^2 \doteq 9.81 \text{ m/sec}^2.$$

In accord with the flattening of the earth amounting to about 20 km, the earth's gravitational acceleration will be less at the equator

(9.78 m/sec²) and greater at the poles (9.83 m/sec²) than this average acceleration.

According to the law of gravitation, this average acceleration exerted by the earth will decrease rapidly as the distance from the center of the earth increases.

Referred to a flight altitude h over the assumed average surface of the earth discussed earlier, the acceleration will be:

$$g_h = g_0 \left(\frac{R}{R + h} \right)^2.$$

At the extreme height $h = 60$ km of interest in rocket flight, the acceleration will be

$$g_{60} = 9.81 \cdot 0.993 = 9.73 \text{ m/sec}^2.$$

We shall not discuss this slight decrease in any greater detail in our subsequent calculations, in any case, and we may be content to use the constant acceleration due to gravity $g = 9.81 \text{ m/sec}^2$.

32. THE HIGH-ALTITUDE FLIGHT PHASE

The high-altitude flight of a rocketplane is characterized by the fact that the aerodynamic lift A plus the centrifugal force F of the trajectory curvature are consistently equal, in the perpendicular direction, to the remaining gross flying weight G , so that the flight altitude is maintained consistently. The air drag W associated with A in terms of the aircraft lift/drag ratio must continually be compensated by a rocket thrust of equal magnitude. We have $F \gg A$ at appropriately high flight velocities, so that the required rocket thrust is very low and the fuel consumption rate associated with it is inconsiderable.

Next we take up, separately, the magnitudes of the three forces acting in perpendicular directions on the aircraft.

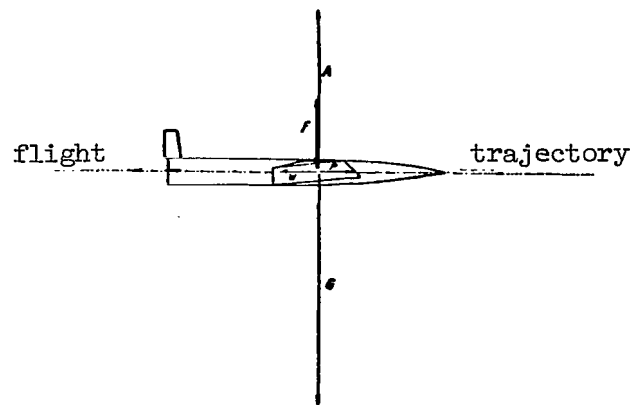


Fig. 79.

The external forces on the rocketplane during the high-altitude phase.

321. The Centrifugal Force

Since the flight altitude is assumed to be constant in the high-altitude flight phase, the only possible causal factor for the centrifugal force to be considered is the trajectory curvature resulting from the osculation of the flight trajectory with the course of the earth's surface. If we put the mean curvature of

this surface as $R = 6.37755 \cdot 10^6$ m, we then have for the centrifugal force:

$$F = \frac{M v^2}{\rho} = \frac{G v^2}{g h (R + h)} = \frac{G v^2 (R + h)}{g \cdot R^2} = \frac{G v^2}{g R}$$

The magnitude of this centrifugal force per unit weight, the F/G ratio for relief of the centrifugal force, appears in Fig. 80 of the next section as a function of the flight velocity.

When the centrifugal force becomes so great that it attains the value of the weight G , so that F/G equals 100 %, then the appropriate flight velocity at that point will be the angular velocity, and its magnitude will be found from $G = F$:

$$v_{ang} = R \sqrt{\frac{g}{R + h}} .$$

Table 34 lists the values of the angular velocity at various flight altitudes. The flight velocity of the rocketplane cannot exceed the angular velocity constantly, since the preponderant centrifugal force would otherwise drive the plane away from the earth and into outer space.

TABLE 34

Angular Velocity at Various Altitudes

Flight altitude (km)	Angular velocity (m/sec)
0	7906
10	7902
20	7896
30	7890
40	7884
50	7878

[Table 34 cont'd. next page]

[Table 34 continued]

60	7872
70	7865
80	7859
90	7853
100	7847

The angular velocity thus represents, in present-day engineering understanding, the highest possible circumterrestrial cruising speed.

322. The Aerodynamic Lift

This factor is computed most commonly by using the familiar formula

$$A = c_a \cdot \gamma / 2g \cdot F \cdot v^2.$$

By hypothesis, the air density decreases with height in obedience to the equation

$$\gamma = (1 - h/400\,000)^{49} \gamma_0.$$

For the lift coefficient, over the flight velocity range with which we are exclusively concerned here, i.e., over 1.5 times the speed of sound, we may use the limiting formula

$$c_a = 165 \cdot 300/v^2 + 0.01$$

(here, α is put at about 6°).

We then have the aerodynamic lift:

$$A = (165 \cdot 300/v^2 + 0.01) \cdot (1 - h/400\,000)^{4.9} \cdot \gamma_0/2g \cdot F \cdot v^2$$

From the ground-level flight characteristics, we have:

$$A_0 = G_0 = c_{a0} \cdot \gamma_0/2g \cdot F \cdot v_0^2,$$

and hence

$$\gamma_0/2g \cdot F = G_0/c_{a0} v_0^2.$$

If, further, we put the flying weight in the high-altitude trajectory equal to the k -th part of the take-off flying weight G_0 (for which

see Section 323), we then have

$$\gamma_0/2g \cdot F = k_1 G/c_{a0} v_0^2 = \bar{k} \cdot G, \quad \text{when} \quad \bar{k} = k_1/c_{a0} v_0^2$$

and finally, we have the lift:

$$A = \bar{k} \cdot G \cdot (165 \cdot 300/v^2 + 0.01)(1 - h/400\,000)^{49} \cdot v^2,$$

where \bar{k} is specified primarily by the flight characteristics at ground level and by the ratio of the fuel load to the take-off weight.

323. The Gross Flying Weight

The take-off gross flying weight G_0 of the rocketplane diminishes to a fraction during the ascent to the high altitudes of the mid-course high-altitude flight phase, because of the formidable fuel consumption rate of the operating rocket. The flying weight G remaining when the high-altitude flight trajectory is reached remains practically constant, however, since the subsequent fuel consumption is negligible. In our calculations, therefore, we take the flying weight in the high-altitude mid-course phase as

$$G = G_0/k_1 = \text{const.}$$

324. Height and Flight Velocity of the
High-Altitude Mid-Course Trajectory

On equating the three perpendicular forces mentioned

$$A + F = G$$

we obtain a relationship linking the altitude of the high-altitude flight trajectory and the constant flight velocity required at that altitude:

$$\bar{k} \cdot G \cdot (165\,300/v^2 + 0.01)(1 - h/400\,000)^{49} \cdot v^2 + G v^2/g_0 R^2 \cdot (R + h) = G,$$

and hence

$$v = \sqrt{\frac{1 - \bar{k} (1 - h/400\,000)^{49} 165\,300}{0.01 \bar{k} (1 - h/400\,000)^{49} + (R + h)/g_0 R^2}}.$$

Putting $k = 1/1000$ (corresponding more or less to a flight velocity of 80 m/sec near the earth and to a fuel load amounting to 80 % of the take-off flying weight), we obtain, by means of this formula, the flight velocities required at each altitude, as shown in Fig. 80.

The altitude of the mid-course flight trajectory is included in this diagram for the case where the lift coefficient is constant at all velocities, which is in some measure the case up to about

$$v = 1.5 a.$$

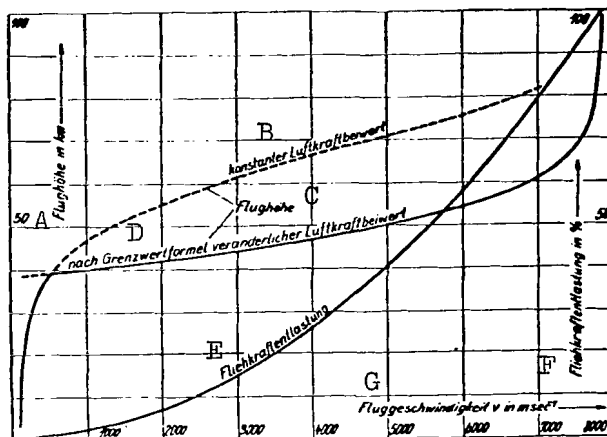


Fig. 80.

Flight altitude and relief of the centrifugal force (F/G ratio) of the mid-course flight trajectory, plotted flight velocity.

- A. Flight altitude in km, B. constant aerodynamic force coefficient, C. Flight altitude, D. aerodynamic force coefficient varying according to limiting formula, E. F/G ratio, F. F/G ratio, in %, G. Flight velocity v in m sec^{-2} .

We find from the two curves that flight at a purely supersonic velocity first becomes possible upwards of 40 km altitude, so that stratospheric flight which has become the object of repeated efforts in recent times can lead to relatively modest flight velocities at flight altitudes below 40 km. Because of the steep drop in the lift coefficient curve in response to pure

supersonic flow, the flight altitudes increase very slowly as the flight velocity is stepped up still further, so that the flight velocity will increase from about 700 m/sec to 7000 m/sec in the altitude range between 40 and 60 km.

At flight velocities upwards of about 7600 m/sec, the flight velocity will increase again with increasing height, but still at a slower rate, since only very slight aerodynamic lifts are required because of the relief of the centrifugal force which will be predominant at those heights, and these lift forces will be possible at enormous flying velocities again only at extraordinarily high flight altitudes with their very slight air densities.

/192

Finally, a curve was plotted for the relief of the centrifugal force to indicate the percentage of the flying weight carried by the centrifugal force associated with the curvature of the trajectory, and to indicate what further percentage would then have to be carried by the wings, and consequently the engine thrust required.

Flight altitudes above 80 km, where the relief of the centrifugal force approaches 100 % and the high-altitude flight becomes almost a purely planetary motion, thereby making it possible to cover the remaining portion of the flight almost without having to use the engine, are of particular interest. For example, we find the relief of the centrifugal force to be about 99 % at 80 km altitude, about 99.9 % at 100 km, at flight velocities of about 7,800 m/sec and 7840 m/sec, respectively. Because of the not entirely reliable air density formula and the equally uncertain air resistance formula, these relationships might turn about to be correct at slightly different altitudes, but in any case they must take place, qualitatively speaking. Overexactness in our calculations would not be justified at the present state of our knowledge.

If we take a F/G ratio (relief of the centrifugal forces) of 99 % from Fig. 80, at 80 km altitude and 7800 m/sec flight velocity, this will mean that, at a lift/drag ratio $\epsilon = 1.5$, despite the fantastic flight velocity, an engine output of only about 260 HP or a total rocket thrust of only 2 kg per ton flying weight is required, and this would entail a fuel consumption per second of 1/50 (one fiftieth of a kilogram) gasoline-oxygen mixture.

To visualize this, the reader may imagine a somewhat high-powered sports airplane featuring the flight weight and engine output figures referred to, with the lift/drag ratio diminished to a hundredth of the usual value, so that it could attain a hundred times the usual speed with the same engine output.

The high-altitude flight of the rocketplane will consequently occur at very great heights with actually negligible fuel consumption over travel path lengths as long as we wish.

To minimize this very minute power output down to the absolute zero value (i.e. pure planetary motion) would require an increase in

flight altitude by a factor of 10 or 20, and would consequently range into the domain of pure space travel, which lies beyond the scope of this book.

Even the pure high-altitude flight depicted here with its persistently negligible engine power output is of no direct theoretical interest for rocket flight, as the next sections will demonstrate. Of much greater importance would be those high-altitude flight trajectories, even at altitudes around 40 km, for rocketplanes of the type of the Gorokhov planes mentioned earlier. If an air chamber were provided in the airplane, the chamber being connected to the external air at the nose of the airplane, then a certain pressure determined by the dynamic pressure would be maintained in the chamber independently of the barometric pressure outside, because of the unaltered dynamic pressure in the chamber. Appropriately designed air compressors can be used to drive the air from this chamber into the combustion chamber of the rocket engine, where the oxygen of the air will act as oxidizer for the fuel, while the residual gases of the air will serve as stabilizing masses in the sense of Fig. 2 and Tables 19 and 20. The exhaust velocity of the combustion gases from the air-gasoline mixture would have to reach about 1300 m/sec at 40 km altitude, and the flight velocity could attain like figures at that altitude. The external rocket efficiency would then be unity. At an average lift/drag ratio $\epsilon = 0.2$, the fuel consumption requirements per ton average flying weight and per hour would be about 150 kg, and this means that a range of about 24,500 km or 5 hours flying time would become possible for a cruise speed of about 4700 km per hour.

The unattainability of this highly intriguing prospect lies, as emphasized at an earlier point, in the inadequacy of presently available compressors.

Near the earth, where the required intake pressure of the air drawn into the combustion chamber would be more easily attainable, the exhaust velocities would again be greater and the flight velocities attainable would be much smaller, so that the external rocket engine efficiency would fall off considerably and the rocket power plant would no longer feature any advantages over the propeller power plant.

In order to facilitate the intake of fresh air, with the aid of the dynamic pressure, we might consider the idea of an intermittent operating mode of this rocket propulsion plant, somewhat in the manner of explosion type gas turbines (e.g. the Holzwarth turbines). At the same time, the exhaust velocity might be substantially reduced by means of a generous excess of air in the combustion process, so that the external efficiency would take on favorable values even in the case of low flight velocities. On

giving this matter a bit of thought, though, we see that the internal efficiency of this type of rocket propulsion unit is extraordinary low, principally on account of circulation losses, and will become steadily lower as the air excess is increased, i.e., as the external efficiency increases at low flight velocities. The circulation losses arise primarily as the fresh air is brought in after a pressure balance is achieved in the rocket combustion chamber through the displacement of the expanded but still hot combustion gases present in the combustion chamber. These circulation losses increase with the air excess beyond any bounds, at low exhaust velocities.

33. THE ASCENT PATH

330. Ascent Path. General.

According to the arguments advanced in Section 32, the rocket aircraft flying at 60 km altitude has a total of about $2.6 \cdot 10^6$ kg-m total energy, both kinetic and potential, referred to the take-off point, per kilogram of gross flying weight. Since 1 kg of the propellant mixture considered possesses only about $1.0 \cdot 10^6$ kg-m calorific value, this final energy of the craft flying weight at the end of the trip can, of course, be attained only by expelling most of the propellant en route before the high velocities are reached, so that the propellant would be without effect on the terminal velocity and terminal altitude of the aircraft.

If the aircraft has about $0.8 \cdot 10^6$ kg-m chemical-thermal energy on the average per kilogram of take-off flying weight, and if this energy is finally imparted to one-fifth of the take-off weight as kinetic and potential energy, then this will amount to $4 \cdot 10^6$ kg-m per kilogram of the remaining gross weight during the high-altitude mid-course flight, and could indeed attain the value stipulated

above of $2.6 \cdot 10^6$ kg-m/kg, when the inevitable losses are taken into account.

The ascent path therefore serves the purpose of providing the rocket with a total (kinetic and potential) energy appropriate to the specified terminal flight altitude discussed in section 32.

During the ascent, a fairly large quantity of energy has to

be withdrawn from the propellant, in order for the rocketplane to attain the required energy in the high-altitude course, with all the losses accounted for.

The ratio of the energy of the aircraft applied in the form of chemical-thermal propellant energy to the energy finally available in the form of potential energy and kinetic energy can be designated as the ascent efficiency, taking into account the path usefully traversed during the ascent phase.

This ratio can be used to state, at each altitude, the required total propellant per kilogram flying weight in the high-altitude phase.

The ascent efficiency is determined by the amounts of calorific propellant energy required not only to lift and accelerate the terminal gross weight, but also to ensure high-altitude flight. These are essentially:

1. Energy losses due to imperfections in the rocket motor as a machine, which can be accounted for in terms of the internal efficiency η_i .

2. Energy losses due to the kinetic energy of the exhaust gases, when these still possess some velocity relative to the take-off point after they have been expelled. These losses will be accounted for in terms of the rocket engine external efficiency η_a .

3. Energy losses due to the potential energy of the exhaust gases, originating in the fact that the propellant materials must be carried aloft for a portion of the ascent path prior to being exhausted.

4. Energy losses which originate in the retarding effect of the earth's gravitational field and which are proportional to the duration of the ascent phase.

5. Finally, the energy losses incurred in overcoming the drag encountered in traversing the ascent path.

The last two energy contributions were already accounted for in terms of the rocket motor efficiency.

331. Differential Equation of the Ascent Path

In the diagram of the ascent path, Fig. 81, we have:

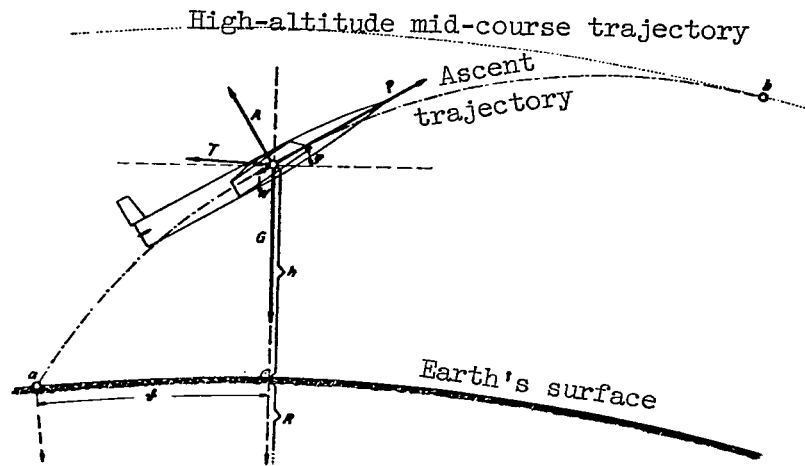


Fig. 81.

External forces acting on the rocketplane during its ascent.

- A the aerodynamic lift,
- P the rocket motor thrust,
- G the instantaneous flying weight,
- W the drag on the aircraft,
- T the d'Alembert force of inertia due to the first four forces.

In setting up the equation of the trajectory, we again assume the take-off point a to be at rest. The deviations resulting from the actual state of motion of the take-off point a will be dealt with in summary fashion after other factors have been considered.

The resultants of the external forces acting on the aircraft in the direction tangential to the trajectory ($-T_t$) and in the direction normal to the trajectory ($-T_n$) are found from Fig. 81 to be:

$$- T_t = P - G \sin \varphi - W,$$

$$- T_n = G \cos \varphi - A.$$

The total result of the external forces, hence, will be:

$$\begin{aligned} - T &= \sqrt{(-T_t)^2 + (-T_n)^2} = \\ &= \sqrt{A^2 + P^2 + G^2 + W^2 - 2(AG \cos \varphi + PG \sin \varphi - WG \sin \varphi + PW)}. \end{aligned}$$

The differential equation of the ascent path will now be derived from the fundamental equation of dynamics

$$- T = M \frac{dv}{dt} = M \frac{d^2 s}{dt^2}$$

whose components in the directions tangential and normal to the trajectory are, respectively:

$$- T_t = M dv/dt$$

$$- T_n = M v^2 / \rho$$

so that

$$\begin{aligned} A^2 + P^2 + G^2 + W^2 - 2 (AG \cos \varphi + PG \sin \varphi - WG \sin \varphi + PW) = \\ = M^2 (dv/dt)^2 + M^2 (v^4 / \rho^2). \end{aligned}$$

The external forces A, P, G, and W acting on the aircraft are themselves functions of the elements of the trajectory, and apply to those elements when we refer all of the forces to the unit weight of the aircraft at take-off:

$$A/G_0 = c_a v^2 / c_{a_0} v_0^2 \cdot (1 - h/400000)^{49},$$

where c_a is constant for flight velocities in the subsonic region, and can be put equal to c_{a_0} , while we must have

$$c_a = 165300/v^2 + 0.01$$

in the supersonic region.

The specific thrust of a rocket performing constantly over a period of time is

$$P/G_0 = k_0/g \cdot c,$$

where k_0 tells us what portion of the take-off flying weight G_0 passes through the rocket to exhaust per second, and c denotes the exhaust velocity of the gases.

The corresponding weight would then be:

$$G/G_0 = 1 - k_0 t.$$

As the mass of the aircraft diminishes in the course of the rocket's constant activity, the effective acceleration of the craft will ultimately increase to such high values that it will exceed the limits set for biological reasons.

/197

It has become quite commonplace in rocket engineering to reckon with an acceleration kept as constant as possible over the entire ascent path, with the value of that acceleration being fixed by the biological limiting value. In that case, P/G rather than P/G_0 must be kept constant and equal to kc/g , the rocket must be

throttled more and more as the ascent proceeds, whereupon k_0 assumes the variable value

$$k_0 = k \cdot e^{-kt}.$$

The weight variation of the standard weight per second is kept constant and equal to k , so that the weight variation of the entire aircraft per second will be equal to Gk , and therefore will decrease with G . The decrement in weight of the entire aircraft, dG , over a time interval dt , is then:

$$- dG = G \cdot k \cdot dt,$$

and hence

$$G/G_0 = e^{-kt},$$

which is what we also obtain quite directly from the so-called fundamental equation of rocketry. The rocket thrust itself is then:

$$P/G_0 = kc/g \cdot e^{-kt}.$$

But even this assumption is not expedient for the purposes of rocket flight practice, since no possible practical ascent trajectory could be actually found on which the aerodynamic forces would not increase beyond any bearable bounds in a very short time when the aircraft acceleration is kept constant.

Rather, the aircraft acceleration and, concomitantly, the rocket thrust must be functions of the time such that the aerodynamic forces, and in particular the lift force on the wings, will stand in a certain ratio to the flying weight and respectively to the forces acting downwards on the plane, on an ascent trajectory held within certain bounds. There is no point in going here into greater detail on this function.

Finally, the air drag is expressed as:

$$W/G_0 = \epsilon c_a v^2 / c_{a0} v_0^2 \cdot (1 - h/400000)^{49},$$

where the symbol A/G_0 accounts for the coefficients of the aerodynamic

forces.

Now we are in a position to set up the differential equation of the ascent path. Double integration while taking into account all of the boundary conditions to be partially indicated will yield the equation of the ascent path, but the computational difficulties of this integration are so formidable, and even after these difficulties have been overcome the possibly closed formula for the ascent path is likely to be so unwieldy that we will have to forbear any deeper-going exact treatment, which would be hardly justifiable in any case because of the numerous uncertainties in the assumption, and we shall have to be satisfied with an estimate-based calculation which will suffice for our purposes.

/198

332. Approximate Ascent Path in the Subsonic Region

Our point of departure in calculating the approximate subsonic ascent path is that the aircraft pilot will hardly be able to maintain a complicated mathematically defined flight trajectory in the few minutes that the ascent phase lasts, and under such unfavorable biological conditions at that, and that on the other hand an approximately straight ascent path with simultaneous control of the rocket thrust, say by visual monitoring a dynamic pressure indicator, would be easier in practice.

With that in mind, we assume:

1. The subsonic ascent path should be a straight line inclined through a constant angle φ to the earth's surface, on approximately assuming the latter to be level.

2. The velocity on this rectilinear ascent path is to be kept such that the lift force on the wings will be consistently equal to the component of the gross weight normal to the trajectory, so that the resultant forces and with them the accelerations will not be applied transverse to the rectilinear ascent path.

Moreover, the subsonic ascent path, the main purpose of which is to facilitate the attainment of a high potential energy (i.e., altitude), will be distinguished by the approximately constant aerodynamic force coefficients c_a and c over the entire path.

Now a simple argument will convince the reader that, under these assumptions, the sound barrier should be attained only at a height of about 35,000 meters.

At $\varphi = 30^\circ$, we obtain an oblique ascent path such that $s = h/\sin \varphi = 70 \text{ km}$ and an average acceleration on this path of $\bar{b} = v^2/2s = 2 \text{ m/sec}^2$, a very low value as we see.

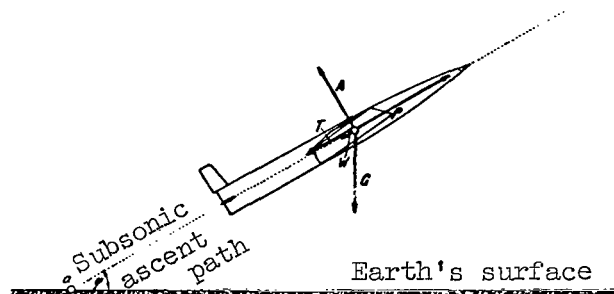


Fig. 82.

External forces acting on the rocket-plane during a practically favorable subsonic ascent.

The acceleration at first must be even lower than this value, in order to avoid too rapid an increase in the aerodynamic forces, but can exceed this value at some later point.

By equating with zero the resultant forces in the directions parallel to the axes and in the normal direction, we find for the required rocket propulsive force:

$$P = G \sin \varphi + W + T,$$

$$A = G \cos \varphi,$$

and hence:

$$P = G (\sin \varphi + \epsilon \cos \varphi) + T$$

or:

$$P/G = (\sin \varphi + \epsilon \cos \varphi + 1/g \cdot dv/dt).$$

From the second equation of equilibrium and from the expression for A in Section 331, we obtain, as a further defining equation:

$$(v/v_0)^2 (1 - s \sin \varphi / 400000)^{4.9} = G/G_0 \cdot \cos \varphi.$$

If, to a first approximation, we put G/G_a equal to a constant k_1 , the average gross flying weight over the subsonic ascent path, then we obtain for v:

$$v = ds/dt = v_0 \sqrt{k_1 \cos \varphi (1 - s \sin \varphi / 400000)^{-24.5}},$$

where G_a is the gross weight at the beginning of the subsonic path.

By a single integration, we obtain from the above, taking boundary conditions into account:

$$t = \frac{15700}{v_0 \sqrt{k_1 \cos \varphi \sin \varphi}} [1 - (1 - s \sin \varphi / 400000)^{25.5}]$$

and accordingly

$$s = 400000 / \sin \varphi \cdot [1 - (1 - v_0 t \sqrt{k_1 \cos \varphi \sin \varphi} / 15700)^{1/25.5}].$$

The required dv/dt is found with the aid of the fundamental relation $dv/dt = v \, dv/ds$:

$$dv/dt = v_0^2 k_1 \sin 2 \varphi / 32640 \cdot (1 - s \sin \varphi / 400000)^{-50}.$$

From this we now obtain the specific thrust:

$$P/G = kc/g = \sin \varphi + \epsilon \cos \varphi +$$

$$+ v_0^2 k_1 \sin 2 \varphi / 32640 g \cdot (1 - s \sin \varphi / 400000)^{-50}$$

or

$$P/G = kc/g = \sin \varphi + \epsilon \cos \varphi +$$

$$+ v_0^2 k_1 \sin 2 \varphi / 32640 g \cdot (1 - v_0 \sin \varphi \sqrt{k_1 \cos \varphi} \cdot t / 15700)^{-1.96}$$

and

$$k = g/c \cdot [\sin \varphi + \epsilon \cos \varphi +$$

$$+ v_0^2 k_1 \sin 2 \varphi / 32640 g \cdot (1 - v_0 \sin \varphi \sqrt{k_1 \cos \varphi} \cdot t / 15700)^{-1.96}].$$

The total weight decrease over the subsonic ascent path will then be, at each instant of time:

/200

$$dG = - G \cdot k \cdot dt$$

$$G/G_0 = e^{-g/c \cdot (\sin \varphi + \epsilon \cos \varphi) - v_0/c \cdot \sqrt{k_1 \cos \varphi} [(1 - v_0 \sin \varphi \sqrt{k_1 \cos \varphi} \cdot t / 15700)^{-1.96} - 1]}.$$

At the end of the ascent path, we have by definition:

$$G/G_0 = 2k_1 - 1.$$

Hence

$$2k_1 - 1 = e^{-g/c \cdot (\sin \varphi + \epsilon \cos \varphi) - v_0/c \cdot \sqrt{k_1 \cos \varphi} [(1 - v_0 \sin \varphi \sqrt{k_1 \cos \varphi} \cdot t / 15700)^{-1.96} - 1]}.$$

Now

$$t = \frac{15700}{v_0 \sqrt{k_1 \cos \varphi} \sin \varphi} \left[1 - (v_0/v \cdot \sqrt{k_1 \cos \varphi})^{1.04} \right] = \frac{15700 (v - v_0 \sqrt{k_1 \cos \varphi})}{v_0 v \sin \varphi \sqrt{k_1 \cos \varphi}}$$

allows us to infer that:

$$2k_1 - 1 = e - \frac{15700 g (v - v_0 \sqrt{k_1 \cos \varphi}) (\sin \varphi + \epsilon \cos \varphi)}{v_0 v c \sin \varphi \sqrt{k_1 \cos \varphi}} - \frac{v - v_0 \sqrt{k_1 \cos \varphi}}{c} =$$

$$= e - \frac{v - v_0 \sqrt{k_1 \cos \varphi}}{c} \left[\frac{15700 g (\sin \varphi + \epsilon \cos \varphi)}{v_0 v \sin \varphi \sqrt{k_1 \cos \varphi}} + 1 \right]$$

The angle of climb φ for the subsonic path is deliberately chosen such that the propellant consumption will be minimized, so that k_1 will then be maximized. Given the assumptions applying earlier:

$$v_0 = 80 \text{ m/sec}, v = 530 \text{ m/sec}, c = 3700 \text{ m/sec and } \epsilon = 0.2,$$

the relationship between k_1 and φ indicated in Fig. 83 shows a flat-topped maximum for k_1 near $\varphi \approx 30^\circ$, and this angle can be accepted as the most favorable angle of ascent, under the assumptions entertained. The final weight will be

$$G \approx 0.4 G_0.$$

The effective rocket thrust P/G , flight velocity v , the length of path traversed s , and the actual acceleration dv/dt on the aircraft, all characterizing the performance during the ascent phase, are shown in Fig. 84 as functions of time, at $\varphi = 30^\circ$ and $k = 0.7$. The absolute value of the rocket thrust P will remain

pretty much constant during the subsonic ascent phase, and this assures extracting optimum performance from the rocket motor.

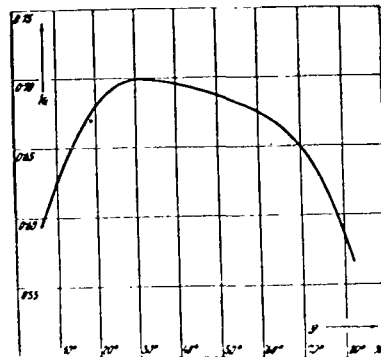
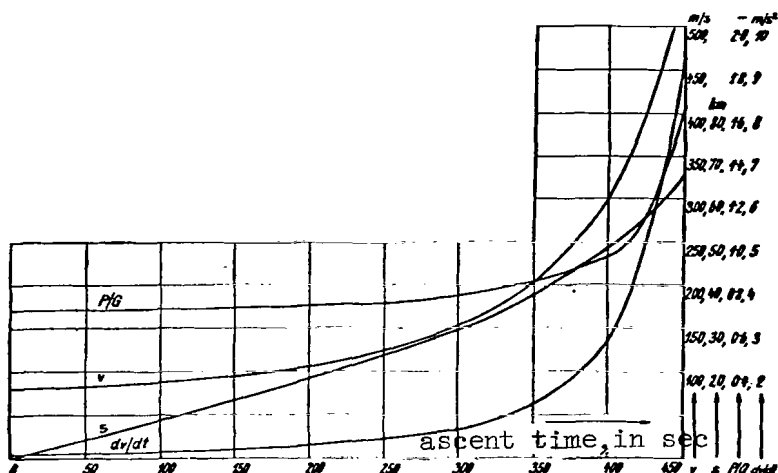


Fig. 83.

Propellant consumption in the subsonic ascent phase as a function of the angle of inclination.

The first conspicuous point to note is that the applicable ascent accelerations must be kept within modest limits if we are to prevent the aerodynamic forces from surpassing all bounds during the ascent phase and thus hindering rather than favoring the ascent.

Summing up, we can state that the subsonic ascent trajectory can be approximated well enough as a straight line that must be flown with a low and so variable an acceleration that the lift force on the wings remains equal to the gross weight component normal to the trajectory.



[commas represent decimal points]

Fig. 84.

Plot of the: velocity v , flight path s , rocket thrust P/G , and acceleration on the rocketplane dv/dt as a function of the ascent time elapsed.

The effect of the low accelerations during the ascent will be that the ascent process will not constitute any acrobatic maneuver accompanied by pressure increments hazardous to the lives of the pilot or eventual crew and passengers, will mean an appreciable simplification in the design of the rocket motor for the low thrust required and a lightening of the inertia loads on the plane, and

finally will make it easier to avoid overheating and hot spots in the aircraft skin through friction with the relative wind. The most favorable angle of climb depends solely on the aircraft characteristics, and is a fixed value for any particular aircraft. Slight deviations from the most favorable angle of climb will not result in any substantial increase in fuel consumption.

333. Approximate Ascent Path in the Supersonic Region

In contrast to the subsonic ascent path, the supersonic load extends over relatively enormous horizontal stretches, with which the vertical-ascent path lengths can hardly compare. The principal aspect of this region is the larger kinetic energy (velocity) required. Corresponding to the slight inclination of the trajectory and in view of the difficulties mentioned in Section 332 on the mathematically exact piloting of the rocketplane, as an approximation we can assume the aircraft axis to be steadily horizontal for the supersonic load of the ascent trajectory. The values of the discrete forces acting on the rocketplane, and plotted in Fig. 85, are taken from Section 331 or 321, and are:

/202

$$A/G_0 = v^2/c_{a0} v_0^2 \cdot (165\,300/v^2 + 0.01)(1 - h/400\,000)^{49},$$

$$F/G_0 = v^2/g R e^{kt},$$

$$P/G_0 = kc/g e^{kt},$$

$$G/G_0 = 1/e^{kt},$$

$$W/G_0 = v^2/\epsilon/c_{a0}v_0^2 \cdot (165\,300/v^2 + 0.01)(1 - h/400\,000)^{49},$$

$$T/G_0 = 1/g \cdot e^{kt} \cdot dv/dt.$$

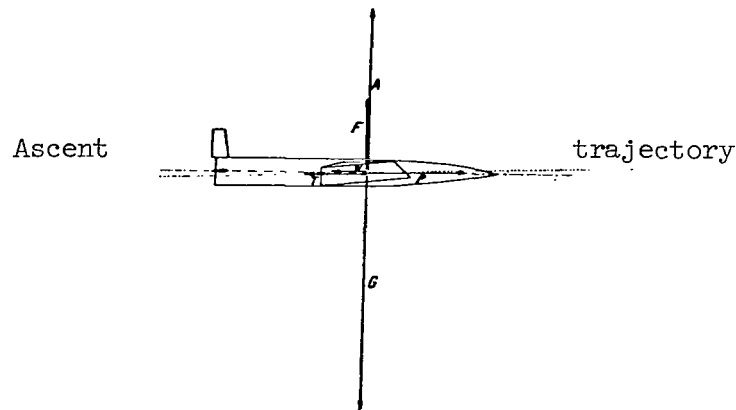


Fig. 85.

External forces acting on the rocketplane during a practically favorable supersonic ascent phase.

In the process, we assume a rocket thrust in the supersonic region decreasing at a rate such that the effective acceleration will remain constant, and its value will be given, moreover, by the value attained at the end of the subsonic ascent phase.

Still higher thrusts would probably be permissible here because the aerodynamic forces increase more slowly with the velocity, but in this region even low airplane accelerations lead to no great losses, and the rocket motor design should not be scaled to higher thrusts than those needed in any case in the subsonic region.

By putting the force resultants in the vertical and horizontal directions equal to zero, we obtain:

$$\Sigma V = 0 \dots v^2/g R e^{kt} +$$

$$= v^2/c_{a0} v_0^2 \cdot (165\ 300/v^2 + 0.01)(1 - h/400\ 000)^{49} = 1/e^{kt},$$

$$\Sigma H = 0 \dots kc/g e^{kt} =$$

$$= v^2 \epsilon/c_{a0} v_0^2 \cdot (165\ 300/v^2 + 0.01)(1 - h/400\ 000)^{49} + 1/ge^{kt} \cdot dv/dt.$$

When h is eliminated from both equations, we obtain the differential equation linking v and t which is of primary interest to us:

/203

$$dv/dt = kc - \epsilon g + \epsilon v^2/R.$$

By a simple integration we obtain:

$$t = \frac{1}{\sqrt{\epsilon/R \cdot (kc - \epsilon g)}} \arctan \frac{\sqrt{\epsilon R (kc - \epsilon g)} (v - v_a)}{R (kc - \epsilon g) + \epsilon v_a v}$$

$$v = \frac{v_a \sqrt{\epsilon R (kc - \epsilon g) + R(kc - \epsilon g) \tan t} \sqrt{\epsilon/R \cdot (kc - \epsilon g)}}{\sqrt{\epsilon R (kc - \epsilon g) - \epsilon v_a \tan t} \sqrt{\epsilon/R \cdot (kc - \epsilon g)}},$$

where v_a denotes the limiting velocity between the subsonic and the pure supersonic regions, and t represents the time elapsed from the beginning of the supersonic phase.

The flight speed attained is thus known at each instant.

The corresponding flight altitude may be found directly from the above equation $\Sigma V = 0$ in terms of v and t .

By repeated integration of the differential equation, we obtain the horizontal path length covered at each instant. We avoid, however, the resulting highly cumbersome formula for s , which has only the apparent but unjustified appeal of very high exactitude, and estimate the horizontal path length covered during the supersonic ascent phase by assuming an average constant aircraft acceleration in terms of the quantity:

$$dv/dt \approx \text{const} = kc - \epsilon g + \frac{\epsilon}{R} \left(\frac{v - v_a}{2} \right)^2$$

so that

$$s \approx \frac{v^2}{2b} \frac{v^2}{2kc - 2\epsilon g + \epsilon/2 R \cdot (v + v_a)^2}.$$

The supersonic ascent path can be investigated in approximate fashion by means of the formulas so derived. It should be noted that here the time t is reckoned from the beginning of the supersonic ascent path. In Fig. 86, the velocities, the horizontal path lengths of the supersonic ascent path, and the propellant consumption are plotted as functions of the time elapsed under the assumptions:

$$\epsilon = 0.2 \text{ and } kc = 15 \text{ m/sec}^2.$$

Because of the lifting work left out of account in the more exact calculation during the supersonic ascent phase, the velocities attained in the rocket performance will actually turn out to be a few percent lower than indicated in Fig. 86. The slight departure of the more exact v/t -curve from the averaged v/t -straight line shown as a broken line, at constant average acceleration, is also clearly seen in the diagram. The justification of the simple s/t -curve is thereby demonstrated.

/204

334. Efficiency of the Ascent Path

During the subsonic ascent phase, the unit of weight of the gross weight available for conversion to energy at the end of the phase was:

1. Potential energy at 32 km altitude...	32,000 kgm/kg
2. Kinetic energy at 530 m/sec flight speed ...	14,260 kgm/kg
3. Usefully applied transportation work to cover a horizontal path of 55.5 km at $\epsilon = 0.2$...	11,100 kgm/kg
	<hr/>
	57,360 kgm/kg

Since Section 332 yields $G/G_0 = 0.4$ at the end of the ascent trajectory in the subsonic region, 1.5 kg propellant becomes consumed for $1.01 \cdot 10^6 \text{ kgm/kg}$ energy content per kilogram of gross weight at the end of the trajectory, i.e., $1.515 \cdot 10^6 \text{ kgm}$ of chemical-thermal propellant energy. Of this total quantity of energy, about 3.8 % is used to the aircraft's advantage, according to the above discussion. This value seems very low when compared to the total efficiency of over 20 % attained in conventional airplane power plants.

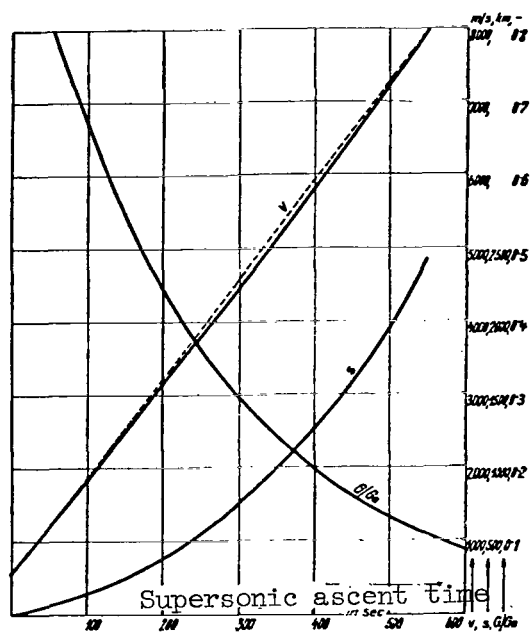


Fig. 86.

Flight velocity v , of the supersonic flight path length s , and propellant consumption G/G_0 , as functions of the supersonic ascent time elapsed.

The reason lies first of all in the relatively low external efficiency of the rocket motor itself, which amounts to 14 % when the average flight speed is about 265 m/sec at $c = 3700$ m/sec, according to Section 1221. Given the known internal efficiency of $\eta_i = 0.7$, the losses due to these causes, independent of the

nature of the ascent trajectory, amount to about 90 %, from which we may infer that no perceptibly improved efficiency is to be attained by any other mode of ascent based on a different principle, when we bear in mind the remaining 6 % losses accounted for by the air resistance, the retarding effect of the earth's attraction, etc.

The low efficiency of the subsonic ascent trajectory thus has to be accepted as inherent in the nature of rocket propulsion.

The efficiency of the supersonic ascent trajectory defined in the same sense is not a fixed value, but depends on the duration of the supersonic ascent phase. In Fig. 87, the energies supplied usefully to the corresponding final gross weight of the airplane are separated into the three components (potential energy, kinetic energy, and transportation work) and plotted with the aid of Fig. 86. The G/G_0 curve furthermore yields the expenditure in

chemical-thermal fuel energy (see Fig. 86). The efficiency curve in Fig. 87 was determined thereby. The efficiency of the supersonic portion of the ascent trajectory turns out to be consistently extraordinarily high, reaching an extremely flat-topped peak of 48 % at about $v = 4,000$ m/sec. The reason for this favorable behavior may be ascribed first of all to the high external efficiency of the rocket motor in the velocity ranges concerned.

The efficiency of the entire ascent trajectory from take-off to the point where the required flight altitude and airspeed are attained is spectacular. It is found as the ratio of the total extracted energy (kinetic plus potential plus transportation) per kilogram of final weight of the airplane to the energy content of the total propellant consumed per kilogram terminal craft weight.

Numerically, it is computed from the two partial efficiencies mentioned earlier, after these have been reduced to the common final weights, and we arrive with ease at the values plotted in Fig. 87.

We learn from the diagram, for instance, that a gasoline-oxygen propellant mixture of about 16 kg per kilogram final weight of the airplane would be required to generate a flight speed of about 6,700 m/sec (sufficient, according to what we shall learn in the later discussion, to reach the opposite pole of any take-off point on the earth in a gliding flight) at an ascent trajectory efficiency of 19.3 %.

This highest attainable total efficiency appears at first

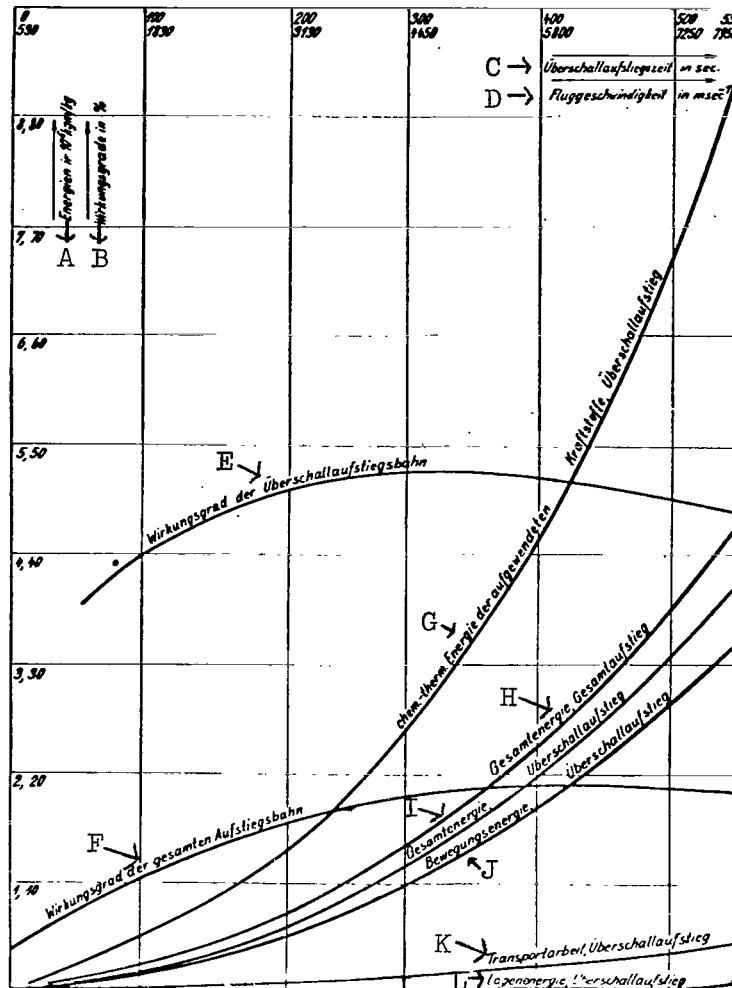


Fig. 87.

Energy and Efficiency relations for the ascent trajectory.

A. Energies in 10^6 kgm/kg, B. Efficiencies in %
 C. Supersonic ascent time in sec, D. Flight speed
 in $\text{m} \cdot \text{sec}^{-1}$, E. Efficiency of supersonic ascent

[Cont'd. next page]

[legend cont'd.]

trajectory, F. Efficiency of total ascent trajectory, G. Chemical-thermal energy of propellant used, supersonic ascent, H. Total energy, total ascent, I. Total energy, supersonic ascent, J. Potential energy, supersonic ascent, K. Transportation work, supersonic ascent, L. Potential energy, supersonic ascent.

to be unjustifiably small compared to the rocket engine efficiencies discussed in Section 12.

The greatest total efficiency at flight in a gravity-free, drag-free field is found to be 45 % at constant flight acceleration. Under conditions of gravity this figure undergoes a correction to about 38 % in view of the limit on the aircraft accelerations permissible on biological grounds. The remaining 18 % of the energy losses with respect to the efficiency of our ascent trajectory are ascribed primarily to the low accelerations applied and to the air resistance.

These energy losses could hardly be kept at a much lower level in the case of a fixed-wing rocketplane traversing other ascent trajectories.

34. DESCENT PATH. GENERAL.

If the power is shut off during the high-altitude flight or at the end of the ascent path, then the rocketplane will begin to describe its descent trajectory under the influence of the retarding air drag. Since the angle between the tangent to the trajectory and the horizon is very small over the extensive upper-lying portions of the descent trajectory, we can then apply the force diagram valid for the high-altitude flight as an approximation in our investigation of the relationships prevailing in the descent phase. Here we need only replace the rocket thrust P by the force of inertia T , which arises from the retardation of the aircraft by the air drag, and which accordingly must be supplied from the potential energy of the aircraft's mass.

/207

The descent path is characterized, then, by the fact that the total kinetic energy $G/2gv^2$ and the potential energy Gh of the rocketplane over that trajectory must be used up in overcoming the air drag which at first is quite negligible. The descent path may extend over enormous distances, depending on the available energies. Given the relationships underlying the situation depicted in Fig. 80, the numerical values of the kinetic energy and potential energy of the rocketplane in the high-altitude phase of the course yield the numerical values indicated in Fig. 89 per kilogram gross weight G .

/208

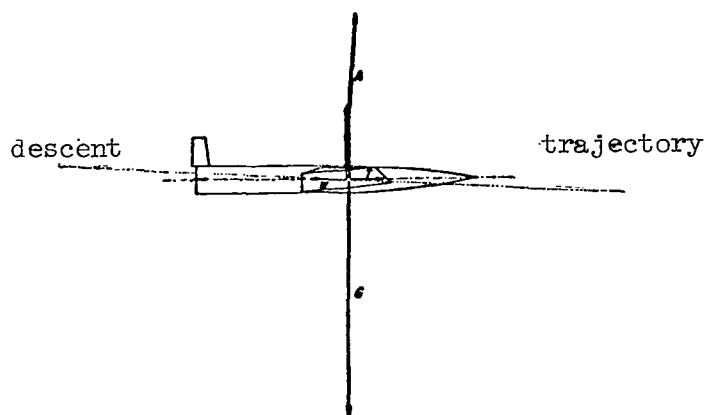


Fig. 88.

External forces acting on the rocketplane during the descent phase.

341. Descent Path in the Supersonic Region

Given the negligible value of the potential energy compared to the kinetic energy at the initial altitudes in question, and

given the very poor gliding capability of the rocketplane, we can begin by leaving the potential energy completely out of consideration in our treatment, and subsequently we can summarily estimate its effect in increasing the length of the descent path. A more exact calculation would have very little practical point at the present time because of the uncertainty in our air density and air drag formulas.

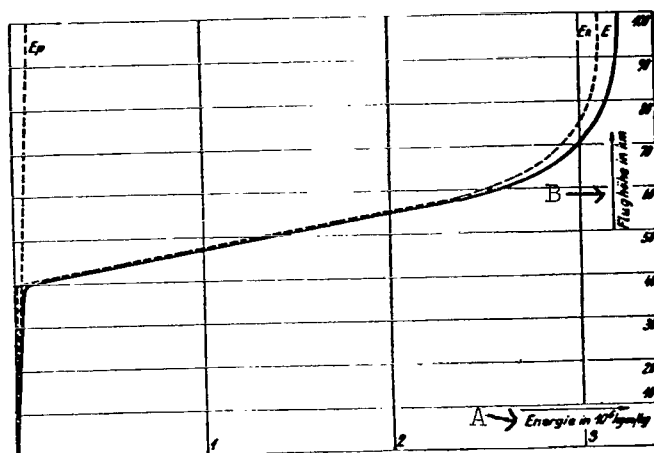


Fig. 89.

Illustration of the kinetic energy (E_k), potential energy (E_p), and total energy (E) available for the descent path per kilogram gross weight, as a function of the initial altitude.

A. Energy, in 10^6 kgm/kg, B. Altitude, in km.

Next, referring back to Section 32, we find the individual forces depicted in Fig. 88 to be, in value:

$$F \doteq G v^2 / R g,$$

$$A = kG (165 \cdot 300/v^2 + 0.01)(1 - h/400\,000)^{49} v^2,$$

$$G = \text{const} = G,$$

$$W = A \cdot \epsilon = k \epsilon G (165 \cdot 300/v^2 + 0.01)(1 - h/400\,000)^{49} v^2,$$

$$T = G/g \cdot dv/dt.$$

On equating with zero, the sum of the forces in the vertical and horizontal directions, we get:

$$\Sigma V = 0 \dots k(165 \cdot 300/v^2 + 0.01)(1 - h/400\,000)^{49} v^2 + v^2/g R = 1,$$

$$\Sigma H = 0 \dots k\epsilon(165 \cdot 300/v^2 + 0.01)(1 - h/400\,000)^{49} v^2 = 1/g \cdot dv/dt.$$

The descent trajectory is uniquely and completely determined in the flight velocity range of pure supersonic flow by these two equations.

When h is eliminated from these equations, we obtain as a differential expression in v and t :

$$g \epsilon - v^2 \epsilon / R = dv/dt = d^2 s / dt^2.$$

A single integration yields:

$$v = \sqrt{g R} \frac{e^{2\epsilon t \sqrt{g/R}} - (\sqrt{g R} + v_0)/(\sqrt{g R} - v_0)}{e^{2\epsilon t \sqrt{g/R}} + (\sqrt{g R} + v_0)/(\sqrt{g R} - v_0)}$$

or

$$t = \frac{1}{2 \epsilon \sqrt{g/R}} \frac{\ln(\sqrt{g R} + v_0)(\sqrt{g R} - v)}{(\sqrt{g R} - v_0)(\sqrt{g R} + v)},$$

where v_0 represents the flight speed at the initial altitude. The flight speed, and with it also the flight altitude, will then be known at each instant of time, in line with Section 324.

By repeated integration of the differential equation, we find the horizontal distance traversed by each instant of time:

$$s = t \sqrt{g R} + \frac{R}{2 \epsilon} \ln \left(\frac{1 + (\sqrt{g R} + v_0)/(\sqrt{g R} - v_0)}{e^{2\epsilon t \sqrt{g/R}} + (\sqrt{g R} + v_0)/(\sqrt{g R} - v_0)} \right)^2.$$

With the equations derived here, the descent path can be mathematically traced starting from any initial altitude so long as the flight speed remains in the purely supersonic region, i.e., the air drag law adopted must be valid for a variable c_a value. This will be the case

in general down to altitudes of about 40 km. Furthermore, in this reasoning the negligible vertically acting force of inertia ensuing from the vertical component of the descent trajectory was disregarded. Its path-lengthening effect can be estimated to sufficient exactness, however, when we lengthen the horizontal descent path lengths with respect to the ratio of the potential energy to the kinetic energy at any given moment, with a lengthening of about 3 % in a descent from 100 km to 40 km altitude. Because of the uncertainty of many of the assumptions underlying our calculations, an uncertainty to which reference has been made repeatedly, such improvements would be entirely superfluous.

342. Descent Path in the Subsonic Region

Since the F/G ratio, or compensation of the centrifugal force, no longer applies in practice in the subsonic velocity range of the descent path, and the coefficients of the aerodynamic forces must be treated as constant, the air resistance will be constant over the entire remainder of the descent path, and the length of the descent path can be calculated most simply from the available energy and from this air resistance.

Any more precise statements about the subsonic part of the descent trajectory would require dealing with force relationships similar to those discussed in Section 341, but because this branch of the trajectory is so short we can bypass any such steps and treat it as a straight line in an approximation.

/210

343. Features of the Descent Path

According to Fig. 80, the borderline separating the supersonic and subsonic parts of the descent trajectory will be found in the vicinity of 40 km altitude. According to Fig. 89, the total available energy at that point amounts to about 60,000 kg-m per kilogram gross weight. If we again assume a L/D ratio of $\epsilon = 0.2$

for the rocketplane in the subsonic region, despite the very low load on the wings, we will find the constant air drag per kilogram gross weight to be 0.2 kg, and the length of the subsonic descent path will be simply

$$s_u = 60000/0.2 = 300 \text{ km.}$$

The flight velocity on this subsonic descent trajectory will drop from the initial figure of about 1,900 km/h to a final figure of about 150 km/h near the earth's surface, so that the dynamic pressure will remain constant despite the different air density, and the entire subsonic portion of the trajectory will have been traversed in about $3/4$ h.

These values are entirely independent of the initial altitude at which the descent began, provided that altitude is upwards of 40 km.

The supersonic part of the descent trajectory extends over even far greater cruising distances. The dependence of the length of its trajectory and of the time required to cover the length starting from the final altitude of the high-altitude phase may be seen in Fig. 80 and in the values arrived at in Section 341 for the relations shown in Fig. 90, provided we again assume $\epsilon = 0.2$.

One of the first things we note are the enormous distances over which a descent trajectory starting at higher altitudes will stretch. Since the greatest circumterrestrial cruise distance cannot be greater than about 20,000 km by its very nature, the highest altitudes involved in traffic from one point on the earth to another will be about 58 km, inasmuch as the descent trajectory starting at that altitude will already cover the entire length of the required distance. The time required to complete this descent will be about 85 min in the supersonic region, another 45 min in the subsonic region, so that the entire trip plus the ascent time will take about 2 h.

Rocket flight, insofar as it is used for traffic between different points on the earth, will actually take place only in the two lower layers of the atmosphere, the troposphere and the stratosphere, with only very brief segments of the trajectory, however, traversing the troposphere.

One particularly characteristic property of the supersonic descent trajectory is the fact that the airplane is barely steerable in practice on the trajectory. The eventual course of the

supersonic portion of the flight is completely determined by the magnitude and direction of the initial flight speed on the high-altitude trajectory, and can hardly be influenced by the pilot through any steering maneuvers. Any arbitrary alterations of the trajectory, theoretically conceivable because of the slight aerodynamic forces in operation, will be limited in practice because such maneuvers would place the aircraft in a risky position with respect to its direction of propulsion, with the chances of heating of the air in front of the aircraft greatly enhanced. Because of this guided motion, the descent trajectory will be completely and uniquely specified as a function of the initial conditions, and the relations derived in Sections 324 and 341 can be used to define the trajectory analytically.

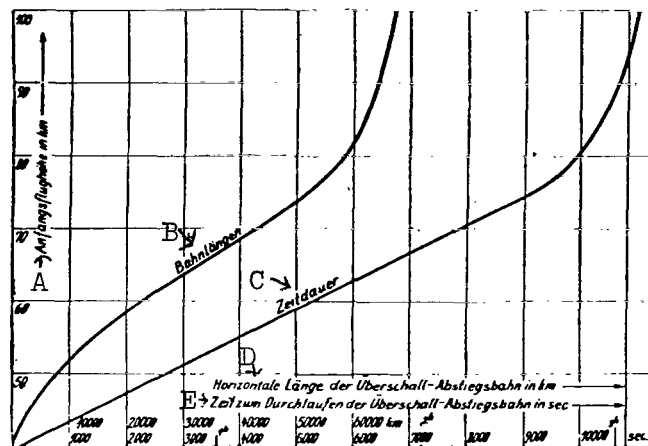


Fig. 90.

Lengths of trajectory and duration of descent from high-altitude flight until the subsonic velocity is reached.

A. Initial altitude in km, B. Trajectory lengths, C. Duration, D. Horizontal length of supersonic descent path, in km, E. Time to traverse supersonic descent path, in sec.

The trajectory equation s/h , ensuing from the combination of the relations reigning between v/h , v/t and s/t at any given moment, yields, if need be, all the closer information desired.

The piloting relations are altered as soon as the subsonic portion of the descent trajectory is reached, where the kinetic energy plays only a very minor role and the aircraft therefore begins to obey piloting maneuvers. This is of utmost importance for the landing operations, since it permits the pilot to home in, from an altitude of about 40 km, on a suitable landing site within a radius of 300 km, and to approach the selected landing area in a gliding flight via curves, spirals, etc., with almost one full hour at the pilot's disposal.

/212

35. PERFORMANCE OF A ROCKET AIRCRAFT. GENERAL.

The more prominent performance criteria of the rocketplane are its flight velocity and its flight altitude.

In these two respects, the rocketplane presents not so much a continuous further development, as a basic multiplication of the performance achieved to date with tropospheric aircraft. The flying range is of paramount importance as a third performance factor. The principal causes of limitations on the velocity ranging from about 400 to 750 km/h in conventional tropospheric aircraft as well as the more recent stratospheric aircraft are well known, and will be mentioned here, in part, as:

1. The limited range of speeds between the landing speed and the maximum speed, the limitations placed by considerations of safety on the landing speed being decisive.
2. The unsatisfactory capability of the superchargers for flights at a very high atmospheric altitude, since the engine performance cannot be maintained because of the lack of oxygen.
3. Deterioration of the aerodynamic properties as the speed of sound is approached, with increased power requirements and impaired propeller efficiency resulting.
4. The impossibility of increasing the propeller rpm figures because of considerations of material strength.
5. Exorbitant engine weight associated with the increased power requirements imposed by increased flight velocities.

These difficulties are obviated in the rocketplane by:

1. The use of rocket propulsion which does not require any air propeller to generate propulsive forces, and develops a many times greater power output per unit engine weight,

2. The fact that the oxygen required to burn the fuel is carried on board, so that the engine power plant is enabled to operate independent of the oxygen present in the air.

These basic principles make it possible to aim for very high flight altitudes independently of shortcomings in superchargers, and theoretically make it possible to utilize contemporary engineering know-how to achieve the highest possible speeds in terrestrial traffic at these altitudes.

According to the previous discussion, we see that not only do the flight altitude and flight speed affect each other very intimately, but that the range of the rocketplane is most intimately bound up with these factors. Since this last factor is the principal determinant of the practical usefulness of the rocketplane, it will be the first of the points to be discussed.

351. Range of a rocket aircraft

The range is determined, just as in the conventional airplane, by the quantity of fuel carried on board. In this respect, the rocket aircraft poses entirely extraordinary demands to the designer, and, according to Section 332, the propellant alone must amount to 60 % of the initial gross flying weight in order to achieve pure supersonic speeds, and this is a percentage which could not be far surpassed by our most capable long-range aircraft. On the other hand, possibilities hitherto unknown are opened up by the low weight of the rocket engine plant and by the very high load permitted on the wings by the high take-off thrust and the excellent take-off properties.

Once supersonic speeds and the associated flight altitudes have been attained, the aircraft has two choices open to it for reaching a remote destination.

On the one hand, the already achieved flight speed could be simply increased to the point required to assure sufficient rocket efficiency, about 1850 to 2000 m/sec according to the assumptions so far, whereupon a pure high-altitude cruising phase

could be maintained at that speed until the destination becomes attainable by a gliding flight. The horizontal length of this gliding flight would then be about 2000 km, according to Section 343.

On the other hand, there is the possibility of increasing the previously achieved supersonic speed until the high flight speed achieved after a few minutes will suffice to reach the destination in gliding flight, with the engine completely shut off, from the instantaneous position of the plane.

This latter possibility rests on the fact, alluded to in Section 343, that the aircraft will be capable of completely flying around the earth with the engine cut off in gliding flight at a flight speed of about 7,500 m/sec, and of reaching the antipode of the instantaneous position of the craft, with the engine cut off in gliding flight, at $v = 6,400$ m/sec.

Destinations lying closer than say 2,400 km from the take-off point do not require an actual high-altitude course in any case, since the horizontal paths of the ascent trajectory and descent trajectory will completely cover this range.

But even for the remaining still greater distances, the choice is readily in favor of the second possibility, with no actual high-altitude phase at constant flight speed and with the engine operating, when we consider that, according to Section 324, the high-altitude flight phase takes place with a F/G ratio of barely 7 % at 2,000 m/sec and at about 42 km flight altitude, so that it takes place in practice against the total air drag which requires

a work output of about $6 \cdot 10^6$ kg-m/kg in the high-altitude phase alone, at $\epsilon = 0.2$ and 20,000 km total cruising distance, as com-

pared with $3 \cdot 10^6$ kg-m/kg work, according to Section 333, put into stepping up the cruising speed from 2,000 m/sec to 6,400 m/sec at 56 km altitude, where the flight can be continued for the most part with over 60 % F/G ratio, i.e., against a very slight air drag. This advantage holds good even for shorter flights. Moreover, the cruising speed does increase quite a bit in the second cruising mode, the rocket engine need be activated for a much shorter time, and most of the flight will take place independently of the behavior of the engine.

Further reasoning will then apply exclusively to long-range flights consisting solely of the two branches of the ascent trajectory and the immediately following descent trajectory, with no intervening high-altitude phase.

The shortest cruise distance in practice is obtained in the case where the rocketplane climbs till it achieves pure supersonic speed and then descends to about 350 km.

Short flights of this type by means of a rocketplane would be ruled out by economic considerations.

The advantage offered by the rocketplane over the conventional tropospheric airplane with respect to energy, in the sense that the former requires smaller quantities of energy than a high-performance propeller-driven airplane, to transport a certain final payload over a specified distance would become a reality only beyond the cruising range of the propeller aircraft. Even this point cannot be made with justification, since to date, no matter what vehicle is used the higher cruising speed must be paid for in terms of higher ton-kilometers work output. The rocketplane is a clear departure from the past, and a highly advantageous one, comparatively speaking, since the ton-kilometer work output in long-range flights is of about the same order of magnitude as that for propeller-driven aircraft, despite the 30-fold or greater cruising speed. We shall return to this point below, in Section 353.

The range itself depends primarily on the load ratio G/G_0 , on the attainable exhaust velocity c , and partially also on the lift/drag ratio of the airplane.

If we reapply the earlier assumptions to these last two parameters and to the other influences, we find the relationship represented in Fig. 91 between the load ratio G/G_0 , the range s ,

and the maximum flight speed v . Figure 91 is plotted with ease by means of the relations derived in Sections 32, 33, and 34. It is well to note that the distance covered in the subsonic region independently of the total travel distance amounts to about 370 km, with about 70 km accounted for by the subsonic ascent trajectory and about 300 km accounted for by the supersonic descent trajectory. The principal distances in question are traversed at supersonic speed, as we see. The supersonic ascent trajectory extends to over 1,000 km distance only when the final velocities exceed $v = 5,000$ m/sec, so that the supersonic descent trajectory accounts for an overwhelming section of the route covered.

At the load factor $G/G_0 = 0.3$ already occasionally achieved in conventional aircraft of today, the range could hardly extend to about 1,000 km of the horizontal course (see Fig. 91). Load factors of about from $G/G_0 = 0.15$ to 0.13, which already lie on the border-

line of present-day design capabilities, would be required to attain the great non-stop distances achieved by propeller-driven aircraft. Of course, there is no point in discussing any significant payload figures in this context.

Achievement of an adequate range is accordingly the most important problem now facing the rocketplane designer.

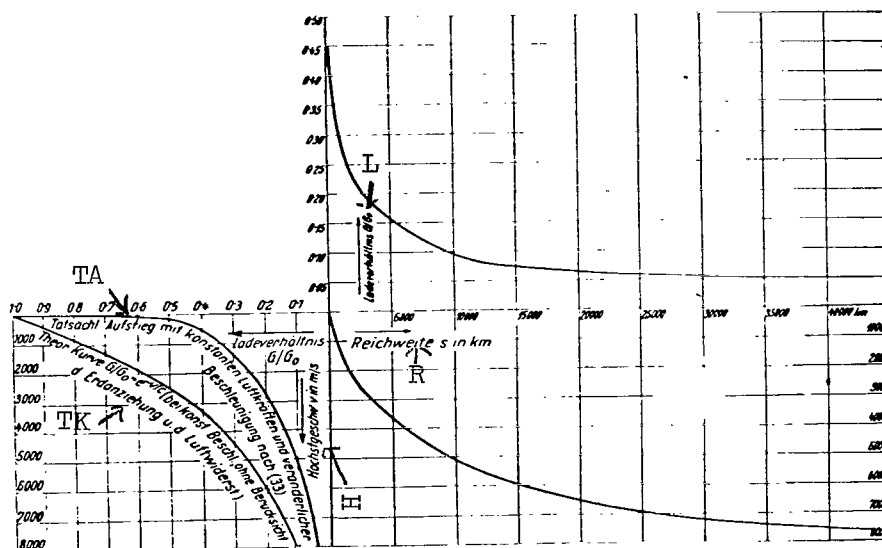


Fig. 91.

Relationships linking: load factor G/G_0 ; range s ; peak flight speed v .

L. load factor G/G_0 , R. Range s , in km, H. Peak flight speed v , in m/s, TA. Actual ascent with aerodynamic forces constant and variable acceleration, according to (33), TK. theoretical curve, G/G_0 vs. $e^{-v/c}$ at constant acceleration, ignoring gravitational acceleration and air drag.

Abstracting from any special revolutionary discoveries in the realm of fuels and propellants, the main problem we have to solve is to find the optimum among the following partially contradictory influences:

With the use of superior energy-rich propellants, there is in general an increase not only in the hazard presented by these materials, but in the measures required to accommodate them on board the aircraft, with a concomitant increase in the dead weight of the aircraft. Beyond a certain mass, then, the range will again shorten despite the high exhaust velocities.

As larger rocket nozzle diameters are used, the internal efficiency of the rocket will increase, and the exhaust velocity c will likewise increase for given propellants, but the blunt-tailed rocket extremity will bring about a considerable impairment in the lift/drag ratio of the airplane, particularly in the subsonic region (where at least three-fourths of the total amount of fuel will be consumed).

But even granting the figures used here, which are certainly not the most favorable estimates, a non-stop range stretching to 4000 or 5000 km can be confidently anticipated, and we note that there is a cruising range greater than that available to most airplanes we have knowledge of, including the fastest.

The competitive capabilities of the rocket aircraft compared to the propeller aircraft are therefore quite plausible even in the initial stage of development, with respect to the cruising range.

The earth's rotation exerts no substantial influence on the cruising range within the region of maximum speeds that we have to consider primarily. Any such influence may be taken into account, however, in an approximation by considering the velocity component of the take-off point lying in the direction of the trajectory to add algebraically to the maximum velocity, so that it will be included in the summed value in Fig. 91. In this way, we find that east-to-west flights will have a somewhat longer range than flights in the opposite direction.

The earth's rotation will be an important influence, however, in flight ranges extending over 20,000 km, hardly attainable at the present state of the art; in those cases it will have to be completely taken into account.

352. Cruising and maximum speeds of a rocket aircraft

The most outstanding superiority of the rocket aircraft over propeller aircraft lies in the flight speed.



The top flight speeds are themselves limited by the load factor G/G_0 , and on their part limit the flying range, as we see from Fig. 91. At a 50,000-km flight the maximum flight speed amounts to about 3,700 m/sec, i.e., 13,300 km/h.

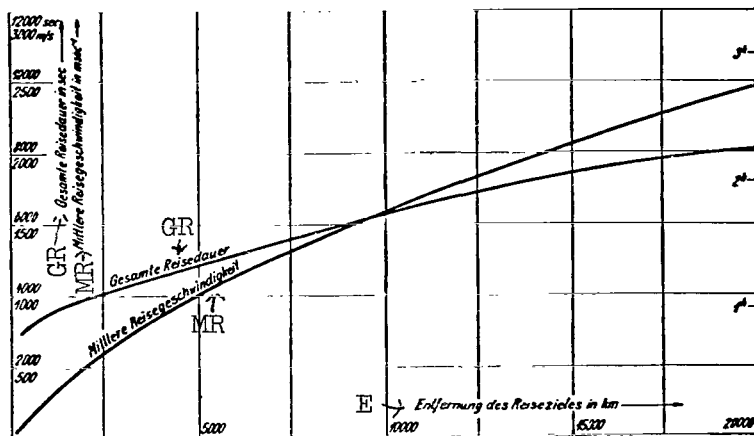


Fig. 92.

Dependence of entire duration of flight and of intermediate cruising speed on the distance of the destination point.

GR - total duration of trip [in sec], MR - intermediate cruising speed [in m/sec], E - distance to destination, in km.

This speed comes within reach only during a very short period at the end of the ascent path, however. The average cruising speed for a 5,000-km flight is calculated for the individual branches of the trajectory in terms of time requirements.

According to Section 332, the subsonic ascent lasts about 400 sec. According to Section 333, the supersonic ascent phase up to the point where a speed $v = 3,700$ m/sec is attained lasts about 240 sec.

According to Section 343, the supersonic descent trajectory starting from this speed lasts about 1,600 sec and the adjoining subsonic descent trajectory is about $3/4$ h, or 2,700 sec.

Taken altogether, the 5,000-km flight will take place in about 5,000 sec or at an average cruising speed of 1,000 m/sec or 3,600 km/h.

Therefore, we see that the cruising speed of the rocket-plane at such a cruising range will be approximately 10-fold to 20-fold that of the currently conventional cruising speeds. These cruising speeds would increase to a considerable extent with the longer cruising distances, which are to be sure not yet attainable without further improvements. Figure 92 provides an overall view of the intermediate cruising speeds as a function of the length of the non-stop travel distance.

Plotted in the same diagram, we have the directly derived durations of the trips as functions of the distance to the destination.

353. Flight altitudes of a rocket aircraft

The flight trajectories treated in this book are primarily for the purpose of transportation between different points on the earth. Therefore, only those flight altitudes required for specific flight speeds are maintained on these trajectories.

The figures arrived at have nothing to do directly with the peak altitude attainable by rocket aircraft, on that account.

If it is to attain much higher altitudes the aircraft would have to be designed from a slightly different point of view and the calculations discussed here would not provide a basis for that work, but we have no need to go into this in greater detail here.

The rocket aircraft altitudes required for the transportation purposes are associated in the first instance with the attainable peak velocities, and therefore in turn with the length of the flight. Nevertheless, the range of altitudes is a relatively narrow one. Since the aircraft attains the region of pure supersonic speeds only at altitudes from 35 to 40 km, the flight altitudes will definitely have to be above that number. But since the aerodynamic forces

increase only very slowly, with speed in the pure supersonic region, altitudes higher than 50 km will hardly be required for the peak velocities attainable within a foreseeable span of time, according to Section 324, so that the top ceilings attainable on long-range flights will fluctuate between 35 and 50 km. The more exact value appropriate to each particular flying range may be read with ease from Fig. 90 and Fig. 80.

FARADAY TRANSLATIONS
15 PARK ROW
NEW YORK 38, N. Y.